Universidade de Aveiro
2019

Departamento de Química

Marina da Conceição da Silva Matos

DESENVOLVIMENTO DE POLÍMEROS E MATERIAIS COMPÓSITOS MAIS SUSTENTÁVEIS A PARTIR DO ÁCIDO 2,5-FURANODICARBOXÍLICO

DEVELOPMENT OF MORE SUSTAINABLE POLYMERS AND COMPOSITE MATERIALS BASED ON 2,5-FURANDICARBOXYLIC ACID

Universidade de Aveiro Departamento de Química
2019

Marina da Conceição da Silva Matos

DESENVOLVIMENTO DE POLÍMEROS E MATERIAIS COMPÓSITOS MAIS SUSTENTÁVEIS A PARTIR DO ÁCIDO 2,5-FURANODICARBOXÍLICO

DEVELOPMENT OF MORE SUSTAINABLE POLYMERS AND COMPOSITES MATERIALS BASED ON 2,5-FURANDICARBOXYLIC ACID

Dissertação apresentada à Universidade de Aveiro para cumprimento dos requisitos necessários à obtenção do grau de Doutor em Química Sustentável, realizada sob a orientação científica do Doutor Armando Jorge Domingues Silvestre, Professor Catedrático do Departamento de Química da Universidade de Aveiro e da Doutora Paula Andreia Fernandes de Sousa, Investigadora de Pós-Doutoramento do Departamento de Química da Universidade de Aveiro.

Apoio financeiro da FCT e do POPH/FSE (PD/BD/52501/2014) no âmbito do III Quadro Comunitário de Apoio.

FCT
Fundação para a Ciência e a Tecnologia
MINISTÉRIO DA EDUCAÇÃO E CIÊNCIA

POPH
PROGRAMA OPERACIONAL POTENCIAL HUMANO

QREN
QUADRO DE REFERÊNCIA ESTRATÉGICO NACIONAL

UNIÃO EUROPEIA
Fundo Social Europeu

Dedico este trabalho à minha família.

o júri

presidente

Prof. Doutor Silvina Maria Vagos Santana
professora catedrática da Universidade de Aveiro

Prof. Doutor Jorge Fernando Jordão Coelho
professor catedrático da Faculdade de Ciências e Tecnologia da Universidade de Coimbra

Doutor Shanmugam Thiyagarajan
Investigador da Universidade de Wageningen

Doutor Jorge Alberto Salgueiro Vigário Moniz Dos Santos
Gerente de inovação na OMNOVA Solutions Portugal

Doutora Carmen Sofia Da Rocha Freire Barros
Equiparada a Investigadora Principal com agregação da Universidade do Porto

Doutora Paula Andreia Fernandes De Sousa
Investigadora de Pós-doutoramento da Universidade de Aveiro

agradecimentos

Em primeiro lugar gostaria de agradecer aos meus orientadores, ao professor Doutor Armando Silvestre e Doutora Andreia Sousa, pela orientação, esforço e disponibilidade que demonstraram ao longo de todo este percurso.

À Doutora Patrícia Mendonça pela disponibilidade, constante alegria, e precioso auxílio com as inúmeras análises de SEC efectuadas ao longo dos anos.

Gostaria também de agradecer ao Professor Doutor Jorge Coelho pela ligação com a CIRES S.A. no âmbito da preparação dos filmes de PVC, e mais ainda pelas diversas conversas construtivas e apoio prestado.

À Engenheira Cristina Costa da CIRES S.A. pelas amostras de PVC e pelo uso das instalações e equipamentos na fábrica.

Ao Professor Doutor Adélio Mendes e à Mestre Márcia Andrade pela disponibilidade prestada com a determinação das permeabilidades barreira.

À Doutora Rosemeyre Cordeiro e ao Professor Doutor Henrique Faneca pela disponibilidade e auxílio prestados com os ensaios de citotoxicidade.

Aos meus colegas dos três laboratórios que, directa ou indirectamente contribuíram para que estes quatro anos fossem um importante marco da minha vida. Um especial agradecimento à Patrícia Ramos, ao André Lopes, ao Nuno Gama, à Maria João Soares, à Catarina Moreirinha e à Inês Mendes pelo apoio, motivação e trocas de conhecimentos valiosas.

Aos colegas do laboratório PATH: Tánia Sintra, Helena Passos, Pedro Carvalho, Catarina Neves, Maria Jorge Pratas, Márcia Neves, Mónia Martins, entre muitos outros, que muito me auxiliaram, tanto em equipamento, material, conhecimento e boa disposição.

Um agradecimento especial à Sandra Magina e à Belinda Soares pelos anos de sólida amizade, carinho, incentivo e acima de tudo o meu pilar dentro da Universidade de Aveiro.

Gostaria também de agradecer aos meus Pais pelo apoio incondicional que me deram ao longo de toda a minha vida.

Finalmente o meu maior agradecimento vai para o meu marido José Pedras e para o meu filho Tiago, pela compreensão, apoio, incentivo e amor diários.

palavras-chave

Ácido 2,5-furanodicarboxílico, recursos renováveis, 5-hidroximetilfurfural, poliésteres furânicos, nanocompósitos, plastificantes não tóxicos.

resumo

Nos dias de hoje, os problemas ambientais, as mudanças climáticas, os recursos fósseis limitados e sua flutuação de preço, associados à atividade industrial (muitas vezes muito pouco ecológicas) são as forças motrizes para governos, empresas e cientistas encontrarem alternativas para os materiais preparados a partir de recursos fosséis. Neste cenário, o ácido 2,5-furandicarboxílico (FDCA), em produto químico de origem renovável, surgiu como o substituto mais promissor do ácido tereftálico na síntese de diversos materiais, particularmente poliésteres, que possuem propriedades térmicas e mecânicas semelhantes. Estes materiais podem ser utilizados nas aplicações existentes, e em outras novas aplicações, inovadoras e de alto valor. Neste contexto, o desenvolvimento de polímeros e materiais sustentáveis a partir dos furanos é oportuno e bastante relevante. Precisamente, esta tese tem como principal objetivo o desenvolvimento polímeros e materiais compósitos mais sustentáveis a partir do FDCA e uma panóplia de compostos alifáticos selecionados pela sua origem renovável. Posteriormente, foi ainda avaliado o potencial de um novo monómero éster preparado a partir do FDCA como plastificante para a substituição parcial do não renovável tereftalato de di(2-etilhexilo) em formulações de cloreto de polivínilo (PVC).

No primeiro estudo, foi preparado um poliéster parcialmente renovável a partir do FDCA e do 1,4-ciclohexanodiol, nomeadamente o poli(2,5-furanodicarboxilato de 1,4-ciclohexileno) (PCdF) com o objectivo de se obter um novo material com propriedades térmicas melhoradas. A sua síntese foi efetuada a partir de duas abordagens distintas, nomeadamente via policondensação em solução e politransesterificação em estado sólido. Por motivos comparativos, foi ainda sintetizado o homopolímero poli(2,5-furandicarboxilato de 1,4-ciclohexanodimetileno) (PCF), devido à semelhança estrutural entre ambos. Homopolímeros com pesos moleculares diferentes foram obtidos de acordo com a abordagem de síntese e catalisadores utilizados (valores de M_n e $Đ$ variando entre 4 300-14 100 g/mol e 1.2-1.7, respetivamente). Os materiais resultantes revelaram possuir carácter semi-cristalino com elevadas temperaturas de transição vítrea (valores de T_g de 175 e 105 ºC, para o PCdF e PCF, respetivamente) e estabilidade térmica até aos 377 ºC. Verificou-se ainda que, a ausência do grupo metileno no homopolímero PCdF, deu origem a um material com estrutura de cadeia polimérica mais rígida, e consequentemente um valor de T_g mais elevado.

Num segundo estudo, vários copolímeros do poli(2,5-furanodicarboxilato de 1,4-butileno)-co-poli(2,5-furanodicarboxilato de poli(óxido de propileno)) (PBF-co-PPOF) poli(éster-éter)s foram sintetizados a partir do 2,5-furanodicarboxilato de dimetilo e diferentes rácios molares do 1,4-butanodiol e do poli(óxido de propileno.

resumo (continuação)

Os copolímeros resultantes apresentaram caráter semi-cristalino quando quantidades superiores de PBF foram usadas, líquidos viscosos completamente amorfos quando o rácio PBF/PPOF usado foi igual a 1. Mais ainda, estes materiais apresentaram elevada estabilidade térmica (temperaturas de degradação máxima entre 340-365 ºC, e baixas Tg´s (valores a variar entre os -42.3 a -32.6 ºC), facilitando desta forma o seu processamento a mais baixas temperaturas.

Adicionalmente, num terceiro estudo, abrangendo a preparação de uma série de nanocompósitos à base de FDCA, preparados usando os copolímeros poli(2,5-furanodicarboxilato de 1,4-butileno)-co-poli(diglicolato de 1,4-butileno) (PBF-co-PBGD e celulose bacteriana acetilada (Ac-BC). Numa primeira etapa, os copolímeros foram sintetizados; seguida da preparação de filmes de nanocompósitos, obtidos através da abordagem de evaporação de solvente. Curiosamente, para uma maior incorporação de unidades de BDG, estes materiais reforçados demonstraram um aumento de rigidez (módulo de Young até 1239 MPa) e elasticidade aceitável (valores alongamento até à ruptura entre 0.6 até 25.0 %) quando comparados com os seus (co)polímeros homólogos puros. Além disso, foram observados valores similares para as permeabilidade ao oxigénio dos nanocompósitos e (co)polímeros, expandindo a exploração destes materiais para aplicações como embalagens.

Finalmente, um quarto estudo, abordou a possibilidade de usar um éster furânico como aditivo para formulações de poli(cloreto de vinilo) (PVC) (Capítulo VI). A combinação dos plastificantes 2,5-furanodicarboxilato de di(2-etilhexilo) (DEHF) com o tereftalato de di(2-etilhexilo) (DEHT) foi efetuada de forma a aumentar o 'conteúdo verde' das formulações de PVC. Estes materiais demostraram possuir maior compatibilidade com a matriz do PVC comparativamente com os preparados apenas com o DEHF. Mais ainda, apresentaram características térmicas comparáveis aos preparados apenas com o DEHT (T_g's entre 19.2 e 23.8 ºC) e um aumento do alongamento até à rutura (até 330%). Além disso, os testes de migração revelaram muito baixas percentagens de perda de massa, não excedendo os 0.3% e os 0.2%, respetivamente, para a água e para a solução PBS. Mais importante, resultados preliminares em testes de viabilidade celular *in vitro* (concentrações até 500 µM e máximo de 72 h) revelaram um perfil não-tóxico para ambos os plastificantes, DEHF e DEHT.

Todos os materiais e químicos preparados a partir do FDCA dentro do âmbito desta dissertação são uma importante contribuição para a crescente procura por novos materiais de origem renovável, dentro de uma abordagem sustentável. Mais, estes materiais e químicos apresentaaram propriedades semelhantes ou melhoradas às dos preparados a partir de recursos petrolíferos.

keywords

2,5-furandicarboxilic acid Renewable resources, 5-hydroxymethylfurfural, furanic polyesters, nanocomposites, non-toxic plasticisers.

abstract

Nowadays environmental problems, climate changes, limited fossil resources and their price fluctuation, associated with industrial activity (often ecologically unsound) are the strong driving forces for governments, companies and scientists to find alternatives to the fossil-based materials. In this scenario 2,5-furandicarboxylic acid (FDCA), a renewable platform chemical has emerged as the most promising substitute to terephtalic acid for the synthesis of several materials, particularly polyesters, which possess similar thermal and mechanical proprieties. These materials could be applied to current applications and, could even be applied in new, innovative and high value applications. In this context, the development of sustainable FDCA-based polymers and materials is timely and quite relevant. Precisely, the main objective of this thesis is the development of more sustainable polymers and composites based on FDCA and a wide panoply of aliphatic compounds selected for their renewable origin (PART B) and/or the improved thermal and mechanical properties they can impart the ensuing materials. Furthermore, the potential of a new FDCA-based ester monomer as plasticiser for partial replacement of the non-renewable di(2-ethylhexyl) terephthalate on PVC formulations was also evaluated (PART C).

In the first study, a partially renewable polyester based on FDCA and 1,4-cyclohexanediol, namely poly(1,4-cyclohexylene 2,5-furandicarboxylate) (PCdF) was prepared aiming at preparing a new material with enhanced thermal properties. Its synthesis was performed by two distinct approaches, namely *via* solution polycondensation and bulk polytransesterification. For comparative purposes, poly(1,4-cyclohexanedimethylene 2,5-furandicarboxylate) (PCF) homopolyester was also synthesised, due to their related structural resemblance. Homopolyesters with different molecular weights (M_n and $Đ$ values ranging between 4 300-14 100 g/mol and 1.2-1.7, respectively) were obtained, depending on the synthesis approach and catalyst used. The resulting materials revealed to possess semi-crystalline character with high glass transition temperatures (T_g values of 175 and 105 ºC for PCdF and PCF, respectively), and thermal stablility up to 377 ºC. It was also found that, the absence of the methylene group on PCdF homopolyester, lead to a more rigid polymer chain backbone, and accordingly to a highest T_g.

Other studies, focused on the development of copolyesters enterelly based on renewable-based monomers, namely those based on FDCA, 1,4-butanediol and poly(propylene oxide) or diglycolic acid were performed.

abstract (continuation)

In a second study, several poly(1,4-butylene 2,5-furandicarboxylate)-co-poly(poly(propylene oxide) 2,5-furandicarboxylate) (PBF-co-PPOF) poly(ester-ether)s copolymers were synthesised using dimethyl 2,5-furandicarboxylate and different molar ratios of 1,4-butanediol and poly(propylene oxide). The ensuing copolyesters presented either semi-crystalline character when using higher PBF feed amounts, or completely amorphous viscous liquid was obtained instead when using a PBF/PPOF ratio equal to 1 . Moreover, these materials presented high thermal stability (maximum degradation temperatures between 340-365 ºC), and low T_gs (values ranging from -42.3 to -32.6 ºC), facilitating their processability at lower temperatures.

Further, in a third stud, comprised the preparation of a series of FDCA-based nanocomposites were prepared using poly(1,4-butylene 2,5-furandicarboxylate)-co-poly(1,4-butylene diglycolate) (PBF-co-PBDG) copolyesters and acetylated bacterial cellulose (Ac-BC). In a first step, PBF-co-PBDG (co)polyesters were synthesised; followed, in a second step, by the preparation of nanocomposites films obtained by solvent-casting approach. Interestingly, for higher incorporation of BDG moieties, these reinforced materials showed an increased stiffness (Young's modulus up to 1239 MPa) and reasonable elasticity (elongation at break values between 0.6 to 25.0 %) compared to their neat (co)polyester counterparts. Furthermore, similar values of oxygen permeability of nanocomposites and (co)polyesters were observed, expanding the exploitation of these materials for packaging applications.

Finnaly, a fourth study, addressed the possibility of using a furanic ester as an additive for poly(vinyl chloride) (PVC). A combination of di(2-ethylhexyl) 2,5-furandicarboxylate (DEHF) and di(2-ethylhexyl) terephthalate (DEHT) plasticisers was performed into an attempt to increase the 'green content' of PVC formulations. These materials have shown to possess higher compatibility with the PVC matrix compared with DEHF as single plasticizer, confirmed by FTIR spectroscopy. Furthermore, they displayed thermal features comparable to those prepared with DEHT as single plasticizer (T_g's between 19.2 to 23.8 ºC), and increased elongation at break (up to 330%). Moreover, migration tests revealed very low weight loss percentages, not exceeding *ca.* 0.3 and 0.2%, for water and PBS solution, respectively. More important, preliminary results of *in vitro* cell viability tests (concentrations up to 500 µM for a maximum of 72 h) revealed a non-toxic profile (around 100 %) for both DEHF and DEHT plasticisers.

All FDCA-based materials and chemicals prepared under the scope of this dissertation are an important contribute for the increasing demand for new renewable-based products, within a sustainable approach. Further, these materials and chemicals, presented similar or improved properties to those prepared from petroleum-based resources.

TABLE OF CONTENTS

LIST OF ABBREVIATIONS AND SYMBOLS

AA	Adipic acid
Ac-BC	Acetylated bacterial cellulose
ATR FTIR	Attenuated total reflectance Fourier transform infrared
BD	1,4-Butanediol
2,3-BD	2,3-Butanediol
BDG	Butylene diglycolate moiety
BF	Butylene 2,5-furandicarboxylate moiety
BHAFDC	Bis(hydroxyalkyl)-2,5-furandicarboxylate
BHEFDC	Bis(hydroxyethyl)-2,5-furandicarboxylate
BHEPDC	Bis(hydroxypropyl)-2,5-furandicarboxylate
$\mathbf{CA}_{water}$	Water contact angle
CALB	*Candida Antartica* Lipase B
CBDO	2,2,4,4-Tetramethyl-1,3-cyclobutanediol
CHD	1,4-cyclohexanediol
CHDM	1,4-cyclohexadimethanol
$Đ$	Polydispersity index
DBTO	Dibutyltin (IV) oxide
DEG	Diethylene glycol
DEHF	Di(2-ethylhexyl) 2,5-furandicarboxylate
DEHT	Di(2-ethylhexyl) terephthalate
DGA	Diglycolic acid
DMF	Dimethylformamide
DMFDC	2,2-Dimethyl-1,3-propanediol
DMPD	Dimethyl-2,5-furandicarboxylate
DMTA	Dynamic mechanical thermal analysis
DPn	Degree of polymerisation in number
$\overline{DP_n}$	Number-average degree of polymerisation
DS	Degree of substitution
DSC	Differential scanning calorimetry
E	Young's modulus
E'	Storage modulus
EF	Ethylene 2,5-furandicarboxylate moiety
EG	Ethylene glycol
FDCA	2,5-Furandicarboxylic acid
FDCDCl	2,5-Furandicarbonyl chloride
GC-MS	Gas chromatography-mass spectrometry
GTR	Gas trasmition rate
5-HMF	5-Hydroxymethylfurfural
M_n	Number-average molecular weight
M_w	Weight-average molecular weight

NMR	^{1}H, ^{13}C Nuclear magnetic resonance
PBA	Poly(butylene adipate)
PBDG	Poly(butylene diglycolate)
PBF	Poly(1,4-butylene 2,5-furandicarboxylate)
2,3-PBF	Poly(2,3-butylene 2,5-furandicarboxylate)
PBS	Poly(butylene succinate)
PBF-co-PBA	Poly(1,4-butylene 2,5-furandicarboxylate-co-1,4-butylene adipate)
PBF-co-PBDG	Poly(1,4-butylene 2,5-furandicarboxylate-co-1,4-butylene diglycolate)
PBF-co-PBS	Poly(1,4-butylene 2,5-furandicarboxylate-co-1,4-butylene succinate)
PBT	Poly(1,4-butylene terephthalate)
PBF-co-PEGF	Poly(1,4-butylene 2,5-furandicarboxylate)-co-poly(poly(ethylene glycol) 2,5-furandicarboxylate)
PBF-co-PBGF	Poly(1,4-butylene 2,5-furandicarboxylate)-co-poly(poly(butylene glycol) 2,5-furandicarboxylate)
PBF-co-PPOF	Poly(1,4-butylene 2,5-furandicarboxylate)-co-poly(poly(propylene oxide) 2,5-furandicarboxylate)
PBT-co-PEGT	Poly(1,4-butylene terephtalate)-co-poly(poly(ethylene glycol) terephthalate)
PBT-co-PBGT	Poly(1,4-butylene terephthalate)-co-poly(poly(butylene glycol) terephthalate)
PCdF	Poly(1,4-cyclohexylene 2,5-furandicarboxylate**)**
PCF	Poly(1,4-cyclohexanedimethylene 2,5-furandicarboxylate**)**
PCF-co-PIsF	Poly(1,4-cyclohexanedimethylene 2,5-furandicarboxylate**)**-co-poly(isosorbide 2,5-furandicarboxylate)
PCT	Poly(1,4-cyclohexanedimethylene terephthalate**)**
PD	1,3-Propanediol
PDeF	Poly(1,10-decylene 2,5-furandicarboxylate)
PDEGF	Poly(diethylene glycol 2,5-furandicarboxylate)
PDMPF	Poly(2,2-dimethylpropylene 2,5-furandicarboxylate)
PDoF	Poly(1,12-dodecylene 2,5-furandicarboxylate)
PEEs	Poly(ester-eter)s copolymers
PEF	Poly(ethylene 2,5-furandicarboxylate)
PEF-co-PCBDOF	Poly(ethylene 2,5-furandicarboxylate**)**-co-poly(2,2,4,4-tetramethyl-1,3-cyclobutylene 2,5-furandicarboxylate)
PEF-co-PCF	Poly(ethylene 2,5-furandicarboxylate**)**-co-poly(1,4-cyclohexanedimethylene 2,5-furandicarboxylate)
PEF-co-PES	Poly(ethylene 2,5-furandicarboxylate-co-ethylene succinate)
PEF-co-PIsF	Poly(ethylene 2,5-furandicarboxylate**)**-co-poly(isosorbide 2,5-furandicarboxylate)
PEF-co-PLA	Poly(ethylene 2,5-furandicarboxylate)-co-poly(lactic acid)
PEF-co-PPF	Poly(ethylene 2,5-furandicarboxylate-co-1,3-propylene 2,5-furandicarboxylate)

PEG	Poly(ethylene glycol
PEGF	Poly(poly(propylene glycol) 2,5-furandicarboxylate)
PES	Poly(ethylene succinate)
PET	Poly(ethylene terephthalate)
PET-co-PES	Poly(ethylene terephthalate-co-ethylene succinate)
PGA	Poly(glycolic acid)
PHF	Poly(1,6-hexylene 2,5-furandicarboxylate)
PHeF	Poly(1,7-heptylene 2,5-furandicarboxylate)
PIDF	Poly(isodide-2,5-dimethylene 2,5-furandicarboxylate)
PIsF	Poly(isosorbide 2,5-furandicarboxylate)
PLA	Poly(lactic acid)
PLGA	Poly(lactide-co-glycolide)
PMePF	Poly(2-methyl-1,3-propylene 2,5-furandicarboxylate)
PNF	Poly(1,9-nonylene 2,5-furandicarboxylate)
POE	Polyorthoesters
POF	Poly(1,8-octylene 2,5-furandicarboxylate)
PPF	Poly(1,3-propylene 2,5-furandicarboxylate)
PPeF	Poly(1,5-pentylene 2,5-furandicarboxylate)
PPO	Poly(propylene oxide)
PVC	Poly(vinyl chloride)
SA	Succinic acid
SEC	Size-exclusion chromatography
SEM	Scanning electron microscopy
SSP	Solid-state ppolimerisation
SSP	Solid-state ppolimerisation
TBT	Tetrabutyl titanate
T_d or $T_{d,max}$	Maximum degradation temperature
$T_{d,\mathrm{on}}$	Onset degradation temperature
$T_{d,5\%}$	Degradation temperature at 5% weight loss
T_c	Crystallisation temperature
T_{cc}	Cold-crystallisation temperature
T_g	Glass transition temperature
T_m	Melting temperature
TGA	Thermogravimetric analysis
TPA	Terephthalic acid
XRD	X-ray diffraction
$\mathcal{E}_b$	Elongation at break
σ_m	Tensile strength

TABLE OF FIGURES

TABLE OF TABLES

PART A

Chapter I – General Introduction

"Fortunately, an increasing number of polymer chemists – both academic and industrial are considering the sustainability of their creations. The two overarching goals are to employ renewable resources – instead of fossil fuels – and to engineer degradation pathways that can operate under reasonable time frames – decades instead of millennia."

Stephen A. Miller

(*Polymer Chemistry* 5, 3117-3118, 2014)

1. The context

In the last decades, the depletion of fossil resources and their price instability, as well as the environmental problems and climate changes associated with their massive consumption, have driven the scientific community to find renewable and sustainable alternatives to replace petro-based feedstocks for energy/fuels, chemicals and materials production. In this context the attention on biomass feedstocks has increased exponentially, since it is a carbon-neutral and renewable resource that can be converted into energy/fuels, chemicals and materials, through a bio-refinery process (Figure 1.1).[1,2]

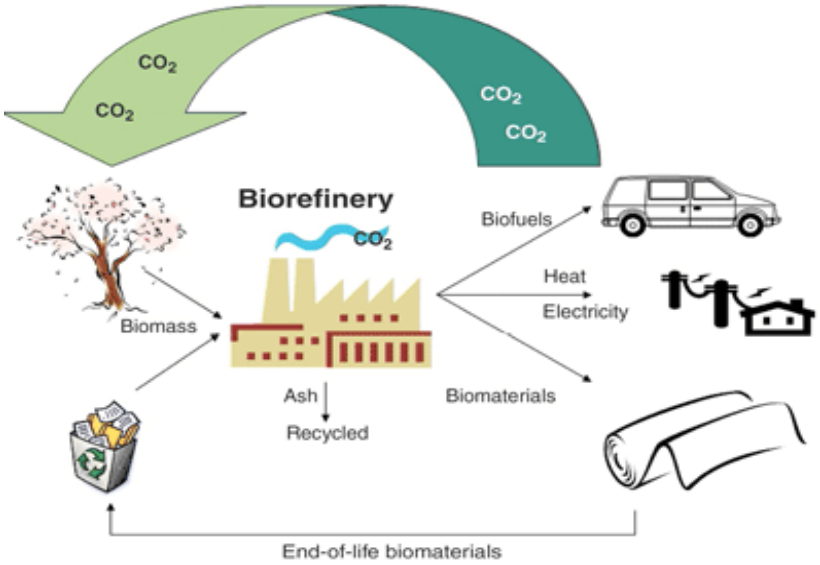

Figure 1.1. Biorefinery concept (adapted from reference [2]).

Biomass components specially polysaccharides and the ensuing monosaccharides, due to their abundance, will play a central role in the production of high quantities of chemical building-blocks, produced by hydrolysis, oxidation, reduction, dehydration, isomerisation, and hydrogenation, among other reactions, through biorefineries.[3–6] One of the most important sugar derived building block is 5-hydroxymethylfurfural (5-HMF), obtained from hexoses. 5-HMF is considered a key precursor of a wide variety of chemicals and biofuels,[7,8] among which 2,5-furandicarboxylic acid (FDCA) is by far the most important.[6]

FDCA is an heteroaromatic diacid (also detected in the human body),[9] with high chemical stability, that can be used under the typical polymerisation reaction conditions, particularly in polyesters synthesis.[10,11] Further, due to the structure similarity between FDCA and 1,4-

terephthalic acid (TPA) (Figure 1.2),[12,13] FDCA is considered as a potential renewable substitute of the former for the the preparation of several polymeric materials (which includes thermoplastics), plasticisers and thermosets, among others.[14]

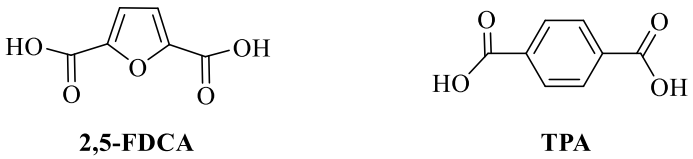

Figure 1.2. Chemical structures of FDCA and TPA.

Among FDCA-based polyesters, poly(ethylene 2,5-furandicarboxylate) (PEF) and poly(1,4-butylene 2,5-furandicarboxylate (PBF) are the most studied due to their structural resemblance with poly(ethylene 1,4-terephtalate) (PET) and poly(butylene 1,4-terephthalate) (PBT), their petroleum-based counterparts.[15,16] Moreover, FDCA has been also used in the synthesis of several other polyesters,[17,18] mainly incorporating aliphatic diols possessing short to long linear chains from 3 to 20 carbon atoms, as well as branched and cyclic ones.[18,19] The resulting FDCA-based homopolyesters have displayed wide range of thermal and mechanical properties, which could be very useful for the production of a variety of polyesters derived materials. Moreover, most of these polyesters are still entirely prepared from renewable resources. For example, furanic-based homopolyesters prepared with medium to long chain linear diols, tend to be flexible materials (more than PEF and/or PBF), and at same time they show adequate thermal stability, finding potential applications as films and fibers.[20–23] Oppositely, when branched diols are incorporated into the homopolyester chains, stiffer materials are obtained, mostly due to their constricted molecular structure, typically presenting higher glass transition temperatures (T_g) and increased thermal stability compared to linear homopolyesters with the same carbon number chain.[24–27] In the same line, the incorporation of more rigid cyclic monomers, such as 1,4:3,6-dianhydrohexitols or 1,4-cyclohexanedimethanol in the backbone of FDCA-based polyesters has been used as an approach to obtain materials with enhanced thermal properties.[26,28–31]

Nevertheless, thinking on their life-time ending, several studies reported their hydrolytic and enzymatic degradation, revealing that these materials could be degraded in specific medium conditions,[24,32] however their biodegradability is still far from the desired specifications.[33] In this context, in order to obtain materials with enhanced thermal and

mechanical properties, as well as biodegradable, the copolymerisation between FDCA (or derivatives) and aliphatic comonomers has been studied.

Copolymerisation enables the possibility to obtain unlimited variety of materials with tuned properties, simply by changing the aliphatic and/or aromatic nature and relative amounts of the comonomers in the copolymer backbone. Moreover, to overcome the limited biodegradability of FDCA-based homopolyesters, copolymerisation with aliphatic diacids or hydroxyacids, namely succinic acid (SA), adipic acid (AS) and poly(lactic acid) (PLA), has proved to be a promising strategy to obtain materials with tuned biodegradability, and at same time with enhanced thermal and mechanical properties. Indeed, recently, copolyesters prepared from PEF and variable amount of PLA oligomers, showed relevant (bio)degradability, namely through hydrolytic degradation and soil degradation tests.[34,35] These studies have introduced a completely new renewable, biodegradable and non-toxic aromatic-aliphatic generation of copolymers.

Nevertheless, besides the interest around FDCA-based polyesters, other materials have also been explored aiming to achieve enhanced and/or refined properties, namely better processability and crystallinity, such as composites or hybrid materials. Nanocomposites prepared with PEF and small quantities of nanocrystalline cellulose (around 4 wt %) have demonstrated an enhanced crystallization process in the presence of fibers.[36] Furthermore, PEF-derived hybrid materials were also prepared by compounding PEF with SiO_2 and TiO_2 (added during the synthesis of the polymer), revealing an increase on the PEF molecular weight.[37]

Finally, the use of FDCA in the preparation of other products has also been attempted, such as for example, in the synthesis of plasticizers, namely di(2-ethylhexyl) 2,5-furandicarboxylate (DEHF).[38,39]

In this scenario, the main aim of the present work was to develop FDCA-based materials with enhanced properties including thermal, mechanical, gas barrier and degradability properties, as well as, products that could act as plasticisers, and in the future replace, fossil-based materials.

2. Objectives and Outline of the thesis

Several problems associated to the use of petroleum-based materials have been reported in the last decadesrelated with sustainability. It has become clear that to achieve a more sustainable environment it is imperative to find new renewable alternatives to polymer materials. In this context, this thesis emerged to fulfil that necessity, reporting the synthesis and characterisation of several FDCA-based materials with interesting properties, very similar to those obtained from non-renewable resources.

This appraisal is divided into four parts and seven chapters focusing firstly on a general background to furanic-based polyesters and subsequently on the description of the polyesters, nanocomposites and chemicals developed using FDCA.

In **PART A** is provided a general introduction to the context of this thesis (**Chapter I**). The synthesis, ensuing properties and main applications of FDCA-based polyesters are briefly reviewed in **Chapter II**.

PART B is divided in three chapters, and it is focused on the synthesis of FDCA-based polyesters and nanocomposites.

In **Chapter III** is described the synthesis and characterisation of poly(1,4-cyclohexylene 2,5-furandicarboxylate) (PCdF). In addition, a comparative study between PCdF and poly(1,4-cyclohexanedimethylene 2,5-furandicarboxylate) (PCF) is also described.

Chapter IV is devoted to the study of the almost unexplored furanic poly(ester-ether)s (PEEs) copolymers. In this Chapter is is described the synthesis and characterisation of a series of copolymers based on PBF and poly(propylene oxide) (PPO).

Chapter V deals with the preparation of several nanocomposites, prepared using poly(butylene 2,5-furandicarboxylate)-co-(butylene diglycolate) (PBF-co-PBDG) copolyesters and acetylated bacterial cellulose (Ac-BC).

PART C is dedicated to the study of di(2-ethylhexyl) 2,5-furandicarboxylate (DEHF) as a plasticiser for poly(vinyl chloride) (PVC). **Chapter VI** handles with the synthesis of DEHF and the preparation of PVC blends incorporating both DEHF and di(2-ethylhexyl) terephthalate (DEHT) in order to assess the progressive replacement of the non-renewable DEHT in PVC formulations.

Finally, in **PART D** the main conclusions of the work carried out under the auspices of this thesis are presented, together with some perspectives for future work.

References

(1) Cherubini, F. The Biorefinery Concept: Using Biomass Instead of Oil for Producing Energy and Chemicals. *Energy Convers. Manag.* **2010**, *51* (7), 1412–1421.

(2) Ragauskas, A. J.; Williams, C. K.; Davison, B. H.; Britovsek, G.; Cairney, J.; Eckert, C. A.; Frederick Jr., W. J.; Hallett, J. P.; Leak, D. J.; Liotta, C. L.; et al. The Path Forward for Biofuels and Biomaterials. *Science* **2006**, *311* (5760), 484–489.

(3) Ma, J.; Yu, W.; Wang, M.; Jia, X.; Lu, F.; Xu, J. Advances in Selective Catalytic Transformation of Ployols to Value-Added Chemicals. *Chinese J. Catal.* **2013**, *34* (3), 492–507.

(4) McNeff, C. V.; Nowlan, D. T.; McNeff, L. C.; Yan, B.; Fedie, R. L. Continuous Production of 5-Hydroxymethylfurfural from Simple and Complex Carbohydrates. *Appl. Catal. A Gen.* **2010**, *384* (1–2), 65–69.

(5) Rosatella, A. A.; Simeonov, S. P.; Frade, R. F. M.; Afonso, C. A. M. 5-Hydroxymethylfurfural (HMF) as a Building Block Platform: Biological Properties, Synthesis and Synthetic Applications. *Green Chem.* **2011**, *13* (4), 754.

(6) Tong, X.; Ma, Y.; Li, Y. Biomass into Chemicals: Conversion of Sugars to Furan Derivatives by Catalytic Processes. *Appl. Catal. A Gen.* **2010**, *385* (1–2), 1–13.

(7) Kuster, B. 5-Hydroxymethylfurfural (HMF). A Review Focussing on Its Manufacture. *Starch-Stärke* **1990**, *42* (8), 314–321.

(8) Teong, S. P.; Yi, G.; Zhang, Y. Hydroxymethylfurfural Production from Bioresources: Past, Present and Future. *Green Chem.* **2014**, *16* (4), 2015–2026.

(9) Witten, T. A.; Levine, S. P.; Killian, M. T.; Boyle, P. J. R.; Markey, S. P. Gas-Chromatographic-Mass-Spectrometric Determination of Urinary Acid Profiles of Normal Young Adults . II . The Effect of Ethanol. *Clin. Chem.* **1973**, *19* (9), 963–966.

(10) Zia, K. M.; Noreen, A.; Zuber, M.; Tabasum, S.; Mujahid, M. Recent Developments and Future Prospects on Bio-Based Polyesters Derived from Renewable Resources: A Review. *Int. J. Biol. Macromol.* **2016**, *82*, 1028–1040.

(11) Dam, E. D. J. M. A.; Gruter, L. S. G. M. Furandicarboxylic Acid (FDCA), A Versatile Building Block for a Very. *Prog. Polym. Sci.* **2012**, 1–13.

(12) Werpy, T.; Petersen, G.; Aden, A.; Bozell, J. *Top Value Added Chemicals from Biomass Volume I—Results of Screening for Potential Candidates from Sugars and*

Synthesis Gas; Oak Ridge, 2004.

(13) Bozell, J. J.; Petersen, G. R. Technology Development for the Production of Biobased Products from Biorefinery Carbohydrates—the US Department of Energy's "Top 10" Revisited. *Green Chem.* **2010**, *12* (4), 539.

(14) Choi, S.; Song, C. W.; Shin, J. H.; Lee, S. Y. Biorefineries for the Production of Top Building Block Chemicals and Their Derivatives. *Metab. Eng.* **2015**, *18*, 223–239.

(15) Gandini, A.; Silvestre, A. J. D.; Neto, C. P.; Sousa, A. F.; Gomes, M. M. The Furan Counterpart of Poly (Ethylene Terephthalate): An Alternative Material Based on Renewable Resources. *J. Polym. Sci. Polym. Chem.* **2009**, *5* (c), 295–298.

(16) Eerhart, J. J. E.; Faaij, P. C.; Patel, M. K. Replacing Fossil Based PET with Biobased PEF; Process Analysis, Energy and GHG Balance. *Energy Environ. Sci.* **2012**, *5* (4), 6407–6422.

(17) Tsanaktsis, V.; Terzopoulou, Z.; Exarhopoulos, S.; Bikiaris, D. N.; Achilias, D. S.; Papageorgiou, D. G.; Papageorgiou, G. Z. Sustainable, Eco-Friendly Polyesters Synthesized from Renewable Resources: Preparation and Thermal Characteristics of Poly(Dimethyl-Propylene Furanoate). *Polym. Chem.* **2015**, *6* (48), 8284–8296.

(18) Zhang, D.; Dumont, M. J. Advances in Polymer Precursors and Bio-Based Polymers Synthesized from 5-Hydroxymethylfurfural. *J. Polym. Sci. Polym. Chem.* **2017**, *55* (9), 1478–1492.

(19) Papageorgiou, G. Z.; Papageorgiou, D. G.; Terzopoulou, Z.; Bikiaris, D. N. Production of Bio-Based 2,5-Furan Dicarboxylate Polyesters: Recent Progress and Critical Aspects in Their Synthesis and Thermal Properties. *Eur. Polym. J.* **2016**, *83*, 202–229.

(20) Knoop, R. J. I.; Vogelzang, W.; van Haveren, J.; van Es, D. S. High Molecular Weight Poly(Ethylene-2,5-Furanoate); Critical Aspects in Synthesis and Mechanical Property Determination. *J. Polym. Sci. Polym. Chem.* **2013**, *51* (19), 4191–4199.

(21) Jiang, M.; Liu, Q.; Zhang, Q.; Ye, C.; Zhou, G. A Series of Furan-Aromatic Polyesters Synthesized via Direct Esterification Method Based on Renewable Resources. *J. Polym. Sci. Polym. Chem.* **2012**, *50* (5), 1026–1036.

(22) Tsanaktsis, V.; Terzopoulou, Z.; Nerantzaki, M.; Papageorgiou, G. Z.; Bikiaris, D. N. New Poly(Pentylene Furanoate) and Poly(Heptylene Furanoate) Sustainable Polyesters from Diols with Odd Methylene Groups. *Mater. Lett.* **2016**, *178* (May),

64–67.

(23) Soares, M. J.; Dannecker, P. K.; Vilela, C.; Bastos, J.; Meier, M. A. R.; Sousa, A. F. Poly(1,20-Eicosanediyl 2,5-Furandicarboxylate), a Biodegradable Polyester from Renewable Resources. *Eur. Polym. J.* **2017**, *90*, 301–311.

(24) Haernvall, K.; Zitzenbacher, S.; Amer, H.; Zumstein, M. T.; Sander, M.; McNeill, K.; Yamamoto, M.; Schick, M. B.; Ribitsch, D.; Guebitz, G. M. Polyol Structure Influences Enzymatic Hydrolysis of Bio-Based 2,5-Furandicarboxylic Acid (FDCA) Polyesters. *Biotechnol. J.* **2017**, *12* (9), 1600741.

(25) Gubbels, E.; Jasinska-Walc, L.; Koning, C. E. Synthesis and Characterization of Novel Renewable Polyesters Based on 2,5-Furandicarboxylic Acid and 2,3-Butanediol. *J. Polym. Sci. Polym. Chem.* **2013**, *51* (4), 890–898.

(26) Terzopoulou, Z.; Kasmi, N.; Tsanaktsis, V.; Doulakas, N.; Bikiaris, D. N.; Achilias, D. S.; Papageorgiou, G. Z. Synthesis and Characterization of Bio-Based Polyesters: Poly(2-Methyl-1,3-Propylene-2,5-Furanoate), Poly(Isosorbide-2,5-Furanoate), Poly(1,4-Cyclohexanedimethylene-2,5-Furanoate). *Materials* **2017**, *10* (7).

(27) Genovese, L.; Lotti, N.; Siracusa, V.; Munari, A. Poly(Neopentyl Glycol Furanoate): A Member of the Furan-Based Polyester Family with Smart Barrier Performances for Sustainable Food Packaging Applications. *Materials* **2017**, *10* (9).

(28) Moore and J. E. and Kelly, J. A. Polyesters Derived from Furan and Tetrahydrofuran Nuclei. *Macromolecules* **1978**, *11* (3), 568–573.

(29) Gomes, M.; Gandini, A.; Silvestre, A. J. D. D.; Reis, B. Synthesis and Characterization of Poly(2,5-Furan Dicarboxylate)s Based on a Variety of Diols. *J. Polym. Sci. Polym. Chem.* **2011**, *49* (17), 3759–3768.

(30) Wu, J.; Eduard, P.; Thiyagarajan, S.; Noordover, B. a J.; van Es, D. S.; Koning, C. E. Semi-Aromatic Polyesters Based on a Carbohydrate-Derived Rigid Diol for Engineering Plastics. *ChemSusChem* **2015**, *8* (1), 67–72.

(31) Storbeck, R.; Ballauff, M. Synthesis and Properties of Polyesters Based on 2,5-Furandicarboxylic Acid and 1,4:3,6-Dianhydrohexitols. *Polymer* **1993**, *34* (23), 5003–5006.

(32) Weinberger, S.; Haernvall, K.; Scaini, D.; Ghazaryan, G.; Zumstein, M. T.; Sander, M.; Pellis, A.; Guebitz, G. M. Enzymatic Surface Hydrolysis of Poly(Ethylene Furanoate) Thin Films of Various Crystallinities. *Green Chem.* **2017**, *19* (22), 5381–

5384.

(33) Bioplastics, E. Standardisation http://en.european-bioplastics.org/standards/standardization/ (accessed May 26, 2015).

(34) Matos, M.; Sousa, A. F.; Fonseca, A. C.; Freire, C. S. R.; Coelho, J. F. J.; Silvestre, A. J. D. A New Generation of Furanic Copolyesters with Enhanced Degradability: Poly(Ethylene 2,5-Furandicarboxylate)-Co-Poly(Lactic Acid) Copolyesters. *Macromol. Chem. Phys.* **2014**, *215* (22), 2175–2184.

(35) Wu, H.; Wen, B.; Zhou, H.; Zhou, J.; Yu, Z.; Cui, L.; Huang, T.; Cao, F. Synthesis and Degradability of Copolyesters of 2, 5-Furandicarboxylic Acid, Lactic Acid, and Ethylene Glycol. *Polym. Degrad. Stabil.* **2015**, *121*, 100–104.

(36) Codou, A.; Guigo, N.; van Berkel, J. G.; de Jong, E.; Sbirrazzuoli, N. Preparation and Crystallization Behavior of Poly(Ethylene 2,5-Furandicarboxylate)/Cellulose Composites by Twin Screw Extrusion. *Carbohyd. Polym.* **2017**, *174* (July), 1026–1033.

(37) Achilias, D. S.; Chondroyiannis, A.; Nerantzaki, M.; Adam, K. V.; Terzopoulou, Z.; Papageorgiou, G. Z.; Bikiaris, D. N. Solid State Polymerization of Poly(Ethylene Furanoate) and Its Nanocomposites with SiO2 and TiO2. *Macromol. Mater. Eng.* **2017**, *302* (7), 1–15.

(38) Yu, Z.; Zhou, J.; Zhang, J.; Huang, K.; Cao, F.; Wei, P. Evaluating Effects of Biobased 2,5-Furandicarboxylate Esters as Plasticizers on the Thermal and Mechanical Properties of Poly (Vinyl Chloride). *J. Appl. Polym. Sci.* **2014**, *131* (20), 1–10.

(39) Sanderson, R. D.; Schneider, D. F.; Schreuder, I. Synthesis and Evaluation of Dialkyl Furan-2,5-Dicarboxylates as Plasticizers for PVC. *J. Appl. Polym. Sci.* **1994**, *53* (13), 1785–1793.

Chapter II – The State of the Art

Part of this chapter has been published in:

Sousa, A. F.; Vilela, C.; Fonseca, A. C.; Matos, M.; Freire, C. S. R.; Gruter, G. J. M.; Coelho, J. F. J.; Silvestre, A. J. D. Biobased Polyesters and Other Polymers from 2,5-Furandicarboxylic Acid: A Tribute to Furan Excellency. Polym. Chem. 2015, 6 (33), 5961–5983

1. FDCA-based monomers and polymers: synthesis, properties and main applications

1.1. FDCA-based polyesters prepared through polyesterification reactions

FDCA is a dicarboxylic acid derived from biomass. Typically obtained from sugars *via* dehydration of 5-HMF, followed by oxidation. FDCA or its derivatives, such as 2,5-furandicarbonyl chloride (FDCDCl), dimethyl 2,5-furandicarboxylate (DMFDC), or bis(hydroxalkyl) 2,5-furandicarboxylates (BHAFDC) (Figure 2.1) are used in polyesterification reactions in order to obtain FDCA-based polyesters.[1–3]

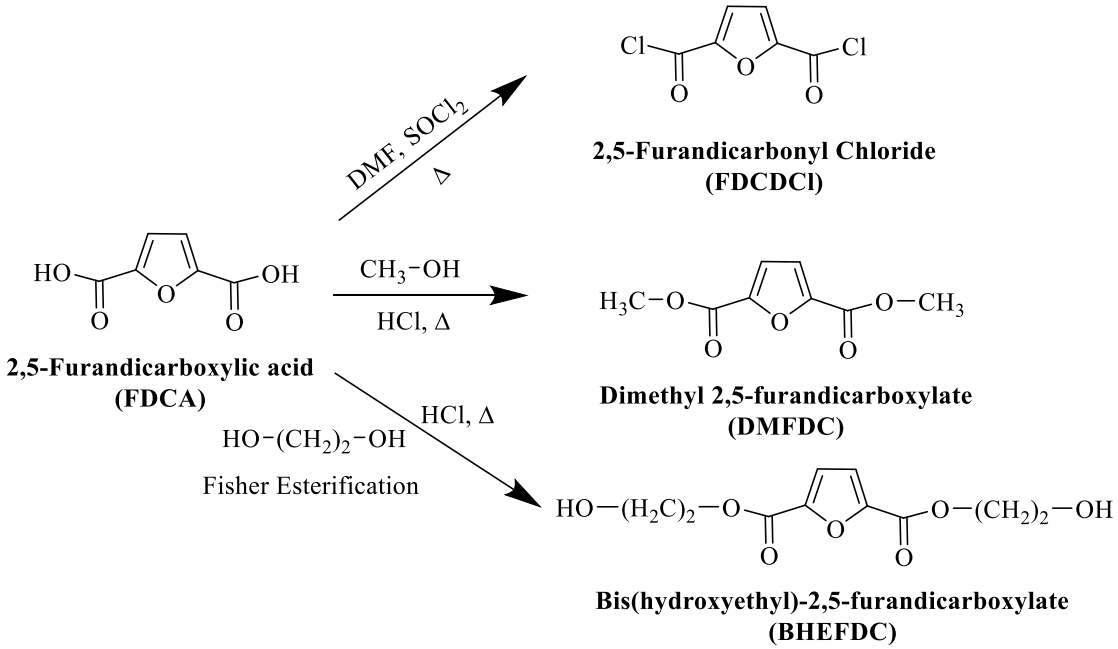

Figure 2.1. Synthesis of the starting FDCA-based comonomers.

Polyesters, such as those based on FDCA, are typically prepared by step-growth polymerisation. In step-growth polymerisation, the polymer grows by a series of steps (Figure 2.2), and high molecular weight polymers result from a large number of steps. In the case of polyesters, this kind of polymerisation is usually referred to as polycondensation and/or polytransesterification, depending if water or either low-molecular weight products (such as or alcohols) are being released during the formation of the polymer chains, respectively.[4]

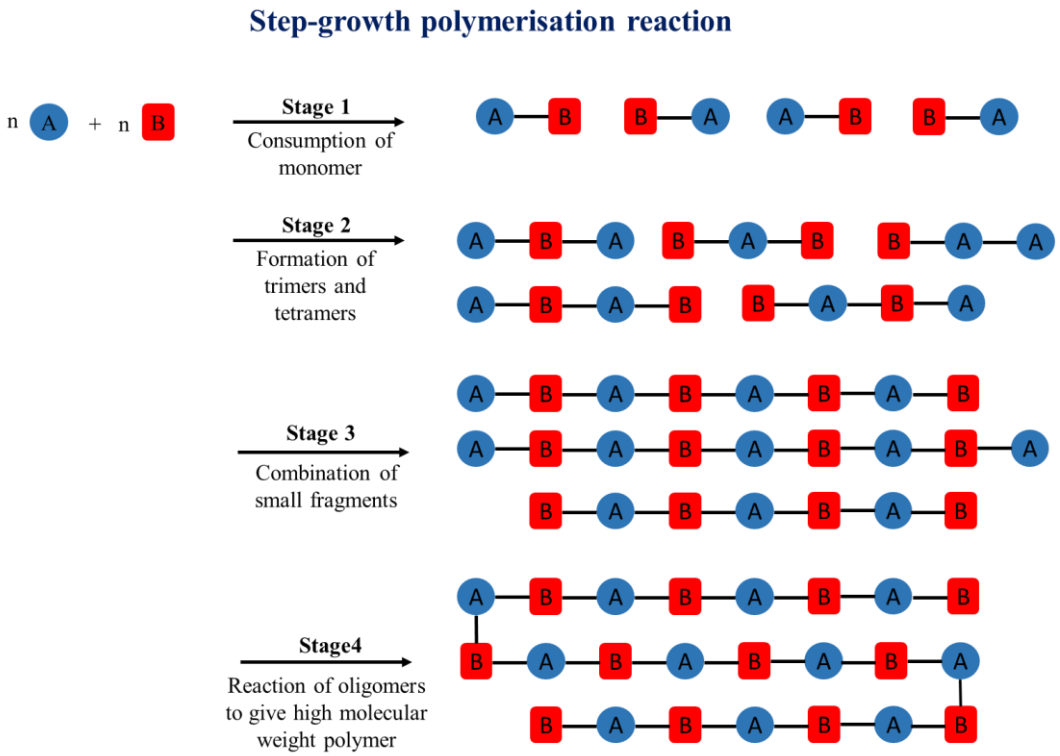

Figure 2.2. Generic representation of a step-growth polymerisation reaction (adapted from reference [4]).

In this polymerisation reaction, initially a monomer reacts with another monomer to form a dimer, then the dimer may react with another dimer to produce a tetramer, or with another monomer to form a trimer, and so on, until a high molecular weight polymer is obtained (Figure 2.2).[4]

This process is governed by random intermolecular reactions between species with different molecular sizes, where the average molecular weight increases slowly until near the end of the polymerisation where it increases rapidly.[5] Carothers in 1929 was the pioneer in the study of polyester synthesis by polytransesterification.[6,7] In his work an array of combinations of aliphatic diacids and aliphatic diols were employed in the preparation of several aromatic and aliphatic polyesters.

Importantly, Carothers studies provided the fundamentals for the polymerisation kinetics, establishing a relation between the number-average degree of polymerisation ($\overline{DP_n}$) and the extent of reaction (Carothers' equation) for linear polyesterifications (and also polyaddition):

$$\overline{DP_n} = \frac{1}{1-p} \quad (1)$$

where p, is the fraction of the functional groups that have reacted at time t.

A consequence of Carothers' equation is that to achieve high *DPs* in step-growth polymerisation a high conversion of the initial reagents (*p*) is required, and for that goal to be achieved an absolutely accuracy between stoichiometry together with the constant removal of by-products is fundamental. These reactions require, in general, long reaction times, high temperatures and often high vacuum.[8]

The polytransesterification reaction could be performed through several approaches such as, in bulk, solution and interfacial, depending on the final application of the resulting polymers, as well as the nature of the corresponding monomers.[9] One of the most used method to prepare FDCA-based polyesters is definitely bulk polyesterification, and mainly performed in two steps. The first step could involve: i) transesterification of a dimethyl ester with a diol to form an intermediate diester; or ii) the direct esterification of a diacid with a diol. In the second step, a bulk polytransesterification is performed to achieve the corresponding homopolymer (Figure 2.3).[10]

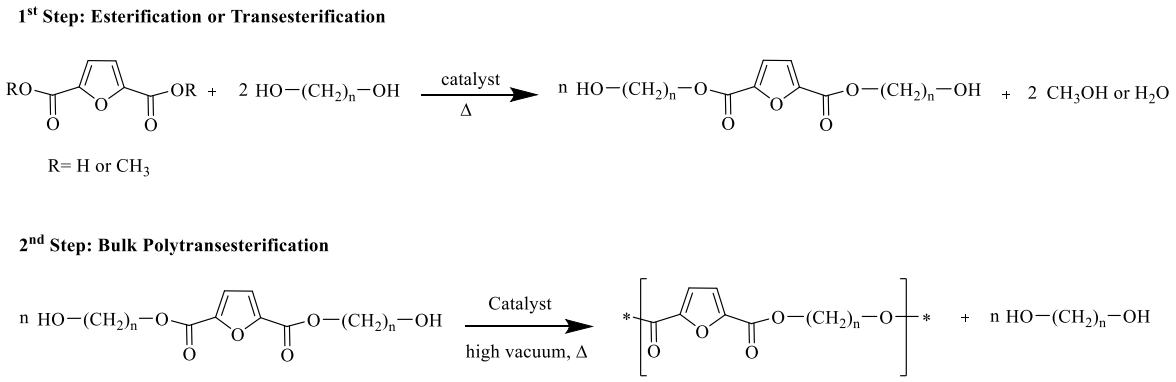

Figure 2.3. Polyesters syntheses through the two-step polycondensation reaction approach.

As mentioned before, polyesters can also be prepared through direct solution polycondensation reaction (Figure 2.4).[1,11] The exploitation of that approach, typically allows the use of moderate reaction conditions, in terms of, for example, temperature and pressure. Hence, enabling, the use of a variety of volatile or thermally unstable diols.

Typically, these reactions are performed with diacid dichlorides between 0 to 50 ºC, using the Schotten-Baumann reaction (Figure 2.4).[8]

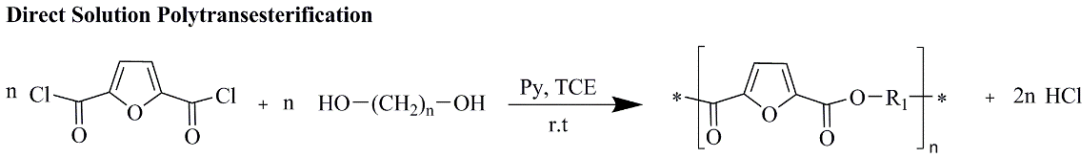

Figure 2.4. Direct solution polytransesterification reaction of a diacid dichloride with a diol.

Finally, in some studies a third polymerisation step called solid-state polymerisation (SSP) can be introduced after polytransesterification,[10] to raise the molecular weights of the FDCA-based homopolyester (which cannot be achieved in the typical bulk polytransesterification process).[12–17] This post-polymerisation step is highly used industrially to increase polyesters molecular weight, enabling their use in specific applications, namely in the manufacture of bottles, packaging, and fibbers.[17] Nevertheless, the SSP process is very complex and still not fully understood, mainly due to the influence of the diffusion process and crystallisation on the reaction kinetics. The SSP occurs when a semi-crystalline polymer is heated above the glass transition temperature (T_g) of the amorphous phase, but below the melting temperature (T_m) of the crystalline phase, enabling the chain mobility necessary to allow further polycondensation reactions to take place (Figure 2.5).[18]

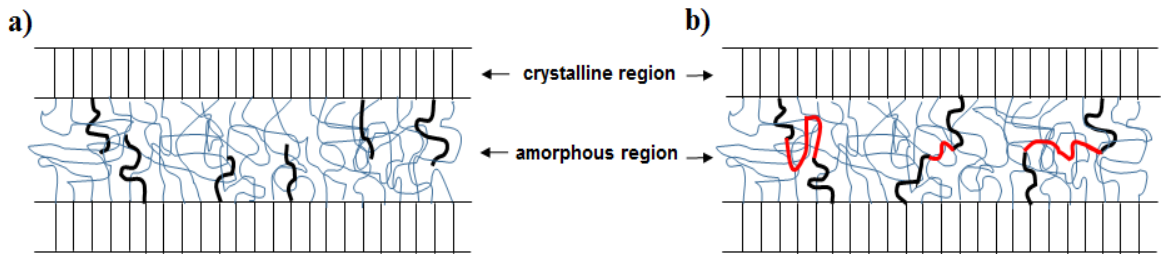

Figure 2.5. Schematic representation of limited mobility of the end groups in the amorphous region a) before and b) after SSP (adapted from reference [18]).

The reaction equilibrium shifts in favour of the polycondensation due to by-products removal from the reaction system by an inert gas flow, or under vacuum. Due to the use of

lower temperatures than those usually applied in bulk polytransesterification, side reactions and thermal degradation are limited in SSP. [13,14]

The understanding and careful control of all the variables concerning polytransesterification reaction is absolutely critical, and they have to be taken into consideration to successfully prepare FDCA based polyesters, as will be discussed in more detailed in the next sections.

1.2. FDCA-based polyesters

As already mentioned in Chapter I, in the last decades, the need to promote a new paradigm of sustainable development based on renewable resources, led to a tremendous increase in the interest on polymers from renewable resources, and particularly in FDCA-based polyesters.[1–3] In fact, the synthesis of polyesters bearing furan moieties started in 1946, with the synthesis of poly(ethylene 2,5-furandicarboxylate) (PEF) by the British Celanese.[19] However, only 32 years later by the hand of Moore and Kelly,[20,21] their study was again reported.

Among the myriad of FDCA-based polyesters, those possessing aliphatic diols have been the most investigated.[22–27] Actually, short linear aliphatic chains, as well as, branched and/or cyclic aliphatic diols, and some aliphatic diacids and hydroxyacids (Figure 2.6) have been used in the synthesis of FDCA-based polyesters. For example, PEF, poly(1,3-propylene 2,5-furandicarboxylate) (PPF) and PBF, among others, were the most studied FDCA-based polyesters.[3,28] These polyesters have a wide range of interesting thermal and mechanical properties, and in the latter case, also potential (bio)degradability. These furanic-aliphatic polyesters will be described in more detail in the following sections. Furthermore, furanic-aliphatic polyesters have been proposed for the most variable applications, such as, beverage packaging, films, fibbers, powder coatings, among others, revealing that they could be the renewable alternative to PET and other TPA-based polyesters.[28]

Other FDCA-based polyesters, are entirely aromatic in nature, are being prepared using FDCA and other aromatic compounds (Figure 2.7), in order to obtain more rigid materials, with enhanced thermal properties, as well as, aiming to prepare liquid crystalline polyesters.[11,20,22,29–35]

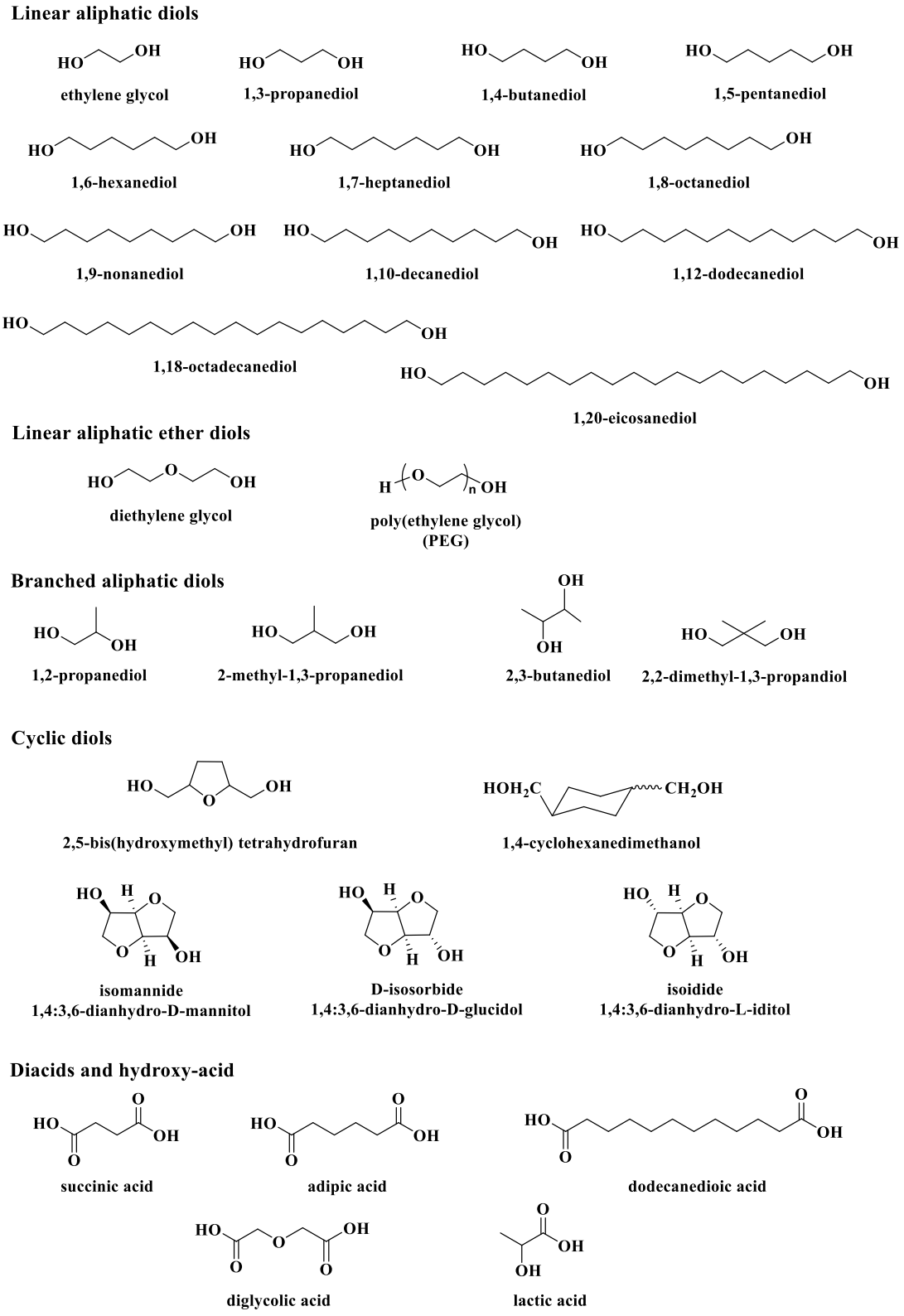

Figure 2.6. Examples of (mainly renewable) aliphatic comonomers already used to produce FDCA-based polyesters.[36]

The studies involving these furanic-aromatic polyesters have been described both in scientific papers,[11,20,22,32,33,35] and patents,[29–31,34] and were essentially focused in lignin-based monomers, such as, vanillic, syringic, salicylic, isophthalic and 4-hydroxybenzoic acids, among others, and also on sugar-based monomers like for example the 2,5-bis(hydroxymethyl)furan (Figure 2.7).

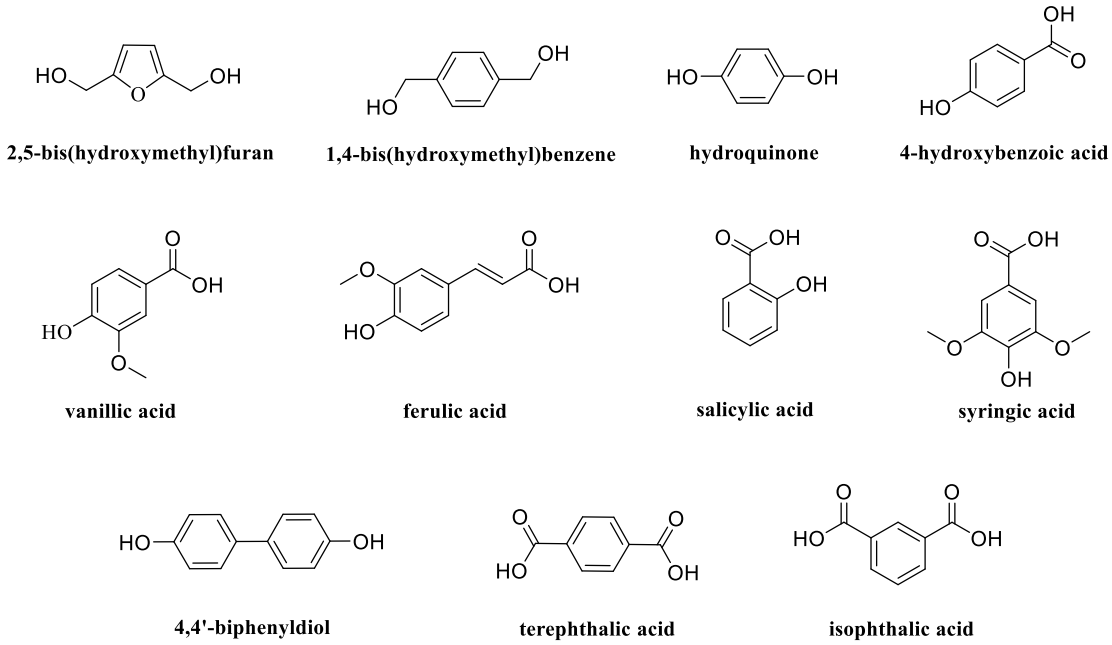

Figure 2.7. Example of aromatic monomers used in the synthesis of furanic-aromatic polyesters.[36]

Despite the number of furanic-aromatic polyesters described in the literature, this group of polyesters will not be further described because it is out of scope of the present thesis.

1.2.1. Furanic-aliphatic homopolyesters

The furanic-aliphatic homopolyesters are the most investigated FDCA-based polyesters derived from FDCA, mostly due to the resemblance in terms of thermal and mechanical properties with those obtained from TPA, as will be demonstrated in the following sub-sections. In this vein, the following paragraphs will be devoted to the discussion of their synthesis, thermal and mechanical features, and presented in an increasing order of number of methylene groups, starting for the linear, followed by branched, and finally for the cyclic ones.

1.2.1.1. Synthesis

The most highlighted FDCA-based polyester is PEF (Figure 2.8), the furan counterpart of PET, due to their similar thermal and mechanical properties.[1] In fact, as mentioned before, PEF is the potential substitute of PET, and for that reason, an extensible literature is found devoted to its synthesis and characterisation (Table 2.1).[12,36,37,41,53–55,57–69,70–73]

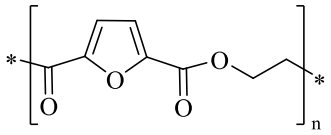

Poly(ethylene 2,5-furandicarboxylate) (PEF)

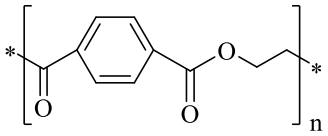

Poly(ethylene terephtalate) (PET)

Figure 2.8. Chemical structure of PEF and PET.

Table 2.1. Reaction conditions to prepare PEF and related properties.

Precursor	*Reaction conditions*			$M_n \times 10^4$ [a] (g mol^{-1})	Đ[b]	Ref.[c]
	T (°C)	*t (h)*	*catalyst*			
BHEFDC	70 – 250	-	Sb_2O_3	2.24	1.92	1,11,22
FDCDCl	r.t.	-	pyridine	0.20	1.25	11,22
FDCA	160 – 220	7.5	-	-	-	19,51
	200 – 255	15	Sb_2O_3	0.48	-	38
	180 – 240	5	$Ti(OBu)_4$	1.55	1.21	45
	150 – 245	5 – 9.2	$Ti(OPr)_4$	1.25 – 10.53	2.39 – 2.60	15,23
	180 – 240	5	$Sn(Oct)_2$	3.20	1.24	45
	180 – 240	5	SnOBu	4.74	1.42	
	180 – 240	5	GeO_2	3.42	1.32	
	180 – 240	5	$Sb(Ac)_3$	2.41	1.78	
DMFDC	160 – 220	7.5	-	-	-	19,51
	150 – 230	5 – 16	$Ti(OPr)_4$	1.45 – 1.91	1.80 – 2.44	15,26
	150 – 230	5	BTTO; TNPP	5.68	3.00	15
	160 – 250	-	$Ti(OBu)_4$	1.12	-	40,43,44
	170 – 240		SnOxa			44
	170 – 280	4	Sb_2O_3	-	-	38,44,46
	170 – 240		$Sb_2(EG)_3$			44
	- [d]	- [d]	- [d]	4.70	2.34	39,41
	180 – 240	4	SnOBu	4.61	1.31	45
With SSP approach						
	195	24	- [d]	8.30	1.95	14
	195	-	$Ti(OPr)_4$ / Sb_2O_3	3.10	2.58	13
			$Ti(OBu)_4$	1.27	-	
	225	5	$Ti(OPr)_4$	1.31	-	16,17
			DBTO	1.00	-	

[a] Number-average molecular weight determined by SEC; [b] Polydispersity index; [c] References; [d] PEF provided from Coca-Cola company.

PEF and in general other FDCA-based homopolyesters have been routinely prepared by the two-step polytransesterification of FDCA, DMFDC and other FDCA derivatives (bis(hydroxyalkyl) 2,5-furandicarboxylate), with different aliphatic diols, such as ethylene glycol (EG), 1,3-propanediol (PD), 1,4-butanediol (BD), 2,3-butanediol (2,3-BD), 2,2-dimethyl-1,3-propanediol (DMPD), diethylene glycol (DEG), among others (Figure 2.9). Other interesting approaches studied were ring-opening polymerisation (ROP)[47,52] or biocatalysis processes using *Candida Antarctica* Lipase B (CALB) enzyme.[53] The most relevant properties of furanic-aliphatic homopolyesters are summarised in Table 2.2.

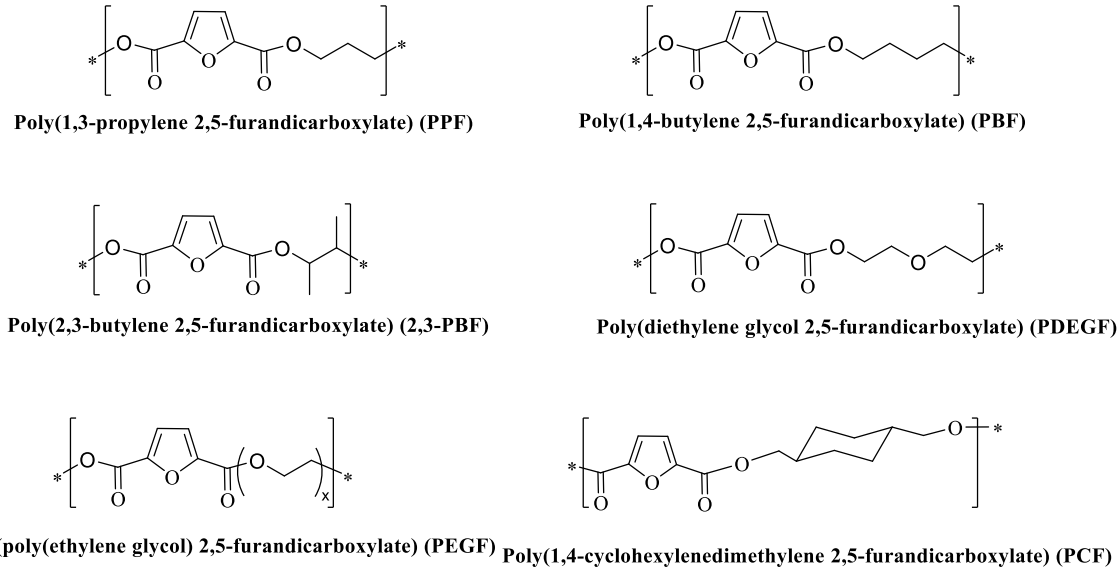

Figure 2.9. Illustration of some furanic-aliphatic homopolyesters.

FDCA-based homopolyesters synthesis has been performed in a relative large array of conditions, with a range of temperatures between 90 to 230 ºC (up to 280 ºC in case of PEF), for several hours (4 to 24 h), and in the presence of different catalysts, such as, dibutyltin(IV) oxide (DBTO), titanium(IV) isopropoxide ($Ti(OPr)_4$), antimony(III) oxide (Sb_2O_3), tetrabutyl titanate ($Ti(OBu)_4$), among others.[3,27] In fact, several works were devoted to the study how catalysts influence the molecular weight and coloration of the final polyesters.[12,13,15,19,42,45,54]

The effect of several other catalysts on the molecular weight of PEF prepared *via* direct polytransesterification of FDCA (Table 2.1), revealed that $Ti(OPr)_4$ was the most effective catalyst to achieve high number-average molecular weights (M_n) , while Sb_2O_3 was the less effective.

Table 2.2. Relevant thermal and mechanical properties of linear FDCA-based polyesters.

Polyester	Diol	Synthetic procedure	$M_n \times 10^4$ [a] (g mol^{-1})	Đ[b]	T_g[c] (ºC)	T_m[d] (ºC)	$T_{d,5\%}$[e] (ºC)	E (MPa)	σ_m (MPa)	ε_b (%)	Ref.[e]
Linear diols											
PEF	EG	A; B; C; D	0.48 – 10.53	1.8 – 2.6	71 – 91	205 – 226	300 – 376	1 900 – 2 450	35 – 85	3 – 4	12,36,37,41,53–55,57–69,70–73
PPF	1,3-propanediol (PD)	A	0.12 – 6.02	1.3 – 2.4	40 – 65	169 – 180	300 – 333	1 150	68	46	11,14,23,26,37,55–59
PBF	1,4-butanediol (BD)	A; D	0.12 – 23.21	1.4 – 3.3	25 – 39	163 – 177	304 – 370	1 100 – 1 900	20 – 56	3 – 284	14,23,62–64,26,37,38,47,52,55,60,61
PPeF	1,5-pentanediol (PeD	A	-[g]	-[g]	5 – 19	83 – 94	-	-	-	-	43,65
PHF	1,6-hexanediol (HD)	A; B; D	1.31 – 3.21	1.5 – 2.1	5 – 28	141 – 157	375	496	36	210	20,23,25,53,58
PHeF	1,7-heptanediol (HeD)	A	-[g]	-[g]	5	83	-	-	-	-	65
POF	1,8-octanediol (OD)	A; D	0.33 – 4.10	1.5 – 2.3	-5 – 22	118 – 149	340 – 384	311 – 407	20 – 28	14 – 160	23,24,37,43,53,66,67
PNF	1,9-nonanediol (ND)	A	2.10 – 4.00	1.7 – 2.1	-30 – -4	69 – 92	387	145 – 252	19 – 20	149 – 658	2,65–67
PDeF	1,10-decanediol (DeD)	A; D	2.0 –5.16	1.6 – 2.1	-8 – 1	108 – 116	363 –386	200 – 275	11 – 17	52 – 160	27,37,43,53,66,67
PDoF	1,12-dodecanediol (DoD)	A	2.54 – 3.94	1.8 – 2.3	-22 – -5	104 – 111	390	181 – 267	10 – 16	82 – 130	43,58,66–68
POdF	1,18-octadecanediol (OdD)	A	2.21	2.1	-	98	-	-	-	-	58
PE20F	1,20-eicosanediol (E20D)	A	3.12	1.4	7[h]	107[h]	358	-	-	-	69
PEGF	Poly(ethylene glycol) (PEG)	A; D	0.18 – 1.33	1.3 – 1.8	-35 – -7	49	248 – 318	-	-	-	70
PDEGF	diethylene glycol (PDEG)	B; D	0.10 – 3.29	1.1 – 2.7	13 – 40	56	314 – 375	-	-	-	53,71
Branched diols											
1,2-PPF	1,2-propanediol (1,2-PD)	A	1.41	2.5	89	-	-	-	-	-	71
2,3-PBF	2,3-butanediol (2,3-BD)	A; B; D	0.20 – 13.00	1.5 – 2.6	71 – 113	-	276 – 301	-	-	-	26,53,72
PMePF	2-methyl-1,3-propanediol (MePD)	A	-[g]	-[g]	55	-	> 300	-	-	-	73
PDMPF	2,2-dimethyl-1,3-propanediol (DMPD)	A	0.12 – 6.02	1.3 – 4.0	68 – 71	197 – 198	356	1 648	45	4	59,74,75
Cyclic diols											
PBHMTF	2,5-bishydroxymethyltetrahydrofuran	B	-	-	-	-	-	-	-	-	20,21
PIF	isoidide	B	0.5 7 – 2.15	1.3	140 – 196	-	275	-	-	-	11,22,76
PIDF	isodide-2,5-dimethanol	A	3.03	2.0	94	250	375	-	-	-	77
PImF	isomannide	B	1.49 – 2.04	-	187 – 191	-	-	-	-	-	76
PIsF	isosorbide	A; B; D	0.90 – 2.50	1.7	137 – 194	-	350	-	-	-	11,22,53,73,76,78
PCF	1,4-cyclohexylenedimethanol (CHDM)	A; B	-	-	74 – 86	262	> 300	-	-	-	73,79–82

[a] Number-average molecular weight determined by SEC; [b] Polydispersity index [c] Glass transition temperature determined from the DSC 2nd heating scan. [d] Melting temperature determined from DSC 1st heating scan. [e] Degradation temperature at 5% weight loss. [f] References; [g] Not determine by SEC; [h] Determined from DMTA.
Synthetic procedure: A- Two-step bulk polytransesterification; B- Direct solution polytransesterification; C- Ring-opening polymerisation (ROP); D- Biocatalytic process.

Another important aspect regarding furanic-aliphatic homopolyesters synthesis was the colour of the resulting materials due to its importance in some applications. In this context, several studies were focused on the effect of different catalysts, feed monomer, temperature, among others, on the colour of the achieved materials.[12,13,15,19,42] In fact, when FDCA is the starting monomer coloured polymers were obtained, since higher temperatures were needed.[15]

Furthermore, titanate-based catalysts were found to be the most effective on the increasing of molecular weights compared with tin-based catalysts, however exhibiting more intense coloration.[42]

In addition, polytransesterification reactions combining long time and high temperatures also revealed an increase on the colour intensity, mostly due to the decomposition of by-products.[54] For these reasons, high molecular weight furanic-aliphatic homopolyesters synthesis has been performed using DMFDC as starting monomer, as well as, in the presence of titanium-based catalysts at less drastic temperatures (90-220 ºC) (Table 2.2).

Other FDCA diester monomer derivatives were also used to synthesise PEF and poly(1,3-propylene 2,5-furandicarboxylate) (PPF), namely bis(hydroxyethyl) 2,5-furandicarboxylate (BHEFDC) and bis(hydroxypropyl) 2,5-furandicarboxylate (BHPFDC), respectively, leading to polymers with M_n of 22 400 and 21 600 g/mol, respectively.[1,11,22] However, when compared with DMFDC, bis(hydroxyalkyl) 2,5-furandicarboxylates have the disadvantage of needing hard purification procedures involving, long periods of time (several days) and high vacuum to the complete elimination of the excess diol that remain from the esterification reaction.

In some cases, the direct solution polytransesterification reaction was adopted, in order to avoid the problems of decomposition and discoloration that typically occur due to bulk polytransesterification reactions conditions adopted needed. However, the molecular weight of the ensuing polymers are typically modest. For example, PEF was prepared through this procedure by Gandini *et al.*,[1,11] and a PEF with a degree of polymerisation (DPn) of about 70 was reported,[11] instead a DPn of 250 obtained from the two-stage bulk polytransesterification approach.[1] Also a series of poly(poly(ethylene glycol) 2,5-furandicarboxylate) (PEGF) homopolyesters were prepared by Sousa *et al.*[70] *via* direct solution polytransterification reaction of FDCDCl with PEG, comprising different molecular

weights, namely 200, 400 or 2000 g/mol. The resulting homopolyesters presented M_n and Đ values from 1 800 to 13 300 g/mol and 1.3 to 1.8, respectively.

Direct solution polytransesterification is also very useful when diols with high boiling point are used, *e.g.* cyclic ones.[11,20–22,76,79] Several homopolyesters were prepared from FDCDCl and cyclic aliphatic diols, such as, 2,5-bis(hydroxymethyl) tetrahydrofuran,[20,21] 1,4:3,6-dianhydrohexitols (isomannide, isosorbide and isoidide)). Moore and Kelly in 1978[20,21] reported the first study of direct polytransesterification of FDCDCl with 2,5-bishydroxymethyltetrahydrofuran, however no characterisation was provided (Figure 2.10).

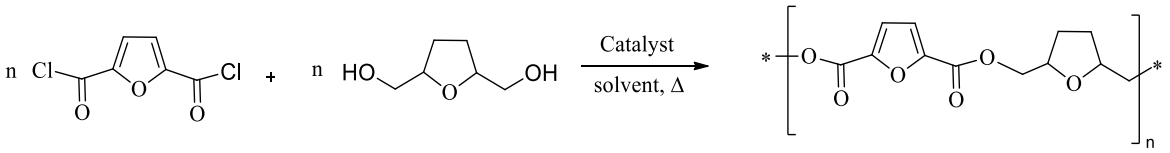

Figure 2.10. Direct solution polytransesterification of PBHMTF.[20,21]

SSP has sometimes been introduced after bulk polytransesterification to increase the molecular weights of polyesters. In the particular case of PEF,[12–14,16,17] for example, Knoop *et al.*[14] reported the increase in the initial PEF M_n from 8 000 g/mol to 25,000 g/mol, and then to 83,000 g/mol, after 24 and 72 h, respectively, at 180 ºC. SSP revealed to be an important tool to obtained materials with high molecular weights that could be used for the manufacturing process of packaging and bottles applications.[17]

1.2.1.2. Thermal and crystallinity behaviour

The study of the interesting thermal properties of FDCA-based homopolyesters was also deeply investigated. [12,14,24,25,27,40,41,56,60,62–64,67,68,74,83–95] The majority of these studies where devoted to the determination of the main thermal properties of these polyesters, namely glass transition (T_g) and melting transition (T_m) temperatures. However, other authors were more focused on their thermal stability and decomposition kinetics, crystallisation kinetics and dynamics, as well as, on their chain conformations.[1,11,12,14,26,38,40–43,45,54,55,83–96]

PEF has been described as a highly crystalline polymer (maximum degree of crystallisation around 60%), thermally stable up to 300 ºC, and with T_g and T_m temperatures between 71-91 ºC and 205-226 ºC, respectively (Table 2.2). Like PEF, PPF and PBF are also semi-crystalline polymers, with T_g values ranging from 40-65 and 31-39 ºC, and T_m values

of 169-180 and 163-177 ºC, respectively (Table 2.2). Typically, FDCA-based homopolyesters prepared from linear diols presented semi-crystalline character, with T_g´s and T_m´s values decreasing with the increasing number of even methylene groups of the corresponding diol chain (Table 2.2). In the case of homopolyesters prepared with odd number of methylene groups, namely poly(1,5-pentylene 2,5-furandicarboxylate) (PPeF), poly(1,7-heptylene 2,5-furandicarboxylate) (PHeF) and poly(1,9-nonylene 2,5-furandicarboxylate) (PNF), their T_m´s also decreased with the methylene group number increasing, and they are lower than those observed for other furanic-even-number-aliphatic homopolyesters (Table 2.2).

Moreover, a series of PEGFs' were prepared with PEG, comprising different molecular weights, namely 200, 400 or 2000 g/mol.[70] The resulting homopolyesters displayed in their DSC traces T_g values of -6.5, -29.0, and -35.1 ºC for PEGF200, PEGF400 and PEGF2000, respectively. The only T_m peak was observed for PEGF2000 with the value of 49.1 ºC, associated with the longer flexible PEG segment.

On the contrary, furanic-aliphatic homopolyesters prepared with branched and cyclic diols, usually results in more amorphous materials, displaying only T_g´s on their DSC traces (Table 2.2). In the case of the polyesters reported in Table 2.2 prepared from branched diols, T_g values were higher than the corresponding homopolyesters synthesised with linear diols with the same number of carbon atoms. Moreover, the highest T_g values reported are attributed to homopolyesters prepared with cyclic diols, due to their structural rigidity and more constricted mobility chain. Although, only few homopolyesters do not follow this tendency, displaying a semi-crystalline nature (Table 2.2), which is the case of poly(2,2-dimethyl-1,3-propylene 2,5-furandicarboxylate) (PDMPF), PIDF and PCF. The presence of branched and/or side groups in the chains of the latest polymers, namely methyl and methylene ones (in the case of the branched and cyclic diols, respectively), promoted a more stable chain configuration, thus facilitating the molecular mobility, and consequently increase the crystallinity of the related homopolyesters.

Nevertheless, some studies reported the existence of three distinct peaks in DSC heating traces, for samples crystallized at different temperatures for some semi-crystalline furanic-aliphatic homopolyesters.[12,14,24,25,27,40,41,56,60,62–64,67,68,74,83–95] For example, in Figure 2.11 is represented this multiple melting behaviour for PBF samples crystallized at different temperatures and heating rates.

A very small peak (peak I) can be observed just after the cold-crystallization temperature (T_{cc}) and it is usually attributed to the melting of the secondary crystals. The middle temperature peak (peak II) corresponds to the melting of the original crystals formed during the isothermal crystallization stage, and finally, the third melting peak (peak III) is related to the re-melting process (reorganisation mechanism). These results suggest that, rather than re-crystallisation, two populations of lamellae with different stabilities were responsible for these multiple melting behaviour.[40]

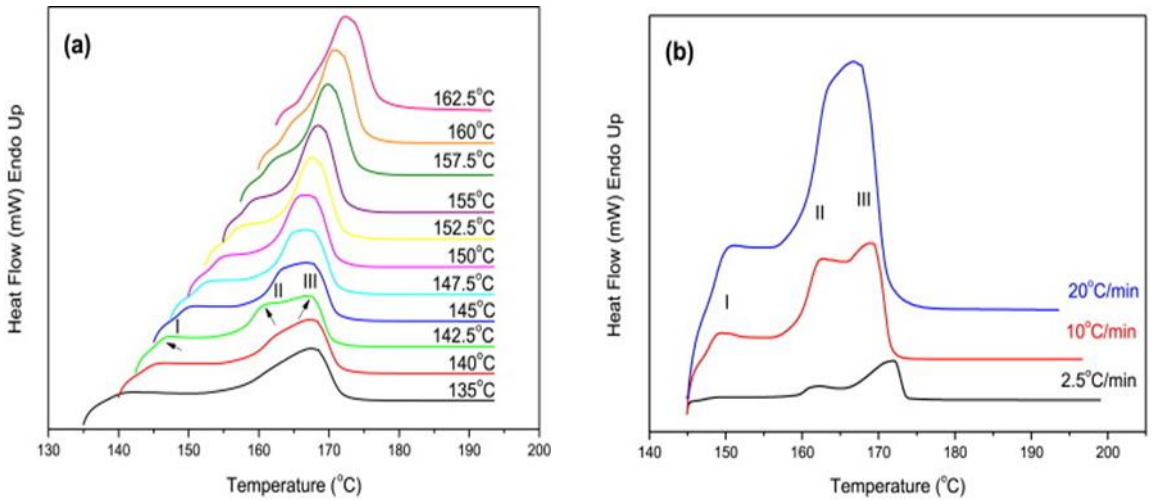

Figure 2.11. DSC heating scans of PBF a) at 20 C/min for samples crystallized from the melt at different temperatures and b) at different heating rates for PBF samples crystallized at 145 ºC for 15 min (adapted from reference [62]).

Apart from the extended literature on the crystallisation dynamics of furanic-aliphatic homopolyesters, several other studies have been focused on their thermal stability and decomposition kinetics.[2,43,54,55,73,74] From Table 2.2 it is possible to observe that, in general all homopolyesters are high thermally stable materials with degradation temperature at 5% weight loss ($T_{d.5\%}$) ranging from 248 (PEGF) to 390 ºC (poly(1,12-dodecylene 2,5-furandicarboxylate)-PDoF), depending on their structure and molecular weights. It was noted that $T_{d.5\%}$ values increase with the increasing of the carbon atoms of the diol used.

Moreover, Bikiaris and Papageorgious group[2,43,54,55,73,74] presented a detailed investigation on the thermal stability and decomposition kinetics of several furanic-aliphatic polyesters, namely PEF, PPF, PBF, PPeF, PHF, POF, PNF, PDef, PDoF, PMePF, PDMPF, PIsF and PCF using TGA and pyrolysis-gas chromatography/mass spectrometry (Py-

GC/MS). In general, for linear furanic polyesters the *β*-hydrogen bond scission was the primary decomposition mechanism (Figure 2.12), with vinyl- and carboxyl-terminated compounds formed as main degradation products.[2,43] Furanic-cyclic aliphatic polyesters also followed the *β*-scission mechanism.[73]

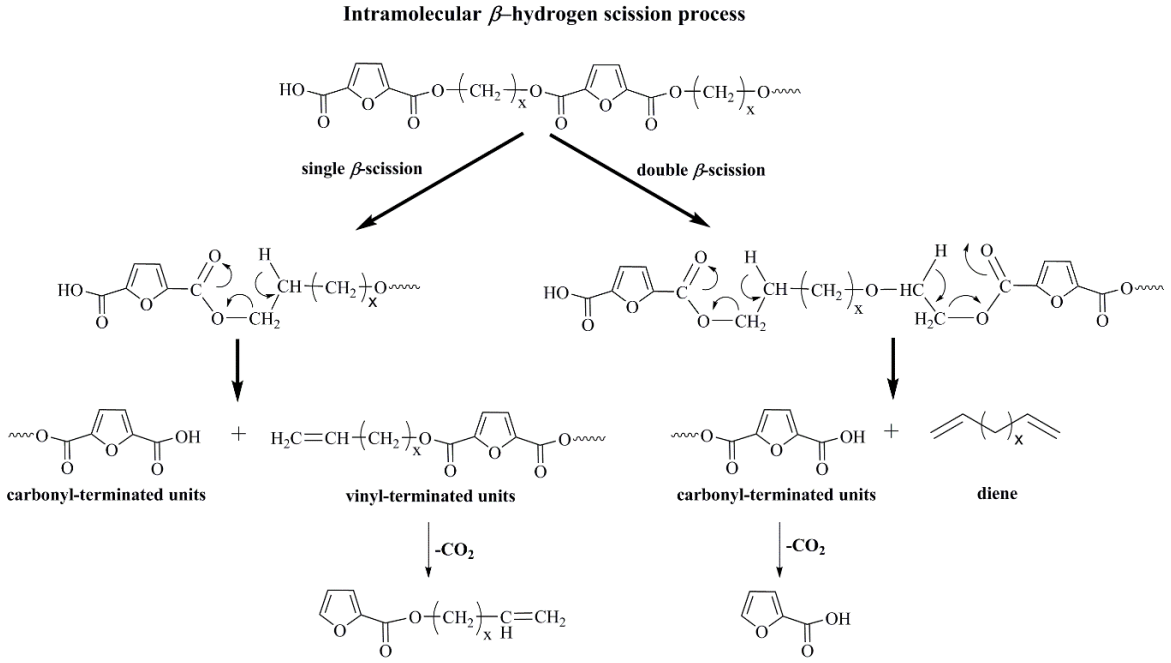

Figure 2.12. Intermolecular *β*-hydrogen bond scission (adapted from reference [43]).

A more distinct decomposition mechanism was observed for PMePF polyester.[74] Due to the fact that this polyester do not possess *β*-hydrogens, and that no vinyl-terminated compounds were detected, the *β*-hydrogen scission was excluded as decomposition mechanism. In this particular case, the authors proposed a new decomposition mechanism, where only radical scission processes take place.

These results were quite important, since they could help to choose the most suitable methods or fillers to enhance the thermal stability of the ensuing polyesters.

1.2.1.3. Mechanical properties

Tensile tests have been extensively used to mechanically characterise furanic-aliphatic homopolyesters.[14,23,27,41,59,61,66,67,75] In general, for these polymers the Young's modulus (*E*) decreased with the increasing number of methylene groups, oppositely to the elongation at

break (ε_b) that increased instead (Table 2.2). This has been associated to the increase chain mobility with the increasing number of methylene groups, resulting in high flexible materials. Moreover, all furanic-aliphatic polyesters represented in Table 2.2 are mechanically stable materials with PEF exhibiting the highest Young's Modulus at 2 450 MPa and PNF the lowest, at 252 MPa, and elongations at break ranging from 4 to 658%. PEF and PPF exhibit the highest tensile strength, 85 and 68 MPa, respectively, followed from PBF (56 MPa) while PDeF and PDoF have the lowest 17 and 16 MPa, respectively.

1.2.1.4. Barrier properties

The oxygen, carbon dioxide, and water permeabilities of PEF, PPF and PDMPF was extensively study by several authores,[39,41,57,59,75,97–101] showing that these homopolyesters exhibit higher barrier properties than PET. In fact, PEF pocesses ~11 times lower oxygen permeability than its petroleum-based counterpart (0.114 and 0.0107 barrer for PET and PEF, respectively).[41] Moreover, in the case of carbon dioxide, this difference was even higher, both in terms of permeability as diffusivity.[97] A reduction of 19 and 31 times was observed in PEF permeability and diffusivity values, respectively, when compared to PET. The reduced permeability in PEF is a result of the reduced diffusion, associated to chain motion reduction.[41] This is mainly associated to furan ring-flipping hindrance. Burgess *et al.*[41] pointed out that the non-linear axis of furan ring rotation and ring polarity is thought to hinder this mechanism.

The kinetic and equilibrium sorption on water was also evaluated for PEF and PET polyesters.[98,99] PEF showed a higher equilibrium water uptake (~1.8x) as compared to PET due to its higher affinity with water.[98] Additionally, PEF exhibited a significant reduction in the water diffusion coefficient compared to PET (~2.8x), due to the PEF chain restriction mobility.[99]

With respect to gas barrier properties of PPF, they have shown to be inferior to those of PEF.[57] In fact, PPF showed a gas permeability to O_2 and CO_2 of 2.44×10^{-3} and 2.88×10^{-3} $cm^3m^{-2}day^{-1}bar^{-1}$, and PEF of 7.02×10^{-3} and 1.71×10^{-1} $cm^3m^{-2}day^{-1}bar^{-1}$, respectively. These authors,[57] suggested that the presence of an additional methylene group in the PPF subunit with respect to PEF, could favoured the *syn* conformation of FDCA and consequently increase the C–H···O interactions, improving the barrier properties of PPF. Furthermore,

from the gas permeability tests, PDMPF also presented 2.17 and 7.67 times lower CO_2 and O_2 gas barrier, respectively, than those observed for PET.[57]

1.2.1.5. Main applications of FDCA-based homopolyesters

Due to their interesting thermal and mechanical properties, FDCA-based homopolyesters could easily find applications in the most variable fields. For example, PEF as the renewable substitute of PET, and a high-performance engineering thermoplastic as well, had shown enhanced gas barrier and attractive thermal and mechanical properties, enabling a series of industrial applications, such as beverage packaging, films and fibers.[48,102–107] In fact, in 2011 Avantium[107] in collaboration with Alpla, the Coca-Cola Company and Danone, announced the production of the first bio-based bottle entirely from PEF for soft drinks, water, alcoholic beverages, through the so-called YXY technology. Thus expanding PEF to the industrial scale (Figure 2.13).

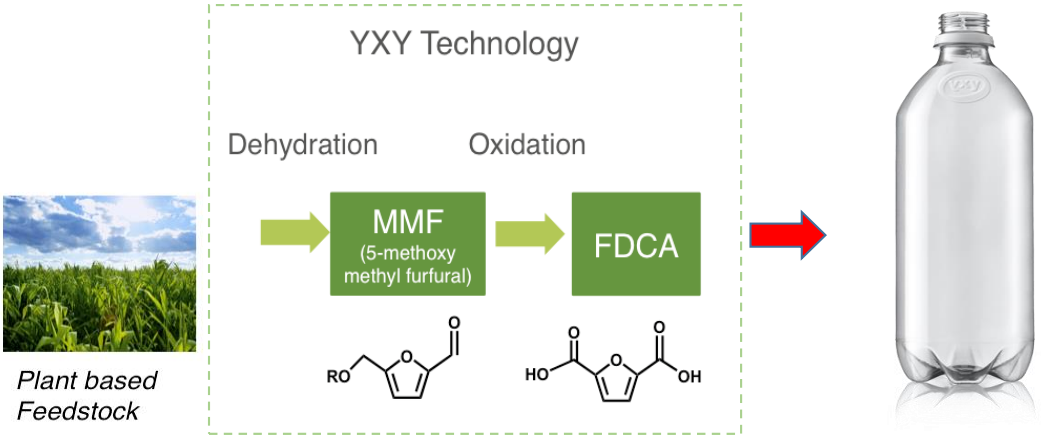

Figure 2.13. Synthesis of FDCA trough the YXY technology and the first PEF bottle (adapted from reference [107]).

Moreover, recently it was found that PEF it is a material highly suitable for rapid 3D printing with low resolution, and slow 3D printing with high resolution. Furthermore, the quality of the 3D printed objects was superior in terms of fusion of the layers and smoothness of the surface as compared to the standard PLA material.[108]

PPF and PBF owning very similar thermal and mechanical properties to PPT and PBT, can find applications such as in packaging materials, and in injected products and fibers.[57,61,62,109] Moreover, according to Tsanaktis *et al.*,[65] PPeF, PHeF and PNF can also be

used for films, fibers and containers for beverages and water. Furthermore, PHF due to its mechanical properties and slow crystallization rates, can be used for produce cast polymeric parts.[23] Also, PDeF, PDoF and PEGF could be interesting for applications where less rigid materials are needed.[66,68,70]

In general terms, packaging seems to be a transversal application proposal for several homopolyesters by different authors.[26,75,78,80–82]

1.2.1.6. Recyclability and degradability

In terms of FDCA-based homopolyesters recycling, processes like chemical recycling (depolymerisation of polyesters through hydrolysis, methanolysis or glycolysis), as well as, mechanical recycling (re-introduction in extrusion process) are also an alternative to the waste management and consequent contribution to the development of circular economy. A patent from Furanix Technologies B.V.,[12] described the PEF base catalysed depolymerisation mechanism thought hydrolysis and methanolysis (using sodium methoxide or 1,5,7-triazabicyclo[4.4.0]dec-5-ene), with DMFDC and FDCA as final products. Results showed a methanolysis rate for PEF much higher than for PET, i.e., after only 90 min, 52% of the initial PEF sample weight were recovery from methanol compared to only 2% of PET.

Another interesting finding was that, when recycle streams of PET and PEF were mixed (with total PEF addition of 5% (w/w) into the re-extrusion process), no significant effect on the mechanical and physical properties of PET was observed.[12]

Even in the context of recycling, it was demonstrated that PEF is an efficient material for 3D printing, possessing optimal adhesion, thermoplasticity, lack of delamination and low heat shrinkage.[108] Moreover, due to the high thermal stability and relatively low temperature of extrusion, PEF is an optimal candidate for recycling printed objects. Finally, authors also referred the capacity of PEF be recycled several times without noticeable loss of 3D printing characteristics.

Moreover, information on the enzymatic hydrolysis of polyesters is of particular interest because enzymes are suitable biocatalysts for environmentally friendly degradability or recycling processes.[110] In the case of FDCA-based homopolyesters, some studies on their enzymatic degradation, namely, trough enzymatic hydrolysis were reported.[71,108,110–113]

In the case of PEF, its enzymatic hydrolysis was reported in several studies.[110–112] In 2016,[110] enzymatic hydrolysis of amorphous PEF powders (M_n values of 6 000, 10 000 and

40 000 g/mol; crystallinity <1%), using the *Thermobifida cellulosilytica* cutinase was reported, observing the release of 2,5-furandicarboxylic acid (Table 2.3) and oligomers up to DPn ~ 4.

Table 2.3. Results of the amount of FDCA released after enzymatic hydrolysis of different homopolyesters.

Polyester	M_n (g mol^{-1})	Đ	Degree of crystallinity (%)	Released FDCA (mmol L^{-1})[a]	References
PEF	5 700	-	< 1	5.7 ± 0.45	110
	10 200	-	< 1	10.2 ± 0.64	
	13 000	-	< 1	13.0 ± 1.18	
PEF	18 000	1.6	< 1	2.4 ± 0.04 (d< 180 μm) 2.6 ± 0.12 (180 < d < 425 μm)	111
	55 000	1.9	46	1.4 ± 0.28 (d< 180 μm) 0.8 ± 0.14 (180 < d < 425 μm)	
1,2-PPF	14 100	2.5	< 1	7.5 ± 0.1	71
PPF	21 000	2.8	< 1	2.0 ± 0.1	
PPeF	17 800	3.1	< 1	22.2 ± 2.9	
PHF	14 200	2.9	27	1.2 ± 0.04	
POF	9 3600	3.1	37	0.5 ± 0.02	
PNF	16 600	3.0	< 1	16.7 ± 1.3	
PDoF	11 100	2.5	30	3.3 ± 0.3	
PDEGF	32 900	3.7	< 1	42.2 ± 2.4	

[a] Amount of recovered FDCA after 72 h of enzyme-catalysed hydrolysis, average of three independent samples and the standard deviation among the triplicates.

More recently, Weinberg *et al.*[111] evaluated the enzymatic hydrolysis of PEF powders with different M_n´s, particle size and crystallinity, using the *T. cellulosilytica* cutinase under similar reaction conditions to those reported by Pellis *et al.*[110]. Contrary to the first study, materials with lower M_n and small particle sizes (d < 180 μm) were hydrolysed faster than those with higher molecular weights (Table 2.3). The enzymatic degradation of amorphous PEF films was also studied using *Humicola insolens* or *T. cellulosilytica* cutinases, showing that a 100% hydrolysis was achieved after only 72 h of incubation with *H. insolens* cutinase in a 1 M potassium phosphate buffer solution (pH=8) at 65 ºC. After 96 h, not only PEF films have been completely degraded, as well as >95% of the oligomers have been completely hydrolysed into monomers.[111]

In a different study also from 2017, the same authors highlighted the different hydrolysis patterns of PEF and PET.[112] The enzymatic hydrolysis of thin films with different crystallinity (0, 10 and 20%) was reported to be 1.7 times faster than that for PET. Once

again, *H. insolens* cutinase revealed to be more active on both PEF (and PET) films than *T. cellulosilytica* cutinase.

Taking in consideration the other furanic-aliphatic homopolyesters besides PEF, Haernvall *et al.*[71] studied the influence of the polyol structure on the enzymatic hydrolysis of furanic-aliphatic homopolyesters, such as 1,2-PPF, PPF, PPeF, PHF, POF, PNF, PDoF e PDEGF. *T. cellulosilytica* cutinase, in a 0.1 M potassium phosphate buffer (pH=7.0) at 50 ºC during 72 h. These polyesters were almost amorphous, presenting a crystallinity values lower than 1%, except for PHF, POF and PDoF with crystallinities of 27, 37, and 30%, respectively. The main results have shown (Table 2.3) that *T. cellulosilytica* cutinase had hydrolysed all tested polyesters, with preference to those containing 1,5-pentanediol and 1,9-nonanediol. Furthermore, from Table 2.3 it is also possible to observe that semi-crystalline homopolyesters, namely PEF, PHF, POF and PDoF were the less hydrolysable, especially in the case of amorphous PEF, in which the amount of FDCA released was almost the double.

Moreover, it was clear that enzyme activity increased when the linear diol was replaced by a branched diol or ether derivatives (Table 2.3). In fact, the latter displayed the highest FDCA release amount among the tested diol-based polyesters (Table 2.3), showing that ether group strongly favour the degradation of this material. Indeed, the introduction of ethoxy units into the FDCA-based polyester chain doubled the hydrolytic activity.

1.2.2. FDCA-based copolyesters

As mentioned above, copolymerisation between FDCA and other comonomers, such as diols and diacids or hydroxyacids, could be a simple way to prepare materials with tuned properties,[22,114,123–132,115,133–142,116,143–152,117,153–162,118,163,164,119–122] including, (bio)degradability. This has been accomplished by combining FDCA with EG, PD, BD, oligomeric poly(lactic acid) (PLA), succinic acid (SA), and/or adipic acid (AA), as comonomers (Figure 2.6).

These copolymers have been prepared both through random or block copolymerisation. Although, random copolymerisation strategy is definitely the most used.

In the next sub-sections the synthesis, thermal, mechanical and barrier properties of several important copolyesters will be discussed in detail.

1.2.2.1. Copolymerisation between FDCA and different diols

Several studies were reported focusing the synthesis of FDCA-based copolyesters combining two different linear diols, such as among others EG, PD, BD, 2,2-dimethyl-1,3-propanediol, as well as oligomeric ones like poly(ethylene glycol) (PEG), , in order to tune the thermal and/or mechanical properties of the final materials.[22,70,123,114–121]

Gomes *et al.*[22] reported the synthesis of poly(ethylene 2,5-furandicarboxylate-co-1,3-propylene 2,5-furandicarboxylate) (PEF-co-PPF) with 24% of ethylene units *via* a two-step polytransesterification reaction in the presence of Sb_2O_3 as catalyst (Figure 2.14).

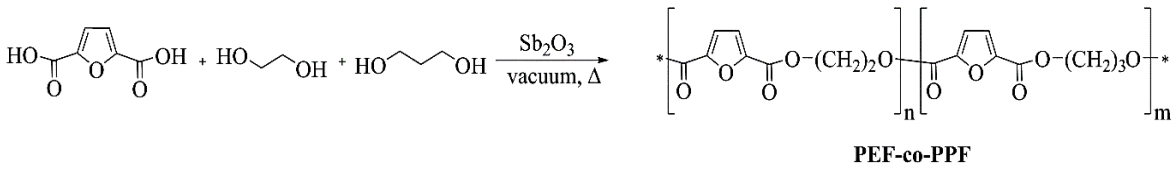

Figure 2.14. Synthesis of PEF-co-PPF.[22]

A semi-crystalline copolyester was obtained with M_n in the range of 14 100 g/mol and Đ equal to 2.27 and a T_g and T_m of 80 and 215 ºC, respectively, quite similar to those values typically reported for PEF.

Sousa *et al.*[115] prepared several random poly(1,4-butylene 2,5-furandicarboxylate)-co-poly(poly(ethylene glycol) 2,5-furandicarboxylate) (PBF-co-PEGF) copolyesters with different BD and PEG_{1000} ratios, namely 80/20, 65/35, 50/50 and 34/66 (Figure 2.15 and Table 2.4). Semi-crystalline copolyesters were obtained. They had M_n values between 5 400 and 37 000 g/mol, and T_g and T_m ranging from -35.4 to -43.1 ºC and 30.3 to 107.1 ºC, respectively. The ensuing materials will be referend as PBF-co-PEGF-80/20, -65/65, -50/50 and -34/66, corresponding to their PBF/PEGF feed ratio, and same nomenclature will be adopted for all copolyesters that will be described forward.

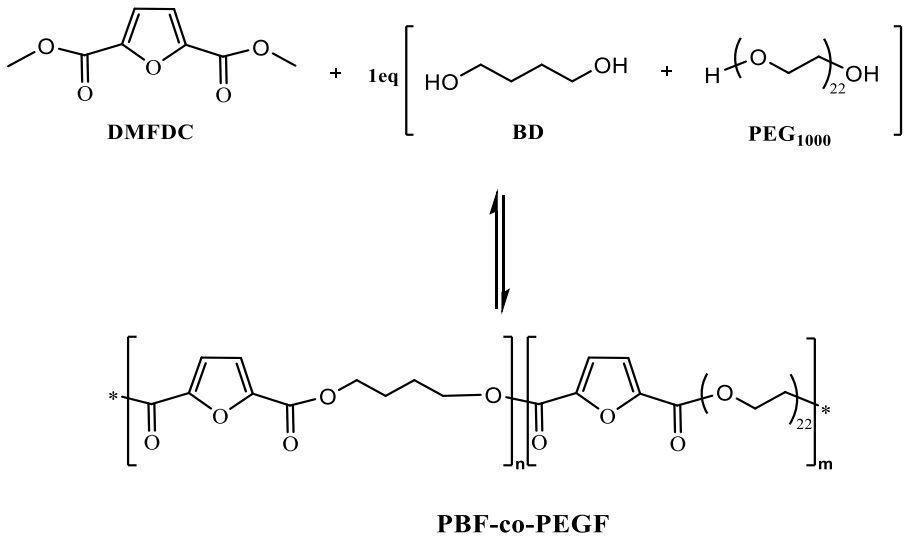

Figure 2.15. Synthesis of random PBF-co-PEGF copolyesters.[115]

Table 2.4. Main results obtained for copolyesters prepared with DMFDC, BD and PEG_{1000}.[115]

Polyester	BF_{real} [a] (mol %)	M_n (g mol^{-1})	T_g [b] (ºC)	T_m (ºC)	$T_{d,on}$ [c] (ºC)	$T_{d,max}$ (ºC)
PBF	-	-	71.1	171.1	351	381
PBF-co-PEGF-80/20	86	-[d]	-35.4	107.1	352	352
PBF-co-PEGF-65/35	50	5 400	-36.8	30.3	370	370
PBF-co-PEGF50/50	32	21 900	-35.4	37.9	380	380
PBF-co-PEGF34/66	≈ 0	37 0000	-43.1	41.1	374	374
PEGF	-	4 200	-35.8	41.7	364	364

[a]Real molar percentage of PBF incorporated in the copolyester, determined by ^{1}H NMR; [b]T_g determined by DMTA at 1 Hz; [c] $T_{d,on}$: Extrapolated onset temperature of weight loss step; [d]Not determined due to the solubility issues;

This study showed a tendency to incorporate more 1,4-butylene 2,5-furandicarboxylate (BF) moieties than PEGF units in the polymer backbone, especially for higher BD/PEG ratios, suggesting a higher reactivity of BD compared to PEG.[150] It was also found that the incorporation of PEG units into the backbone of the polymer clearly decreased both T_g and T_m, reaching values even lower than their related homopolyesters, however a gain in the thermal stability was noted. Nevertheless, PBF-co-PEGF-80/20 showed to have a segmented behaviour, displaying a T_g associated to the amorphous soft PEGF segment and a high T_m related with crystalline PBF units.

Moreover, other copolymers were prepared also incorporating EG, PD and BD but also rigid aliphatic comonomers in order to improve the thermal and mechanical properties of the ensuing materials.[116,117]

For example, in Figure 2.16 is represented the synthesis of PEF copolyesters incorporating 2,2,4,4-tetramethyl-1,3-cyclobutanediol (CBDO) as comonomer, and Table 2.5 summarises the main results obtained for all copolyesters synthesised in these studies.[116,117]

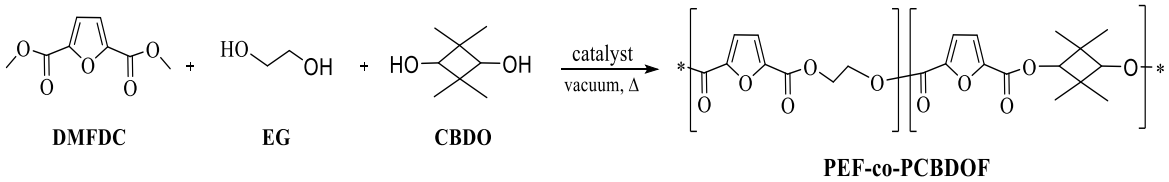

Figure 2.16. Synthesis of poly(ethylene glycol 2,5-furandicarboxylate)-co-poly(2,2,4,4-tetramethyl-1,3-cyclobutylene 2,5-furandicarboxylate) (PEF-co-PCBDOF).[116,117]

From Table 2.5 is possible to observe that the resulting copolyesters revealed some loss of crystallinity compared to PEF, PPF and PBF, since only T_g was displayed in their DSC traces, with the only exception being PBF-co-PCBDOF-10 that presented both T_g and T_m.

But, the incorporation of PCBDOF units does not affected the thermal stability of the ensuing copolyesters, showing values close to those of PEF, PPF and PBF homopolyesters (Table 2.5). As expected, an increase in the Young's modulus and tensile strength was observed with the CBDO content increase, attributed to the higher rigidity of PCBDOF unit. The same tendency was observed in terms of barrier properties, showing a slight increase in the O_2 and CO_2 permeabilities for higher content of CBDO, however still much lower than PET, PPT and PBT.[116,117]

Several other studies reported the synthesis of poly(ethylene glycol 2,5-furandicarboxylate)-co-poly(1,4-cyclohexylenedimethylene 2,5-furandicarboxylate) (PEF-co-PCF) copolyesters from DMFDC, EG and different CDHM isomer ratios, *via* a two-step bulk polytransesterification approach (Figure 2.17) to improve the mechanical properties of PEF.[118–120]

Table 2.5. Composition, thermal, mechanical and barrier properties of CBDO-based copolyesters.[116,117]

Polyester	$CBDO_{real}$[a] (mol%)	M_η[b] (g mol^{-1})	T_g (ºC)	T_m (ºC)	$T_{d,5\%}$ (ºC)	E (MPa)	σ_m (MPa)	ε_b (%)	O_2[d] (barrer)	CO_2[d] (barrer)
PEF	-	69 000	87.0	211.9	373	2 800	85	5	0.011	0.010
PEF-co-PCBDOF-96/4	3.6		88.9	-[c]	372	3 000	95	6	-	-
PEF-co-PCBDOF-90/10	10.3	56 000	90.9	-[c]	368	3 100	97	6	0.013	0.019
PEF-co-PCBDOF-85/15	15.4		92.1	-[c]	365	3 400	97	5	-	-
PEF-co-PCBDOF-82/18	18.2	51 000	91.1	-[c]	369	3 300	98	4	0.028	0.059
PEF-co-PCBDOF-77/23	22.7		94.2	-[c]	364	3 500	98	4	0.028	0.059
PPF	-	65 000	55.5	173.6	367	2 700	53	50	0.09	0.016
PPF-co- PCBDOF-90/10	9.8	71 000	61.1	-[c]	370	2 750	63	56	0.010	0.018
PPF-co- PCBDOF-82/18	17.8	53 000	63.5	-[c]	361	2 800	78	30	0.036	0.020
PBF	-	76 000	39.0	168.6	367	2 000	62	290	0.018	0.018
PBF-co- PCBDOF-90/10	9.6	74 000	42.5	154.4	368	2 100	72	274	0.025	0.027
PBF-co- PCBDOF-82/18	17.9	69 000	43.5	-[c]	365	2 200	80	220	0.042	0.055

[a] Real mol percentage of CBDO incorporated on the copolyester, determined by ^{1}H NMR; [b] Viscosity average molecular weight ($M\eta$) calculated using Mark–Houwink equation; [c] Not determinate; [d] Oxygen and carbon dioxide permeability coefficient, at 30 °C and 0.1001 MPa (1 barrer= 10^{-10} cm^3 cm/cm^2·s·cm Hg).

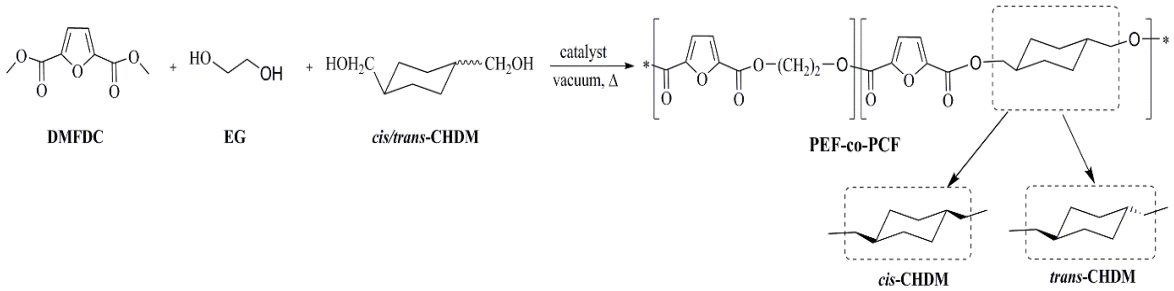

Figure 2.17. Representative synthesis of PEF-co-PCF copolyesters from DMFD, EG and CHDM with different *trans/cis* isomers.[118–120]

The influence on properties of the CHDM/EG ratio was assessed (Table 2.6).[118–120] Hong *et al.*[118] reported the synthesis of PEF-co-PCF (75/25, 50/50, 30/70), but with a non-specified ratio of CHDM isomers.

Table 2.6. Main results from molecular and thermal characterisation of PEF-co-PCF copolyesters.[118–120]

Polyester	*cis/trans*	CHDM$_{real}$[a] (mol%)	$M_n \times 10^3$ (g mol^{-1})	T_g (ºC)	T_m (ºC)	$T_{d,5\%}$ (ºC)	E (MPa)	σ_m (MPa)	ε_b (%)	O_2[c] (barrer)	CO_2[c] (barrer)	Ref.
PEF		-	33.7	87.0	211.9	372 – 383	2 800 – 3 702	73 – 85	1 – 5	0.011	0.010	118,119
PEF-co-PCF-85/15		15.1	29.6	84.9	-	369	2 300	75	8	-	-	
PEF-co-PCF-68/32	[d]	32.0	43.2	83.8	-	367	2 200	71	50	0.014	0.012	119
PEF-co-PCF-41/59		59.2	51.6	81.7	206.5	368	1 740	59	186	0.017	0.027	
PEF-co-PCF-24/76		75.9	34.4	80.6	225.4	365	1 760	63	155	-	-	
PEF-co-PCF-75/25		25.8	29.3	82.0	-	-	-	-	-	-	-	
PEF-co-PCF-50/50	70/30	51.0	32.0	80.0	-	-	2 763		20	-	-	118
PEF-co-PCF-30/70		81.6	27.6	81.0	239.0	-	2 317		79			
	90/10	10.4[b]	27.2	-	189.1	380	1 700	52	155	0.026	0.054	
	75/25	24.9[b]	33.2	-	-	383	1 780	65	200	-	-	
	60/40	39.8[b]	40.1	-	195.1	386	1 810	67	195	-	-	
PEF-co-PCF-50/50	45/55	55.3[b]	30.2	78.9	214.9	387	1 830	73	190	0.014	0.026	120
	32/68	67.8[b]	48.0	82.5	226.8	389	1 850	75	175	-	-	
	15/85	85.1[b]	44.6	-	250.7	390	1 880	74	160	-	-	
	2/98	97.7[b]	48.4	-	252.3	391	1 900	80	105	0.009	0.019	
PCF		100	18.0 – 29.2	79.5 – 84.0	263 – 268	~ 370	2 100 – 2 195	56 – 62	18 – 180	-	-	118,119

[a] Real mol percentage of CHDM incorporated on the copolyester, determined by ^{1}H NMR [b] Real mol percentage of *trans*-CHDM incorporated on the copolyester, determined by ^{1}H NMR [c] Oxygen and carbon dioxide permeability coefficient, at 30 °C and 0.1001 MPa (1 barrer= 10^{-10} cm^3 cm/cm^2·s·cm Hg). [d] Not determinate.

Also Wang *et al.*[119] prepared a series of PEF-co-PCF (85/15, 64/32, 41/59, 24/76) but using a CHDM *cis/trans* isomers ratio of 70/39. Copolyesters with M_n values between 27 600 and 51 600 g/mol were obtained, and showed that they were thermally stable up to 369ºC (Table 2.6).

Additionally, in a very interesting study the influence of the ratio on the final thermal and mechanical properties was also evaluated (Table 2.6).[120] The ratio of CHDM and EG was keep constant and equal to 1, and the *trans*/*cis* ratio varied from 10/90 to 98/2 mol% in the feed. PEF-co-PCF copolyesters with high molecular weights and enhanced thermal stability were obtained (Table 2.6). In addition, T_g and T_m increased significantly with the increasing content of *trans*-CHDM, revealing that this isomer impairs higher rigidity but also ability to crystallise to the related copolyesters, compare to *cis* isomer. Once again, mechanical properties reflected the increasing of the rigidity of the polymer chain, presenting increasing Young's modulus and tensile strength values with the incorporation of more *trans*-CHDM segments of PEF-co-PCF polymer chains, although the ε_b followed an opposite trend.

The copolymerisation with CHDM leaded to polymers with increased permeability to O_2 and CO_2, compared to *e.g.* PEF.[118,119] However, a decrease was noted with the incorporation of 98 % of *trans*-CHDM, suggesting that tuning *cis/trans*-CHDM ratio could lead to an even better gas barrier properties.

Similar to the homopolyesters, also copolyesters development studies addressed the possibility of improving the thermal properties, by using isosorbide diol monomers in copolymerisation reactions. In this vein, Sousa *et al.*[70] proposed the modification of PEGF homopolyesters with isosorbide, through direct solution polytransesterification, of FDCDCl, isosorbide and PEG with molecular weight of 2 000 g/mol (Figure 2.18).

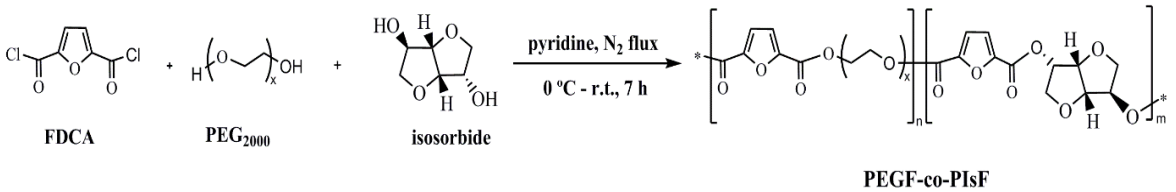

Figure 2.18. Synthetic route to prepare PEGF-co-PIsF copolyesters.[70]

The diols ratio in the feed was equal to 1, and a poly(poly(ethylene glycol) 2,5-furandicarboxylate)-co-poly(isosorbide 2,5-furandicarboxylate) (PEGF-co-PIsF)

copolyester with M_n and Đ of 11 000 g/mol and 1.1, respectively, was obtained. Moreover, it was found that the real incorporation of isosorbide into the copolyester backbone was much higher than PEG, resulting in a copolymer formed essentially with PIsF moieties with the incorporation of some PEGF moities (PIsF/PEGF ratio of 76/23).[70] This polymer showed to be a thermally stable material ($T_{d,5\%}$= 352.2 ºC), and also constituted by different phase block segments, *i.e.*, two distant T_g´s were observed, one associated to the PEGF soft segments and the other to the PIsF rigid segments (-26.5 and 168.7 ºC, respectively).

The incorporation of two cyclic diols in the same copolymer was only performed by Kasmi *et al.*[123] (Figure 2.19) where CHDM and isosorbide were incorporated in different proportions, in order to modify the crystallinity of the resulting polymers, as well as tuning their thermal properties.

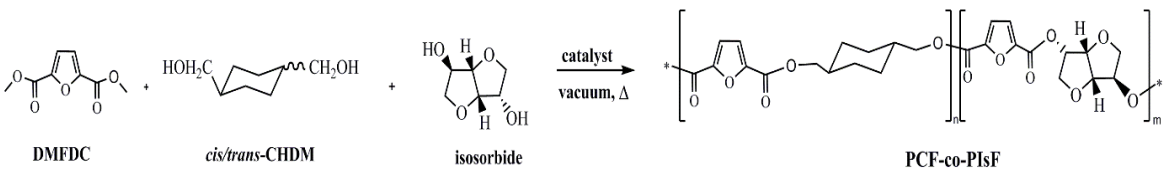

Figure 2.19. Synthesis of PCF-co-PIsF from DMFDC, CHDM and isosorbide.[123]

The resulting random PCF-co-PIsF presented molar composition in agreement with the corresponding feed ratios (Table 2.7); and T_g and T_m ranging from 75.3 to 103.5 ºC and 219.7 to 257.2 ºC, respectively.

Table 2.7. Main results from molecular and thermal properties of PCF-co-PIsF.[123]

Polyester	CHDM$_{real}$[a] (mol%)	T_g (ºC)	T_m (ºC)	$T_{d,5\%}$ (ºC)	Ref.
PIsF	100	157 – 180	-	350.0	11,22,73
PCF-co-PIsF-5/95	95.6	75.3	257.2	372.4	
PCF -co-PIsF-10/90	88.7	82.6	249.5	370.5	
PCF -co-PIsF-15/85	84.5	87.0	243.7	362.0	
PCF -co-PIsF-20/80	82.2	90.0	234.8	375.0	
PCF -co-PIsF-30/70	74.7	97.8	219.7	366.1	
PCF -co-PIsF-40/60	64.9	103.5	-	362.8	
PCF	100	76.9	264.5	379.7	123

[a] Real mol percentage of CHDM incorporated on the copolyester, determined by ^{1}H NMR.

Furthermore, increasing the isosorbide content, the crystallinity and thermal stability was directly affected, *i.e.*, T_g strongly increased, however the T_m and $T_{d,5\%}$ decreases, which is in accordance with the increase of rigid PIsF amorphous units that inhibit the mobility of molecular chains, as well as the crystallisation ability of the resulting materials. These results were corroborated by WAXD diffractograms, where peaks became less sharp with the introduction of the isosorbide content along the macromolecular chains. In fact, PCF-co-PisF-40/60 is a completely amorphous copolyesters, displaying an amorphous halo in its diffractogram.[123]

With the respect of their thermal stability, PCF-co-PIsF were found to be thermally stable up to 375 ºC (Table 2.7). However, these values were slightly lower than PCF homopolyester, yet still higher than that reported in the literature for PIsF.[11,22]

In conclusion, the improved thermal stability and broad working window of PCF-co-PIsFs ensure their processability at high temperatures, turning it into a suitable candidate for injection moulding applications, in these properties respect.

1.2.2.2. Copolymerisation between FDCA and different aliphatic diacids and hydroxy-acids

As mentioned above the copolymerisation of FDCA with aliphatic diacids or hydroxy-acids, namely SA, AA, dodecanoic acid (DA), diglycolic acid (DGA) and PLA, was also considered in several studies aiming at obtaining materials with well-defined thermal, mechanical properties and resulting in materials with some degree of degradability.[124,125,134,135,137–142,126–133] Similar to FDCA-based homopolyesters, copolyesters synthesis was typically performed through the chemical two-step bulk polytransesterification.

Poly(ethylene succinate) (PES) is a commercial homopolyester with excellent processability and biodegradability, which finds a wide variety of applications.[153] In order to improve the biodegradability of PEF, Yu *et al.*,[124] described the synthesis of poly(ethylene 2,5-furandicarboxylate-co-ethylene succinate) (PEF-co-PES), *via* the two-step bulk polytransesterification reaction, using FDCA, SA, an excess of EG and $Ti(OBu)_4$ as catalyst (Figure 2.20).

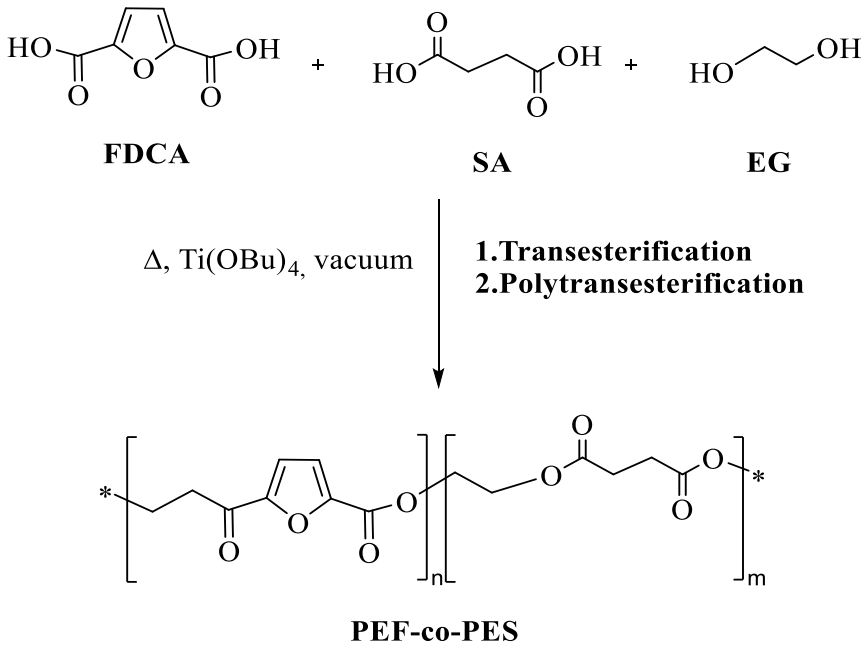

Figure 2.20. Two-step polytransesterification of FDCA,SA and EG.[124]

In general, PEF-co-PES were obtained as random copolyesters, incorporating 12-91 mol% of ethylene 2,5-furandicarboxylate moieties (EF) in their backbone structures, and possessing M_n values ranging from 25 600 to 57 400 g/mol (Table 2.8). These copolyesters only showed crystalline behaviour when EF content was lower than 10 mol% or higher than 70 mol%.

Table 2.8. Most relevant physical properties of PEF-co-PES.[124]

(co)Polyester	*EF/ES*[a]	$M_n \times 10^4$ (g mol^{-1})	T_g (ºC)	T_m (ºC)
PES	0/100	2.48	-10	115
PEF-co-PES-10/90	12/88	4.12	-	72
PEF-co-PES-30/70	33/67	5.74	21.93	-
PEF-co-PES-50/50	52/48	4.25	32.36	-
PEF-co-PES-70/30	74/26	3.93	-	146
PEF-co-PES-90/10	91/9	2.56	-	173
PEF	100/0	0.5 – 31.0	71 – 90	205 – 225

[a] Molar ratio of EF and ES in feed.

These modified PEF copolymers, showed thermal properties similar to those of their petrochemical counterparts, poly(ethylene terephthalate-co-ethylene succinate) (PET-co-

PES).[154] The authors also refereed that PEF-co-PES can be degraded under specific conditions, however without presenting any specific details.

In the same perspective, poly(propylene furandicarboxylate-co-propylene succinate) (PPF-co-PPS) were prepared from DMFDC or FDCA, PD and SA.[126,127] These copolyesters were also random materials, and they had high M_n, ranging from 39 600 to 81 600 g/mol (Table 2.9).

Table 2.9. Most relevant physical and barrier properties of PPF-co-PPS copolyesters.

(co)Polyester	$M_n \times 10^4$ (g mol^{-1})	T_g (ºC)	$T_{d,5\%}$ (ºC)	σ_m (MPa)	E (MPa)	ε_b (%)	O_2[a] (barrer)	CO_2[b] (barrer)	H_2O[c] (g·cm/cm^2·s·Pa)	Ref.
PPF	3.96	57.3	372	98.5	2 600	5	0.006	0.06	1.39*10^{-14}	
PPF-co-PPS-90/10	4.89	47.7	378	87.3	2 374	6	0.0072	0.07	3.52*10^{-14}	
PPF-co-PPS-80/20	4.96	28.9	373	48.1	1 237	196	0.018	0.27	4.46*10^{-14}	126
PPF-co-PPS-70/30	5.02	28.7	370	14.0	200	500	0.023	0.30	4.93*10^{-14}	
PPF-co-PPS-60/40	4.93	17.0	369	4.4	20	687	0.025	0.37	5.78*10^{-14}	
PPF-co-PPS-50/50	6.83	8.8	366	2.9	12	1 255	0.027	0.57	6.37*10^{-14}	
PPF-co-PPS-50/50	1.53	-7.2	323	-	-	-	-	-	-	127
PPF-co-PPS-40/60	7.66	-0.2	370	0.4	7	1 485	0.04	0.60	9.37*10^{-14}	
PPF-co-PPS-30/70	7.63	-8.3	372	0.3	4	1 590	-	-	-	
PPF-co-PPS-20/80	7.52	-16.1	367	0.2	3	1 700	-	-	-	126
PPF-co-PPS-10/90	8.16	-24.6	366	0.2	1	1 730	-	-	-	
PPS	6.28	-30.8	356	4.6	211	3	-	-	-	

[a] Oxygen permeability coefficient, at 23 °C, 50% relative humidity and 0.1001 MPa. 1 barrer= 10^{-10} cm3 cm/cm2·s·cm Hg. [b] Carbon dioxide permeability coefficient, at 23 °C, 50% relative humidity and 0.1001 MPa; [c] Water vapour transmission rate, at 38 °C, 90% relative humidity.

In addition, PPF-co-PPS presented a decrease in the T_g with the PS content increasing, related to the incorporation of more soft moieties. It was also observed that Young´s modulus and tensile strength, strongly decreased with the increasing of PS content, and the elongation at break increased up to 1 700%.[126]

It is worth to mention that the gas permeability of PPF-co-PPS-90/10 was close to that of PPF (Table 2.9), but for lower PF content, a decrease in the gas barrier was noted, however still showing superior properties than those of PBAT (permeability to O_2 and CO_2 of 0.76 and 5.9 barrer, respectively),[126] These gas barrier results could be an advantage for food packaging and agricultural films applications.

PBF, as described before, is an interesting linear furanic-aliphatic polyester, however possessing low biodegradability when compared with other aliphatic renewable polyesters such as poly(butylene succinate) (PBS), and poly(butylene adipate) (PBA).

Copolymerisation with SA and/or AA and BD can be a simple method to tune biodegradability of PBF, and at same time maintaining its thermal and mechanical properties, as noted for other FDCA-based polymers.[128–135]

Poly(butylene furandicarboxylate-co-butylene succinate) (PBF-co-PBS) and poly(butylene furandicarboxylate-co-butylene adipate) (PBF-co-PBA) copolyesters were usually prepared by the two-step polytransesterification approach of FDCA, SA and/or AA and BD, using $Ti(OBu)_4$ or $Zr(OBu)_4$ as catalysts. Random copolyesters with M_n values ranging between 15 700-85 700 g/mol and 26 400-68 700 g/mol to (PBF-co-PBS) and (PBF-co-PBA) (Table 2.10) were obtained, respectively.

Table 2.10. Most relevant physical properties of PBF-co-PBS and PBF-co-PBA.

(co)Polyester	$M_n \times 10^4$ (g mol^{-1})	T_g (ºC)	T_m (ºC)	$T_{d,5\%}$ (ºC)	σ_m (MPa)	E (MPa)	ε_b (%)	Ref.
PBF	0.12 – 23.21	25 – 39	163 – 180	304 – 370	68	1 100 – 1 900	3 – 284	128,129,131
PBF-co-PBS-5/95	5.82	-31	111	-	14	172	174	128
PBF-co-PBS-10/90	2.21 – 8.35	-27.6 – -25.0	102 – 105	339	20 – 77	20 – 372	160 – 1 027	128,129,131
PBF-co-PBS-20/80	1.99 – 6.17	-24.2 – -20.0	90 – 93.1	342	20 – 115	21 – 550	320 – 1 423	128,129
PBF-co-PBS-30/70	2.21	-17.9	71.0	344	-[b]	-[b]	580	129
PBF-co-PBS-40/60	2.90 – 7.83	-10.5	57.1 – 70.7	349	-[b]	-[b]	660	129,132
PBF-co-PBS-45/55	8.27	-	73.1	-	56	64	758	132
PBF-co-PBS-50/50	1.85 – 8.57	-3.5	75.5 – 85.6	344	46	99	758	129,132
PBF-co-PBS-55/45	7.94	-	96.8	-	49	167	706	132
PBF-co-PBS-60/40	0.13 – 4.08	-21.0 – 6.5	54 – 112.0	345	27	300	434	128,129,132
PBF-co-PBS-70/30	2.2100	14.6	131.0	339	-[b]	-[b]	-[b]	129
PBF-co-PBS-80/20	1.57	22.0	147.0	347	-[b]	-[b]	-[b]	129
PBF-co-PBS-90/10	-[a]	30.5	159.0	345	-[b]	-[b]	-[b]	129
PBS	0.77 – 8.42	-33 – -36	114	404 – 423	44	432	303	131,155,156
PBF-co-PBA-10/90	3.30 – 4.13	-53.2	49 – 55	342	12 – 17	110 – 122	748 –759	130,135
PBF-co-PBA-20/80	3.39 – 5.70	-48.1 – -44	27 – 30	369	11	55	976	130,135
PBF-co-PBA-30/70	2.64 – 4.10	-38.0	50	370	2.6	0.1	1 850	130,135
PBF-co-PBA-40/60	3.23 – 5.18	-30.2 – -28.0	47 – 54	382	9 – 28	2 – 34	613 – 1 521	130,132,135
PBF-co-PBA-45/65	6.87	-	74	-	28	47	896	132
PBF-co-PBA-50/50	2.85 – 5.04	-20	70 – 87	377	15 – 35	10 – 73	365 – 1 040	130,132,135
PBF-co-PBA-55/75	-	-	99	-	26	117	800	132
PBF-co-PBA-60/40	4.30 – 5.06	-11	108 –112	369	26 – 43	56 – 185	418 – 798	132,135
PBF-co-PBA-70/30	3.50	-1	132	386	35	44	469	135
PBF-co-PBS-75/25	3.13	7	134	-	30	76	425	130
PBF-co-PBA-80/20	3.00	10.6	146	388	42	51	407	135
PBF-co-PBA-90/10	-[c]	23.3	156	382	36	111	304	135
PBA	1.70 – 6.20	-60 – -78	58 – 60	340 – 404	15 – 139	162 – 168	463 – 680	128–130,135,155–160

[a] Not determinate because of the insolubility in chloroform. [b] Not determinated. [c] Not measured due to the limitation of the instrument used.

From Table 2.10 it is possible to conclude that with the increasing of BS or BA content, the T_g clearly decreased, mostly due to the incorporation of soft aliphatic moieties in higher quantities. Similar trend was also noted in the T_m, but not so evident.

Further, these copolyesters were found to be thermally stable up to 388 ºC, possessing better thermal stability than PBF ($T_{d,5\%}$ between 304 to 370 ºC) (Table 2.10).

Both, PBF-co-PBS and PBF-co-PBA copolymers exhibited lower values of E and σ_m than PBF, but they have higher elongation at break (Table 2.10). Furthermore, these polyesters have also presented enhanced biodegradability (soil degradation tests), even when only 10 mol% of BF moieties were incorporated, and in some cases even higher than the corresponding homopolyesters.[128,130,132,136,165]

In terms of their applications, both PBF-co-PBS and PBF-co-PBA copolymers were proposed to find wide applications as thermoplastics, bottles, packaging and films, as well as elastomers or impact modifiers simply by tuning the relative amount of BF units content introduced.[128–130,132,133] Jacquel *et al.*[138] patented in 2013, PBF-co-PBS copolyesters for films and packaging applications.

Recently, Soccio *et al.*[140] reported the synthesis of poly(butylene 2,5-furandicarboxylate)-co-poly(butylene diglycolate) (PBF-co-PBDG), *via* bulk polytransesterification method (Figure 2.21). In this study, the BF content was comprised from 60 to 90 mol% in the feed, and the ensuing copolyesters presented semi-crystalline nature (Table 2.11).

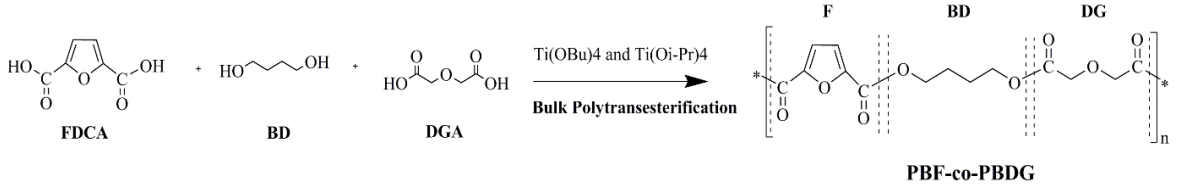

Figure 2.21. Synthesis of PBF-co-PBDG *via* bulk polytransesterification reaction.[140]

PBF-co-PBDG copolymers have shown a good thermal stability, with maximum degradation temperatures between 380 to 388 ºC, even higher than PBF homopolymer ($T_{d,max}$=366 ºC).

Table 2.11. Main thermal and mechanical results of PBF-co-PBDG.[140]

(co)Polyester	T_g (ºC)	T_m (ºC)	$T_{d,max}$ (ºC)	σ_m (MPa)	E (MPa)	ε_b (%)
PBF	35	164	366	34	1 283	102
PBF-co-PBDG-90/10	26	153	383	10	373	419
PBF-co-PBDG-80/20	19	140	380	26	688	241
PBF-co-PBDG-70/30	11	128	382	18	353	415
PBF-co-PBDG-60/40	6	106	388	9	130	414

As already pointed out before for other copolymers, the thermal features were quite dependent of the BF/BDG ratio, *i.e.*, both T_g and T_m decreased with the increasing of BDG segments incorporated into the polymer chains. BDG units provide softer polymer consequently decreasing the T_g, and at same time disrupting the crystalline ability of PBF due to high random degree, leading to the formation of less perfect crystals decreasing the T_m. In addition, with introduction of more BDG segments into the PBF chain, a progressive decrease of the Young's modulus and tensile strength was observed, as well as also due to the incorporation of more soft segments, and consequently increasing the elongation at break. Further, by increasing the BDG unit content, there is a modest increase in the gas permeability values consequent to the decrease of the glass transition temperature, which attributed higher flexibility to the polymer chains.

The copolymerisation of FDCA with hydroxy-acids, namely oligomeric PLA, has also been investigated in two studies.[141,142] Matos *et al.*[141] performed the synthesis of poly(ethylene 2,5-furandicarboxylate)-co-poly(lactic acid) (PEF-co-PLA), through the copolymerisation of BHEFDC and PLA ($M_n \approx 5\ 000$ g/mol), in the presence of Sb_2O_3 or $SnCl_2.2H_2O$ as catalyst (Figure 2.22). Wu *et al.*[142] also reported the synthesis of this copolymer but using $Ti(OBu)_4$ as catalyst, and PLA with $M_n \approx 2\ 900$ g/mol.

The results obtained showed that $Ti(OBu)_4$ was a better catalyst, since polymers with much higher molecular weights were achieved.

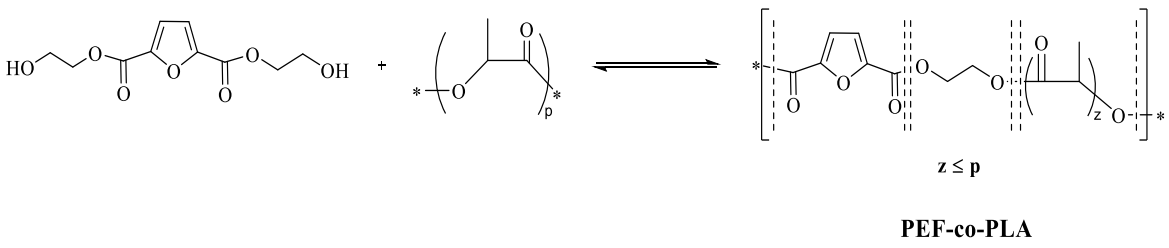

Figure 2.22. Polytransesterification reaction between BHEFDC and PLA.[141,142]

However, in both approaches[141,142] the obtained copolyesters presented a random structure and were essentially amorphous, with high thermal stability (T_d > 282 ºC), and T_g's that can be very close to PEF (Table 2.12).

Table 2.12. Main results obtained for PEF-co-PLA.[141,142]

(co)Polyester	$M_n \times 10^4$ (g mol^{-1})	T_g (ºC)	T_m (ºC)	$T_{d,5\%}$ (ºC)	Ref.
PEF	2.21	80	-	-	142
PEF-co-PLA-73/27	0.69	76.4	-	324	
PEF-co-PLA-54/46	0.70	67.5	-	301	141
PEF-co-PLA-23/77	0.73	69.2	-	320	
PEF-co-PLA-7/93	0.83	25.0	119.6	230	
PEF-co-PLA-20/80	2.16	68	-	282	
PEF-co-PLA-30/70	2.64	70	-	287	142
PEF-co-PLA-40/60	6.47	79	-	300	
PLLA	0.29 – 0.50	54	151.2	257	141,142

The degradability of these copolyesters was investigated through hydrolytic and tests have revealed that these polyesters possess enhanced hydrolytic degradability, even higher than the corresponding PLA homopolyester (Figure 2.23).

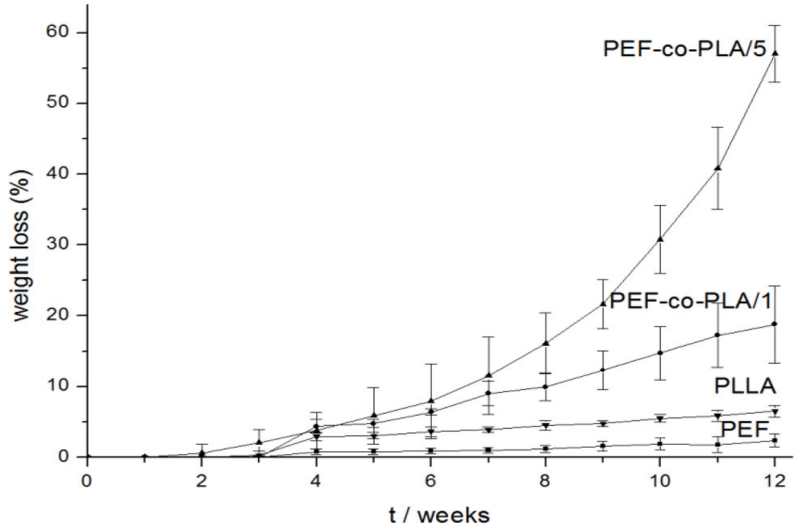

Figure 2.23. Variation of the weight loss along with the hydrolytic degradation time (adapted from reference [141]).

1.2.3. FDCA-based copolyesters and their biodegradability

Biodegradability can be defined as the ability of a given material to be degraded under defined conditions, safely and relatively quickly, that after can disappear into the environment.[161]

In Europe, to be considered as (bio)degradable, and according to EN 13432 or EN 14995 standards,[137] a material has to degrade biologically to at least 90 %, in less than 180 days. Moreover, biodegradable polyesters can decompose in the environment because of the characteristics of their main-chain structure and to certain extent of hydrophilicity and crystallinity.[162]

In fact, a balance between the hydrophilic/hydrophobic of polyesters molecules seems to be crucial for the enzyme to bind to the substrate and the subsequent hydrolytic action of the enzyme. Furthermore, lipases, the most used estereases for hydrolytic degradation, have the ability to hydrolyse aliphatic polyesters in contrast to aromatic polyesters because the flexibility of the main chain and the hydrophilicity of aliphatic polyesters.[162] On the contrary, almost all aromatic polyesters tend to be non-biodegradable essentially due to their rigid structures and hydrophobicity, that prevent the entrance of the water to hydrolyse the ester linkages.[163]

Some studies have shown that copolymerisation of FDCA with aliphatic diacids or hydroxyacids can be used to achieve materials with some degree of biodegradability. [125,130,136,139,141,142] Actually, the introduction of aliphatic ester moieties in the backbone of copolyesters have facilitated the chemical or enzymatic attack as well as the penetration of water to break the ester linkage.[164] For example, PEF-co-PLA copolyesters prepared from FDCA and oligomeric lactic acid (PEF-co-PLA) have demonstrated enhanced soil degradability when compared with PEF.[142] Soil degradation tests of these copolyesters displayed quite interesting results, since the copolyester with higher EF content still presents weight loss higher than 10% (Figure 2.24).[142]

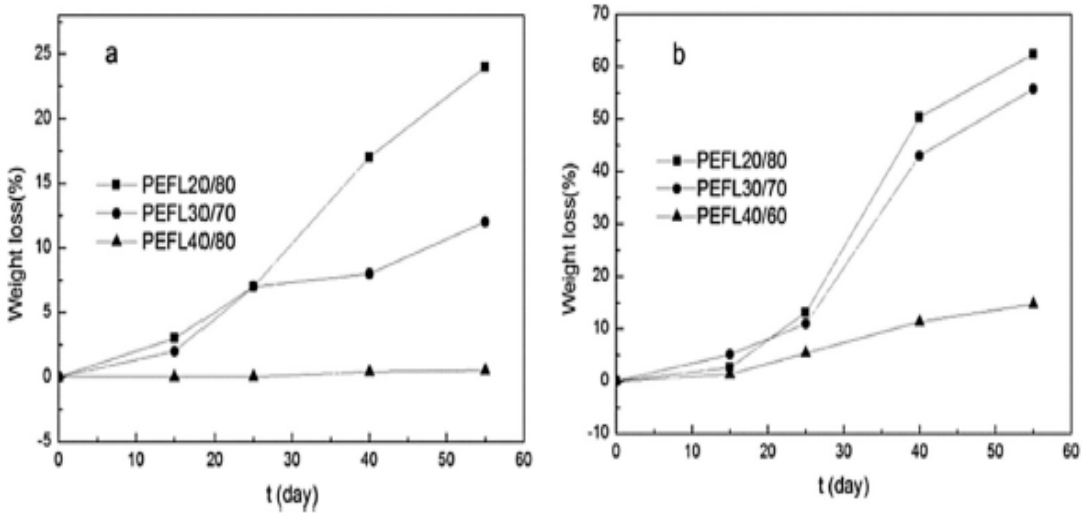

Figure 2.24. Weight loss of copolyesters degradation in PBS (a) and soil (b) (adapted from reference [142]).

The biodegradation of PBF and PBF-co-PBDG copolymers was also evaluated through composting tests. Polyesters were incubated in compost for 21, 35 and 62 days, and the corresponding weight loss was measured (Figure 2.25). It was clear, that higher BDG content lead to higher weight losses, with the maximum weight loss value being observed for PBF-co-PBGD-60/40 (40 %), while no significant changes in PBF weight were observed.

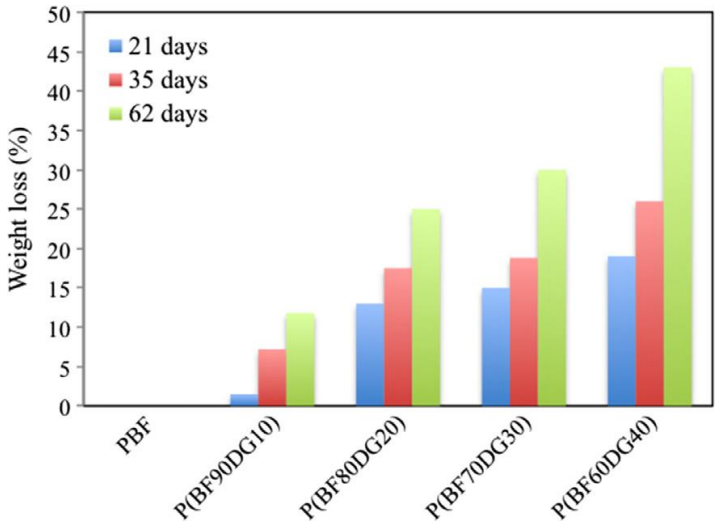

Figure 2.25. Weight loss (%) for the samples under study at different incubation times (adapted from reference [140]).

Moreover, copolyesters prepared from FDCA and aliphatic diacids, such as adipic and succinic acids, also have shown some biodegradability. In the case of PBF-co-PBA, just incorporating only 10 mol% of BF content a higher biodegradability was achieved, even when compared with PBA.[130] For PBF-co-PBS copolyesters, compostability tests have revealed that all samples were biodegradable up to 90 % in less than 180 days, as required by the European Standard.[128,165] A recent patent from Novamont[136] reinforces these results, where 91.6 % of compostability was achieved for PBF-co-PBS just in 90 days.

Copolymerisation between FDCA and aliphatic diacids and/or hydroxylacids had revealed to be an excellent approach to obtained very interesting materials with enhanced biodegradability.

2. Conclusions

The synthesis of furanic-aliphatic FDCA-based homopolyesters has been intensively studied during the last few decades through several routes, resulting in polymers with enhanced thermal and mechanical properties, and/or degradability, depending on the monomers used. It is also noteworthy, that all materials described in this survey are almost bio-based renewable materials, possessing thermal and mechanical features quite similar and for some even better than those currently derived from petroleum.

The synthesis of FDCA-based copolyesters was also performed using a myriad of linear, branched and cyclic diols, as well as, different diacids and hydroxyacids, leading to materials with tuneable properties and in some cases with enhanced biodegradability, which can open a wide variety of applications.

References

(1) Gandini, A.; Silvestre, A. J. D.; Neto, C. P.; Sousa, A. F.; Gomes, M. M. The Furan Counterpart of Poly (Ethylene Terephthalate): An Alternative Material Based on Renewable Resources. *J. Polym. Sci. Polym. Chem.* **2009**, *5* (c), 295–298.

(2) Terzopoulou, Z.; Tsanaktsis, V.; Nerantzaki, M.; Papageorgiou, G. Z.; Bikiaris, D. N. Decomposition Mechanism of Polyesters Based on 2,5-Furandicarboxylic Acid and Aliphatic Diols with Medium and Long Chain Methylene Groups. *Polym. Degrad. Stabil.* **2016**, *132* (March), 127–136.

(3) Zhang, D.; Dumont, M. J. Advances in Polymer Precursors and Bio-Based Polymers Synthesized from 5-Hydroxymethylfurfural. *J. Polym. Sci. Polym. Chem.* **2017**, *55* (9), 1478–1492.

(4) Mandal, B. M. Step Polymerization. In *Fundamentals of Polymerization*; World Scientific Publishing Co. Pte. Ltd: Londo, 2013; pp 37–95.

(5) Hamielec, Archie E.; Tobita, H. Polymerization Processes, 1. Fundamentals. In *Encyclopedia of Industrial Chemistry*; Wiley-VCH Verlag GmbH & Co.: Weinheim, 2012; p 136.

(6) Carothers, Wallace H.; Arvin, J. A. Vol. 51. *J. Am. Chem. Soc.* **1929**, *51* (11), 2560–2570.

(7) Carothers, W. H. Studies on Polymerization and Ring Formation. I. An Introduction to the General Theory of Condensation Polymers. *J. Am. Chem. Soc.* **1929**, *51* (1833), 2548–2559.

(8) Edlund, U.; Albertsson, A. Polyesters Based on Diacid Monomers. *Adv. Drug Deliv. Rev.* **2003**, *55* (4), 585–609.

(9) He, Zhiqun; Whale, Eric A.; Davis, F. J. Step-Growth Polymerization-Basics and Development of New Materials. In *Polymer Chemistry - The Practical Approach in Chemistry Series*; Davis, F. J., Ed.; Oxford University Press: Oxford, UK, 2004; pp 126–127.

(10) Pang, K.; Kotek, R.; Tonelli, a. Review of Conventional and Novel Polymerization Processes for Polyesters. *Prog. Polym. Sci.* **2006**, *31* (11), 1009–1037.

(11) Gandini, A.; Coelho, D.; Gomes, M.; Reis, B.; Silvestre, A. Materials from Renewable Resources Based on Furan Monomers and Furan Chemistry: Work in Progress. *J. Mater. Chem.* **2009**, *19* (45), 8656.

(12) Sipos, L. A Process for Preparing a Polymer Having a 2,5-Furandicarboxylate Moiety within the Polymer Backbone and Such (Co)Polymers. WO2010077133 A1, 2010.

(13) Berkel, J. G. Van; Guigo, N.; Kolstad, J. J.; Sipos, L.; Wang, B.; Dam, M. a.; Sbirrazzuoli, N. Isothermal Crystallization Kinetics of Poly(Ethylene 2,5-Furandicarboxylate). *Macromol. Mater. Eng.* **2015**, *300* (4), 466–474.

(14) Knoop, R. J. I.; Vogelzang, W.; van Haveren, J.; van Es, D. S. High Molecular Weight Poly(Ethylene-2,5-Furanoate); Critical Aspects in Synthesis and Mechanical Property Determination. *J. Polym. Sci. Polym. Chem.* **2013**, *51* (19), 4191–4199.

(15) Gruter, G. M.; Sipos, L.; Dam, M. A. Accelerating Research into Bio-Based FDCA-Polyesters by Using Small Scale Parallel Film Reactors. *Comb. Chem. High Throughput Screen.* **2011**, *14*, 1–9.

(16) Kasmi, N.; Majdoub, M.; Papageorgiou, G. Z.; Achilias, D. S.; Bikiaris, D. N. Solid-State Polymerization of Poly(Ethylene Furanoate) Biobased Polyester, I: Effect of Catalyst Type on Molecular Weight Increase. *Polymers* **2017**, *9* (11).

(17) Kasmi, N.; Papageorgiou, G. Z.; Achilias, D. S.; Bikiaris, D. N. Solid-State Polymerization of Poly(Ethylene Furanoate) Biobased Polyester, II: An Efficient and Facile Method to Synthesize High Molecular Weight Polyester Appropriate for Food Packaging Applications. *Polymers* **2018**, *10* (5), 1–21.

(18) Steinborn-Rogulska, I.; Rokicki, G. Solid-State Polycondensation (SSP) as a Method to Obtain High Molecular Weight Polymers. *Polymery* **2013**, *58* (1), 1–11.

(19) Drewitt, J. G. N.; Lincoln, J. Improvements in Polymers. GB 621971 (A), 1946.

(20) Moore and J. E. and Kelly, J. A. Polyesters Derived from Furan and Tetrahydrofuran Nuclei. *Macromolecules* **1978**, *11* (3), 568–573.

(21) Moore, J. E.; Kelly, J. A. Thermally Initiated Crosslinking of an Unsaturated Heterocyclic Polyester. *J. Polym. Sci. Polym. Chem. Ed.* **1978**, *16*, 2407–2409.

(22) Gomes, M.; Gandini, A.; Silvestre, A. J. D. D.; Reis, B. Synthesis and

Characterization of Poly(2,5-Furan Dicarboxylate)s Based on a Variety of Diols. *J. Polym. Sci. Polym. Chem.* **2011**, *49* (17), 3759–3768.

(23) Jiang, M.; Liu, Q.; Zhang, Q.; Ye, C.; Zhou, G. A Series of Furan-Aromatic Polyesters Synthesized via Direct Esterification Method Based on Renewable Resources. *J. Polym. Sci. Polym. Chem.* **2012**, *50* (5), 1026–1036.

(24) Papageorgiou, G. Z.; Guigo, N.; Tsanaktsis, V.; Papageorgiou, D. G.; Exarhopoulos, S.; Sbirrazzuoli, N.; Bikiaris, D. N. On the Bio-Based Furanic Polyesters: Synthesis and Thermal Behavior Study of Poly(Octylene Furanoate) Using Fast and Temperature Modulated Scanning Calorimetry. *Eur. Polym. J.* **2015**, *68*, 115–127.

(25) Papageorgiou, G. Z.; Tsanaktsis, V.; Papageorgiou, D. G.; Chrissafis, K.; Exarhopoulos, S.; Bikiaris, D. N. Furan-Based Polyesters from Renewable Resources: Crystallization and Thermal Degradation Behavior of Poly(Hexamethylene 2,5-Furan-Dicarboxylate). *Eur. Polym. J.* **2015**, *67*, 383–396.

(26) Thiyagarajan, S.; Vogelzang, W.; J. I. Knoop, R.; Frissen, A. E.; Van Haveren, J.; Van Es, D. S. Biobased Furandicarboxylic Acids (FDCAs): Effects of Isomeric Substitution on Polyester Synthesis and Properties. *Green Chem.* **2014**, *16* (4), 1957–1966.

(27) Tsanaktsis, V.; Bikiaris, D. N.; Guigo, N.; Exarhopoulos, S.; Papageorgiou, D. G.; Sbirrazzuoli, N.; Papageorgiou, G. Z. Synthesis, Properties and Thermal Behavior of Poly(Decylene-2,5-Furanoate): A Biobased Polyester from 2,5-Furan Dicarboxylic Acid. *RSC Adv.* **2015**, *5* (91), 74592–74604.

(28) Papageorgiou, G. Z.; Papageorgiou, D. G.; Terzopoulou, Z.; Bikiaris, D. N. Production of Bio-Based 2,5-Furan Dicarboxylate Polyesters: Recent Progress and Critical Aspects in Their Synthesis and Thermal Properties. *Eur. Polym. J.* **2016**, *83*, 202–229.

(29) Vriesema, B. K.; Miniaci, F. Aromatic Polyester. EP 0294863 A1, 1987.

(30) Fujioka, Y.; Mochizuki, M.; Nagara, Y. Liquid Crystalline Polyester. JP 2010000275036, 2010.

(31) Wilsens, C. H. R. M.; Rastogi, S.; Veld, M. A. J.; Klop, E. A.; Noordover, B. A. J. Liquid Crystalline Furandicarboxylic Acid-Based Aromatic Polyesters. WO

2013092667 A1, 2011.

(32) Wilsens, C. H. R. M.; Noordover, B. a. J.; Rastogi, S. Aromatic Thermotropic Polyesters Based on 2,5-Furandicarboxylic Acid and Vanillic Acid. *Polymer* **2014**, *55* (10), 2432–2439.

(33) Wilsens, C. H. R. M.; Verhoeven, J. M. G. A.; Noordover, B. A. J.; Hansen, M. R.; Auhl, D.; Rastogi, S. Thermotropic Polyesters from 2,5-Furandicarboxylic Acid and Vanillic Acid: Synthesis, Thermal Properties, Melt Behavior, and Mechanical Performance. *Macromolecules* **2014**, *54* (7), 1034–1040.

(34) Y. Kanetaka; Kimura, K.; Uchida, T.; Yamasaki, S. Manufacture of Polyester Involves Mixing and Polymerizing Furan-Dicarboxylic Acid, (Formyloxy)Phenyl Formatecontaining Compound, and (Formyl Oxy) Phenyl Formate Containing Compound, and Obtaining Polyester Having Liquid Crystallinity. JP2014034611–A, 2014.

(35) Morales-huerta, J. C.; Martí, A. Partially Renewable Poly(Butylene 2,5-Furandicarboxylate-Co-Isophthalate) Copolyesters Obtained by ROP. *Polymers* **2018**, *10* (5), 483.

(36) Sousa, A. F.; Vilela, C.; Fonseca, A. C.; Matos, M.; Freire, C. S. R.; Gruter, G. J. M.; Coelho, J. F. J.; Silvestre, A. J. D. Biobased Polyesters and Other Polymers from 2,5-Furandicarboxylic Acid: A Tribute to Furan Excellency. *Polym. Chem.* **2015**, *6* (33), 5961–5983.

(37) Jiang, Y.; Woortman, A. J. J.; Alberda Van Ekenstein, G. O. R.; Loos, K. A Biocatalytic Approach towards Sustainable Furanic-Aliphatic Polyesters. *Polym. Chem.* **2015**, *6* (29), 5198–5211.

(38) Gopalakrishnan, P.; Narayan-Sarathy, S.; Ghosh, T.; Mahajan, K.; Belgacem, M. N. Synthesis and Characterization of Bio-Based Furanic Polyesters. *J. Polym. Res.* **2014**, *21* (1).

(39) Burgess, S. K.; Karvan, O.; Johnson, J. R.; Kriegel, R. M.; Koros, W. J. Oxygen Sorption and Transport in Amorphous Poly(Ethylene Furanoate). *Polymer* **2014**, *55* (18), 4748–4756.

(40) Papageorgiou, G. Z.; Tsanaktsis, V.; Bikiaris, D. N. Synthesis of Poly(Ethylene

Furandicarboxylate) Polyester Using Monomers Derived from Renewable Resources: Thermal Behavior Comparison with PET and PEN. *Phys. Chem. Chem. Phys.* **2014**, *16* (17), 7946–7958.

(41) Burgess, S. K.; Leisen, J. E.; Kraftschik, B. E.; Mubarak, C. R.; Kriegel, R. M.; Koros, W. J. Chain Mobility, Thermal, and Mechanical Properties of Poly(Ethylene Furanoate) Compared to Poly(Ethylene Terephthalate). *Macromolecules* **2014**, *47* (4), 1383−1391.

(42) Terzopoulou, Z.; Karakatsianopoulou, E.; Kasmi, N.; Tsanaktsis, V.; Nikolaidis, N.; Kostoglou, M.; Papageorgiou, G. Z.; Lambropoulou, D. A.; Bikiaris, D. N. Effect of Catalyst Type on Molecular Weight Increase and Coloration of Poly(Ethylene Furanoate) Biobased Polyester during Melt Polycondensation. *Polym. Chem.* **2017**, *8* (44), 6895–6908.

(43) Terzopoulou, Z.; Tsanaktsis, V.; Nerantzaki, M.; Achilias, D. S.; Vaimakis, T.; Papageorgiou, G. Z.; Bikiaris, D. N. Thermal Degradation of Biobased Polyesters: Kinetics and Decomposition Mechanism of Polyesters from 2,5-Furandicarboxylic Acid and Long-Chain Aliphatic Diols. *J. Anal. Appl. Pyrolysis* **2016**, *117*, 162–175.

(44) Wu, J.; Xie, H.; Wu, L.; Li, B. G.; Dubois, P. DBU-Catalyzed Biobased Poly(Ethylene 2,5-Furandicarboxylate) Polyester with Rapid Melt Crystallization: Synthesis, Crystallization Kinetics and Melting Behavior. *RSC Adv.* **2017**, *7* (23), 13877.

(45) Yu, Z.; Zhou, J.; Cao, F.; Zhang, Q.; Huang, K.; Wei, P. Synthesis, Characterization and Thermal Properties of Bio-Based Poly(Ethylene 2,5-Furan Dicarboxylate). *J. Macromol. Sci. Part B Phys.* **2016**, *55* (12), 1135–1145.

(46) Wang, J. G.; Liu, X. Q.; Zhu, J. From Furan to High Quality Bio-Based Poly(Ethylene Furandicarboxylate). *Chinese J. Polym. Sci.* **2018**, *36* (6), 720–727.

(47) Morales-Huerta, J. C.; Martínez De Ilarduya, A.; Muñoz-Guerra, S. Poly(Alkylene 2,5-Furandicarboxylate)s (PEF and PBF) by Ring Opening Polymerization. *Polymer* **2016**, *87*, 148–158.

(48) Poulat, F.; Reutenauer, P. Method of Making a Bottle Made of Fdca and Diol Monomers and Apparatus for Implementing Such Method. WO2014032731 A1,

2014.

(49) L.T. Brandão, A.; F. Oechsler, B.; W. Gomes, F.; G. Souza, F.; Carlos Pinto, J. Modeling and Parameter Estimation of Step-Growth Polymerization of Poly(Ethylene-2,5-Furandicarboxylate). *Polym. Eng. Sci.* **2018**, *58* (5), 729–741.

(50) Miura, Toshinari; Kakinuma, Hirokazu, Kawano, Takenobu; Matsuhisa, H. A 2,5-Disubstituted Furan Having Functional Groups Selected from a Hydroxymethyl Group, a Formyl Group and a Carboxyl Group, Is Oxidized with a Metal Permanganate in an Alkaline Environment Containing an Alkali Metal or Alkali Earth Metal Hydroxide. US 7411078 B2, 2008.

(51) Lincoln, J.; Drewitt, J. G. N. Polyesters From Heterocyclic Components. US2551731 A, 1951.

(52) Pfister, D.; Storti, G.; Tancini, F.; Costa, L. I.; Morbidelli, M. Synthesis and Ring-Opening Polymerization of Cyclic Butylene 2,5-Furandicarboxylate. *Macromol. Chem. Phys.* **2015**, *216* (21), 2141–2146.

(53) Jiang, Y.; Woortman, A. J. J.; Alberda Van Ekenstein, G. O. R.; Loos, K. A Biocatalytic Approach towards Sustainable Furanic-Aliphatic Polyesters. *Polym. Chem.* **2015**, *6* (29), 5198–5211.

(54) Terzopoulou, Z.; Karakatsianopoulou, E.; Kasmi, N.; Majdoub, M.; Papageorgiou, G. Z.; Bikiaris, D. N. Effect of Catalyst Type on Recyclability and Decomposition Mechanism of Poly(Ethylene Furanoate) Biobased Polyester. *J. Anal. Appl. Pyrolysis* **2017**, *126* (January), 357–370.

(55) Tsanaktsis, V.; Vouvoudi, E.; Papageorgiou, G. Z.; Papageorgiou, D. G.; Chrissafis, K.; Bikiaris, D. N. Thermal Degradation Kinetics and Decomposition Mechanism of Polyesters Based on 2,5-Furandicarboxylic Acid and Low Molecular Weight Aliphatic Diols. *J. Anal. Appl. Pyrolysis* **2015**, *112*, 369–378.

(56) Papageorgiou, G. Z.; Papageorgiou, D. G.; Tsanaktsis, V.; Bikiaris, D. N. Synthesis of the Bio-Based Polyester Poly(Propylene 2,5-Furan Dicarboxylate). Comparison of Thermal Behavior and Solid State Structure with Its Terephthalate and Naphthalate Homologues. *Polymer* **2015**, *62*, 28–38.

(57) Guidotti, G.; Soccio, M.; Lotti, N.; Gazzano, M.; Siracusa, V.; Munari, A.

Poly(Propylene 2,5-Thiophenedicarboxylate) vs. Poly(Propylene 2,5-Furandicarboxylate): Two Examples of High Gas Barrier Bio-Based Polyesters. *Polymers* **2018**, *10* (7), 785.

(58) Grosshardt, O.; Fehrenbacher, U.; Kowollik, K.; Tübke, B.; Dingenouts, N.; Wilhelm, M. Synthese Und Charakterisierung von Polyestern Und Polyamiden Auf Der Basis von Furan-2,5-Dicarbonsäure. *Chemie Ing. Tech.* **2009**, *81* (11), 1829–1835.

(59) Genovese, L.; Soccio, M.; Lotti, N.; Munari, A.; Szymczyk, A.; Paszkiewicz, S.; Linares, A.; Nogales, A.; Ezquerra, T. A. Effect of Chemical Structure on the Subglass Relaxation Dynamics of Biobased Polyesters as Revealed by Dielectric Spectroscopy: 2,5-Furandicarboxylic Acid vs. Trans -1,4-Cyclohexanedicarboxylic Acid. *Phys. Chem. Chem. Phys.* **2018**, *20* (23), 15696–15706.

(60) Zhu, J.; Cai, J.; Xie, W.; Chen, P.; Gazzano, M.; Scandola, M.; Gross, R. A. Poly(Butylene 2,5-Furandicarboxylate), a Biobased Alternative to PBT: Synthesis, Physical Properties, and Crystal Structure. *Macromolecules* **2013**, *46* (3), 796–804.

(61) Ma, J.; Yu, X.; Xu, J.; Pang, Y. Synthesis and Crystallinity of Poly(Butylene 2,5-Furandicarboxylate). *Polymer* **2012**, *53* (19), 4145–4151.

(62) Papageorgiou, G. Z.; Tsanaktsis, V.; Papageorgiou, D. G.; Exarhopoulos, S.; Papageorgiou, M.; Bikiaris, D. N. Evaluation of Polyesters from Renewable Resources as Alternatives to the Current Fossil-Based Polymers. Phase Transitions of Poly(Butylene 2,5-Furan-Dicarboxylate). *Polymer* **2014**, *55* (16), 3846–3858.

(63) Matsuda, K.; Matsuhisa, H.; Horie, H.; Komuro, T. Polymer Compound and Method of Sinthesizing the Same. US0124763 A1, 2009.

(64) Soccio, M.; Martínez-Tong, D. E.; Alegría, A.; Munari, A.; Lotti, N. Molecular Dynamics of Fully Biobased Poly(Butylene 2,5-Furanoate) as Revealed by Broadband Dielectric Spectroscopy. *Polymer* **2017**, *128*, 24–30.

(65) Tsanaktsis, V.; Terzopoulou, Z.; Nerantzaki, M.; Papageorgiou, G. Z.; Bikiaris, D. N. New Poly(Pentylene Furanoate) and Poly(Heptylene Furanoate) Sustainable Polyesters from Diols with Odd Methylene Groups. *Mater. Lett.* **2016**, *178* (May), 64–67.

(66) Shen, Y.; Yao, B.; Yu, G.; Fu, Y.; Liu, F.; Li, Z. Facile Preparation of Bio-Based

Polyesters from Furandicarboxylic Acid and Long Chain Diols via Asymmetric Monomer Strategy. *Green Chem.* **2017**, *19* (20), 4930–4938.

(67) Tsanaktsis, V.; Papageorgiou, G. Z.; Bikiaris, D. N. A Facile Method to Synthesize High-Molecular-Weight Biobased Polyesters from 2,5-Furandicarboxylic Acid and Long-Chain Diols. *J. Polym. Sci. Polym. Chem.* **2015**, *53* (22), 2617–2632.

(68) Papageorgiou, D. G.; Guigo, N.; Tsanaktsis, V.; Exarhopoulos, S.; Bikiaris, D. N.; Sbirrazzuoli, N.; Papageorgiou, G. Z. Fast Crystallization and Melting Behavior of a Long-Spaced Aliphatic Furandicarboxylate Biobased Polyester, Poly(Dodecylene 2,5-Furanoate). *Ind. Eng. Chem. Res.* **2016**, *55* (18), 5315–5326.

(69) Soares, M. J.; Dannecker, P. K.; Vilela, C.; Bastos, J.; Meier, M. A. R.; Sousa, A. F. Poly(1,20-Eicosanediyl 2,5-Furandicarboxylate), a Biodegradable Polyester from Renewable Resources. *Eur. Polym. J.* **2017**, *90*, 301–311.

(70) Sousa, A. F.; Coelho, J. F. J.; Silvestre, A. J. D. Renewable-Based Poly((Ether)Ester)s from 2,5-Furandicarboxylic Acid. *Polymer* **2016**, *98*, 129–135.

(71) Haernvall, K.; Zitzenbacher, S.; Amer, H.; Zumstein, M. T.; Sander, M.; McNeill, K.; Yamamoto, M.; Schick, M. B.; Ribitsch, D.; Guebitz, G. M. Polyol Structure Influences Enzymatic Hydrolysis of Bio-Based 2,5-Furandicarboxylic Acid (FDCA) Polyesters. *Biotechnol. J.* **2017**, *12* (9), 1600741.

(72) Gubbels, E.; Jasinska-Walc, L.; Koning, C. E. Synthesis and Characterization of Novel Renewable Polyesters Based on 2,5-Furandicarboxylic Acid and 2,3-Butanediol. *J. Polym. Sci. Polym. Chem.* **2013**, *51* (4), 890–898.

(73) Terzopoulou, Z.; Kasmi, N.; Tsanaktsis, V.; Doulakas, N.; Bikiaris, D. N.; Achilias, D. S.; Papageorgiou, G. Z. Synthesis and Characterization of Bio-Based Polyesters: Poly(2-Methyl-1,3-Propylene-2,5-Furanoate), Poly(Isosorbide-2,5-Furanoate), Poly(1,4-Cyclohexanedimethylene-2,5-Furanoate). *Materials* **2017**, *10* (7).

(74) Tsanaktsis, V.; Terzopoulou, Z.; Exarhopoulos, S.; Bikiaris, D. N.; Achilias, D. S.; Papageorgiou, D. G.; Papageorgiou, G. Z. Sustainable, Eco-Friendly Polyesters Synthesized from Renewable Resources: Preparation and Thermal Characteristics of Poly(Dimethyl-Propylene Furanoate). *Polym. Chem.* **2015**, *6* (48), 8284–8296.

(75) Genovese, L.; Lotti, N.; Siracusa, V.; Munari, A. Poly(Neopentyl Glycol Furanoate):

A Member of the Furan-Based Polyester Family with Smart Barrier Performances for Sustainable Food Packaging Applications. *Materials* **2017**, *10* (9).

(76) Storbeck, R.; Ballauff, M. Synthesis and Properties of Polyesters Based on 2,5-Furandicarboxylic Acid and 1,4:3,6-Dianhydrohexitols. *Polymer* **1993**, *34* (23), 5003–5006.

(77) Wu, J.; Eduard, P.; Thiyagarajan, S.; Noordover, B. a J.; van Es, D. S.; Koning, C. E. Semi-Aromatic Polyesters Based on a Carbohydrate-Derived Rigid Diol for Engineering Plastics. *ChemSusChem* **2015**, *8* (1), 67–72.

(78) Ghosh, T.; Mahajan, K.; Sridevi, N.-S.; Belgacem, M. N.; Gopalakrishnan, P. 2,5-Furan Dicarboxylic Acid-Based Polyesters Biomass, Prepared From. WO 2013103574 A1, 2012.

(79) Chen, M.; Yin, H.; Dong, W.; Ni, Z.; Lan, D.; Li, X. Preparation Method of Low-Yellowing 2,5-Furandicarboxylic Acid-Based Polyester. CN 102516513 A, 2011.

(80) Carman, H. S.; Killman, J. I.; Crawford, E. D.; Jenkins, J. C. Polyester Compositions Containing Furandicarboxylic Acid or an Ester Thereof and Ethylene Glycol. US 20130095269 A1, 2011.

(81) Carman, H. S.; Killman, J. I.; Crawford, E. D.; Jenkins, J. C. Polyester Compositions Containing Furandicarboxylic Acid or an Ester Thereof, Cyclobutanediol and Cyclohexanedimethanol. US 20130095270 A1, 2011.

(82) Carman, H. S.; Killman, J. I.; Crawford, E. D.; Jenkins, J. C. Polyester Composition Containing Furandicarboxylic Acid or an Ester Thereof, Ethylene Glycol and Cyclohexanedimethanol. US 20130095271 A1, 2011.

(83) Stoclet, G.; Lefebvre, J. M.; Yeniad, B.; Gobius du Sart, G.; de Vos, S. On the Strain-Induced Structural Evolution of Poly(Ethylene-2,5-Furanoate) upon Uniaxial Stretching: An in-Situ SAXS-WAXS Study. *Polymer* **2018**, *134*, 227–241.

(84) Mao, Y.; Bucknall, D. G.; Kriegel, R. M. Synchrotron X-Ray Scattering Study on Amorphous Poly(Ethylene Furanoate) under Uniaxial Deformation. *Polymer* **2018**, *139*, 60–67.

(85) Mao, Y.; Bucknall, D. G.; Kriegel, R. M. Simultaneous WAXS/SAXS Study on Semi-

Crystalline Poly(Ethylene Furanoate) under Uniaxial Stretching. *Polymer* **2018**, *143*, 228–236.

(86) Kazaryan, L.G.; Medvedeva, F. M. V. S. X-Ray Study of Poly(Ethylene Furan-2,5-Dicarboxylate) Structure. *Ser. B* **1968**, *10*, 305–306.

(87) Mao, Y.; Kriegel, R. M.; Bucknall, D. G. The Crystal Structure of Poly(Ethylene Furanoate). *Polymer* **2016**, *102*, 308–314.

(88) Maini, L.; Gigli, M.; Gazzano, M.; Lotti, N.; Bikiaris, D. N.; Papageorgiou, G. Z. Structural Investigation of Poly(Ethylene Furanoate) Polymorphs. *Polymers* **2018**, *10* (3).

(89) Araujo, C. F.; Nolasco, M. M.; Ribeiro-Claro, P. J. A.; Rudić, S.; Silvestre, A. J. D.; Vaz, P. D.; Sousa, A. F. Inside PEF: Chain Conformation and Dynamics in Crystalline and Amorphous Domains. *Macromolecules* **2018**, *51* (9), 3515–3526.

(90) Stoclet, G.; Gobius Du Sart, G.; Yeniad, B.; De Vos, S.; Lefebvre, J. M. Isothermal Crystallization and Structural Characterization of Poly(Ethylene-2,5-Furanoate). *Polymer* **2015**, *72*, 165–176.

(91) Codou, A.; Guigo, N.; Berkel, J. Van; Jong, E. De; Sbirrazzuoli, N. Non-Isothermal Crystallization Kinetics of Biobased Poly(Ethylene 2,5-Furandicarboxylate) Synthesized via the Direct Esterification Process. *Macromol. Chem. Phys. Chem. Phys.* **2014**, *215* (21), 2065−2074.

(92) Guigo, N.; van Berkel, J.; de Jong, E.; Sbirrazzuoli, N. Modelling the Non-Isothermal Crystallization of Polymers: Application to Poly(Ethylene 2,5-Furandicarboxylate). *Thermochim. Acta* **2017**, *650*, 66–75.

(93) Tsanaktsis, V.; Papageorgiou, D. G.; Exarhopoulos, S.; Bikiaris, D. N.; Papageorgiou, G. Z. Crystallization and Polymorphism of Poly(Ethylene Furanoate). *Cryst. Growth Des.* **2015**, *15* (11), 5505–5512.

(94) Dimitriadis, T.; Bikiaris, D. N.; Papageorgiou, G. Z.; Floudas, G. Molecular Dynamics of Poly(Ethylene-2,5-Furanoate) (PEF) as a Function of the Degree of Crystallinity by Dielectric Spectroscopy and Calorimetry. *Macromol. Chem. Phys.* **2016**, *217* (18), 2056–2062.

(95) Codou, A.; Moncel, M.; Van Berkel, J. G.; Guigo, N.; Sbirrazzuoli, N. Glass Transition Dynamics and Cooperativity Length of Poly(Ethylene 2,5-Furandicarboxylate) Compared to Poly(Ethylene Terephthalate). *Phys. Chem. Chem. Phys.* **2016**, *18* (25), 16647–16658.

(96) Gomes, M.; Gandini, A.; Silvestre, A. J. D.; Reis, B. Synthesis and Characterization of Poly(2,5-Furan Dicarboxylate)s Based on a Variety of Diols. *J. Polym. Sci. Polym. Chem.* **2011**, *49* (17), 3759–3768.

(97) Burgess, S. K.; Kriegel, R. M.; Koros, W. J. Carbon Dioxide Sorption and Transport in Amorphous Poly(Ethylene Furanoate). *Macromolecules* **2015**, *48* (7), 2184–2193.

(98) Burgess, S. K.; Mikkilineni, D. S.; Yu, D. B.; Kim, D. J.; Mubarak, C. R.; Kriegel, R. M.; Koros, W. J. Water Sorption in Poly(Ethylene Furanoate) Compared to Poly(Ethylene Terephthalate). Part 1: Equilibrium Sorption. *Polymer* **2014**, *55* (26), 6861–6869.

(99) Burgess, S. K.; Mikkilineni, D. S.; Yu, D. B.; Kim, D. J.; Mubarak, C. R.; Kriegel, R. M.; Koros, W. J. Water Sorption in Poly(Ethylene Furanoate) Compared to Poly(Ethylene Terephthalate). Part 2: Kinetic Sorption. *Polymer* **2014**, *55* (26), 6870–6882.

(100) Burgess, S. K.; Wenz, G. B.; Kriegel, R. M.; Koros, W. J. Penetrant Transport in Semicrystalline Poly(Ethylene Furanoate). *Polymer* **2016**, *98*, 305–310.

(101) Vannini, M.; Marchese, P.; Celli, A.; Lorenzetti, C. Fully Biobased Poly(Propylene 2,5-Furandicarboxylate) for Packaging Applications: Excellent Barrier Properties as a Function of Crystallinity. *Green Chem.* **2015**, *17* (8), 4162–4166.

(102) Avantium. YXY process technology http://avantium.com/yxy/YXY-technology/YXY-process-technology.html (accessed Sep 26, 2015).

(103) Besson, J.-P.; Bouffand, M.-B.; Reutenauer, P. Pef Container, Preform & Method for the Manufacture of Said Container by Injection Stretch Blow-Molding. WO2015015243 A1, 2015.

(104) Bouffand, M.-B.; Colloud, A.; Reutenauer, P. Bottle, Method of Making the Same and Use of Fdca and Diol Monomers in Such Bottle. WO2014032730 A1, 2014.

(105) Collias, D. I.; Kellett, P. J. Plastic Bottles for Perfume Compositions Having Improved Crazing Resistance. WO2013158477 A1, 2013.

(106) Matsuda, K.; Horie, H.; Ito, K. Plastic Film. US20120258299 A1, 2012.

(107) Avantium. Avantium and The Coca-Cola Company sign partnership agreement to develop next generation 100% plant based plastic: PEF http://avantium.com/news/2011-2/Avantium-and-The-Coca-Cola-Company-sign-partnership-agreement-to-develop-next-generation-100-plant-based-plastic-PEF.html (accessed Aug 30, 2016).

(108) Kucherov, F.; Gordeev, E.; Kashin, A.; Ananikov, V. P. 3D Printing with Biobased PEF for Carbon Neutral Manufacturing. *Angew. Chemie* **2017**, *129*, 16147–16151.

(109) Shahbazi, S.; Jafari, Y.; Moztarzadeh, F.; Mir Mohamad Sadeghi, G. Evaluation of Effective Parameters for the Synthesis of Poly(Propylene Fumarate) by Response Surface Methodology. *J. Appl. Polym. Sci.* **2014**, *131* (20), 1–8.

(110) Pellis, A.; Haernvall, K.; Pichler, C. M.; Ghazaryan, G.; Breinbauer, R.; Guebitz, G. M. Enzymatic Hydrolysis of Poly(Ethylene Furanoate). *J. Biotechnol.* **2016**, *235*, 47–53.

(111) Weinberger, S.; Canadell, J.; Quartinello, F.; Yeniad, B.; Arias, A.; Pellis, A.; Guebitz, G. Enzymatic Degradation of Poly(Ethylene 2,5-Furanoate) Powders and Amorphous Films. *Catalysts* **2017**, *7* (11), 318.

(112) Weinberger, S.; Haernvall, K.; Scaini, D.; Ghazaryan, G.; Zumstein, M. T.; Sander, M.; Pellis, A.; Guebitz, G. M. Enzymatic Surface Hydrolysis of Poly(Ethylene Furanoate) Thin Films of Various Crystallinities. *Green Chem.* **2017**, *19* (22), 5381–5384.

(113) Sipos, L.; Olson, M. L. Process for the Depolymerization of a Furandicarboxylate-Containing Polyester. WO2012091573A9, 2010.

(114) Ma, J.; Pang, Y.; Wang, M.; Xu, J.; Ma, H.; Nie, X. The Copolymerization Reactivity of Diols with 2,5-Furandicarboxylic Acid for Furan-Based Copolyester Materials. *J. Mater. Chem.* **2012**, *22* (8), 3457–3461.

(115) Sousa, A. F.; Guigo, N.; Pozycka, M.; Delgado, M.; Soares, J.; Mendonça, P. V.;

Coelho, J. F. J.; Sbirrazzuoli, N.; Silvestre, A. J. D. Tailored Design of Renewable Copolymers Based on Poly(1,4-Butylene 2,5-Furandicarboxylate) and Poly(Ethylene Glycol) with Refined Thermal Properties. *Polym. Chem.* **2018**, *9* (6), 722–731.

(116) Wang, J.; Liu, X.; Zhu, J.; Jiang, Y. Copolyesters Based on 2,5-Furandicarboxylic Acid (FDCA): Effect of 2,2,4,4-Tetramethyl-1,3-Cyclobutanediol Units on Their Properties. *Polymers* **2017**, *9* (9).

(117) Wang, J.; Liu, X.; Jia, Z.; Liu, Y.; Sun, L.; Zhu, J. Synthesis of Bio-Based Poly(Ethylene 2,5-Furandicarboxylate) Copolyesters: Higher Glass Transition Temperature, Better Transparency, and Good Barrier Properties. *J. Polym. Sci. Polym. Chem.* **2017**, *55* (19), 3298–3307.

(118) Hong, S.; Min, K.-D.; Nam, B.-U.; Park, O. O. High Molecular Weight Bio Furan-Based Co-Polyesters for Food Packaging Applications: Synthesis, Characterization and Solid-State Polymerization. *Green Chem.* **2016**, *18* (19), 5142–5150.

(119) Wang, J.; Liu, X.; Zhang, Y.; Liu, F.; Zhu, J. Modification of Poly(Ethylene 2,5-Furandicarboxylate) with 1,4-Cyclohexanedimethylene: Influence of Composition on Mechanical and Barrier Properties. *Polymer* **2016**, *103*, 1–8.

(120) Wang, J.; Liu, X.; Jia, Z.; Sun, L.; Zhang, Y.; Zhu, J. Modification of Poly(Ethylene 2,5-Furandicarboxylate) (PEF) with 1, 4-Cyclohexanedimethanol: Influence of Stereochemistry of 1,4-Cyclohexylene Units. *Polymer* **2018**, *137*, 173–185.

(121) Diao, L.; Su, K.; Li, Z.; Ding, C. Furan-Based Co-Polyesters with Enhanced Thermal Properties: Poly(1,4-Butylene-Co-1,4-Cyclohexanedimethylene-2,5-Furandicarboxylic Acid). *RSC Adv.* **2016**, *6* (33), 27632–27639.

(122) Sousa, A. F.; Coelho, J. F. J.; Silvestre, A. J. D. Renewable-Based Poly((Ether)Ester)s from 2,5-Furandicarboxylic Acid. *Polymer* **2016**, *98*, 129–135.

(123) Kasmi, N.; Majdoub, M.; Papageorgiou, G. Z.; Bikiaris, D. N. Synthesis and Crystallization of New Fully Renewable Resources-Based Copolyesters: Poly(1,4-Cyclohexanedimethanol-Co-Isosorbide 2,5-Furandicarboxylate). *Polym. Degrad. Stabil.* **2018**, *152*, 177–190.

(124) Yu, Z.; Zhou, J.; Cao, F.; Wen, B.; Zhu, X.; Wei, P. Chemosynthesis and Characterization of Fully Biomass-Based Copolymers of Ethylene Glycol, 2,5-

Furandicarboxylic Acid, and Succinic Acid. *J. Appl. Polym. Sci.* **2013**, *130* (2), 1415–1420.

(125) Papadopoulos, L.; Magaziotis, A.; Nerantzaki, M.; Terzopoulou, Z.; Papageorgiou, G. Z.; Bikiaris, D. N. Synthesis and Characterization of Novel Poly(Ethylene Furanoate-Co-Adipate) Random Copolyesters with Enhanced Biodegradability. *Polym. Degrad. Stabil.* **2018**, *156*, 32–42.

(126) Hu, H.; Zhang, R.; Wang, J.; Ying, W. Bin; Zhu, J. Fully Bio-Based Poly(Propylene Succinate-Co-Propylene Furandicarboxylate) Copolyesters with Proper Mechanical, Degradation and Barrier Properties for Green Packaging Applications. *Eur. Polym. J.* **2018**, *102*, 101–110.

(127) Hbaieb, S.; Kammoun, W.; Delaite, C.; Abid, M.; Abid, S.; El Gharbi, R. New Copolyesters Containing Aliphatic and Bio-Based Furanic Units by Bulk Copolycondensation. *J. Macromol. Sci. Part A Pure Appl. Chem.* **2015**, *52* (5), 365–373.

(128) Jacquel, N.; Saint-Loup, R.; Pascault, J.-P.; Rousseau, A.; Fenouillot, F. Bio-Based Alternatives in the Synthesis of Aliphatic-Aromatic Polyesters Dedicated to Biodegradable Film Applications. *Polymer* **2015**, *59*, 234–242.

(129) Wu, L.; Mincheva, R.; Xu, Y.; Raquez, J. M.; Dubois, P. High Molecular Weight Poly(Butylene Succinate-Co-Butylene Furandicarboxylate) Copolyesters: From Catalyzed Polycondensation Reaction to Thermomechanical Properties. *Biomacromolecules* **2012**, *13* (9), 2973–2981.

(130) Zhou, W.; Wang, X.; Yang, B.; Xu, Y.; Zhang, W.; Zhang, Y.; Ji, J. Synthesis, Physical Properties and Enzymatic Degradation of Bio-Based Poly(Butylene Adipate-Co-Butylene Furandicarboxylate) Copolyesters. *Polym. Degrad. Stabil.* **2013**, *98* (11), 2177–2183.

(131) Peng, S.; Bu, Z.; Wu, L.; Li, B. G.; Dubois, P. High Molecular Weight Poly(Butylene Succinate-Co-Furandicarboxylate) with 10 Mol% of BF Unit: Synthesis, Crystallization-Melting Behavior and Mechanical Properties. *Eur. Polym. J.* **2017**, *96* (May), 248–255.

(132) Peng, S.; Wu, B. S.; Wu, L.; Li, B. G.; Dubois, P. Hydrolytic Degradation of Biobased

Poly(Butylene Succinate-Co-Furandicarboxylate) and Poly(Butylene Adipate-Co-Furandicarboxylate) Copolyesters under Mild Conditions. *J. Appl. Polym. Sci.* **2017**, *134* (15), 1–10.

(133) Papageorgiou, G. Z.; Papageorgiou, D. G. Solid-State Structure and Thermal Characteristics of a Sustainable Biobased Copolymer: Poly(Butylene Succinate-Co-Furanoate). *Thermochim. Acta* **2017**, *656* (September), 112–122.

(134) Morales-Huerta, J. C.; Ciulik, C. B.; De Ilarduya, A. M.; Muñoz-Guerra, S. Fully Bio-Based Aromatic-Aliphatic Copolyesters: Poly(Butylene Furandicarboxylate-Co-Succinate)s Obtained by Ring Opening Polymerization. *Polym. Chem.* **2017**, *8* (4), 748–760.

(135) Wu, B.; Xu, Y.; Bu, Z.; Wu, L.; Li, B. G.; Dubois, P. Biobased Poly(Butylene 2,5-Furandicarboxylate) and Poly(Butylene Adipate-Co-Butylene 2,5-Furandicarboxylate)s: From Synthesis Using Highly Purified 2,5-Furandicarboxylic Acid to Thermo-Mechanical Properties. *Polymer* **2014**, *55* (16), 3648–3655.

(136) Bastioli, C.; Borsotti, G.; Capuzzi, L.; Vallero, R. Aliphatic-Aromatic Biodegradable Polyester. WO2009135921 A1, 2011.

(137) Bioplastics, E. Standardisation http://en.european-bioplastics.org/standards/standardization/ (accessed May 26, 2015).

(138) Jacquel, N.; Saint-Loup, R.; Fenouillot, R. F.; Pascault, J. P.; Rousseau, A. Polymers, the Process for the Synthesis Thereof and Compositions Comprising Same. WO2013144525 A1, September 1, 2013.

(139) Jia, Z.; Wang, J.; Sun, L.; Zhu, J.; Liu, X. Fully Bio-Based Polyesters Derived from 2,5-Furandicarboxylic Acid (2,5-FDCA) and Dodecanedioic Acid (DDCA): From Semicrystalline Thermoplastic to Amorphous Elastomer. *J. Appl. Polym. Sci.* **2018**, *135* (14).

(140) Soccio, M.; Costa, M.; Lotti, N.; Gazzano, M.; Siracusa, V.; Salatelli, E.; Manaresi, P.; Munari, A. Novel Fully Biobased Poly(Butylene 2,5-Furanoate/Diglycolate) Copolymers Containing Ether Linkages: Structure-Property Relationships. *Eur. Polym. J.* **2016**, *81*, 397–412.

(141) Matos, M.; Sousa, A. F.; Fonseca, A. C.; Freire, C. S. R.; Coelho, J. F. J.; Silvestre,

A. J. D. A New Generation of Furanic Copolyesters with Enhanced Degradability: Poly(Ethylene 2,5-Furandicarboxylate)-Co-Poly(Lactic Acid) Copolyesters. *Macromol. Chem. Phys.* **2014**, *215* (22), 2175–2184.

(142) Wu, H.; Wen, B.; Zhou, H.; Zhou, J.; Yu, Z.; Cui, L.; Huang, T.; Cao, F. Synthesis and Degradability of Copolyesters of 2, 5-Furandicarboxylic Acid, Lactic Acid, and Ethylene Glycol. *Polym. Degrad. Stabil.* **2015**, *121*, 100–104.

(143) Kwiatkowska, M.; Kowalczyk, I.; Kwiatkowski, K.; Szymczyk, A.; Rosłaniec, Z. Fully Biobased Multiblock Copolymers of Furan-Aromatic Polyester and Dimerized Fatty Acid: Synthesis and Characterization. *Polymer* **2016**, *99* (August), 503–512.

(144) Wang, X.; Wang, Q.; Liu, S.; Wang, G. Biobased Copolyesters: Synthesis, Structure, Thermal and Mechanical Properties of Poly(Ethylene 2,5-Furandicarboxylate-Co-Ethylene 1,4-Cyclohexanedicarboxylate). *Polym. Degrad. Stabil.* **2018**, *154*, 96–102.

(145) Atsushi, K.; Satoshi, K. Method for Producing Polyester Resin Including Furan Structure. JP2008/291244, 2008.

(146) Cai, X.; Yang, X.; Zhang, H.; Wang, G. Aliphatic-Aromatic Poly(Carbonate-Co-Ester)s Containing Biobased Furan Monomer: Synthesis and Thermo-Mechanical Properties. *Polymer* **2018**, *134*, 63–70.

(147) Hu, H.; Zhang, R.; Wang, J.; Ying, W. Bin; Zhu, J. Synthesis and Structure-Property Relationship of Bio-Based Biodegradable Poly(Butylene Carbonate-Co-Furandicarboxylate). *ACS Sustain. Chem. Eng.* **2018**, *6* (6), 7488–7498.

(148) Wang, G.; Jiang, M.; Zhang, Q.; Wang, R.; Zhou, G. Biobased Multiblock Copolymers: Synthesis, Properties and Shape Memory Performance of Poly(Ethylene 2,5-Furandicarboxylate)-b-Poly(Ethylene Glycol). *Polym. Degrad. Stabil.* **2017**, *144*, 121–127.

(149) Wang, G.; Jiang, M.; Zhang, Q.; Wang, R.; Qu, X.; Zhou, G. Biobased Multiblock Copolymers: Synthesis, Properties and Shape Memory Behavior of Poly(Hexamethylene 2,5-Furandicarboxylate)-b-Poly(Ethylene Glycol). *Polym. Degrad. Stabil.* **2018**, *153*, 292–297.

(150) Hu, H.; Zhang, R.; Sousa, A.; Long, Y.; Ying, W. Bin; Wang, J.; Zhu, J. Bio-Based Poly(Butylene 2,5-Furandicarboxylate)-b-Poly(Ethylene Glycol) Copolymers with

Adjustable Degradation Rate and Mechanical Properties: Synthesis and Characterization. *Eur. Polym. J.* **2018**, *106* (July), 42–52.

(151) Zhou, W.; Zhang, Y.; Xu, Y.; Wang, P.; Gao, L.; Zhang, W.; Ji, J. Synthesis and Characterization of Bio-Based Poly(Butylene Furandicarboxylate)-b-Poly(Tetramethylene Glycol) Copolymers. *Polym. Degrad. Stabil.* **2014**, *109*, 21–26.

(152) Chi, D.; Liu, F.; Na, H.; Chen, J.; Hao, C.; Zhu, J. Poly(Neopentyl Glycol 2,5-Furandicarboxylate): A Promising Hard Segment for the Development of Bio-Based Thermoplastic Poly(Ether-Ester) Elastomer with High Performance. *ACS Sustain. Chem. Eng.* **2018**, *6* (8), 9893–9902.

(153) Tansengco, M. L.; Tokiwa, Y. Thermophilic Microbial Degradation of Polyethylene Succinate. *World J. Microbiol. Biotechnol.* **1998**, *14*, 133–138.

(154) Luo, S.; Li, F.; Yu, J.; Cao, A. Synthesis of Poly(Butylene Succinate-Co-Butylene Terephthalate) (PBST) Copolyesters with High Molecular Weights via Direct Esterification and Polycondensation. *J. of Applied Polymer Sci.* **2010**, *115*, 2203–2211.

(155) Ahn, B. D.; Kim, S. H.; Kim, Y. H.; Yang, J. S. Synthesis and Characterization of the Biodegradable Copolymers from Succinic Acid and Adipic Acid with 1,4-Butanediol. *J. Appl. Polym. Sci.* **2001**, *82* (11), 2808–2826.

(156) Nikolic, M. S.; Djonlagic, J. Synthesis and Characterization of Biodegradable Poly (Butylene Succinate- Co -Butylene Adipate). *Polym. Degrad. Stabil.* **2001**, *74* (2), 263–270.

(157) Xu, J.; Guo, B.-H. Poly(Butylene Succinate) and Its Copolymers: Research, Development and Industrialization. *Biotechnol. J.* **2010**, *5* (11), 1149–1163.

(158) Pivsa-Art, W.; Chaiyasat, A.; Pivsa-Art, S.; Yamane, H.; Ohara, H. Preparation of Polymer Blends between Poly(Lactic Acid) and Poly(Butylene Adipate-Co-Terephthalate) and Biodegradable Polymers as Compatibilizers. *Energy Procedia* **2013**, *34*, 549–554.

(159) Lai, S.; Gao, Y.; Yue, L. Heterogeneous Catalytic Synthesis of Poly(Butylene Succinate) by Attapulgite-Supported Sn Catalyst. *J. Appl. Polym. Sci.* **2015**, *132* (13), 1–9.

(160) Tserki, V.; Matzinos, P.; Pavlidou, E.; Vachliotis, D.; Panayiotou, C. Biodegradable Aliphatic Polyesters. Part I. Properties and Biodegradation of Poly(Butylene Succinate-Co-Butylene Adipate). *Polym. Degrad. Stabil.* **2006**, *91* (2), 367–376.

(161) Goods, G. Biodegradable and compostable definitions http://www.greengood.com/terms_to_know/biodegradable_and_compostable_definitions.htm (accessed Jan 20, 2016).

(162) Zhang, C. Biodegradable Polyesters : Synthesis , Properties , Applications. In *Biodegradable Polyesters*; Fakirov, S., Ed.; Wiley-VCH Verlag GmbH & Co. KGaA: Weinheim, Germany, 2015; pp 1–19.

(163) Tokiwa, Y.; Calabia, B. P.; Ugwu, C. U.; Aiba, S. Biodegradability of Plastics. *Int. J. Mol. Sci.* **2009**, *10* (9), 3722–3742.

(164) Chen, Y.; Tan, L.; Chen, L.; Yang, Y.; Wang, X. Study on Biodegradable Aromatic/Aliphatic Copolyesters. *Brazilian J. Chem. Eng.* **2008**, *25* (2), 321–335.

(165) Standardization, E. C. for. Requirements for Packaging Recoverable Trough Composting and Biodegradation-Test Scheme and Evaluation Criteria for the Final Acceptance of Packaging (EN 13432 : 2001). 2001.

PART B

FDCA-based polymers and composites

Chapter III – Improving the Thermal Properties of Poly(2,5-furandicarboxylate)s Using Cyclohexylene Moieties: A Comparative Study

This chapter was published in:

Marina Matos, Andreia F. Sousa, Armando J. D. Silvestre. Improving the Thermal Properties of Poly(2,5-furandicarboxylate)s Using Cyclohexylene Moieties: A comparative Study, *Macromolecular Chemistry and Physics*, **2016**, 218 (5), 1600492.

Abstract

The search for new polymers from renewable origin is a sparkling field in polymer chemistry, especially those having promising properties, for example, in terms of their thermal performance. In this vein, in this study, an original renewable 2,5-furandicarboxylic acid-based cycloaliphatic homopolyester, poly(1,4-cyclohexylene 2,5-furandicarboxylate) (PCdF), is synthesised from dimethyl-2,5-furandicarboxylate and 1,4-cyclohexanediol. Poly(1,4-cyclohexanedimethylene 2,5-furandicarboxylate) is also prepared for comparison purposes, since it is the direct renewable substitute of poly(1,4-cyclohexanedimethylene terephthalate) and they are structurally related. The resulting homopolyesters are characterised in detail by using attenuated total reflectance Fourier transform infrared, ^{1}H, ^{13}C and 2D NMR, X-ray and elemental analysis, and thermal properties are assessed by thermogravimetric analysis, differential scanning calorimetry, and dynamic mechanical thermal analysis. PCdF shows to have a semi-crystalline character, exhibiting an extremely high glass transition temperature around 175 ºC. Moreover, this polyester also shows to be a high thermally stable material with a degradation temperature of 380.0 ºC.

Keywords: 1,4-cyclohexanedimethanol; 1,4-cyclohexanediol; 2,5-furandicarboxylic acid; enhanced thermal properties; furanic-cycloaliphatic polyesters.

1. Introduction

Polyesters, well-known as highly versatile materials, have a high importance in a broad range of commodity applications spanning from packaging plastics, typically for soft drinks, water, and alcoholic beverages as well as textiles; to films; sheeting; and resins for moulding up including sophisticated precision pieces for medical and electronic applications.[1]

Poly(ethylene terephthalate) (PET) and poly(butylene terephthalate) (PBT) are the most applied thermoplastics with a wide range of applications, mostly due to their well-known good mechanical properties and excellent chemical resistance, as well as their electrical insulation properties.[2] Furthermore, the fact that these polymers show a combination of high glass transition (T_g) and high melting temperatures (T_m) (75 and 250 ºC for PET, and 35 and 225 ºC for PBT, respectively),[3,4] enables them to maintain their shape and mechanical

properties at high temperatures, positioning them into a privileged position among all thermoplastic materials.[5] Another relevant example, which had some commercial relevance as fibbers (Kodel fibres),[1] is also based on terephthalic acid (TPA) but incorporating the rigid cycloaliphatic monomer, 1,4-cyclohexanedimethanol (CHDM). The ensuing poly(1,4-cyclohexanedimethylene terephthalate) (PCT) is a high performance polyester with a T_m between 278-318 °C, much higher than that of PET or PBT.[6]

Many other polyesters based on TPA have a spotlighted importance in polymer scene, however in recent years, concerns regarding fossil feedstock availability, price instability, as well as environmental issues associated with their massive consumption, CO_2 emissions and improper disposal, lead to an increasing research activity to find sustainable and environmentally friendly alternatives, mainly using plant biomass as the primary raw material.[7–10] In fact, within the biorefinery concept, biomass is expected to be efficiently converted (calling upon sustainable and environmentally friendly processes) into fuels, energy, chemicals and materials.[11] In this context, 2,5-furandicarboxylic acid (FDCA), that can be easily obtained from hexoses, has been considered as one of the most important platform chemicals for a panoply of applications,[8] among which polyester synthesis is probably one of the most promising.[12] In fact, a significant number of FDCA-based materials have already been successfully synthesised, showing often similar properties to those of the TPA counterpart,[13] and in the case of poly(ethylene 2,5-furandicarboxylate) (PEF) already produced at pilot scale.

However, oppositely to the increasing number of FDCA-based polyesters using linear short-chain aliphatic alcohols,[13,14,23–32,15,33,16–22] the studies involving cycloaliphatic monomers are scarce. In fact, only a few studies were dedicated to this specific domain, apart from the pioneering work of Moore and Kelly, in the late 1970's,[34,35] where the direct polycondensation of 2,5-furandicarbonyl dichloride with 2,5-bis(hydroxymethyl) tetrahydrofuran was reported. It was only several decades later that the synthesis of FDCA-based homopolyesters with other cyclic diols, mainly 1,4:3,6-dianhydrohexitols was reported.[2,36–40] Several other results have also been patented, focusing the synthesis or specific applications of FDCA-based polyesters, using dianhydrohexitols[39,40] and other cyclic monomers, such as, dichloro-2,3-*o*-isopropylidene *L*-tartrate,[41] 1,4-cyclohexanedimethanol[42–44] or 2,2,4,4-tetramethylcyclobutane-1,3-diol,[45] as well as combinations of both,[46] with ethylene glycol[47] or 1,4-butanediol.[43]

Recently, Sousa et al.[48] reported the synthesis of FDCA-based copolymers incorporating isosorbide and different number-average molecular weight poly(ethylene glycol) (PEG200, PEG400 or PEG2000). The resulting materials have shown better or comparable T_g to their petro-based counterparts.

In this vein, the incorporation of more rigid cycloaliphatic monomers into the polyesters backbone could be a very interesting approach to obtain materials with enhanced thermal and mechanical properties. To achieve this goal it is expected that the incorporation of 1,4-cyclohexanediol (CHD) in FDCA-based polyesters could lead to materials with enhanced thermal properties and at same time with good processability. Thus, in this study poly(1,4-cyclohexylene 2,5-furandicarboxylate) (PCdF) was synthesized using two approaches, namely the two-step polytransesterification procedure (transesterification followed by a polytransesterification), and the direct polycondensation reaction. Moreover, the synthesis of poly(1,4-cyclohexanedimethylene 2,5-furandicarboxylate) (PCF) was also performed for comparison, since this polyester is the direct furanic-renewable substitute of PCT and they are structurally related.

Finally, the ensuing polyesters were fully characterized by size-exclusion chromatography (SEC), attenuated total reflectance Fourier transform infrared (ATR FTIR), ^{1}H, ^{13}C and HSQC NMR, elemental analysis, as well as by thermogravimetric analysis (TGA), differential scanning calorimetry (DSC), dynamic mechanical thermal analysis (DMTA), and X-ray diffraction (XRD) techniques.

2. Experimental

2.1. Materials

1,4-Cyclohexanediol (99.99 %, cis/trans 43/57), 1,4-cyclohexanedimethanol (99.99 %, cis/trans 46/54), zinc acetate ($Zn(OAc)_2$, > 99.99 %), trifluoroacetic acid (TFA, 99 %), and deuterated trifluoroacetic acid, (TFA-*d*, 99 atom % D) were purchased from Sigma-Aldrich Chemicals Co. 2,5-Furandicarboxylic acid (FDCA, >98%) and 1,1,1,3,3,3-hexafluoro-2-propanol (HFP, >99 %) were purchased from TCI Europe N.V. Concentrated hydrochloric acid (HCl, 37 %) was purchased from Panreac, and methanol, chloroform, dichloromethane, among other solvents (pro-analysis and HPLC grade) were purchased from Fisher Scientific.

Polystyrene standards with molecular weights between 4 290 and 66 350 Da were supplied by Polymer Laboratories. All chemicals were used as received, without further purification.

2.2. Synthesis

2.2.1. Synthesis of dimethyl 2,5-furandicarboxylate (DMFDC)

The synthesis of DMFDC followed a previously reported procedure.[14] Typically, DMFDC was prepared by reacting FDCA with an excess of methanol, under acidic conditions (HCl). The final product was isolated in 71 % yield as a white powder. FTIR (ν/cm^{-1}): 3168 (=CH); 2965 (C-H); 1706 (C=O); 1578, 1522 (C=C); 1288 (C-O); 1024 (furan ring breathing); 969, 825, 757 (2,5-dibustituted furan ring). ^{1}H NMR (300 MHz, $CDCl_3$, δ/ ppm): 7.2 (s, *H*3/*H*4 furan ring); 3.9 (s, 2,5-COOC*H*$_3$). ^{13}C NMR (75 MHz, $CDCl_3$, δ/ppm): 158 (2,5-*C*=O); 147 (*C*2/*C*5 furan ring); 118 (*C*3/*C*4 furan ring); 52 (2,5-COO*C*H$_3$).

2.2.2. Synthesis of 2,5-furandicarbonyl dichloride (FDCDCl)

The synthesis of FDCDCl followed a previously reported procedure.[37] Typically, FDCDCl was prepared in solution using FDCA (≈2 g) dissolved in dimethylformamide (DMF ≈50 μL) and an excess of $SOCl_2$ (≈5 mL). The mixture was refluxed at 80 ºC for 6 h, with constant stirring. Subsequently, the excess of $SOCl_2$ and DMF was removed under vacuum at room temperature and finally the pure dichloride monomer was isolated by vacuum sublimation, at ≈60 ºC. The final product was isolated in 60% yield as a white powder. FTIR (ν/cm^{-1}): 3141, 3109 (=C-H); 1731 (C=O); 1046 (furan ring breathing); 977, 829, 767 (2,5-dibustituted furan ring). ^{1}H NMR (300 MHz, $CDCl_3$, δ/ppm): 7.5 (s, *H*3/*H*4). ^{13}C NMR (75 MHz, $CDCl_3$, δ/ppm): 156 (2,5-*C*=O); 149 (*C*2/*C*5); 123 (*C*3/*C*4).

2.3. Melt polytransesterification reactions

Reactions were carried out in bulk using DMFDC (5.45×10^{-3} mol) and an excess of either CHD or CHDM (1.5:1 diol to dimethyl ester), using ZnAc or TBT as catalysts (1 wt% relative to the total mass of monomers). The mixture was heated progressively from 110 to 180 ºC during the course of the first 3 h under nitrogen atmosphere, and then up to 220 ºC

during 4 h, under vacuum (~10^{-3} mbar) with constant stirring. The reaction mixtures were dissolved in TFA (~20 mL), and then the polymers precipitated, by pouring into an excess of methanol (~1 L) to remove the catalyst, unreacted monomers and the soluble oligomers; the resulting PCdF or PCF were filtered, dried at 40 ºC, and weighted.

2.4. Solution polycondensation reactions

Reactions were carried out in solution following a previously reported procedure.[37] Typically, the dried diol monomer, either CHD or CHDM (1:1 diol to FDCDCl) dissolved in TCE (1.0 ml), were mixed with anhydrous pyridine (1.7 ml). Then, this mixture was allowed to cool down to about 0 ºC using an ice bath, and an equimolar amount of FDCDCl (ca. 1.81 mmol), dissolved in TCE (1.5 ml), was added dropwise, under nitrogen flux, and with vigorous stirring. The reaction was allowed to proceed at room temperature, while its viscosity increased progressively, during ≈ 7 h. The ensuing PCdF and PCF polymers were precipitated in an excess of cold methanol, filtrated, dried at 40 ºC, and finally weighted.

2.5. Characterization methods

SEC analyses of homopolyesters were performed on a home-made chromatographer equipped with a PL-EMD 960 light scattering detector, using a set of two PL HFIP columns (300 mm × 7.5 mm) and one PL HFIP gel guard column (50 mm × 7.5 mm), kept at 40 ºC, and previously calibrated with polystyrene standards in the range of 4 290 to 66 350 Da. A mixture of CH_2Cl_2/$CHCl_3$/HFP (70/20/10 v/v/v%) was used as the mobile phase with a flow rate of 0.7 mL min^{-1}. All polymers were dissolved using the mobile phase (~3 mg mL^{-1}), and filtered through a 0.2 µm PTFE membranes before injection.

Elemental analyses (C and H) were conducted in triplicate using a LECO TruSpec analyser.

ATR FTIR spectra were obtained using a PARAGON 1000 Perkin-Elmer FTIR spectrometer equipped with a single-horizontal Golden Gate ATR cell. The spectra were recorded after 128 scans, at a resolution of 4 cm^{-1}, within the range of 500–4000 cm^{-1}.

^{1}H, ^{13}C and HSQC (2D) NMR spectra were recorded in TFA-*d* using a Bruker AMX 300 spectrometer, operating at 300 or 75 MHz, respectively. All chemical shifts (δ) are expressed as parts per million (ppm), downfield from tetramethylsilane (used as the internal standard).

TGA analyses were carried out with a Setaram SETSYS analyzer equipped with an alumina plate. Thermograms were recorded under a nitrogen flow of 20 mL min^{-1} and heated at a constant rate of 10 ºC min^{-1} from room temperature up to 800 ºC. Thermal decomposition temperatures were taken at the extrapolated onset temperature of weight loss step and at maximum decomposition temperatures from the heated samples ($T_{d,on}$ and T_d, respectively).

DSC thermograms were obtained with a DSC Q100 V9.9 Build 303 (Universal V4.5A) calorimeter from Texas Instruments, using aluminum DSC pans. Scans were carried out under nitrogen with a heating rate of 10 ºC min^{-1} in the temperature range from 0 to 300 ºC. Two heating/cooling cycles were repeated. Glass transitions (T_g) were determined using the midpoint approach (second heating trace), cold crystallization (T_{cc}) and melting temperatures (T_m) were determined as the maximum of the exothermic crystallization peak and the minimum of the melting endothermic peak during the second heating cycle, respectively.

DMTA analyses were performed in a material pocket accessory with a Tritec 2000 DMA Triton, operating in the single cantilever mode. Tests were performed at 1 and 10 Hz and the temperature was varied from -90 to 250 ºC, at 2 ºC/min. T_g were determined as the maximum peak of tan δ, respectively.

XRD measurements were performed using a Philips X'pert MPD diffractometer operating with CuKα radiation (λ = 1.5405980 Å) at 40 kV and 50 mA. Samples were scanned in the 2θ range of 5 to 50º, with a step size of 0.04º, and time per step of 50 s.

3. Results and Discussion

3.1. From PCdF synthesis to its structural characterization

The new PCdF homopolyester was prepared by two distinct approaches, namely melt polyesterification approach (Sheme 1a), or direct polycondensation system (Scheme 1b)) (Table 3.1). In the former case the renewable-based DMFDC and the cycloaliphatic CHD (Scheme 1a)) reacted by applying the conventional two-step melt polyesterification approach,[14] in the presence of TBT or ZnAc catalysts. These reactions were circumspectly conducted at relatively moderate temperatures, not exceeding 220 ºC, to avoid undesirable side reactions involving the furan moiety (*e.g.* decarboxylation reactions leading to color problem issues),[12] or the secondary diol CHD decomposition (*e.g.* through elimination reactions). Reaction time did not exceed 7 hours for the same reasons.

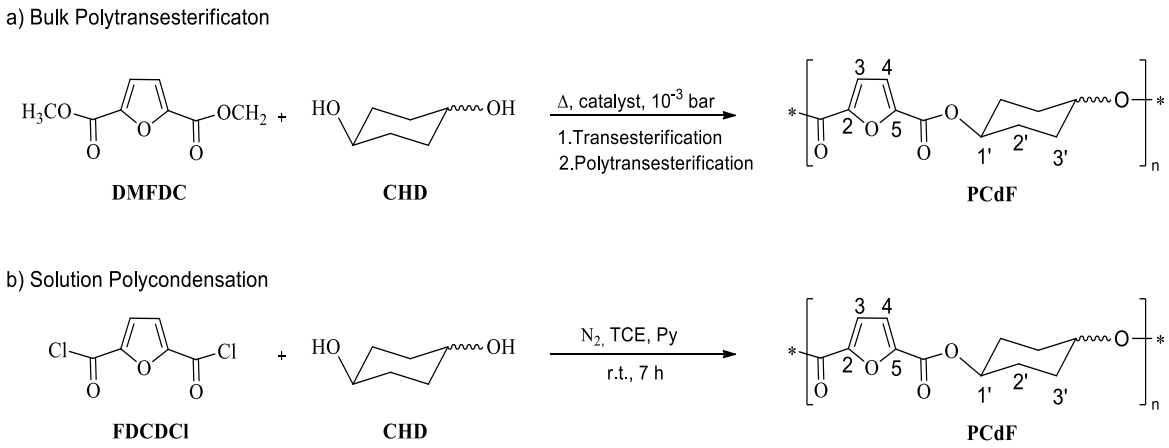

Scheme 1. Synthesis of PCdF via two conventional polymerization approaches: a) bulk polytransesterification reaction, and b) solution polycondensation reaction.

Table 3.1. Experimental data for all the polymerization reactions carried out in this study.

Polyester	Experimental conditions	yield (%)[a)]	M_w[b)]	$Đ$[c)]
PCdF1	**melt polytransesterification; TBT**	50	9 800	1.5
PCdF2	**melt polytransesterification; ZnAc**	33	4 300	1.2
PCdF3	**solution polycondensation**	43	4 300	1.2
PCF1	**melt polytransesterification; TBT**	67	14 100	1.7
PCF2	**melt polytransesterification; ZnAc**	57	11 400	1.7
PCF3	**solution polycondensation**	62	12 100	1.7

[a)] Related to the amount of polymer recovered after precipitation in methanol; [b)] weight-average molecular weight (M_w), determined by SEC in DCM/$CHCl_3$/HFP; [c)] Polidispersity index ($Đ$) determined by SEC in DCM/$CHCl_3$/HFP.

Direct solution polycondensation of FDCDCl and CHD (Scheme 1b)) was also performed at mild reaction conditions to assess their influence on the ensuing reaction products. Additionally, PCF, prepared in this case using CHDM, was also synthesized using similar approaches with the specific aim of providing a comparison point (Table 3.1).

A priori the use of other synthetic approaches could be adopted, including an interesting one recently proposed,[49] however the relatively mild reaction conditions would still have to be applied to avoid side-reaction (vide infra).

The ensuing white PCdF and PCF homopolyesters were isolated, after a purification step to remove the catalyst, unreacted monomers, and low molecular weight soluble oligomers,

in isolation yields ranging from 33 to 67% (Table 3.1), being the highest values obtained for the melt polytransesterification approach using TBT as catalyst (50 and 67% for PCdF and PCF, respectively). However, both polyesters obtained with TBT as catalyst had weight average molecular weight values consistently higher than with the other synthetic conditions (*e.g.*, around 9800 and 4300 for PCdF1 and PCdF2-3, respectively), and the *Đ* values varied between 1.5–1.7. Therefore, the following characterization results refer to the resulting products obtained from melt polyesterification reactions using TBT as catalyst, namely PCdF1 and PCF1, since they had shown the highest isolation yields and accordingly also the highest molecular weight values.

Additionally, also in terms of weight-average molecular weights, PCF had always higher values than PCdF counterpart independent of the synthetic method adopted (*e.g.*, 9800 and 14 100 for PCdF1 and PCF1, respectively). This trend was already previously observed in the synthesis of other CHD-, CHDM-based polycondensates, due most probably to a higher chain stiffness of the CHD-related polymers.[50]

The elemental composition of both homopolymers (Table 3.2) was verified by the elemental analysis of carbon (% C) and hydrogen (% H), while the oxygen content (% O) was assessed by difference to 100% of the former two. The experimental results obtained for both polyesters were found to be in agreement with the calculated elemental composition, excluding a possible presence of low molecular weight oligomers.

Table 3.2. Elemental analysis results (%) of PCdF1 and PCF1.

Polyester	Element	Calculated (%)	Experimental (%)
PCdF1	**C**	61.52	61.13
	H	4.31	4.25
	O	34.17	34.62
PCF1	**C**	60.31	61.33
	H	5.08	5.30
	O	34.61	33.37

The ATR FTIR spectrum (Figure 3.1) of PCdF1 was found to be consistent with its expected macromolecular structure, exhibiting a very intense band near 1720 cm^{-1}, arising from the C=O stretching vibration, typical of ester groups, and the C–O stretching vibration appeared around 1273 cm^{-1}. No significant absorption in the OH stretching region was

detected, suggesting that the polymer had reached a plausibly reaction yield. Additionally, it was also observed two weak bands near 3150 and 3112 cm^{-1} arising from the stretching modes of the =C–H bond of the furanic heterocycle, as well as two weak bands near 2923 and 2854 cm^{-1} assigned to the stretching modes of the C–H bond of cycloaliphatic methylene groups. Moreover, the typical vibration modes of 2,5-disubstituted furans were also observed near 983, 843, and 768 cm^{-1}. The ATR FTIR spectrum of PCF1 (Figure 3.1) was consistent with the characteristic features of PCdF1 counterpart and also with previously published data for PCF.[43]

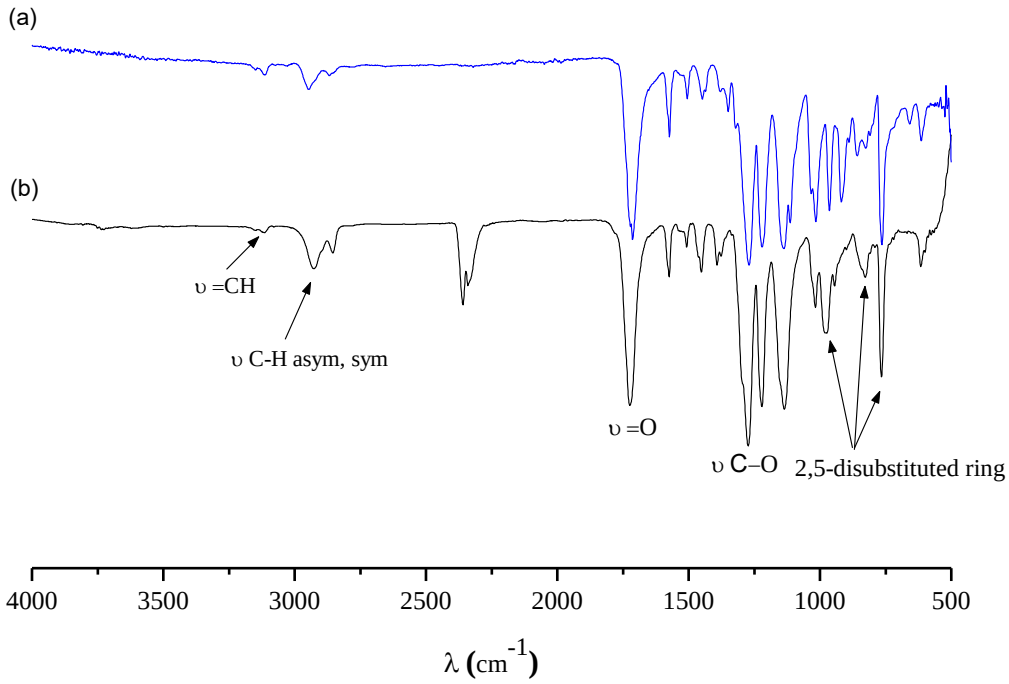

Figure 3.1. ATR FTIR spectra of (a)PCdF1 and (b) PCF1 homopolyesters.

The ^{1}H and ^{13}C NMR spectroscopic analyses have unambiguously confirmed the PCdF1 and PCF1 polyesters'structure (Figure 3.2 a, b and Table 3.3).

The ^{1}H NMR spectrum of PCdF1 (Figure 3.2 a) displayed in the region of $\delta \approx 7.7–4.8$ ppm (dashed square limits of Figure 3.2 a) the typical resonances of H-3 and H-4 of the furan moiety, in the vicinity of *cis*- and *trans*-isomers of the CHD moiety, at around 7.6 and 7.5 ppm, respectively; and the resonances of 2,5-COOC*H* (H-1′) protons attributed to both *cis*- and *trans*-isomers of CHD at 5.5 ppm.

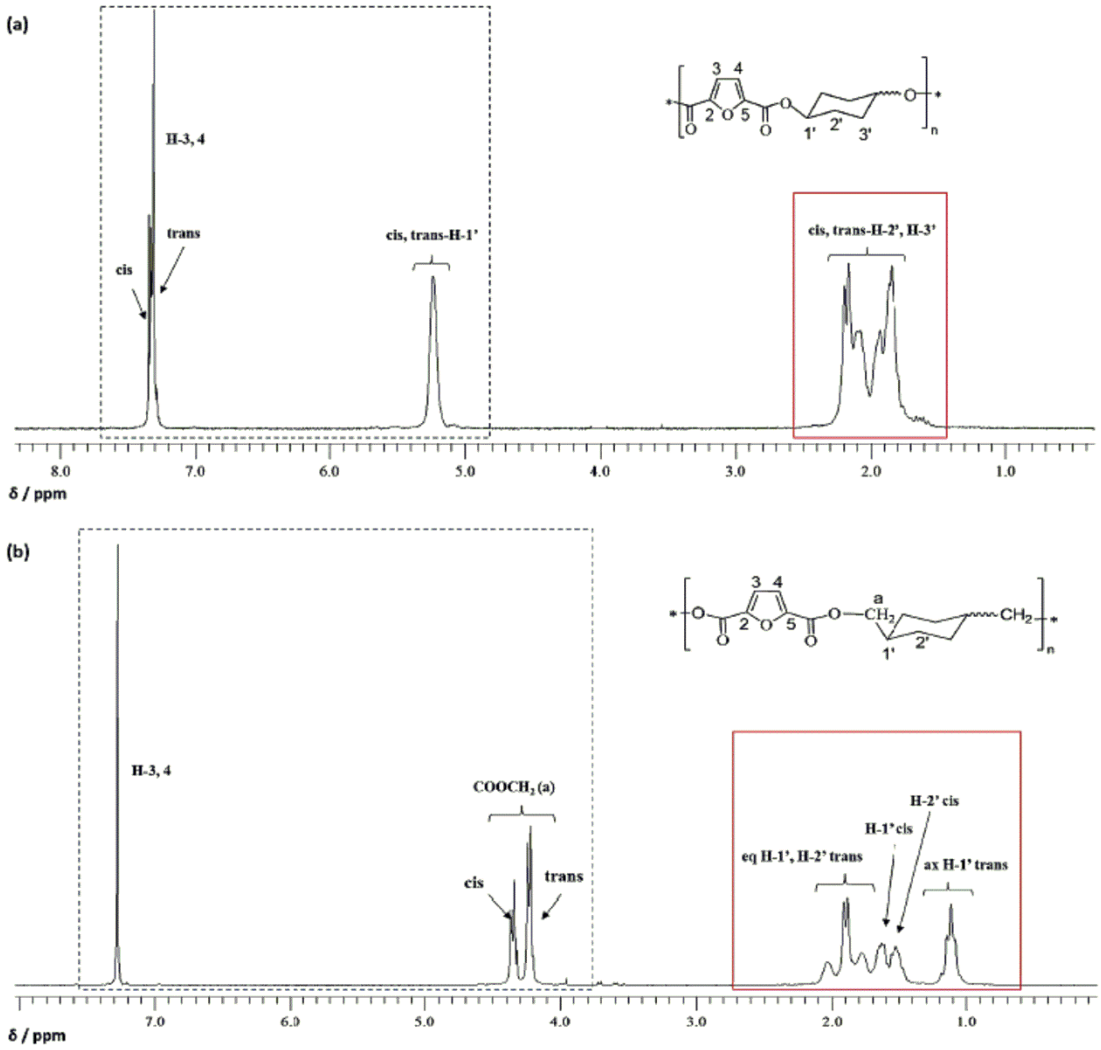

Figure 3.2. ^{1}H NMR spectra of a) PCdF1 and b) PCF1 in TFA-*d*.

In the case of PCF1 polymer (Figure 3.2 b)) the resonances of C*H* protons (H-3 and H-4) from the furan ring were also observed at 7.2 ppm, but no distinguishable split related with *cis*- and *trans*- isomers of CHDM moiety was detected.

Additionally, the spectrum of PCF1 displayed at 4.3 and 4.2 ppm the proton resonances of 2,5-COOCH_2 (H-a) groups attributed to the *trans*- and *cis*-isomers, respectively.

The ^{13}C NMR spectra of PCdF1 and PCF1 were in accordance with their ^{1}H NMR results in the above mentioned region, displaying in both cases the resonances assigned to the furan carbons C-2,5 and C-3,4 at 146.4 and 119.4 ppm, respectively, and the carbonyl carbons at 160.5 ppm.

Table 3.3. Assignment of the ^{1}H and ^{13}C NMR chemical shifts relative to PCdF1 and PCF1.

	PCdF1		PCF1	
Assignment	**^{1}H δ [ppm]**	**^{13}C δ [ppm]**	**^{1}H δ [ppm]**	**^{13}C δ [ppm]**
3, 4	7.6, *cis*- 7.5, *trans*-	119.4	7.3, *cis*- and *trans*-	119.4
2, 5	-	146.4	-	146.4
2,5-COO	-	160.5	-	160.5
($COOCH_2$)	-	-	4.4, *cis*- 4.2, *trans*-	71.5, *trans*- 69.7, *cis*-
1’	5.5, *cis*- and *trans*-	74.5, *trans*- 73.9, *cis*-	1.1, ax, *trans*- 1.6, *cis*-	36.4, *trans*- 33.9, *cis*-
2’	2.5-2.0, *cis*- and *trans*-	26.5, 26.2, 25.7, *cis*- and *trans*-	1.7-2.1, ax, eq, *trans*- 1.5, *cis*-	27.7, *trans*- 24.1, *cis*-
3’			-	-

Moreover, the ^{1}H NMR analysis of PCdF1 in the region comprising $\delta \approx 2.5–1.5$ ppm (line square limits of Figure 3.2 a) displayed the typical chemical shifts of methylene protons (H-2′ and H-3′) of the cyclohexylene moiety; being, however, impossible to distinguish between the different chemical environments attributed to each protons of *cis*- and *trans*-isomers, mostly due to the overlap of their resonances. In the case of PCF1 (Figure 3.2 b)), the resonance of ax H-1′and eq and ax H-2′ are displayed at around 1.1 and 1.7–2.1 ppm, respectively, for the *trans*-isomer. Finally, with the only exception of the resonances displayed at 1.5 and 1.6 ppm, the remaining ones represent the typical resonances of *trans*-isomer resulting polyester, so the formers are attributed to eq and ax H-1′ and H-2′ in the *cis*-isomer. These results were in agreement with previously reported results.[43]

In terms of ^{13}C NMR analysis of the latter region, PCdF1 spectrum displayed several resonances at 74.5, 73.9, 26.5, 26.2, and 25.7 ppm attributed to the COOCH and methylenic carbons (C-1′, C-2′, and C-3′) of the cyclohexylene moiety in the *cis*- and *trans*-isomers (Table 3.3).

For PCF1 polyester the resonances of $COOCH_2$, methinic and also methylenic carbons (a, C-1′ and C-2′) of the cyclohexylene moiety were displayed at 71.5, 69.7, 36.4, 33.9, 27.7, and 24.1 in the *trans*- and *cis*-isomer, respectively (Table 3.3). Furthermore, the NMR results of PCdF1 were also corroborated with the 2D HSQC NMR analysis (Figure 3.3), showing clearly the overlapping of the proton resonances in the region of 2.0–2.5 ppm.

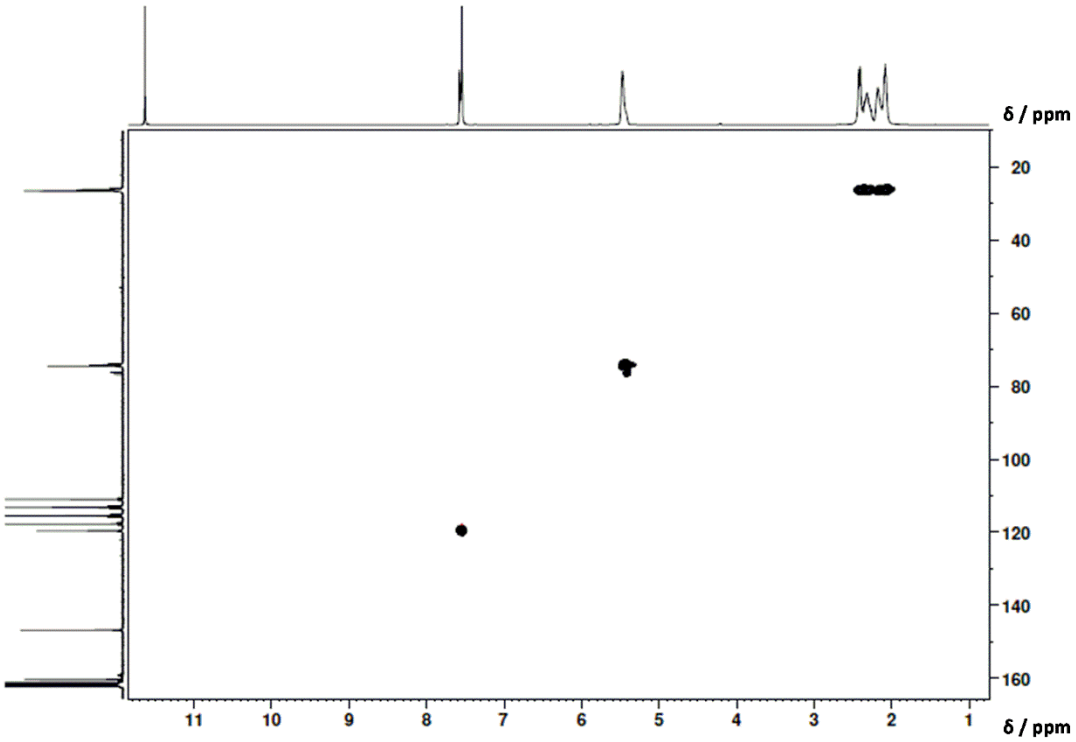

Figure 3.3. 2D HSQC NMR spectrum of PCdF1 in TFA-*d*.

3.1.1. *Cis-/Trans*-1,4-Cyclohexanediol isomers ratio assessment

A deeper analysis of PCdF1 ^{1}H NMR spectrum allowed assessing the ratio between the *cis*- and *trans*-isomers in the polyester backbone by using the furanic H-3 and H-4 resonances. This ratio was estimated to be 25.8/79.3, instead of 43/57 as the starting feed ratio used, showing that the *trans*-isomer is clearly more reactive than the *cis*-counterpart in this polymerization reaction conditions. The modest isolation yields are most plausibly related with this fact. However, in the case of PCF1 polyester (not determined before)[43] the *cis*/*trans* ratio was equal to 39.7/60.3 which is relatively closer to the starting monomers feed ratio (46/54).

3.2. Thermal behavior

The TGA thermograms of PCdF1 (Table 3.4 and Figure 3.4) showed that this polyester is thermally stable ($T_{d,on}$) up to 363.41 ºC, a slightly higher value than that obtained for PCF1 (≈8 ºC). The PCdF1 thermogram exhibited a maximum decomposition temperature (T_d) at

approximately 380.03 ºC (≈39% weight loss), usually assigned to the degradation of the ester linkages within the polymeric chain.[51]

Table 3.4. Decomposition at onset of weight loss, maximum decomposition, glass transition, melting and crystallization temperatures of PCdF1 and PCF1 homopolyesters.

polyester	$T_{d,on}$ / ºC	T_d / ºC	T_g / ºC [a)]	T_g / ºC [b)]	T_m / ºC [a)]	T_c / ºC [a)]
PCdF1	363.41	380.03	174.9	159.0	nd[a]	-
PCF1	354.97	377.46	104.8	102.9	246.7	210.0

[a)] DSC measurements (nd = not detected below 300 ºC); [b)] DMTA measurements.

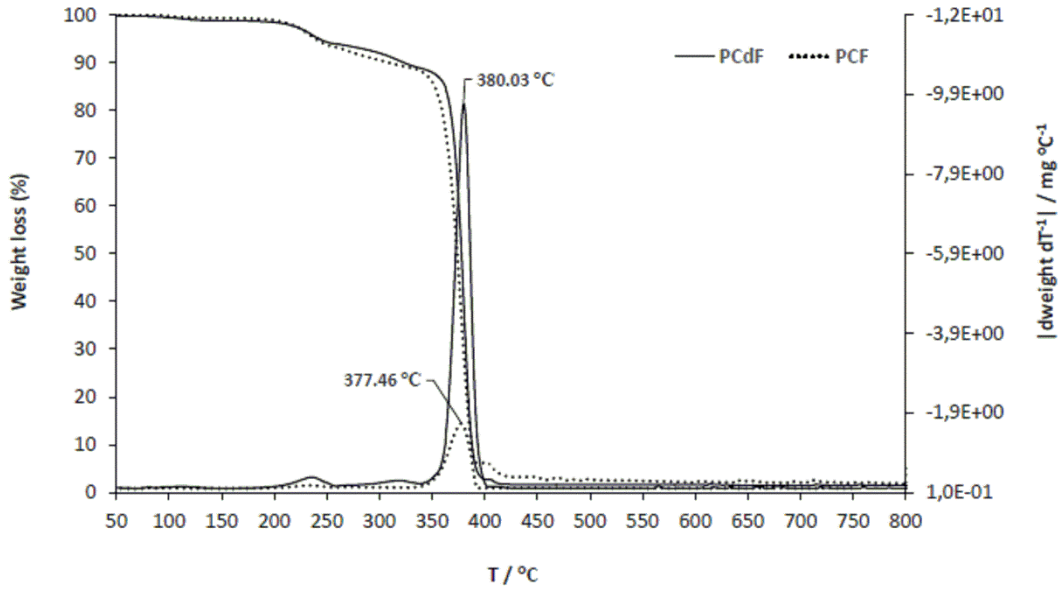

Figure 3.4. TGA and derivative TGA thermograms of PCdF1 and PCF1.

These results are also slightly higher than those obtained for PCF1, which displays a T_d at approximately 377.46 ºC (≈38% weight loss) which is slightly above a reported value.[43] These results indicate that the incorporation of CHD (or even CHDM moiety) into the backbone of FDCA-based polyesters lead to materials with high thermal stability, presenting a very similar behavior compared to those polymers obtained from TPA, namely, PCdT and PCT, having T_d around 290 and 424 ºC, respectively.[5,52,53]

The DSC thermogram of PCdF1 (Table 3.4 and Figure 3.5) exhibited only a T_g at an extremely high temperature, around 174.9 ºC, corroborated by DMTA results displaying in this case a T_g at ≈159.0 ºC.

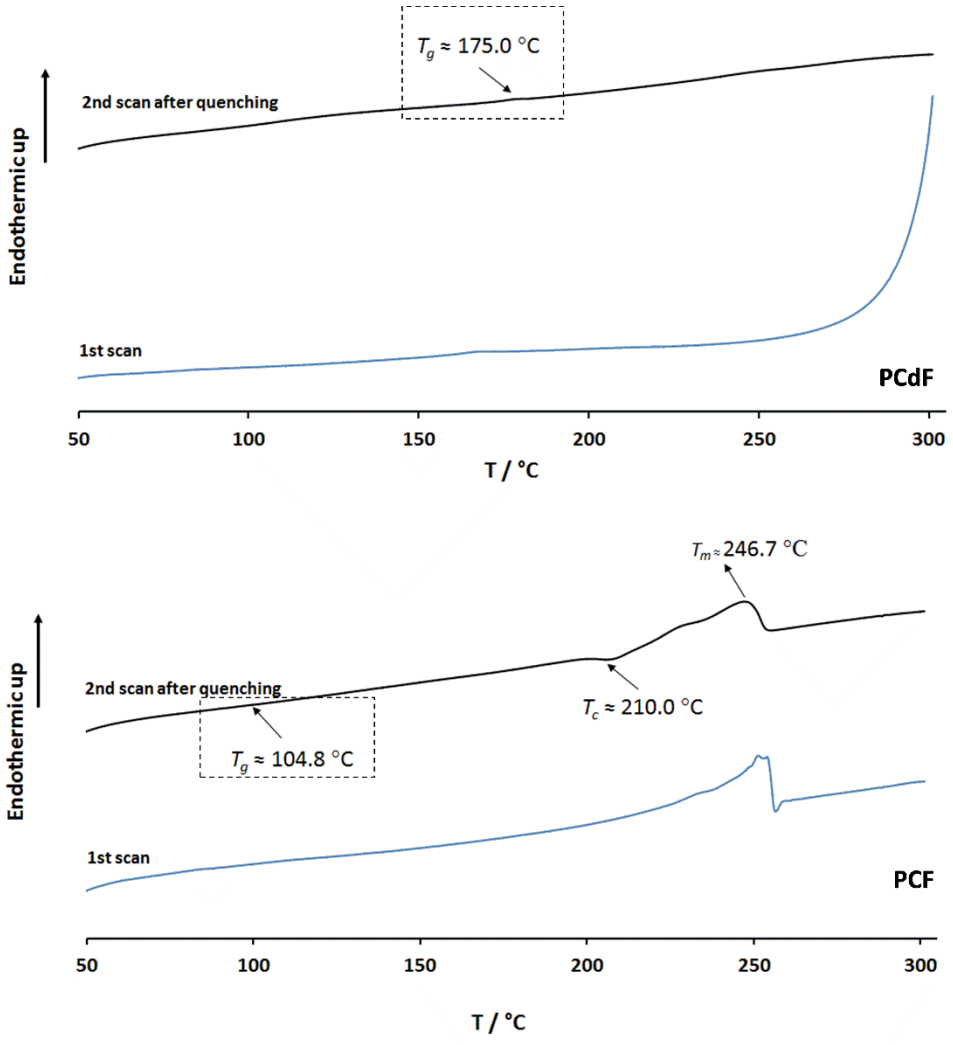

Figure 3.5. DSC thermograms of a) PCdF1 and b) PCF1.

Despite some crystallinity of PCdF1 due to its regular structure, and confirmed by XRD studies (discussed below), no melting event was observed in its DSC tracing up to 300 ºC, very near where its thermal decomposition begun (≈363 ºC). Hence, PCdF is expected to have a very high melting temperature which has some practical implications. The processability of PCdF, in similarity to the petro-based PCT must be carried out very

carefully,[6,54] since there is a narrow processing window between T_m and the initial degradation temperature. This issue could be attenuated by further increasing the molecular weight of this polymer by applying a third stage of solid state polymerization after conventional two-step polytransesterification. Instead, the narrow temperature range between T_g and T_m could also be, at least in part, circumvented by using lower-molecular weight polymers where, *e.g.*, PCdF2 has a $T_m \approx 201.9$ ºC and a $T_d \approx 295.4$ ºC.

PCF1 DSC trace (Table 3.4 and Figure 3.5) also displayed a glass transition but at a lower temperature (104.6 ºC), and crystallization and melting accents, *viz.* around 209.95 and 246.7 ºC, respectively. These results are in accordance with the chemical structure of PCdF1 and PCF1, where the absence/presence of the two methylene groups is associated with distinct thermal transition values. For example, the absence of CH_2 moieties in PCdF1 results in a more rigid polymer chain backbone, and accordingly it has the highest T_g; oppositely, the presence of CH_2 groups in PCF provides flexibility to this polymer chains and consequently a lower T_g was reported.

DMTA analysis (Figure S1, Supporting Information) was used to determine the T_g of the homopolymers, and they have corroborated the DSC results. The tan δ traces of PCdF and PCF homopolyesters displayed T_g features at around 159 and 103 ºC (Table 3.4), respectively. From the previous results for the furan-cycloaliphatic polyesters obtained in this study, we can observe that the thermal properties of these polyesters are typically influenced by the absence/presence of the methylene moieties. Indeed, the restriction in the cyclic ring associated with the absence of methylene moieties in PCdF has resulted in a higher polymer chain rigidity, and subsequently higher thermal behavior in terms of $T_{d,on}$, T_d, and T_g as discussed previously.

3.3. X-Ray diffraction analysis

The XRD pattern (Figure 3.6) of PCdF1 homopolyester synthesized in this work is in agreement with the DSC results described above, exhibiting a semicrystalline character with peaks at $2\theta \approx 18^o$ and 21^o. In general, PCdF1 pattern is very similar to that of the related PCF ($2\theta \approx 17$, 19, and 22^o), although with peaks slightly shifted to lower angles indicating not so closer crystallographic packing.

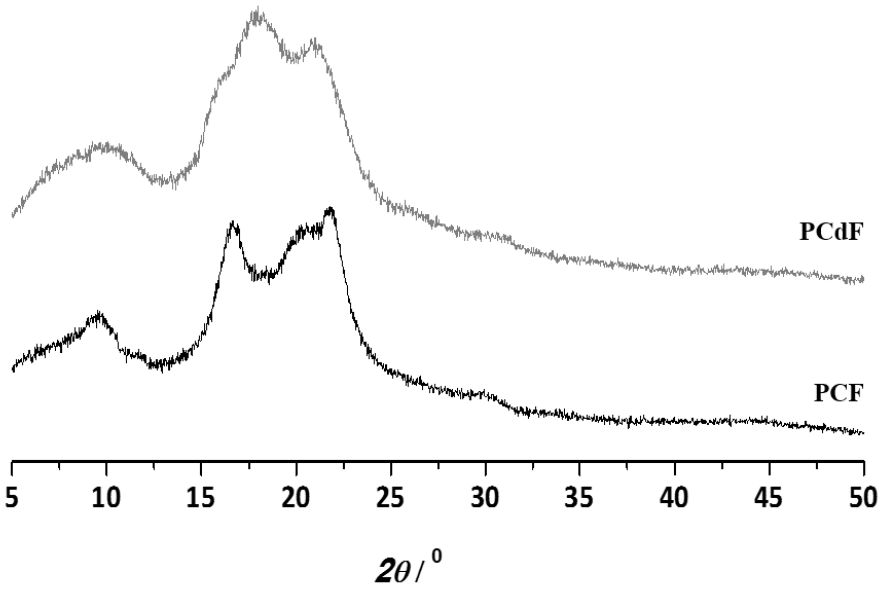

Figure 3.6. XRD patterns of PCdF1 and PCF1 homopolyesters.

4. Conclusions

In summary, the realm of FDCA-based polyesters has been expanded to a new polymer with enhanced thermal properties incorporating 1,4-cyclohexanediol. The ensuing poly(1,4-cyclohexylene 2,5-furandicarboxylate) polyester has shown semicrystalline nature with enhanced thermal stability (T_d around 380.0 ºC and $T_g \approx$ 174.9 ºC). A comparison with the related poly(1,4-cyclohexanedimethylene 2,5-furandicarboxylate) showed that the T_g increased with the stiffness of the linkage of furanic and the cyclohexylene ring. Moreover, these materials could find several interesting industrial applications, namely for optical films or for injection molding materials, similar to PCT polymers.

References

(1) Turner, S. R.; Seymour, R. W.; Dombroski, J. R. Amorphous and Crystalline Polyesters Based on 1,4-Cyclohexanedimethanol. In *Modern Polyesters: Chemistry and Technology of Polyesters and Copolyesters*; Scheirs, J., Long, T. E., Eds.; John Wiley & Sons, Ltd: Chichester, UK, UK, 2004; pp 267–292.

(2) Wu, J.; Eduard, P.; Thiyagarajan, S.; Noordover, B. a J.; van Es, D. S.; Koning, C. E. Semi-Aromatic Polyesters Based on a Carbohydrate-Derived Rigid Diol for Engineering Plastics. *ChemSusChem* **2015**, *8* (1), 67–72.

(3) Burgess, S. K.; Leisen, J. E.; Kraftschik, B. E.; Mubarak, C. R.; Kriegel, R. M.; Koros, W. J. Chain Mobility, Thermal, and Mechanical Properties of Poly(Ethylene Furanoate) Compared to Poly(Ethylene Terephthalate). *Macromolecules* **2014**, *47* (4), 1383−1391.

(4) Sandrolini, F.; Motori, A.; Saccani, A. Electrical Properties of Poly(Butylene Terephthalate). *J. Appl. Polym. Sci.* **1992**, *44* (5), 765–771.

(5) Koo, J. M.; Hwang, S. Y.; Yoon, W. J.; Lee, Y. G.; Kim, S. H.; Im, S. S. Structural and Thermal Properties of Poly(1,4-Cyclohexane Dimethylene Terephthalate) Containing Isosorbide. *Polym. Chem.* **2015**, *6* (39), 6973–6986.

(6) Auerbach, A. B.; Sell, J. W. Evaluation of Poly(1,4-Cyclohexylene Dimethylene Terephthalate) Blends for Improved Processability. *Polym. Eng. Sci.* **1990**, *30* (17), 1041–1050.

(7) Vilela, C.; Sousa, A. F.; Fonseca, A. C.; Serra, A. C.; Coelho, J. F. J.; Freire, C. S. R.; Silvestre, A. J. D. The Quest for Sustainable Polyesters–insights into the Future. *Polym. Chem.* **2014**, *5* (9), 3119–3141.

(8) Gandini, A.; Lacerda, T. M. From Monomers to Polymers from Renewable Resources: Recent Advances. *Prog. Polym. Sci.* **2015**, *48*, 1–39.

(9) Mosiewicki, M. A.; Aranguren, M. I. Recent Developments in Plant Oil Based Functional Materials. *Polym. Int.* **2016**, *65* (1), 28–38.

(10) Sousa, A. F.; Silvestre, A. J. D.; Gandini, A.; Pascoal Neto, C. Synthesis of Aliphatic Suberin-like Polyesters by Ecofriendly Catalytic Systems. *High Perform. Polym.*

2012, *24* (1), 4–8.

(11) Cherubini, F. The Biorefinery Concept: Using Biomass Instead of Oil for Producing Energy and Chemicals. *Energy Convers. Manag.* **2010**, *51* (7), 1412–1421.

(12) Jong, E. de; Dam, M. A.; Sipos, L.; Gruter, G.-J. M.; E. de Jong; M. A. Dam; L. Sipos; G.-J. M. Gruter. Furandicarboxylic Acid (FDCA), a Versatile Building Block for a Very Interesting Class of Polyesters. In *Biobased Monomers, Polymers, and Materials*; Smith, P. B., Gross, R. A., Eds.; ACS Symposium Series; American Chemical Society: Amesterdan, 2012; Vol. 22, pp 1–13.

(13) Sousa, A. F.; Vilela, C.; Fonseca, A. C.; Matos, M.; Freire, C. S. R.; Gruter, G. J. M.; Coelho, J. F. J.; Silvestre, A. J. D. Biobased Polyesters and Other Polymers from 2,5-Furandicarboxylic Acid: A Tribute to Furan Excellency. *Polym. Chem.* **2015**, *6* (33), 5961–5983.

(14) Gandini, A.; Silvestre, A. J. D.; Neto, C. P.; Sousa, A. F.; Gomes, M. M. The Furan Counterpart of Poly (Ethylene Terephthalate): An Alternative Material Based on Renewable Resources. *J. Polym. Sci. Polym. Chem.* **2009**, *5* (c), 295–298.

(15) Hbaieb, S.; Kammoun, W.; Delaite, C.; Abid, M.; Abid, S.; El Gharbi, R. New Copolyesters Containing Aliphatic and Bio-Based Furanic Units by Bulk Copolycondensation. *J. Macromol. Sci. Part A Pure Appl. Chem.* **2015**, *52* (5), 365–373.

(16) Ma, J.; Yu, X.; Xu, J.; Pang, Y. Synthesis and Crystallinity of Poly(Butylene 2,5-Furandicarboxylate). *Polymer* **2012**, *53* (19), 4145–4151.

(17) Ma, J.; Pang, Y.; Wang, M.; Xu, J.; Ma, H.; Nie, X. The Copolymerization Reactivity of Diols with 2,5-Furandicarboxylic Acid for Furan-Based Copolyester Materials. *J. Mater. Chem.* **2012**, *22* (8), 3457–3461.

(18) Jiang, Y.; Woortman, A. J. J.; Alberda Van Ekenstein, G. O. R.; Loos, K. A Biocatalytic Approach towards Sustainable Furanic-Aliphatic Polyesters. *Polym. Chem.* **2015**, *6* (29), 5198–5211.

(19) Matos, M.; Sousa, A. F.; Fonseca, A. C.; Freire, C. S. R.; Coelho, J. F. J.; Silvestre, A. J. D. A New Generation of Furanic Copolyesters with Enhanced Degradability: Poly(Ethylene 2,5-Furandicarboxylate)-Co-Poly(Lactic Acid) Copolyesters.

Macromol. Chem. Phys. **2014**, *215* (22), 2175–2184.

(20) Papageorgiou, G. Z.; Papageorgiou, D. G.; Tsanaktsis, V.; Bikiaris, D. N. Synthesis of the Bio-Based Polyester Poly(Propylene 2,5-Furan Dicarboxylate). Comparison of Thermal Behavior and Solid State Structure with Its Terephthalate and Naphthalate Homologues. *Polymer* **2015**, *62*, 28–38.

(21) Papageorgiou, G. Z.; Guigo, N.; Tsanaktsis, V.; Papageorgiou, D. G.; Exarhopoulos, S.; Sbirrazzuoli, N.; Bikiaris, D. N. On the Bio-Based Furanic Polyesters: Synthesis and Thermal Behavior Study of Poly(Octylene Furanoate) Using Fast and Temperature Modulated Scanning Calorimetry. *Eur. Polym. J.* **2015**, *68*, 115–127.

(22) Papageorgiou, G. Z.; Tsanaktsis, V.; Bikiaris, D. N. Synthesis of Poly(Ethylene Furandicarboxylate) Polyester Using Monomers Derived from Renewable Resources: Thermal Behavior Comparison with PET and PEN. *Phys. Chem. Chem. Phys.* **2014**, *16* (17), 7946–7958.

(23) Papageorgiou, G. Z.; Tsanaktsis, V.; Papageorgiou, D. G.; Chrissafis, K.; Exarhopoulos, S.; Bikiaris, D. N. Furan-Based Polyesters from Renewable Resources: Crystallization and Thermal Degradation Behavior of Poly(Hexamethylene 2,5-Furan-Dicarboxylate). *Eur. Polym. J.* **2015**, *67*, 383–396.

(24) Terzopoulou, Z.; Tsanaktsis, V.; Nerantzaki, M.; Achilias, D. S.; Vaimakis, T.; Papageorgiou, G. Z.; Bikiaris, D. N. Thermal Degradation of Biobased Polyesters: Kinetics and Decomposition Mechanism of Polyesters from 2,5-Furandicarboxylic Acid and Long-Chain Aliphatic Diols. *J. Anal. Appl. Pyrolysis* **2016**, *117*, 162–175.

(25) Tsanaktsis, V.; Bikiaris, D. N.; Guigo, N.; Exarhopoulos, S.; Papageorgiou, D. G.; Sbirrazzuoli, N.; Papageorgiou, G. Z. Synthesis, Properties and Thermal Behavior of Poly(Decylene-2,5-Furanoate): A Biobased Polyester from 2,5-Furan Dicarboxylic Acid. *RSC Adv.* **2015**, *5* (91), 74592–74604.

(26) Tsanaktsis, V.; Terzopoulou, Z.; Exarhopoulos, S.; Bikiaris, D. N.; Achilias, D. S.; Papageorgiou, D. G.; Papageorgiou, G. Z. Sustainable, Eco-Friendly Polyesters Synthesized from Renewable Resources: Preparation and Thermal Characteristics of Poly(Dimethyl-Propylene Furanoate). *Polym. Chem.* **2015**, *6* (48), 8284–8296.

(27) Shahbazi, S.; Jafari, Y.; Moztarzadeh, F.; Mir Mohamad Sadeghi, G. Evaluation of

Effective Parameters for the Synthesis of Poly(Propylene Fumarate) by Response Surface Methodology. *J. Appl. Polym. Sci.* **2014**, *131* (20), 1–8.

(28) Wu, B.; Xu, Y.; Bu, Z.; Wu, L.; Li, B.-G.; Dubois, P. Biobased Poly(Butylene 2,5-Furandicarboxylate) and Poly(Butylene Adipate-Co-Butylene 2,5-Furandicarboxylate)s: From Synthesis Using Highly Purified 2,5-Furandicarboxylic Acid to Thermo-Mechanical Properties. *Polymer* **2014**, *55* (16), 3648–3655.

(29) Wu, L.; Mincheva, R.; Xu, Y.; Raquez, J. M.; Dubois, P. High Molecular Weight Poly(Butylene Succinate-Co-Butylene Furandicarboxylate) Copolyesters: From Catalyzed Polycondensation Reaction to Thermomechanical Properties. *Biomacromolecules* **2012**, *13* (9), 2973–2981.

(30) Wu, H.; Qiu, Z. Synthesis, Crystallization Kinetics and Morphology of Novel Poly(Ethylene Succinate-Co-Ethylene Adipate) Copolymers. *CrystEngComm* **2012**, *14* (10), 3586–3595.

(31) Yu, Z.; Zhou, J.; Cao, F.; Wen, B.; Zhu, X.; Wei, P. Chemosynthesis and Characterization of Fully Biomass-Based Copolymers of Ethylene Glycol, 2,5-Furandicarboxylic Acid, and Succinic Acid. *J. Appl. Polym. Sci.* **2013**, *130* (2), 1415–1420.

(32) Zhou, W.; Wang, X.; Yang, B.; Xu, Y.; Zhang, W.; Zhang, Y.; Ji, J. Synthesis, Physical Properties and Enzymatic Degradation of Bio-Based Poly(Butylene Adipate-Co-Butylene Furandicarboxylate) Copolyesters. *Polym. Degrad. Stabil.* **2013**, *98* (11), 2177–2183.

(33) Zhu, J.; Cai, J.; Xie, W.; Chen, P.-H.; Gazzano, M.; Scandola, M.; Gross, R. A. Poly(Butylene 2,5-Furan Dicarboxylate), a Biobased Alternative to PBT: Synthesis, Physical Properties, and Crystal Structure. *Macromolecules* **2013**, *46* (3), 796–804.

(34) Moore and J. E. and Kelly, J. A. Polyesters Derived from Furan and Tetrahydrofuran Nuclei. *Macromolecules* **1978**, *11* (3), 568–573.

(35) Moore, J. E.; Kelly, J. A. Thermally Initiated Crosslinking of an Unsaturated Heterocyclic Polyester. *J. Polym. Sci. Polym. Chem. Ed.* **1978**, *16*, 2407–2409.

(36) Gandini, A.; Coelho, D.; Gomes, M.; Reis, B.; Silvestre, A. Materials from Renewable Resources Based on Furan Monomers and Furan Chemistry: Work in

Progress. *J. Mater. Chem.* **2009**, *19* (45), 8656.

(37) Gomes, M.; Gandini, A.; Silvestre, A. J. D.; Reis, B. Synthesis and Characterization of Poly(2,5-Furan Dicarboxylate)s Based on a Variety of Diols. *J. Polym. Sci. Polym. Chem.* **2011**, *49* (17), 3759–3768.

(38) Storbeck, R.; Ballauff, M. Synthesis and Properties of Polyesters Based on 2,5-Furandicarboxylic Acid and 1,4:3,6-Dianhydrohexitols. *Polymer* **1993**, *34* (23), 5003–5006.

(39) Ghosh, T.; Mahajan, K.; Sridevi, N.-S.; Belgacem, M. N.; Gopalakrishnan, P. 2,5-Furan Dicarboxylic Acid-Based Polyesters Biomass, Prepared From. WO 2013103574 A1, 2012.

(40) Lincoln, J.; Drewitt, J. G. N. Polyesters From Heterocyclic Components. US2551731 A, 1951.

(41) Bengs, H.; Schoenfeld, A.; Boehm, G.; Weis, S.; Clauss, J. Biodegradable Polymers Based on Natural and Renewable Raw Materials Especially Isosorbite. US 6342300 B1, 1999.

(42) Howard Smith Carman, J.; Jack Irvin Killman, J.; Crawford, E. D.; Jenkins, J. C. Polyester Compositions Containing Furandicarboxylic Acid or an Ester Thereof and Cyclohexanedimethanol. US20130095268 A1, 2011.

(43) Diao, L.; Su, K.; Li, Z.; Ding, C. Furan-Based Co-Polyesters with Enhanced Thermal Properties: Poly(1,4-Butylene-Co-1,4-Cyclohexanedimethylene-2,5-Furandicarboxylic Acid). *RSC Adv.* **2016**, *6* (33), 27632–27639.

(44) Wang, J.; Liu, X.; Zhang, Y.; Liu, F.; Zhu, J. Modification of Poly(Ethylene 2,5-Furandicarboxylate) with 1,4-Cyclohexanedimethylene: Influence of Composition on Mechanical and Barrier Properties. *Polymer* **2016**, *103*, 1–8.

(45) Carman, H. S.; Killman, J. I.; Crawford, E. D.; Jenkins, J. C. Polyester Compositions Containing Furandicarboxylic Acid or an Ester Thereof, Cyclobutanediol and Cyclohexanedimethanol. US 20130095270 A1, 2011.

(46) Carman, H. S.; Killman, J. I.; Crawford, E. D.; Jenkins, J. C. Polyester Compositions Containing Furandicarboxylic Acid or an Ester Thereof and Ethylene Glycol. US

20130095269 A1, 2011.

(47) Carman, H. S.; Killman, J. I.; Crawford, E. D.; Jenkins, J. C. Polyester Composition Containing Furandicarboxylic Acid or an Ester Thereof, Ethylene Glycol and Cyclohexanedimethanol. US 20130095271 A1, 2011.

(48) Sousa, A. F.; Coelho, J. F. J.; Silvestre, A. J. D. Renewable-Based Poly((Ether)Ester)s from 2,5-Furandicarboxylic Acid. *Polymer* **2016**, *98*, 129–135.

(49) Tsanaktsis, V.; Papageorgiou, G. Z.; Bikiaris, D. N. A Facile Method to Synthesize High-Molecular-Weight Biobased Polyesters from 2,5-Furandicarboxylic Acid and Long-Chain Diols. *J. Polym. Sci. Polym. Chem.* **2015**, *53* (22), 2617–2632.

(50) Nemours, P. De. Polyurethanes. 11. Effect of Cis-Trans Isomerism. *J. Polym. Sci.* **1961**, *55* (162), 507–514.

(51) Sousa, A. F.; Fonseca, A. C.; Serra, A. C.; Freire, C. S. R.; Silvestre, A. J. D.; Coelho, J. F. J. New Unsaturated Copolyesters Based on 2,5-Furandicarboxylic Acid and Their Crosslinked Derivatives. *Polym. Chem.* **2016**, *7* (5), 1049–1058.

(52) Osman, M. A. Thermotropic Liquid Crystalline Polymers with Quasi-Rigid Chains. 1. Cyclohexyl Moieties. *Macromolecules* **1986**, *19* (7), 1824–1827.

(53) González-Vidal, N.; Martínez De Ilarduya, A.; Muñoz-Guerra, S.; Ilarduya, A. M. de; Muñozguerra, S. Poly(Ethylene-Co-1,4-Cyclohexylenedimethylene Terephthalate) Copolyesters Obtained by Ring Opening Polymerization. *J. Polym. Sci. Polym. Chem.* **2009**, *47* (22), 5954–5966.

(54) Lee;, S.; Huh, W.; Hong, Y.-S.; Lee, K.-M. Synthesis and Thermal Properties of Poly(Cyclohexylene Dimethylene Terephthalate-Co-Butylene Terephtalate. *Korea Polym. J.* **2000**, *8* (6), 261–267.

Supporting Information

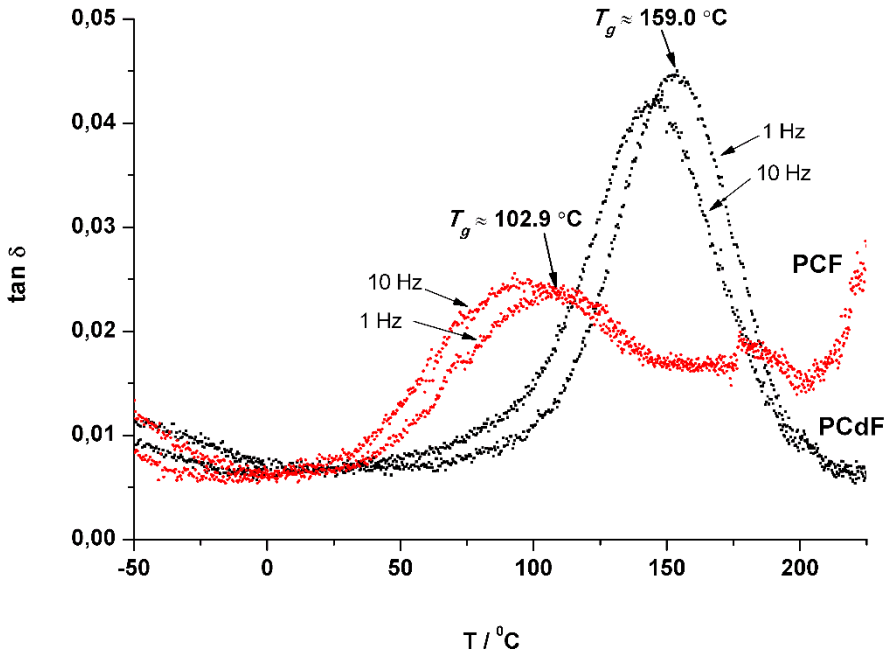

Figure S1. DMTA traces of PCdF1 and PCF1 homopolyesters.

Chapter IV – Copolymers Based on Poly(1,4-butylene 2,5-furandicarboxylate) and Poly(propylene oxide) with Tuneable Thermal Properties: Synthesis and Characterisation

---

This chapter will be submitted as:

Marina Matos, Andreia F. Sousa, P. V. Mendonça, Armando J. D. Silvestre. Copolymers based on poly(1,4-butylene 2,5-furandicarboxylate) and poly(propylene oxide) with tuneable thermal properties: synthesis and characterisation.

Abstract

Poly(ether ester)s (PEEs) represent a promising class of segmented copolyesters, with high commercial interest due to their unique thermal features, namely high thermal stability and low melting temperatures, which enables their industrial processability at lower temperatures than the conventional ones. The synthesis of PEEs based on renewable 2,5-furandicarboxylic acid (FDCA) is still scarce, however the ensuing copolyesters revealed to possess very similar thermal and mechanical properties to those of their petroleum-based counterparts. In this context, a series of poly(1,4-butylene 2,5-furandicarboxylate)-co-poly(poly(propylene oxide) 2,5-furandicarboxylate) copolyesters with different composition of stiff poly(1,4-butylene 2,5-furandicarboxylate) (PBF) and soft poly(poly(propylene oxide) 2,5-furandicarboxylate) (PPOF) moieties were synthesised, *via* a two-step bulk polytransesterification reaction. The molar fraction of the PPOF moieties introduced in the feed was 10, 20 or 50 mol%. All materials were characterised in detail through several techniques, e.g. ATR FTIR, ^{1}H and ^{13}C NMR, TGA, DSC, DMTA and XRD. Finally, their hydrolytic and enzymatic degradation evaluation was also assessed. The ensuing copolyesters presented semi-crystalline nature for higher PBF/PPOF ratios, and for approximately equal amounts of PBF and PPOF an amorphous viscous liquid copolyester was obtained. Moreover, is was observed that the presence of the appending methyl group of PPO unit lead a slightly decreased on the maximum degradation temperatures when compared to PBF, however remaining thermally stable up to 308 ºC. Nevertheless, due to the enhanced range between their glass and melting temperatures (values of -42.3 to -32.6 ºC and 124.2 to 147.6 ºC, respectively), new application fields could be achieved.

Keywords: 2,5-Furandicarboxylic acid; poly(propylene oxide); poly(ester-ether) copolymers; tuneable thermal properties.

1. Introduction

The massive consumption of fossil-based polymers on a variety of commodity objects of daily life has prompted, in the last decades, to the development of renewable-based alternatives with emphasis on their sustainability. Among the renewable-based polymers

polyesters derived from 2,5-furandicarboxylic acid (FDCA) are some of the most promising. FDCA is a renewable-based aromatic monomer building block monomer that has been widely explored as precursor of several homopolyesters, with very similar properties to those obtained their non-renewable counterpart, namely terephthalic acid (TPA).[1,2]

Some examples of polyesters synthesised from FDCA are poly(ethylene 2,5-furandicarboxylate) (PEF)[3] and poly(1,4-butylene 2,5-furandicarboxylate) (PBF), among others, with similar properties to those of their TPA counterparts.[4–11] Furthermore, several other diols besides linear ones have been explored to prepare FDCA-based homopolymers, namely branched diols such as 1,2-propanediol, 2,3-butanediol, 2-methyl-1,3-propanediol and 2,2-dimethyl-1,3-propanediol.[12–18] The ensuing materials presented even higher T_g´s than those of their corresponding homopolyesters synthesised with linear diols with the same number of carbon atoms.

In addition, a demand for new polyesters with specific properties emerged due to the necessity to fulfil specific application gaps, namely in the fields of biomaterials or elastomeric compounds. In this context, some studies[19–23] have focused on the synthesis of FDCA-based poly(ester-ether)s (PEE´s) copolymers composed of polyether soft moieties, e.g., poly(butylene glycol) (PBG)[23] and/or poly(ethylene glycol) (PEG)[21,22] to replace their fossil-based counterparts, such as poly(butylene 1,4-terephthalate)-co-poly(poly(butylene glycol) 1,4-terephtalate) (PBT-co-PBGT) or poly(butylene 1,4-terephthalate)-co-poly(poly(ethylene glycol) 1,4-terephtalate) (PBT-co-PEGT). Commercial PEEs based on TPA, find important applications among the biomedical field.[24,25] Indeed, PBT-co-PEGT copolymers are a well-known commercial PEE´s (under trade mark of PolyActive®)[26], and are widely used for drug delivery systems, presenting high thermal stability, as well as enhanced flexibility when compared to PET. This class of polymers show great potential specially if prepared from FDCA, nonetheless, the literature in furanic PEEs is still scarce.[19–23] Zhou *et al.*[19] presented the first study, reporting the synthesis of poly(1,4-butylene 2,5-furandicarboxylate)-co-poly(poly(butylene glycol) 2,5-furandicarboxylate) (PBF-co-PBGF) copolyesters, with enhanced thermal (maximum decomposition temperatures varying from 363 to 378 ºC) and mechanical properties (elongation at break between 381 to 832%). Sousa *et al.*[20] also reported the synthesis of new poly(ester-ether)s copolymers from FDCA and PEG with different molecular weights (M_n of ~ 200, 400 and 2000 g/mol), and isosorbide, possessing high thermal stability. More recently, a series of poly(1,4-butylene 2,5-

furandicarboxylate)-co-poly(poly(ethylene glycol) 2,5-furandicarboxylate) (PBF-co-PEGF) copolyesters were reported also displaying high thermal stability (up to 380 ºC) and low T_g´s (ranging from -43.1 to -35.4 ºC), enabling their manufacturing process.[21,22] Hydrolytic degradability of PBF-*block*-PEGF was also studied, showing that they can be easily hydrolysed under alkaline conditions (phosphate buffered saline (PBS) solution at pH=12).[22] Further, Chi *et al.*[23] also synthesised several PEE's from FDCA, neopentyl glycol and poly(butylene glycol), with enhanced flexibility (elongation at break values from 38 to 1281%).

However, to our knowledge, the use of poly(propylene oxide) (PPO) as comonomer for the synthesis of PPE's copolymers was not reported in the literature before. In this context, copolymerisation of FDCA, 1,4-butanediol (BD) and PPO, could be an elegant way to obtain materials with low T_g, facilitating its processability, and at same time maintaining the thermal stability, thus enlarging the role of potential applications. Precisely, in this study, a series of poly(1,4-butylene 2,5-furandicarboxylate)-co-poly(poly(propylene oxide)) (PBF-co-PPOF) copolyesters were synthesised by a typical two-step bulk polytransesterification procedure. The ensuing copolyesters were extensively characterised by SEC, ATR FTIR, ^{1}H and ^{13}C NMR, TGA, DSC, and DMTA analysis. Importantly, PBF-co-PPOF bearing 20 mol% of PPOF moieties was also submitted to a hydrolytic and enzymatic degradability evaluation.

2. Experimental

2.1. Materials

1,4-Butanediol (BD, 99%), poly(propylene oxide) (PPO, average M_n ~1 000), deuterated chloroform ($CDCl_3$-*d*, 99 atom % D), titanium(IV) tert-butoxide ($Ti(OBu)_4$, 97 %), sodium phosphate dibasic (≥99%), sodium phosphate monobasic (≥99%) and *Porcine pancreas* lipase (Type II, 100-500 units/mg protein) were purchased from Sigma-Aldrich Chemicals Co. 2,5-Furandicarboxylic acid (FDCA, >98%) was purchased from TCI Europe NV. Concentrated hydrochloric acid (37 %) was purchased from Panreac; and methanol and chloroform (pro-analysis and HPLC grade) were purchased from Fisher Scientific. Polystyrene standards with molecular weights between 4 290 and 66 350 Da were supplied by Polymer Laboratories. All chemicals were used as received, without further purification.

2.2. Synthesis of dimethyl 2,5-furandicarboxylate (DMFDC) monomer

The synthesis of DMFDC followed a previously reported procedure.[3] Typically, DMFDC was prepared by reacting FDCA with an excess of methanol, under acidic conditions (HCl), at 80 ºC for 15 h. The final product was isolated in 71 % yield as a white powder. FTIR (ν/cm^{-1}): 3168 (=C-H); 2965 (C-H); 1706 (C=O); 1578, 1522 (C=C); 1288 (C-O); 1024 (furan ring breathing); 969, 825, 757 (2,5-dibustituted furan ring). ^{1}H NMR (300 MHz, $CDCl_3$, δ/ ppm): 7.2 (s, H3/H4 furan ring); 3.9 (s, 2,5-COOCH_3). ^{13}C NMR (75 MHz, $CDCl_3$, δ/ppm): 158 (2,5-C=O); 147 (C2/C5 furan ring); 118 (C3/C4 furan ring); 52 (2,5-COOCH$_3$).

2.3. Syntheses of poly(1,4-butylene 2,5-furandicarboxylate)-co-poly(poly(propylene oxide)) (PBF-co-PPO) copolymers and poly(1,4-butylene 2,5-furandicarboxylate) (PBF)

The polyesters were prepared by a two-step bulk polytransesterification approach following an adapted procedure reported elsewhere.[20] Reactions were carried out by mixing DMFDC (mg, mmol) and an equimolar amount of BD and PPO (BD/PPO molar ratios of 100/0, 90/10, 80/20, 50/50, Table 4.1), in the presence $Ti(OBu)_4$ as catalyst (1 wt% relative to the total mass of monomers). In the first step, the mixture was heated progressively from 100 up to 190 ºC, for 5 h, under a nitrogen atmosphere and with constant stirring. In the second step, the reaction proceeded under vacuum (10^{-3} bar) and the temperature was slowly raised to 200 ºC for 1h, and finally kept at 210 ºC, for 2 h. The ensuing solid products were purified by dissolving in chloroform (~20 mL), and then pouring in an excess of cold methanol, filtered, dried and weighted. In the case of PBF-co-PPOF 50/50 copolyester (BD/PPO = 50/50), viscous liquid at room temperature, a liquid-liquid extraction procedure using chloroform (~20 mL) was used instead.

Hereafter, the copolyesters will be referred to as PBF-co-PPOF 90/10, 80/20 and 50/50, according to the BD/PPO molar ratio used as feed. Table 4.1 presents the molar amounts of each monomer used as well as the weight average molecular weights (M_w) and dispersity ($Đ = M_w/M_n$) of the polymers.

2.4. Characterization techniques

Size-exclusion chromatography (SEC) analyses of copolyesters were performed on a Viscotek (Viscotek TDAmax) equipped with a differential viscometer (DV) and right-angle laser-light scattering (RALLS, Viscotek) and refractive index (RI) detectors. The column set consisted of a PLgel 5 μm guard column followed by two columns, namely Viscotek T5000 and T4000 column, respectively. A dual piston pump was set with a flow rate of 1 mL min^{-1}. The eluent (DMF with 0.03% LiBr) was previously filtered through a 0.2 μm filter. The system was also equipped with an on-line degasser. The analyses were performed at 60 °C using an Elder CH-150 heater. Before injection, the samples were filtered through a PTFE membrane with 0.2 μm pore. The system was calibrated with narrow poly(methyl methacrylate) standards.

Attenuated total reflectance Fourier transform infrared (ATR FTIR) spectra were obtained using a PARAGON 1000 Perkin-Elmer FTIR spectrometer equipped with a single-horizontal Golden Gate ATR cell. The spectra were recorded after 128 scans, at a resolution of 4 cm^{-1}, within the range of 500 to 4000 cm^{-1}.

^{1}H, ^{13}C nuclear magnetic resonance (NMR) spectra were recorded in $CDCl_3$ using a Bruker AMX 300 spectrometer, operating at 300 or 75 MHz, respectively. All chemical shifts (δ) are expressed as parts per million (ppm), downfield from tetramethylsilane (used as the internal standard). Further, the calculation of the real incorporation of BD/PPO ratio ($PBF/PPOF_{real}$) the integration areas of OCH_2 proton resonance of F-BD diad (δ ≈ 4.40 ppm) and of F-PPO diad (δ ≈ 3.93 ppm) were used, according to the equation: $[A_{OCH2;\,F-BD}/(A_{OCH2;F-BD} + A_{OCH2;F-PPO})] / [A_{OCH2;F-PPO} / (A_{OCH2;F-DB} + A_{OCH2;F-PPO})]$.

The Average PBF sequence length was also calculated by the equation: $L_{n,BF} = 1/[(1 - (PBF_{real}/100))]$[27].

Thermogravimetric analyses (TGA) were carried out with a Setaram SETSYS analyser equipped with an alumina plate. Thermograms were recorded under a nitrogen flow of 20 mL min^{-1} and heated at a constant rate of 10 °C min^{-1} from room temperature up to 800 °C. Thermal decomposition temperatures were taken at 5% weight loss step and at maximum decomposition temperatures from the heated samples ($T_{d,5\%}$ and $T_{d,max}$, respectively).

Differential scanning calorimetry (DSC) thermograms were obtained with a DSC Q100 V9.9 Build 303 (Universal V4.5A) calorimeter from Texas Instruments, using aluminium DSC pans. Scans were carried out under nitrogen with a heating rate of 10 °C min^{-1} in the

temperature range from -90 to 200 °C. Two heating/cooling cycles were repeated. Glass transition temperature (T_g) was determined using the midpoint approach (second heating trace); and cold crystallization (T_{cc}) and melting (T_m) temperatures were determined as the maximum of the exothermic crystallization peak and the minimum of the melting endothermic peak during the second heating scan, respectively.

Dynamic mechanical thermal analyses (DMTA) were performed using a material pocket accessory with a Tritec 2000 DMA Triton, operating in the single cantilever mode. Tests were performed at 1 and 10 Hz and the temperature was varied from -100 to 200 ºC, at 2 ºC min^{-1}. T_g was determined as the maximum peak of tan δ.

X-ray diffraction (XRD) measurements were performed using a Philips X'pert MPD diffractometer operating with CuKα radiation (λ = 1.5405980 Å) at 40 kV and 50 mA. Samples were scanned in the 2θ range of 5 to 50º, with a step size of 0.04º, and time per step of 50 s.

In vitro hydrolytic and enzymatic degradation tests were carried out using press-moulded square-shape samples (*ca.* 69-113 mg) of the prepared polyesters and placed into closed containers with phosphate buffer saline solution (PBS) (10 mL) or with a PBS solution (10 mL) containing *Porcine pancreas* lipase (concentration of 0.1 mg mL^{-1}), for each test, respectively. The specimens were taken out of the related solution at regular intervals (each 7 days), rinsed thoroughly with distilled water, dried at room temperature for 4 h and, weighed. To prevent saturation, both solutions were renewed every 7 days. Each measurement was repeated five times. The weight-loss percentage was calculated using the expression: $Weight\ loss\ (\%) =)[(W_0 - W_d)/W_0] \times 100$, where, W_o and W_d stand for the specimens weights prior and after incubation, respectively.

3. Results and Discussion

3.1. PBF-co-PPOF copolyesters synthesis and structural characterisation

In this study the newly prepared poly(ester-ether)s copolymers are based on poly(1,4-butylene 2,5-furandicarboxylate) (PBF) as rigid unit, and on a soft segment derived from poly(propylene oxide) (PPO) (Scheme 1). Interestingly the poly(ether) selected has a methyl side group which plays an important role on the structure-properties features, as discussed ahead.

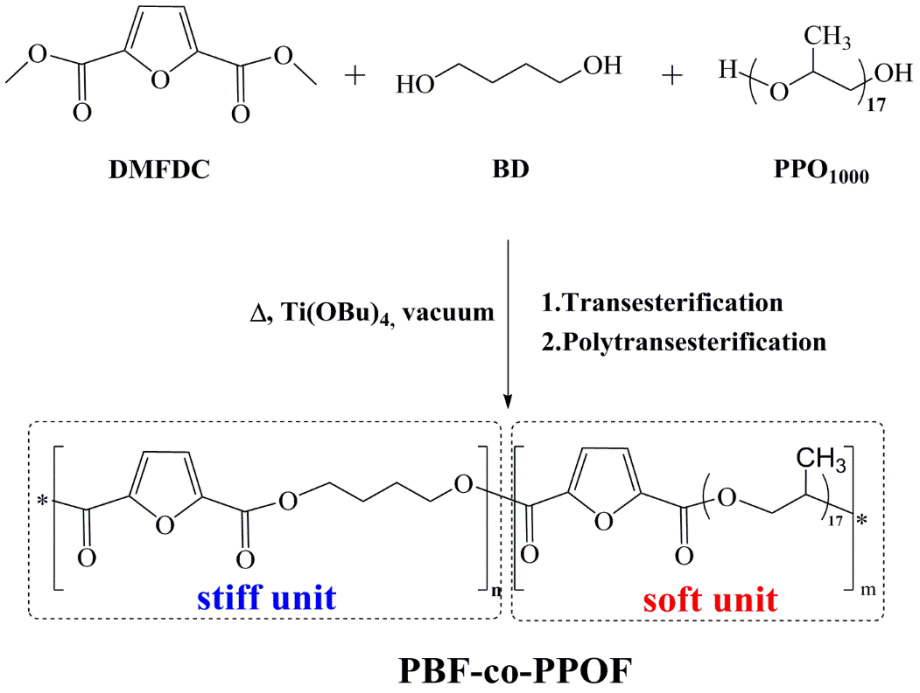

Scheme 1. Synthesis of PBF-co-PPOF copolymers.

PBF-co-PPOF were synthesised *via* a two-step conventional melt polytransesterification approach (Scheme 1),[3] in the presence of $Ti(OBu)_4$ catalyst and at relatively moderate temperatures, not exceeding 210 ºC, to avoid undesirable side reactions involving the furan moiety (*e.g.* decarboxylation reactions which are commonly associated to colour problem issues).[1] The resulting polymers were isolated as powders (PBF, PBF-co-PPOF-90/10 and 80/20) or a viscous liquid (PBF-co-PPOF-50/50) in relatively good yields that ranged from 65 to 71 % (Table 4.1). Furthermore, these copolyesters showed a weight-average molecular weight M_w values between 23 100-41 600, and $Đ$ around 2.

Table 4.1. Molecular characteristics of PBF and PBF-co-PPOF copolymers.

(Co)polymer	BD/PPO$_{feed}$ [a] (mol%)	Yield [b] (%)	M_w	$Đ$
PBF	100/0	71.0	- [c]	- [c]
PBF-co-PPOF-90/10	90/10	64.8	36 700	2.2
PBF-co-PPOF-80/20	80/20	68.1	41 600	2.2
PBF-co-PPOF-50/50	50/50	71.4	48 500	2.1

[a] Molar feed percentage of BD and PPO units, respectively; [b] Isolation yields of purified polyesters in methanol; [C] Not determinate due to the insolubility of PBF in DMF.

The typical ATR FTIR spectra of all PBF-co-PPOF copolyesters and related PBF homopolyester (Figure 4.1) displayed two weak bands near 3150 and 3115 cm^{-1} attributed to the ν C-H bond of the furanic ring. Also, near 2968, 2930, 2893 and 2868 cm^{-1} there are four weak bands attributed to the anti-symmetrical and symmetrical stretching modes (ν C-H *asym* and ν C-H *sym*, respectively) of the C-H bond of methylene and methyl groups related to the BD and PPO moieties, respectively. Additionally, both PBF and copolyesters spectra exhibited a very intense band near 1725 cm^{-1}, arising from the C-O stretching vibration, typical of ester groups. Two bands at 1506 and 1573 cm^{-1}, arising from the C-C bond of the furan ring, and C-O-C stretching vibrations appeared at around 1271 cm^{-1} and the typical vibration modes of 2,5-disubstituted furans were observed at 966, 822, and 769 cm^{-1}, were observed for PBF and PBF-co-PPOF materials. The presence of the above-mentioned bands confirmed the success of the polymerisation reactions.

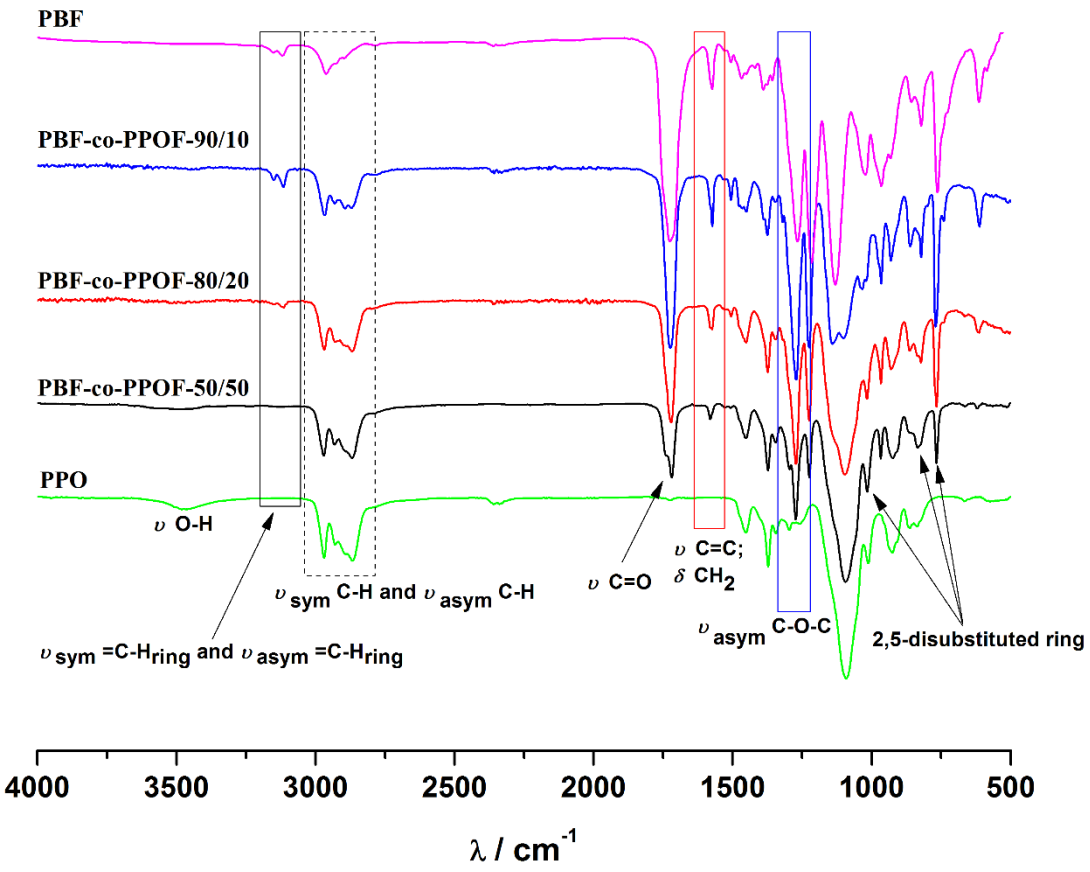

Figure 4.1. ATR FTIR spectra of PBF-co-PPOF copolymers.

The chemical structure characterisation of all PBF-co-PPOF copolyesters and PBF homopolyester was also studied by ^{1}H (Figure 4.2 and Table 4.2) and ^{13}C NMR (Figure S2 and Table 4.4). The main ^{1}H NMR resonances and respective assignments of all polymers studied are summarised in Table 4.2. Figure 4.2 displays the ^{1}H NMR spectrum of PBF-co-PPOF-90/10.

Table 4.2. Main ^{1}H NMR resonances of PBF-co-PPOF copolyesters, and PBF and PPO homopolyester.

δ / ppm	Assignment	Diads	Integration area				
			PBF	PBF-co-PPOF			PPO
				90/10	80/20	50/50	
7.21	***H3 and H4***; C***H***	F-BD; FDCA-PPO	1.00	1.00	1.00	1.00	
5.26	***d, d'*** ; C***H***CH_3	F-PPO	–	0.14	0.37	0.92	
4.40	***a, a'***; C(O)OC***H***$_2$$CH_2$	F-BD	2.01	1.66	1.28	0.46	
3.67	***c, c'***; C(O)OC***H***$_2$	F-PPO	–	0.30	0.84	1.84	
3.54	***f*** ; OC***H***$_2$	PPO-PPO	–	1.91	5.14	17.89	2.01
3.40	***g*** ; OC***H***	PPO-PPO	–	1.03	2.77	9.46	1.00
1.91	***b, b'***; C(O)OCH_2C***H***$_2$	F-BD	2.01	1.66	1.41	0.48	
1.34	***e, e'*** ; CHC***H***$_3$	F-PPO		0.44	1.30	3.04	
1.15	***h*** ; OCHC***H***$_3$	PPO-PPO	–	3.10	8.60	28.50	3.02

The ^{1}H NMR spectra of all polymers (Figure 4.2 and Table 4.2) displayed the typical resonances attributed to the F-BD diad at approximately δ 7.21, 4.40 and 1.91 attributed to the ***H3*** and ***H4*** protons of the furan ring, and to the C(O)O***C******H***$_2$$CH_2$ and C(O)OCH_2C***H***$_2$ protons of the BD moiety, respectively.

In the copolymers spectra the corresponding resonances associated to the PPO-F diads were also detected: δ 5.26, 3.67 and 1.34 ppm, arising from the C(O)OC***H***, C(O)OC***H***$_2$ and C(O)OCHC***H***$_3$ protons, in the neighbouring of the furan ring. Moreover, the protons related to the PPO-PPO units were also identified at 3.54, 3.40, and 1.15 ppm, related to OC***H***$_2$ (ether linkage), OC***H*** and OCHC***H***$_3$, respectively.

Furthermore, the ^{1}H NMR spectra data was used to access the real molar percentage of PBF and PPOF moieties in the copolyesters backbone, due to the important impact this ratio has on the ensuing copolyesters properties. The PBF/PPOF real incorporation was determined using the integration areas of C(O)OC***H***$_2$ proton resonances (in the neighbouring

of furan ring) of the F-BD (δ at 4.40 ppm) and F-PPO (δ at 3.93 ppm) diads, respectively, and the main results are presented in Table 4.3.

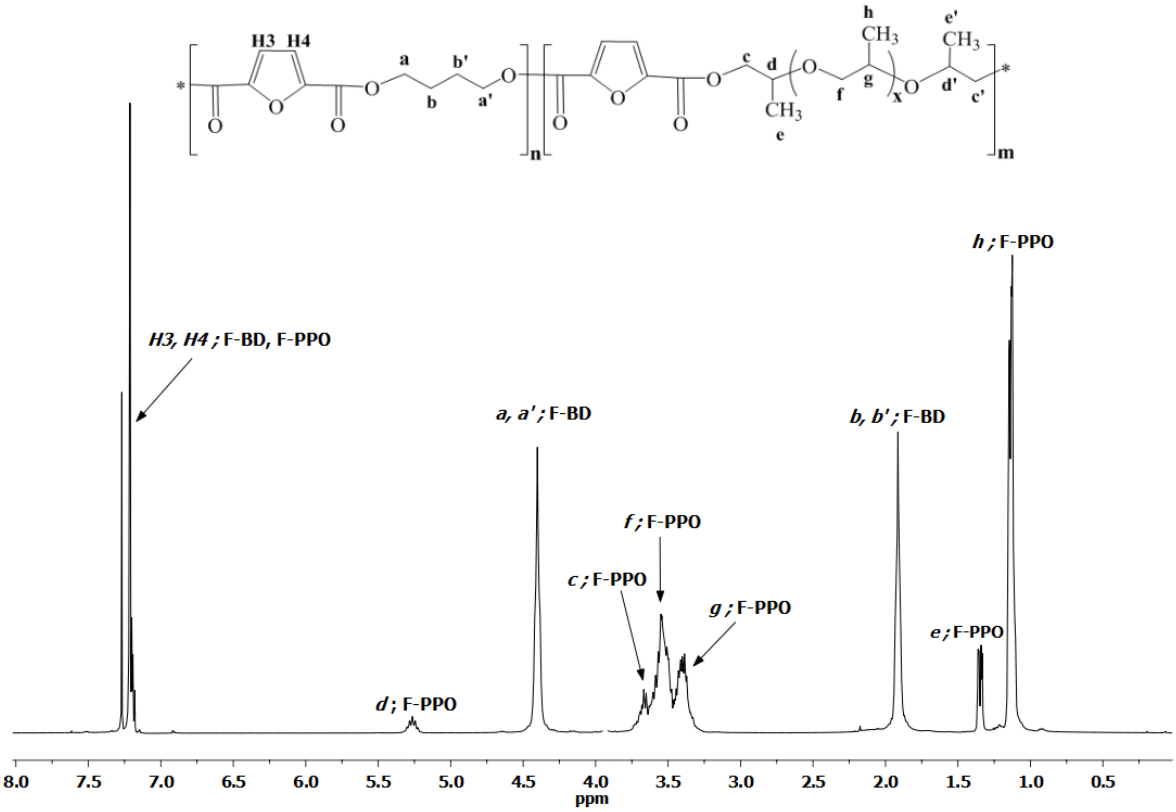

Figure 4.2. ^{1}H NMR spectrum of PBF-co-PPOF-90/10 copolymer in $CHCl_3$-*d*.

Table 4.3. Comparison between the initial target molar percentage and the real molar percentage of PBF and PPOF in the polyesters backbone.

(Co)polymer	PBF/PPOF$_{feed}$ (mol%)	PBF/PPOF$_{real}$ (mol%)	$L_{n,\,BF}$
PBF	100 / 0	100 / 0	–
PBF-co-PPOF-90/10	90 / 10	85 / 15	6.5
PBF-co-PPOF-80/20	80 / 20	76 / 24	4.2
PBF-co-PPPOF-50/50	50 / 50	20 / 80	1.3

[a] PBF/PPOF$_0$ corresponds to the molar feed percentage of BD and PPO, respectively. [b] PBF/PPOF$_{real}$ corresponds to the real incorporation of PBF/PPOF ratio[c] Average PBF sequence length.

From Table 4.3, it is possible to observe that despite the BD and PPO feed ratio, there was a tendency for a higher incorporation of PPOF into copolyesters chains, most probably associated with BD lost during the polytransesterification step due to the high BD volatility.

The number average sequence length of BF unit ($L_{n,BF}$) was also assessed assuming that PBF-co-PPOF copolyesters are random copolyesters. It was found that $L_{n,BF}$ increased with the BF content increasing, according with the theoretically expected values.[20,21,28,29] Importantly, the copolyester with the highest amount of PBF (PBF-co-PPOF-90/10) had a $L_{n,BF}$ of 6.5. This is an important structural feature that is in accordance with a crystalline domain dominated by PBF segments, and corresponding melting behaviour, as discussed above.

In terms of ^{13}C NMR analysis (Table 4.4 and Figure S1), the observed resonances were in agreement with their expected structure and corroborated the above ^{1}H NMR results and also the ATR FTIR data.

Table 4.4. Main ^{13}C NMR resonances of all PBF-co-PPOF copolyesters, and PBF and PPO homopolyester.

Assignment	Diads	δ (ppm)				
		PBF	PBF-co-PPOF			PPO
			90/10	80/20	50/50	
2-CO and 5-CO; ***C***(O)O	F-BD; F-PPO	158.0	158.0	158.0	158.0	-
C2 and C5; ***C***-C(O)O	F-BD; F-PPO	146.8	146.8	146.8	147.0	-
C3 and C4; ***C***-H	F-BD; F-PPO	118.5	118.5	118.5	118.2	-
f ; O***C***H$_2$	PPO-PPO	–	75.4	75.3	75.3	75.3
g ; O***C***H	PPO-PPO	–	73.4	73.4	73.4	74.4
c, c'; C(O)O***C***H$_2$	F-PPO	-	72.9	72.9	72.9	-
d, d' ; ***C***HCH$_3$	F-PPO	–	71.7	71.7	71.3	-
a, a'; C(O)O***C***H$_2$CH$_2$	F-BD	64.9	64.9	64.9	64.8	-
b, b'; C(O)OCH$_2$***C***H$_2$	F-BD	25.4	25.4	25.3	25.0	-
h ; OCH***C***H$_3$	PPO-PPO	-	17.3	17.3	17.3	17.3
e, e' ; CH***C***H$_3$	F-PPO	–	16.9	16.8	16.8	-

3.2. Thermal behaviour

PBF-co-PBDG copolyesters were extensively characterised in terms of their thermal behaviour, through TGA, DSC and DMTA analyses (Figure S2, S3 and S4, and Table 4.5).

In general, the TGA thermograms (Figure S2 and Table 4.5) of the copolyesters (carried out under nitrogen atmosphere) exhibited one major characteristic event at the maximum decomposition temperatures ($T_{d,max}$) of 340-365 ºC. Also, the newly prepared copolymers showed to be thermally stable up to $T_{d,5\%} \approx 308$ ºC.

Table 4.5. Decomposition at 5% weight loss ($T_{d,5\%}$), maximum decomposition ($T_{d,max}$), glass transition (T_g), melting and cold crystallisation temperatures (T_{cc}) of PBF, PPO and PBF-co-PPOF copolyesters.

(Co)polymer	$T_{d,5\%}$ / ºC	$T_{d,max}$ / ºC)	DSC [a]			DMTA[b]	
			T_g (ºC)	T_{cc} (ºC)	T_m (ºC)	T_g (ºC)	T_m (ºC)
PBF	348.7	380.5	- [c]	-	176.1	75.6	166.9
PBF-co-PPOF-90/10	284.7	347.2	-	-	143.8	-32.6	147.6
PBF-co-PPOF-80/20	288.9	340.3	-	29.9	-	-37.2	124.2
PBF-co-PPOF-50/50	308.1	365.2	-55.1	-	-	-42.3	- [c]
PPO	283.0	323.4	-72.0 – -67.0 [d]	-	-	-	-

[a] Determined by DSC analysis; [b] Determined by DMTA analysis; [c] Not observed. [d] Values obtained from references [30,31].

As shown in Table 4.5, the copolymers had both $T_{d,5\%}$ and $T_{d,max}$ results lower than those observed to PBF. These less favourable thermal results could be associated to the presence of the appending methyl group, as already reported for other polyesters also having side groups, such as poly(2,3-butylene 2,5-furandicarboxylate) compared to PBF.[32] Nevertheless, all PBF-co-PPOF copolyesters have higher $T_{d,max}$ than PPO.

The DSC and DMTA thermograms of all copolyesters are shown in Figure S3 and S4, and the main results are summarized in Table 4.5.

From DSC traces (Figure S3 and Table 4.5) it is possible to observe that PBF-co-PPOF-90/10 and -80/20 copolyesters presented only a melting (T_m) or cold transition (T_{cc}) and at -143.8 and 29.9 ºC, respectively. Furthermore, using DTMA analysis (Figure S4) were reported T_g values of 75.6, -32.6, -37.2 and -42.3 ºC, for PBF and PBF-co-PPOF-90/10, 80/20 and 50/50 materials, respectively. In fact, PBF-co-PPOF-80/20 copolyester also displaying a T_m value of 124.2 ºC, maintaining the ability to crystallise similar to PBF (T_m of 166.9 ºC) (Table 4.5). In the case of PBF-co-PPOF-50/50 copolyester, the absence of T_m revealed some loss on the crystallinity, especially for a higher incorporation of PPOF moieties, probably due to some incompatibility among PBF and PPOF crystallinity domains.

Although, copolyesters with higher incorporation of PPOF moieties in their backbone chain have shown lower T_g and T_m values when compared with those that presented a higher incorporation of BF moieties, however much higher when compared with the amorphous PPO homopolyester (T_g between -67 to -72 ºC).[30,31] These results were the expected since the incorporation of more flexible moieties into FDCA-based copolyesters typically results

on a decreased on copolyesters thermal features.[19,21] In fact, the incorporation of PEG soft moieties into PBT and PPT polymer chain also lead to a decreased on both T_g and T_m, due to the flexibility gain of the resulting materials.[19,27,33–35]

3.3. X-ray diffraction analysis

The XRD pattern (Figure 4.3) of the PBF homopolyester synthesized in this work is in agreement with other publish results, [14,36–38] exhibiting diffraction peaks at $2\theta \sim 10$, 18, 23 and 25º.

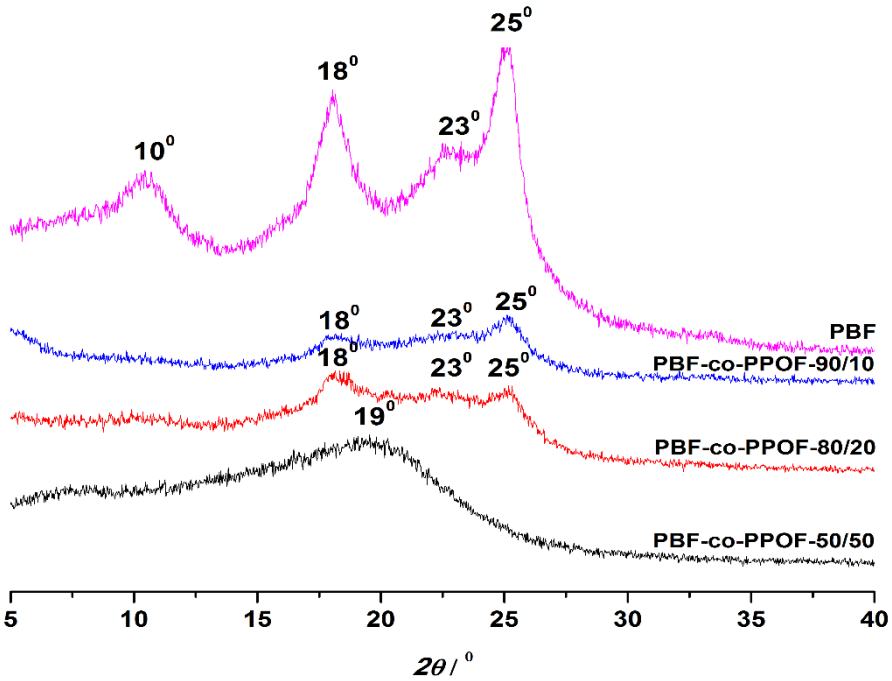

Figure 4.3. XRD patterns of PBF and all PBF-co-PPOF materials.

The XRD patterns of PBF-co-PPOF-90/10 and 80/20 copolymers displayed diffraction peaks at $2\theta \approx 18$, 23 and 25º, quite similar to the PBF pattern. This clearly indicates that the ability of PBF-co-PPOF copolyesters to crystallise is mainly associated to PBF segments (with $L_{n,BF}$ equal to 6.5 and 4.2, respectively). Moreover, these results are in perfect agreement with the above DSC and DMTA data, and also with other FDCA or TPA-based PPEs reported in the literature.[19,21,33,39]

As expected, in the case of the viscous liquid PBF-co-PPOF-50/50 copolyester, only a halo centred at $2\theta \approx 19$ º was observed, in accordance with an essential amorphous nature.

3.4. Hydrolytic and enzymatic degradation tests

As mentioned above, in addition to specific thermal properties, it was also important to understand if the newly prepared materials degrade under hydrolytic and enzymatic conditions. The evaluation of the hydrolytic and enzymatic degradation behaviour was performed evaluated in terms of weight loss percentage versus time (Figure 4.4) for PBF-co-PPOF-80/20 copolyester, with real incorporation of PPOF moieties around 24 mol%. However, the polymer's weight loss under hydrolytic conditions was almost negligible. This result was in the same line with those reported for PBF-co-PEGF copolyesters incorporating similar amount of PBF moieties,22 showing that those copolyesters were not hydrolysable under neutral pH conditions. In fact, also PBT-co-PEGT copolyesters incorporating higher PBT moieties presented very low percentage weight losses (almost zero) in similar hydrolytic conditions used in this study (pH ~ 7 and 37 ºC).34

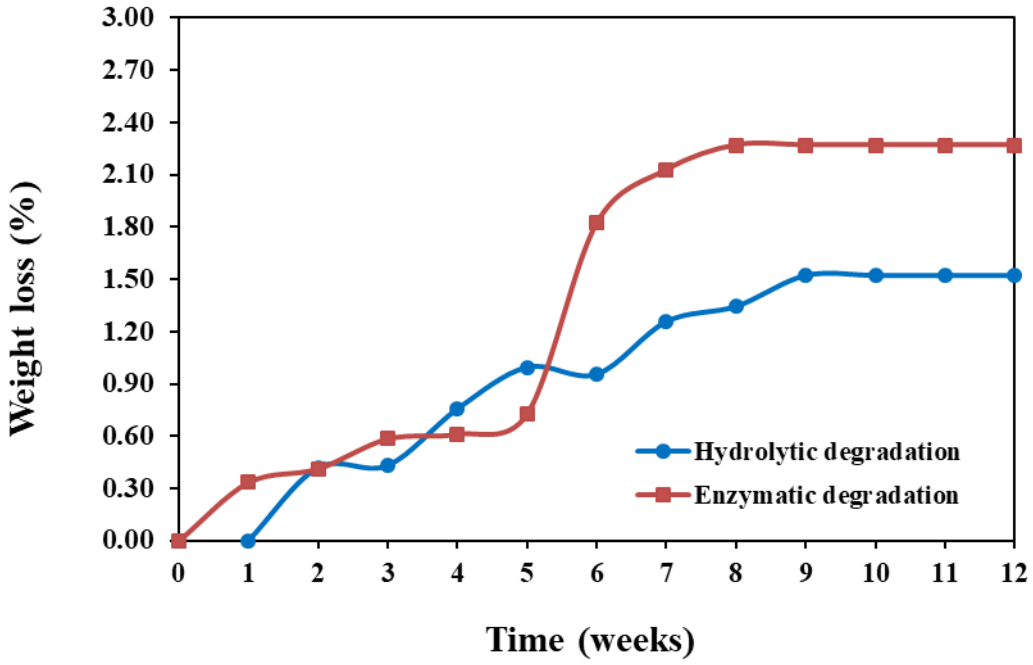

Figure 4.4. Percentage weight loss of PBF-co-PPOF-80/20 copolyester along 12 weeks.

Nevertheless, the incubation with a *Porcine pancreas* lipase in PBS solution slightly increased the weight loss of the ensuing copolyesters. Nevertheless, through hydrolytic and enzymatic degradation tests, just 1.5 and 2.3 % weight loss were achieved, respectively.

Further, incorporation of PPO in the copolymers, is however, expected to counteract this low weight loss.

4. Conclusions

In summary, a new class of FDCA-based poly(ester-ether) copolymers has been accomplished, incorporating both stiff and soft moieties into their copolymer backbone. The ensuing copolyesters have shown high thermal stability ($T_{d,max}$ between 340 to 365 ºC) and T_g at sub-ambient temperatures, namely from -42.3 to -32.6 ºC. Moreover, the semi-crystalline character was only observed for copolyesters with higher BF content, revealing that PBF units were the mainly responsible for the crystalline behaviour of the ensuing materials. Furthermore, PBF-co-PPOF-80/20 copolyester had shown a week hydrolysable behaviour, presenting a maximum percentage weight loss of 2.3 %, after 12 weeks.

Finally, due to their high thermal stability, as well as the presence of both stiff and soft moieties in the copolymer chains, these materials could finding interesting industrial applications, namely as thermoplastic materials.

References

(1) Jong, E. de; Dam, M. A.; Sipos, L.; Gruter, G.-J. M. Furandicarboxylic Acid (FDCA), A Versatile Building Block for a Very Interesting Class of Polyesters. In *Biobased Monomers, Polymers, and Materials*; Smith, Patrick B. ; Gross, R. A., Ed.; American Chemical Society: Amesterdan, 2012; pp 1–13.

(2) Jia, Z.; Wang, J.; Sun, L.; Zhu, J.; Liu, X. Fully Bio-Based Polyesters Derived from 2,5-Furandicarboxylic Acid (2,5-FDCA) and Dodecanedioic Acid (DDCA): From Semicrystalline Thermoplastic to Amorphous Elastomer. *J. Appl. Polym. Sci.* **2018**, *135* (14).

(3) Gandini, A.; Silvestre, A. J. D.; Neto, C. P.; Sousa, A. F.; Gomes, M. M. The Furan Counterpart of Poly (Ethylene Terephthalate): An Alternative Material Based on Renewable Resources. *J. Polym. Sci. Polym. Chem.* **2009**, *5* (c), 295–298.

(4) Sousa, A. F.; Vilela, C.; Fonseca, A. C.; Matos, M.; Freire, C. S. R.; Gruter, G. J. M.; Coelho, J. F. J.; Silvestre, A. J. D. Biobased Polyesters and Other Polymers from 2,5-Furandicarboxylic Acid: A Tribute to Furan Excellency. *Polym. Chem.* **2015**, *6* (33), 5961–5983.

(5) Zhang, D.; Dumont, M. J. Advances in Polymer Precursors and Bio-Based Polymers Synthesized from 5-Hydroxymethylfurfural. *J. Polym. Sci. Polym. Chem.* **2017**, *55* (9), 1478–1492.

(6) Papageorgiou, G. Z.; Papageorgiou, D. G.; Terzopoulou, Z.; Bikiaris, D. N. Production of Bio-Based 2,5-Furan Dicarboxylate Polyesters: Recent Progress and Critical Aspects in Their Synthesis and Thermal Properties. *Eur. Polym. J.* **2016**, *83*, 202–229.

(7) Gomes, M.; Gandini, A.; Silvestre, A. J. D. D.; Reis, B. Synthesis and Characterization of Poly(2,5-Furan Dicarboxylate)s Based on a Variety of Diols. *J. Polym. Sci. Polym. Chem.* **2011**, *49* (17), 3759–3768.

(8) Gandini, A.; Silvestre, A. J. D. A.; Neto, C. P.; Sousa, A. F.; Gomes, M. The Furan Counterpart of Poly(Ethylene Terephthalate): An Alternative Material Based on Renewable Resources. *J. Polym. Sci. Polym. Chem.* **2009**, *47* (1), 295–298.

(9) Matos, M.; Sousa, A. F.; Silvestre, A. J. D. Improving the Thermal Properties of

Poly(2,5-Furandicarboxylate)s Using Cyclohexylene Moieties: A Comparative Study. *Macromol. Chem. Phys.* **2017**, *218* (5).

(10) Soares, M. J.; Dannecker, P. K.; Vilela, C.; Bastos, J.; Meier, M. A. R.; Sousa, A. F. Poly(1,20-Eicosanediyl 2,5-Furandicarboxylate), a Biodegradable Polyester from Renewable Resources. *Eur. Polym. J.* **2017**, *90*, 301–311.

(11) Sousa, A. F.; Coelho, J. F. J.; Silvestre, A. J. D. Renewable-Based Poly((Ether)Ester)s from 2,5-Furandicarboxylic Acid. *Polymer* **2016**, *98*, 129–135.

(12) Haernvall, K.; Zitzenbacher, S.; Amer, H.; Zumstein, M. T.; Sander, M.; McNeill, K.; Yamamoto, M.; Schick, M. B.; Ribitsch, D.; Guebitz, G. M. Polyol Structure Influences Enzymatic Hydrolysis of Bio-Based 2,5-Furandicarboxylic Acid (FDCA) Polyesters. *Biotechnol. J.* **2017**, *12* (9), 1600741.

(13) Gubbels, E.; Jasinska-Walc, L.; Koning, C. E. Synthesis and Characterization of Novel Renewable Polyesters Based on 2,5-Furandicarboxylic Acid and 2,3-Butanediol. *J. Polym. Sci. Polym. Chem.* **2013**, *51* (4), 890–898.

(14) Thiyagarajan, S.; Vogelzang, W.; J. I. Knoop, R.; Frissen, A. E.; Van Haveren, J.; Van Es, D. S. Biobased Furandicarboxylic Acids (FDCAs): Effects of Isomeric Substitution on Polyester Synthesis and Properties. *Green Chem.* **2014**, *16* (4), 1957–1966.

(15) Jiang, Y.; Woortman, A. J. J.; Alberda Van Ekenstein, G. O. R.; Loos, K. A Biocatalytic Approach towards Sustainable Furanic-Aliphatic Polyesters. *Polym. Chem.* **2015**, *6* (29), 5198–5211.

(16) Terzopoulou, Z.; Kasmi, N.; Tsanaktsis, V.; Doulakas, N.; Bikiaris, D. N.; Achilias, D. S.; Papageorgiou, G. Z. Synthesis and Characterization of Bio-Based Polyesters: Poly(2-Methyl-1,3-Propylene-2,5-Furanoate), Poly(Isosorbide-2,5-Furanoate), Poly(1,4-Cyclohexanedimethylene-2,5-Furanoate). *Materials* **2017**, *10* (7).

(17) Tsanaktsis, V.; Terzopoulou, Z.; Exarhopoulos, S.; Bikiaris, D. N.; Achilias, D. S.; Papageorgiou, D. G.; Papageorgiou, G. Z. Sustainable, Eco-Friendly Polyesters Synthesized from Renewable Resources: Preparation and Thermal Characteristics of Poly(Dimethyl-Propylene Furanoate). *Polym. Chem.* **2015**, *6* (48), 8284–8296.

(18) Genovese, L.; Lotti, N.; Siracusa, V.; Munari, A. Poly(Neopentyl Glycol Furanoate):

A Member of the Furan-Based Polyester Family with Smart Barrier Performances for Sustainable Food Packaging Applications. *Materials* **2017**, *10* (9).

(19) Zhou, W.; Zhang, Y.; Xu, Y.; Wang, P.; Gao, L.; Zhang, W.; Ji, J. Synthesis and Characterization of Bio-Based Poly(Butylene Furandicarboxylate)-b-Poly(Tetramethylene Glycol) Copolymers. *Polym. Degrad. Stabil.* **2014**, *109*, 21–26.

(20) Sousa, A. F.; Coelho, J. F. J.; Silvestre, A. J. D. Renewable-Based Poly((Ether)Ester)s from 2,5-Furandicarboxylic Acid. *Polymer* **2016**, *98*, 129–135.

(21) Sousa, A. F.; Guigo, N.; Pozycka, M.; Delgado, M.; Soares, J.; Mendonça, P. V.; Coelho, J. F. J.; Sbirrazzuoli, N.; Silvestre, A. J. D. Tailored Design of Renewable Copolymers Based on Poly(1,4-Butylene 2,5-Furandicarboxylate) and Poly(Ethylene Glycol) with Refined Thermal Properties. *Polym. Chem.* **2018**, *9* (6), 722–731.

(22) Hu, H.; Zhang, R.; Sousa, A.; Long, Y.; Ying, W. Bin; Wang, J.; Zhu, J. Bio-Based Poly(Butylene 2,5-Furandicarboxylate)-b-Poly(Ethylene Glycol) Copolymers with Adjustable Degradation Rate and Mechanical Properties: Synthesis and Characterization. *Eur. Polym. J.* **2018**, *106* (July), 42–52.

(23) Chi, D.; Liu, F.; Na, H.; Chen, J.; Hao, C.; Zhu, J. Poly(Neopentyl Glycol 2,5-Furandicarboxylate): A Promising Hard Segment for the Development of Bio-Based Thermoplastic Poly(Ether-Ester) Elastomer with High Performance. *ACS Sustain. Chem. Eng.* **2018**, *6* (8), 9893–9902.

(24) Deschamps, A. A.; Claase, M. B.; Sleijster, W. J.; Bruijn, J. D. De; Grijpma, D. W.; Feijen, J. Design of Segmented Poly(Ether Ester) Materials and Structures. *J. Control. Release* **2002**, *78* (1–3), 175–186.

(25) Buitinga, M.; Truckenmüller, R.; Engelse, M. A.; Moroni, L.; Ten Hoopen, H. W. M.; van Blitterswijk, C. A.; de Koning, E. J. P.; van Apeldoorn, A. A.; Karperien, M. Microwell Scaffolds for the Extrahepatic Transplantation of Islets of Langerhans. *PLoS One* **2013**, *8* (5), 1–11.

(26) Octoplus. PolyActive^{TM} A biodegradable polymer-based drug delivery system http://www.afinitica.com/arnews/?q=taxonomy/term/130 (accessed Oct 29, 2018).

(27) Deschamps, A. A.; Grijpma, D. W.; Feijen, J. Poly(Ethylene Oxide)/Poly(Butylene Terephthalate) Segmented Block Copolymers: The Effect of Copolymer Composition

on Physical Properties and Degradation Behavior. *Polymer* **2001**, *42* (23), 9335–9345.

(28) Wang, J.; Liu, X.; Jia, Z.; Liu, Y.; Sun, L.; Zhu, J. Synthesis of Bio-Based Poly(Ethylene 2,5-Furandicarboxylate) Copolyesters: Higher Glass Transition Temperature, Better Transparency, and Good Barrier Properties. *J. Polym. Sci. Polym. Chem.* **2017**, *55* (19), 3298–3307.

(29) Wang, J.; Liu, X.; Zhu, J.; Jiang, Y. Copolyesters Based on 2,5-Furandicarboxylic Acid (FDCA): Effect of 2,2,4,4-Tetramethyl-1,3-Cyclobutanediol Units on Their Properties. *Polymers* **2017**, *9* (9).

(30) Allen, G.; Crossley, H. G. Polypropylene Oxide IV-Preparation and Properties of Polyether Networks. *Polymer* **1964**, *5* (C), 553–557.

(31) Vesterinen, A.; Lipponen, S.; Rich, J.; Seppälä, J. Effect of Block Composition on Thermal Properties and Melt Viscosity of Poly[2-(Dimethylamino)Ethyl Methacrylate], Poly(Ethylene Oxide) and Poly(Propylene Oxide) Block Co-Polymers. *Express Polym. Lett.* **2011**, *5* (9), 754–765.

(32) Jiang, Y.; Woortman, A. J. J.; Alberda Van Ekenstein, G. O. R.; Loos, K. A Biocatalytic Approach towards Sustainable Furanic-Aliphatic Polyesters. *Polym. Chem.* **2015**, *6* (29), 5198–5211.

(33) Szymczyk, A. Structure and Properties of New Polyester Elastomers Composed of Poly(Trimethylene Terephthalate) and Poly(Ethylene Oxide). *Eur. Polym. J.* **2009**, *45* (9), 2653–2664.

(34) Chao, G. T.; Fan, L. Y.; Jia, W. J.; Qian, Z. Y.; Gu, Y. C.; Liu, C. B.; Ni, X. P.; Li, J.; Deng, H. X.; Gong, C. Y.; et al. Synthesis, Characterization and Hydrolytic Degradation of Degradable Poly(Butylene Terephthalate)/Poly(Ethylene Glycol) (PBT/PEG) Copolymers. *J. Mater. Sci. Mater. Med.* **2007**, *18* (3), 449–455.

(35) Zhang, Y.; Feng, Z.; Feng, Q.; Cui, F. Preparation and Properties of Poly(Butylene Terephthalate-Co- Cyclohexanedimethylene Terephthalate)-b-Poly(Ethylene Glycol) Segmented Random Copolymers. *Polym. Degrad. Stabil.* **2004**, *85* (1), 559–570.

(36) Gandini, A.; Coelho, D.; Gomes, M.; Reis, B.; Silvestre, A. Materials from Renewable Resources Based on Furan Monomers and Furan Chemistry: Work in Progress. *J. Mater. Chem.* **2009**, *19* (45), 8656.

(37) Jiang, M.; Liu, Q.; Zhang, Q.; Ye, C.; Zhou, G. A Series of Furan-Aromatic Polyesters Synthesized via Direct Esterification Method Based on Renewable Resources. *J. Polym. Sci. Polym. Chem.* **2012**, *50* (5), 1026–1036.

(38) Ma, J.; Yu, X.; Xu, J.; Pang, Y. Synthesis and Crystallinity of Poly(Butylene 2,5-Furandicarboxylate). *Polymer* **2012**, *53* (19), 4145–4151.

(39) Yao, C.; Yang, G. Crystallization, and Morphology of Poly(Trimethylene Terephthalate)/Poly(Ethylene Oxide Terephthalate) Segmented Block Copolymers. *Polymer* **2010**, *51* (6), 1516–1523.

Supporting information

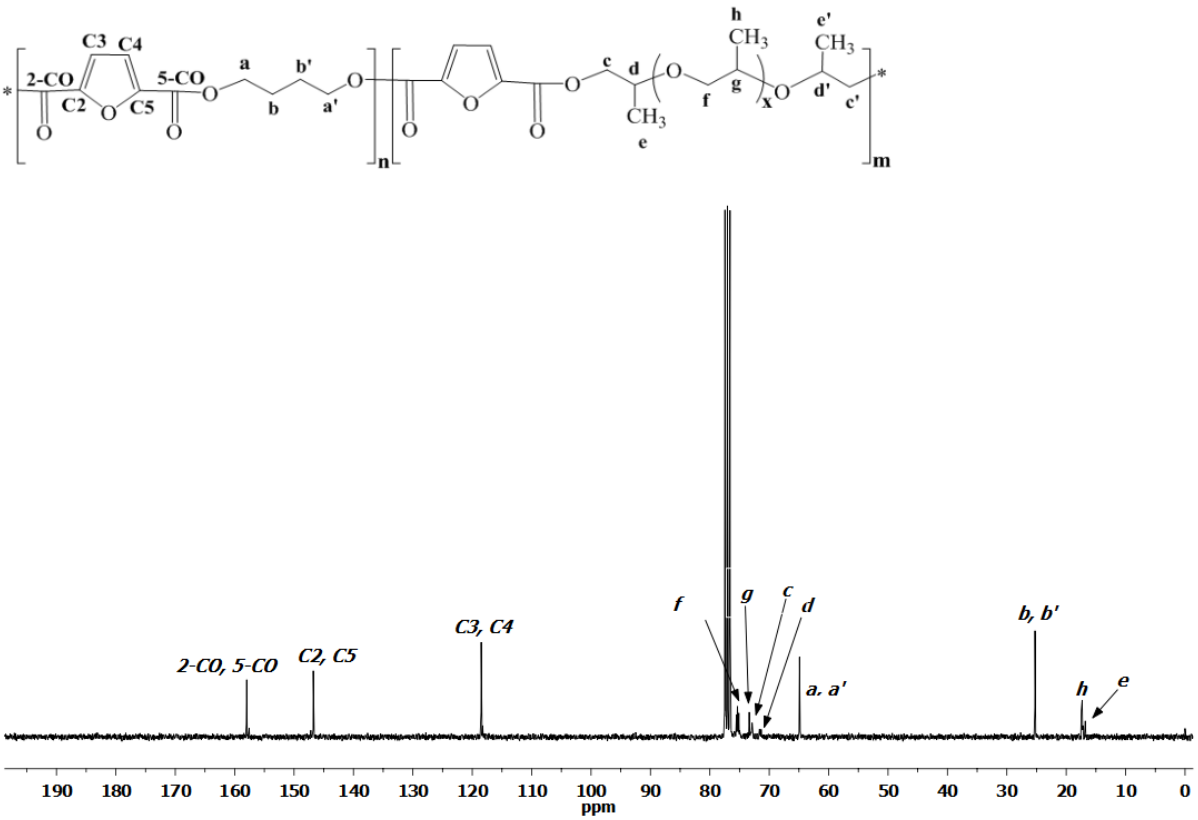

Figure S1. ^{13}C NMR spectra in $CHCl_3$-*d* of PBF-co-PPOF-90/10 copolymer.

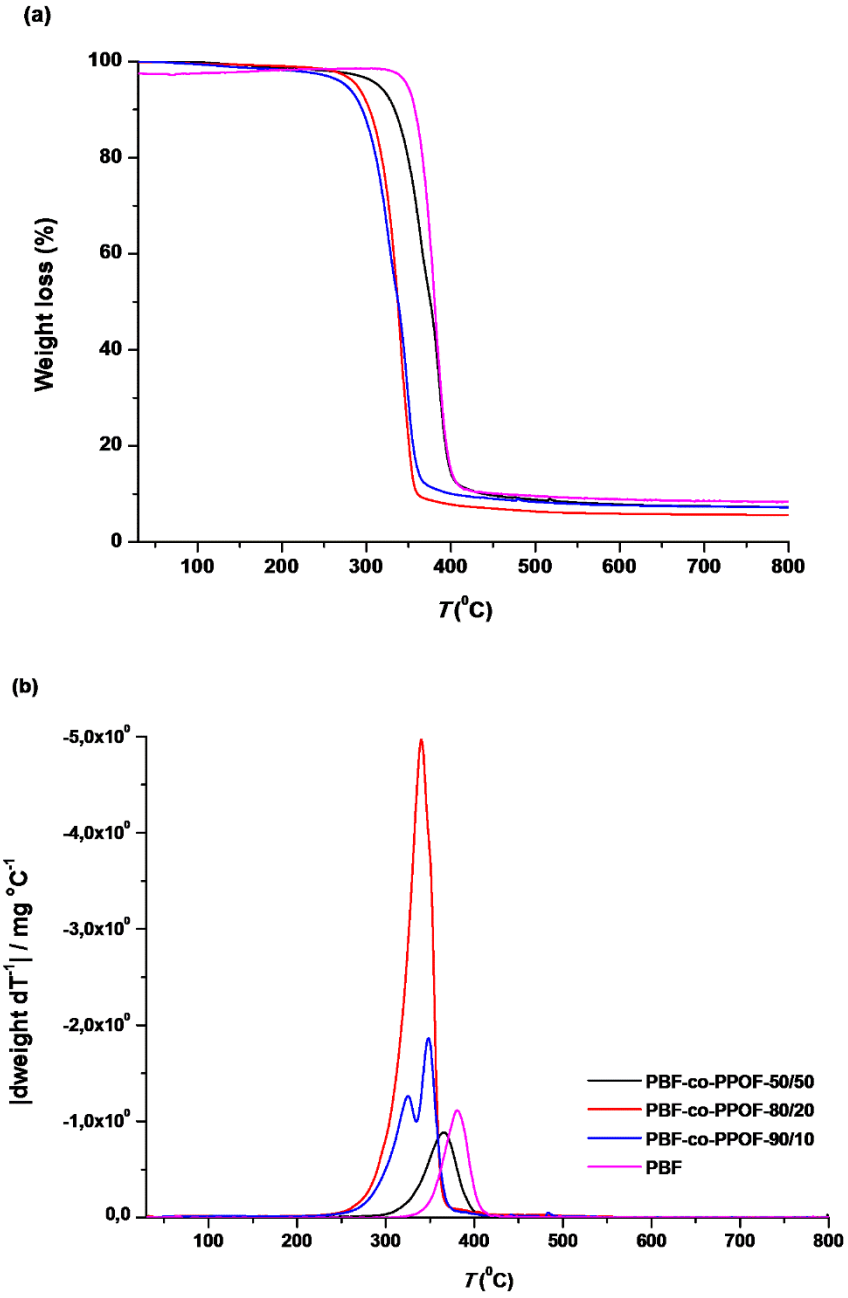

Figure S2. TGA (a) and DTGA (b) thermograms of PBF-co-PPOF copolyesters and PBF homopolyester.

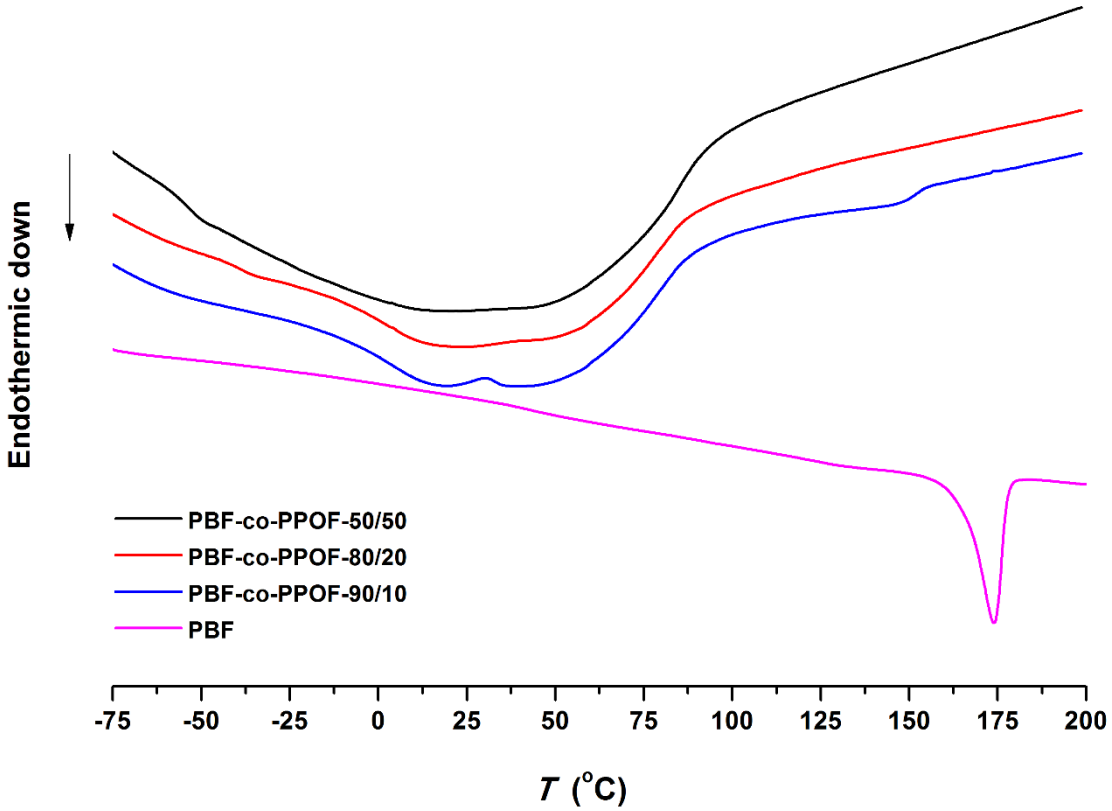

Figure S3. DSC curves of all copolymers and PBF homopolyester.

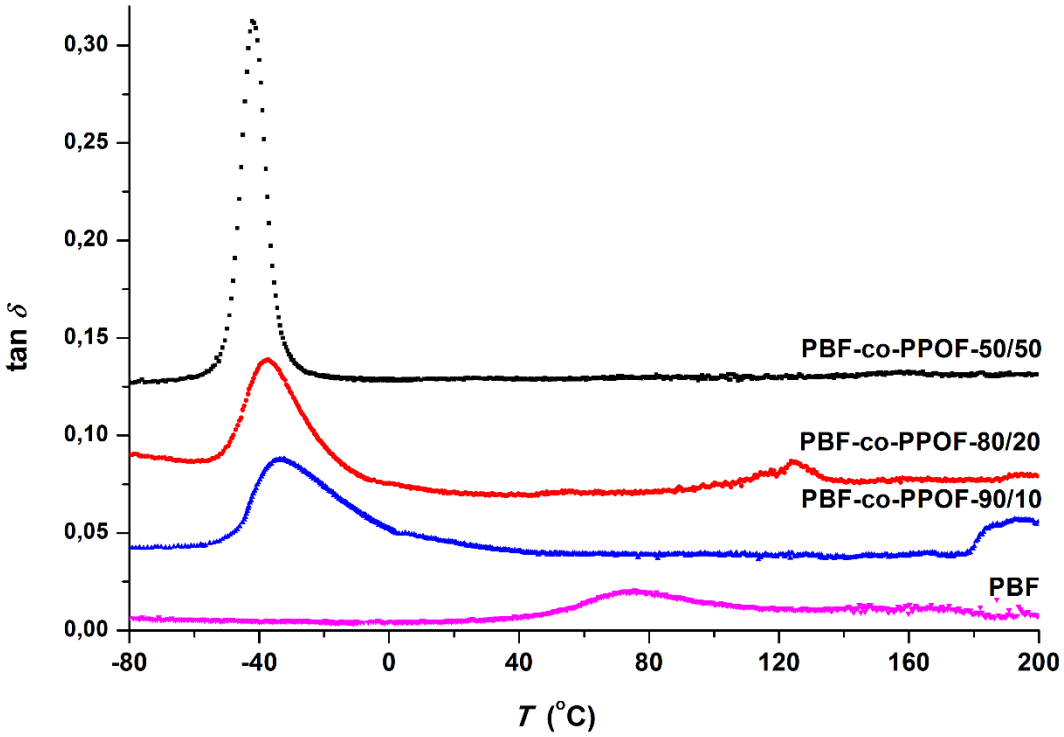

Figure S4. Tan δ of PBF and PBF-co-PPOF (co)polymers, at 1 Hz.

Chapter V – Furanoate-Based Nanocomposites: A Case Study Using Poly(Butylene 2,5-Furanoate) and Poly(Butylene 2,5-Furanoate)-co-(Butylene Diglycolate) and Bacterial Cellulose

---

This chapter was published in:

Marina Matos, Andreia F. Sousa, Nuno H. C. S. Silva, Carmen S. R. Freire, Márcia Andrade, Adélio Mendes, Armando J. D. Silvestre. Furanoate-based nanocomposites: a case study using poly(butylene 2,5-furanoate) and poly(butylene 2,5-furanoate)-co-(butylene diglycolate) and bacterial cellulose, *Polymers*, **2018**, 10 (8), 810.

Abstract

Polyesters made from 2,5-furandicarboxylic acid (FDCA) have been in the spotlight due to their renewable origins, together with the promising thermal, mechanical, and/or barrier properties. Following the same trend, (nano)composite materials based on FDCA could also generate similar interest, especially because novel materials with enhanced or refined properties could be obtained. This paper presents a case study on the use of furanoate-based polyesters and bacterial cellulose to prepare nanocomposites, namely acetylated bacterial cellulose/poly(butylene 2,5-furandicarboxylate) and acetylated bacterial cellulose/poly(butylene 2,5-furandicarboxylate)-co-(butylene diglycolate)s. The balance between flexibility, prompted by the furanoate-diglycolate polymeric matrix; and the high strength prompted by the bacterial cellulose fibres, enabled the preparation of a wide range of new nanocomposite materials. The new nanocomposites had a glass transition between -25–46 ºC and a melting temperature of 61–174 ºC; and they were thermally stable up to 239–324 ºC. Furthermore, these materials were highly reinforced materials with an enhanced Young's modulus (up to 1239 MPa) compared to their neat copolyester counterparts. This was associated with both the reinforcing action of the cellulose fibres and the degree of crystallinity of the nanocomposites. In terms of elongation at break, the nanocomposites prepared from copolyesters with higher amounts of diglycolate moieties displayed higher elongations due to the soft nature of these segments.

Keywords: 2,5-furandicarboxylic acid; poly(1,4-butylene 2,5-furandicarboxylate); biobased materials bacterial cellulose; nanocomposites; mechanical properties

1. Introduction

The last decades have assisted to a burgeoning search for more sustainable chemicals, polymers and materials due to severe environmental concerns and to the announced depletion of fossil resources.[1] In this context, renewable-based chemicals, such as those derived from C5 and C6 biomass sugars, mainly the 2,5-furandicarboxylic acid (FDCA), and the polyesters thereof, have been in the spotlight.[2] Some of the most successful examples, due to their promising properties, comparable to fossil-based terephthalate homologous,

include poly(ethylene 2,5-furandicarboxylate) (PEF),[3,4] and poly(1,4-butylene 2,5-furandicarboxylate) (PBF),[5–14] also known as poly(ethylene 2,5-furanoate) and poly(1,4-butylene 2,5-furanoate), respectively. They are expected to replace poly(ethylene terephthalate) (PET) and poly(1,4-butylene terephthalate) (PBT), respectively, on various conventional applications of thermoplastics, such as for example in packaging materials in the case of PEF or in electronic applications in the case of PBF.[2]

Furthermore, FDCA-derived copolyesters have also been extensively studied aiming to expand, or refine even further the properties and/or potential applications of their parent homopolymers.[7,15–22] Among the wide library of these copolymers, furanoate-aliphatic copolyesters were the most studied,[2,15–17,21–30] and those incorporating ether linkages, such as the work of Lotti *et al*.[29] based on diglycolic acid or of Sousa *et al*.[16] using poly(ethylene glycol), are particularly interesting. For example, the 100% renewable poly(butylene 2,5-furanoate)-co-(butylene diglycolate)s (with 60 to 90 mol% of furanoate moieties), henceforth designated by PBF-co-PBDG, are biodegradable and could have an elongation at break of up to 4 times higher than PBF.[29] In fact, the incorporation of high quantities of soft butylene diglycolate units brings significant improvement in the elongation, but at the expense of the Young's Modulus (roughly 10 times lower compared to PBF). In terms of gas barrier properties, PBF-co-PBDG can exhibit adequate behaviour to packaging materials applications. The oxygen gas transmission rate (GTR) varied between 111-193 $cm^3\ m^{-2}\ d^{-1}\ bar^{-1}$.[29]

More recently, (nano)composite and hybrid materials based on furanoate-based polymeric matrices, have also been developed,[31–36] although still modestly and mostly restricted to PEF. However, the significant properties improvement of the ensuing materials, relevant to their processing and/or application (*e.g.* crystallisation rate improvement), will predictably foster their rapid development in the near future. PEF-derived hybrid materials were prepared by compounding PEF with inorganic fillers, added during the synthesis of the polymer. For example, Bikiaris and co-workers[32] demonstrated that the *in situ* preparation of PEF/SiO_2 and PEF/TiO_2 hybrid materials, during solid state polymerization, lead to slightly higher molecular weight PEF due to the presence of the SiO_2 or TiO_2 nanoparticles. Lotti *et al.*[35] also synthesised hybrid materials based on PEF containing either graphene oxide or multi walled carbon nanotubes (non-functionalised, or functionalised with -COOH or -NH_2 groups). Differential scanning calorimetry analysis indicated that all the fillers acted

as nucleating agents for the PEF crystallisation, albeit in a different extent. Other works are focused on PEF-derived (nano)composites with cellulose fibres,[31,36] organically modified montmorillonite clays and sepiolite clays.[33,34] Of particular interest is the work carried out by the Guigo and Sbirrazzuoli group on PEF composites using small quantities of nanocrystalline cellulose (around 4 %wt) and prepared *via* twin screw extrusion[31] or solvent casting.[36] These composites have enhanced crystallisation properties in the presence of the fibres, namely faster crystallisation[31] and nucleating effect,[36] despite some compatibility problems associated to the hydrophilic nature of pristine cellulose oppositely to PEF homopolyester.[36] Adding to this, nanocellulose fibres, in particular bacterial cellulose (BC) produced by *Gluconoacetobacter sacchari* bacterial strain, in high purity, due to its nanofibrillar structure bring unique physical and chemical properties to the nanocomposites thereof,[37,38] including optically transparency and high mechanical strength.[39] However, to the best of our knowledge, BC has never before been used in the preparation of furanoate-based nanocomposites. In this vein, this study presents a new family of fully bio-based nanocomposites, prepared from a series of PBF-co-PBDG copolyesters, or PBF, and modified bacterial cellulose previously submitted to heterogeneous acetylation (to improve compatibility with the thermoplastic matrices). These PBF-co-PBDG/ and PBF/acetylated-BC nanocomposites were chosen as a case study for a broader development of furanoate-based nanocomposites and in particular due to the potential to enhance the mechanical properties. The newly prepared nanomaterials were fully characterised through several structural, thermal and mechanical techniques, as well as in terms of gas permeability aiming to access their potential use for packaging applications.

2. Experimental

2.1. Materials

Bacterial cellulose in the form of wet membranes was produced using the Gluconoacetobacter sacchari bacterial strain and conventional culture medium conditions, as described elsewhere.[40] 2,5-Furandicarboxylic acid (FDCA, >98%) and 1,1,1,3,3,3-hexafluoro-2-propanol (HFP, >99%) were purchased from TCI Europe NV. Diglycolic acid (DGA, 98%), 1,4-butanediol (BD, 99%), titanium (IV) tert-butoxide (Ti(OBu)4, pro-analysis), trifluoroacetic acid, (TFA, 99%) and deuterated trifluoroacetic acid (TFA-d, 99

atom % D) were supplied by Sigma-Aldrich Chemicals Corporation (Sintra, Portugal). Sulfuric acid (H2SO4, 96%) was supplied by Acros Organic (Geel, Belgium). All chemicals were used as received.

2.2. Heterogeneous acetylation of bacterial cellulose (Ac-BC)

Prior to heterogeneous acetylation, the BC wet membrane was disintegrated using a blender and an Ultra-Turrax equipment (15 min at 20 500 rpm), and solvent exchanged with ethanol and acetone (in triplicate). Heterogeneous acetylation of BC fibres was, then, carried out following a well-stablished protocol described elsewhere.[39] Briefly, acetic anhydride (225 mL) was placed in a 500 mL round flask into an ice bath for 20 minutes, then 1 mL of H_2SO_4 was added and finally the wet BC fibres (≈ 40 g) were added to the mixture. The reaction was allowed to proceed under stirring for 4 h, at 30 ºC. The ensuing BC acetylated fibres (Ac-BC) were filtered and sequentially washed with water, acetone, ethanol, water and again with ethanol. Finally, Ac-BC nanofibres were Soxhlet extracted with ethanol for 12 h to remove any residual trace of acetic anhydride or other impurities, and solvent exchanged with acetone followed by chloroform.

2.3. Preparation of the acetylated BC/Poly(butylene furandicarboxylate-co-butylene diglycolate) nanocomposites (Ac-BC/PBF-co-PBDG)

2.3.1. Synthesis of PBF-co-PBDG copolyesters and corresponding homopolyesters

The polyesters were synthesized *via* a procedure described elsewhere[18,41]: Fisher esterification of FDCA, esterification stage, and finally polycondensation reaction. In brief, firstly, dimethyl 2,5-dimethylfurandicarboxylate (DMFDC) was prepared by reacting FDCA (192.2 mmol) with an excess of methanol (364 mL), under acidic conditions (HCl, 15 mL), at 80 ºC for 15 h. The reaction mixture was allowed to cool down, and the ensuing white precipitate was isolated by filtration in 70% yield. Secondly, DMFDC and DGA (mol% DMFDC / mol% DGA ≈ 90/10, 75/25, 50/50, 25/75 and 10/90) were mixed with an excess of BD (1.5 mol per 1 mol of DMFDC and DGA) under a nitrogen atmosphere. Then, the temperature was raised to 110 ºC, $Ti(OBu)_4$ catalyst (1.4 mmol) added and the temperature was again progressively raised to 200 ºC. Here, a slightly different procedure was followed depending on the polyester being synthesized.

In the case of PBF, PBF-co-PBDG-90/10, 75/25 and 50/50 (*i.e.*, those polyesters prepared from higher amounts of DMFDC) the reaction mixture was kept at 200 ºC for 4 h. Then, the reaction proceeded by applying vacuum (*ca.* 10^{-3} bar) for 1 h. Subsequently, the temperature was raised again to approximately 210 ºC and kept at that maximum temperature for more 4 h. In the other cases of PBDG, PBF-co-PBDG-25/75 and 10/90 the period at 200 ºC was only 2 h, followed by an additional 2 h period, at 210 ºC. In the third-step, the reaction proceeded at 210 ºC under vacuum, and then the temperature was raised to 220 ºC for 4 h. Then, the mixture was purified by dissolving the polymers in TFA (20 mL), and pouring into an excess of cold methanol (*ca.* 1 L), separated by filtration and dried. The isolation yields of the polymers were *ca.* 60%, which is in accordance with previous results.[16]

2.3.2. Preparation of Ac-BC/PBF-co-PBDG nanocomposites, and corresponding homopolyesters nanocomposites

The nanocomposites were prepared by the well-known solvent casting approach. The polyesters (0,21 g) were mixed with a BC or Ac-BC chloroform dispersion (0.0045 g/ml, 20 mL) under magnetic stirring for 3 h. Then, the mixture was deposited into a square Teflon mould (6.5 cm^2) and the films were casted in, at room temperature, for a minimum of 15 h, and finally heated at 30 ºC, under vacuum, for 12 h to remove any remaining solvent. The ensuing films had a thickness of approximately 0.098 ± 0.001 mm.

2.4. Characterisation techniques

Attenuated total reflectance Fourier transform infrared (ATR FTIR) spectra were obtained using a PARAGON 1000 Perkin-Elmer FTIR spectrometer (Villepinte, France) equipped with a single-horizontal Golden Gate ATR cell. The spectra were recorded after 128 scans, at a resolution of 4 cm^{-1}, within a range of 500 to 4000 cm^{-1}. ^{1}H and ^{13}C nuclear magnetic resonance (NMR) spectra were recorded using a Bruker AMX 300 spectrometer (Barcelona, Spain), operating at 300 or 75 MHz, respectively. All chemical shifts (δ) were expressed as parts per million, downfield from tetramethylsilane (used as the internal standard).

Elemental analyses (C and H) were conducted in triplicate using a LECO TruSpec analyser (Madrid, Spain). The degree of substitution (DS) was estimated through the

approach of Vaca-Garcia et al.[42]: DS= (5.13766 − 11.5592 × C)/(0.996863 × C − 0.856277 × *n* + *n* × C) where n and C stand for the number of carbon atoms in the acyl group and for the carbon contents, respectively.

Scanning electron microscopy (SEM) images of the surface and cross-sections of films were acquired using a field emission gun-SEM Hitachi SU70 microscope operating at 4 kV (Dreieich-Buchschlag, Deutschland). Samples were deposited onto a sample holder and coated with carbon twice.

X-ray diffraction (XRD) analyses were performed using a Philips X'pert MPD diffractometer (Valbom, Portugal) operating with CuKα radiation (λ = 1.5405980 Å) at 40 kV and 50 mA. Samples were scanned in the 2θ range of 5º to 50º, with a step size of 0.04º, and a time per step of 50 s.

Differential scanning calorimetry (DSC) thermograms were obtained with a DSC Q100 V9.9 Build 303 (Universal V4.5A) calorimeter from Texas Instruments (Guyancourt, France), using steel DSC pans. Scans were carried out under nitrogen with a heating rate of 10 °C min^{-1} in the temperature range of -90 to 250 ºC. Two heating/cooling cycles were repeated. Glass transition (T_g) was determined using the midpoint approach (second heating trace); melting (T_m) and crystallisation (T_{cc}) temperatures were determined as the maximum of the exothermic crystallisation peak, and the minimum of the melting endothermic peak during the second heating cycle, respectively.

Thermogravimetric analyses (TGA) were carried out with a Setaram SETSYS analyser (Caluire, France) equipped with an alumina plate. Thermograms were recorded under a nitrogen flow of 20 mL min^{-1} and heated at a constant rate of 10 ºC min^{-1} from room temperature up to 800 ºC. Thermal decomposition temperatures were taken at the onset of significant weight loss (5%) and at maximum decomposition temperatures from the heated samples ($T_{d,5\%}$ and T_d, respectively).

Tensile tests were obtained with an Instron 5564 tensile testing machine (Barcelona, Spain,) at a cross-head speed of 10 mm min^{-1} using a 500 N static load cell. The tensile test specimens were rectangular strips (50 mm × 10 mm) pre-conditioned for 72 h at 50% humidity and 30 ºC. Each measurement was repeated at least five times.

Contact angle (CA_{water}) measurements with water were carried out using a Contact Angle System OCA20 goniometer (DataPhysics, Filderstadt, Germany) with SCA20 software using the sessile drop approach, and recorded during 40 s. Water was used as probe liquid,

and for each specimen, drops of 3 μL were deposited using a syringe (50 μL) onto the nanocomposite film surface. The error analysis was obtained by the standard deviation of at least five independent determinations.

Permeation measurements were performed in a system that included a membrane cell connected to a tank with a calibrated volume (at the permeate side) and to a gas cylinder (at the feed side). Prior to permeation tests, the films were glued to steel O-rings with an epoxy glue (Araldite® Standard, Huntsman Advanced Materials, Basel, Switzerland); the glue was also applied along the interface of the steel O-ring and the film, as described elsewhere.[43] A sintered metal disc covered with a filter paper was used as support for the film in the test cell. Single gases were tested at 30 ºC, where the feed pressure was 1 bar and the permeate pressure was ca. 0.03 bar. The tests were performed in a standard pressure-rise setup using an acquisition program based on LabView® platform (National Instruments, Austin, TX, USA). The permeability towards a pure component *i* was determined accordingly to: $L_i = \frac{F_i}{\Delta P_i/l}$, where F_i is the flux of species *I*, ΔP_i is the partial pressure difference of species between the two sides of the membrane, and l is the film thickness. The permeability to the pure component was computed from the experimental data as follows: $L_i = \frac{lV_p v_M}{RTA(P_f - P_p)} \frac{\Delta P_p}{\Delta t}$, where V_p is the volume of the permeate tank, v_M is the molar volume of the gas at normal conditions, *R* is the gas constant, *T* is the absolute temperature, *t* is the time, *A* is the effective permeating area of the film, and P_f and P_p are the feed pressure and permeate pressure, respectively, and ΔP_p is the permeate pressure increment for the elapsed time Δt.

3. Results

3.1. From furanoate-glycolate copolyesters to acetylated bacterial cellulose-based nanocomposites

A series of Ac-BC/PBF-*co*-PBDGs, Ac-BC/PBF, and Ac-BC/PBDG nanocomposites were developed for the first time following a three-step procedure (Scheme 1).

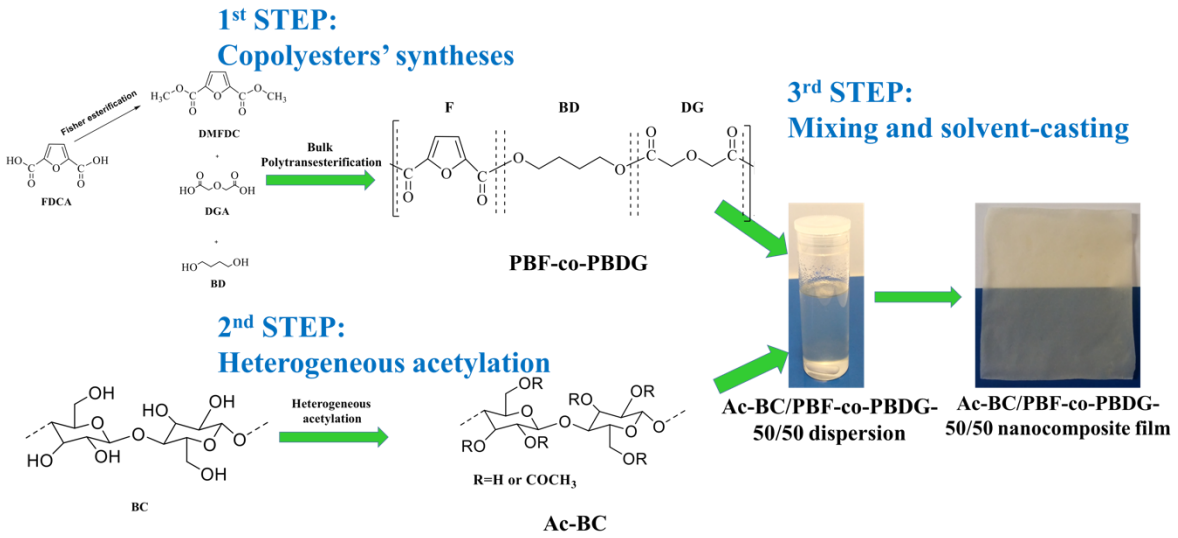

Scheme 1. The Ac-BC/PBF-co-PBDG composite preparation approach.

In the first step, the (co)polyesters were prepared by a conventional bulk polyesterification approach.[18,41] These (co)polyesters spanned from the neat PBF to neat PBDG, and encompassed their copolyesters with different relative furanoate/digycolate amounts (90/10, 75/25, and the never reported 50/50, 25/75, and 10/90 mol %). The selection of these (co)polyesters was based on their promising properties, notably biodegradability and high elongation at break,[29] and aiming to further improve their mechanical properties.

In the second step, heterogeneous acetylation of the BC fibres were performed using acetic anhydride. The degree of acetylation (DS) of the Ac-BC was determined using elemental analysis, by the Vaca-Garcia et al.[42] approach, and the resulting value was 0.87.

In the third step, nanocomposite films of each (co)polyester and Ac-BC were obtained by solvent-casting aiming to obtain novel nanomaterials with enhanced mechanical properties. Importantly, this approach could be generally applied to other furanoate thermoplastics as a strategy to improve their mechanical performance, namely to recycled PEF. Recycled thermoplastics lose some of their high-performance mechanical properties, mostly due to a reduction of the molecular weight. However, compounding these thermoplastics with the Ac-BC nanofibres could play a reinforcing role.

The relative amount of (co)polyester/Ac-BC used in this work in the nanocomposites preparation was approximately equal to 70/30 wt %, based on the fact that a minimum of 30 wt % of Ac-BC was required to form the films. For comparison reasons, films of each individual component of the nanocomposites were additionally prepared. Pure Ac-Bc

generates a white thin film, but the neat copolyesters did not form films by solvent-casting; in fact, this was consistent with the fact that a minimum of 30 wt % of Ac-BC was needed in order to obtain the nanocomposites films.

For comparison reasons, nanocomposites of non-acetylated BC/PBF-*co*-PBDGs were also prepared following a similar approach. However, these materials were shown to be very heterogeneous; hence they were not further investigated. On the contrary the nanocomposite materials prepared using the Ac-BC fibres were homogeneous and translucent, indicating a good dispersion of the modified BC in the thermoplastic polymeric matrices.

3.2. Structure and morphology

The starting (co)polymers components were studied ^{1}H and ^{13}C NMR analysis. The main results are recorded in the Supplementary data (Figure S1, and also Tables S1 and S2), and were consistent with previously published data.[29] One important aspect studied, due to the influence on the final properties of the (co)polyesters and consequently also on the related nanocomposites, were the assessment of the real furanoate/diglycolate incorporation (Table S2). Results indicated a trend towards incorporating slightly more diglycolate moieties in the copolymer back-bone than in the initial feed ratio, except for PBF-*co*-PBDG-50/50 copolyester (7 mol % higher than expected).

All furanoate-based nanocomposites and corresponding components (Ac-BC, PBF-*co*-PBDG, PBF, and PBDG polyesters) were also thoroughly characterised by means of ATR FTIR spectroscopy (Figure 5.1 and Figures S2–S4 of Supplementary data).

The Ac-BC/PBF-*co*-PBDG nanocomposites displayed the typical vibration modes of furanoate-based polyesters[44] and in particular of PBF-*co*-PBDGs: two week bands centred at 3150 and 3115 cm^{-1} arising from the symmetrical and asymmetrical C–H stretching of the furanic ring (ν_{sym} = C–H_{ring} and ν_{asym} = C–H_{ring}), two other weak bands near 2962 and 2890 cm^{-1} arising from the symmetrical and asymmetrical C–H stretching characteristics of the methylene groups of the BD and diglycolate moieties (ν_{sym} C–H and ν_{asym} C–H), and a very intense band centred at 1720 cm^{-1}, arising from the carbonyl stretching vibration, typical of ester groups (ν C=O).

In addition, these spectra also showed a band near 1506 cm^{-1}, assigned to both the C=C stretching and CH_2 in plane deformation (ν C=C, δ CH_2, respectively), a band near 1263

cm^{-1} arising from the ν_{asym} C–O–C stretching, and several vibrations in the finger print region related to the 2,5-disubstitued ring.

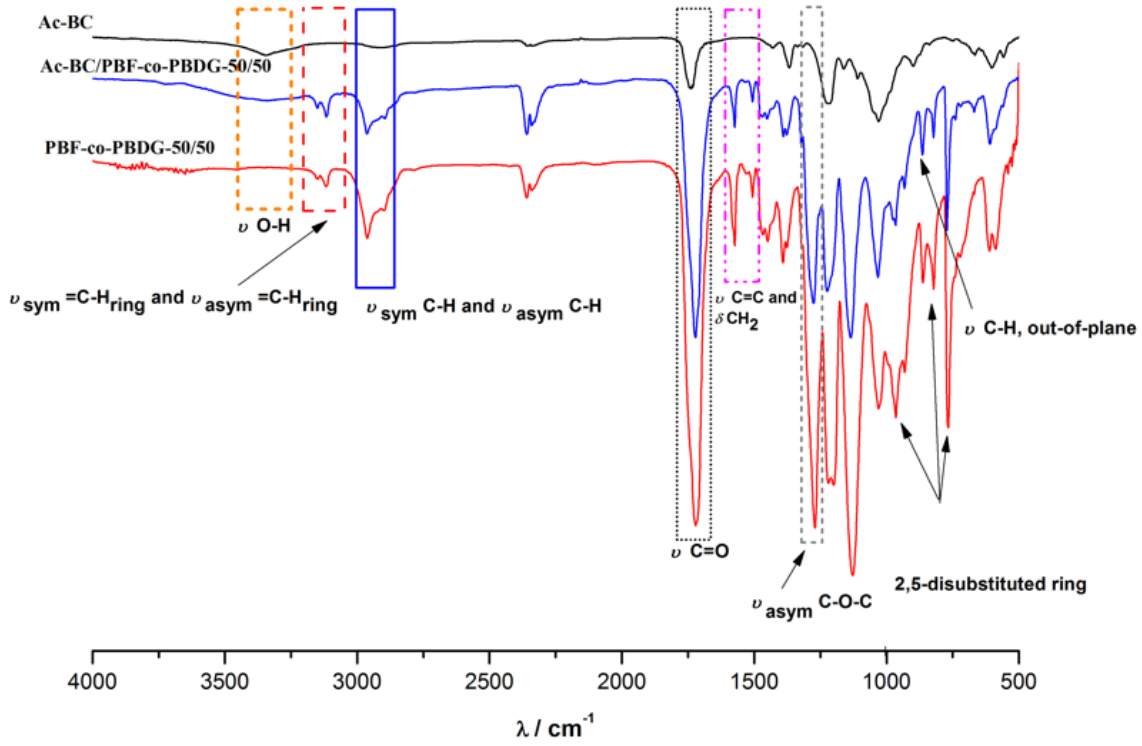

Figure 5.1. Attenuated total reflectance Fourier transform infrared (ATR FTIR) spectra of Ac-BC/PBF-co-PBDG-50/50 nanocomposite and corresponding Ac-BC and PFB-co-PBDG-50/50 components.

The vibrational modes of acetylated BC and those of the polyesters were partially overlapped, as can be confirmed by inspection of the corresponding spectra of Figure 5.1. However, a distinct feature of the nanocomposites spectra due to the cellulose incorporation was the broad band detected near the 3351 cm^{-1} characteristics of the ν O–H. All of the characteristic vibrational features of Ac-BC and BC precursors are summarised in the Supplementary data (Figure S2).

With regards to the morphology, SEM micrographs of the nanocomposites with higher content of diglycolate units (≥50 mol %), collected at different magnifications (Figure 5.2 and Figure S5 of Supplementary data), showed a smoother and uniform surface for those nanocomposites prepared from the high diglycolate quantities, thus indicating enhanced compatibility between the fibres and those polymeric matrices.

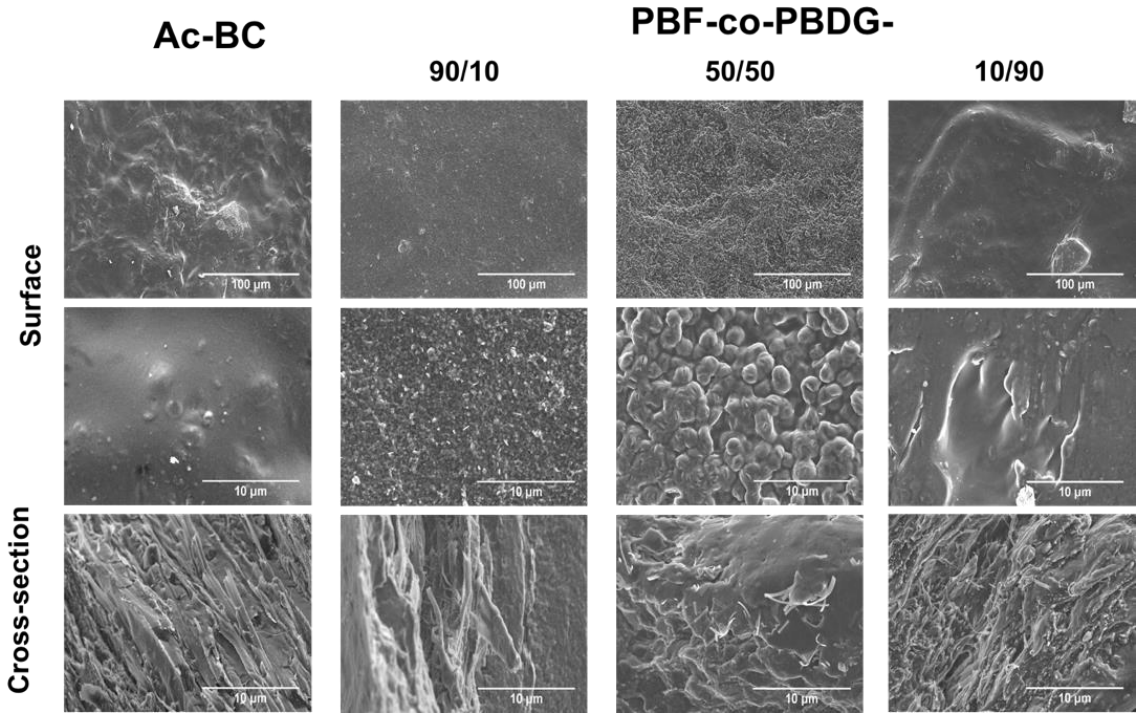

Figure 5.2. Surface (top) and cross-section (bottom) SEM micrographs of Ac-BC film and of selected nanocomposite films.

From this perspective, the amount of Ac-BC used (around 30 wt %) and the heterogeneous acetylation of the cellulose fibres carried out in order to increase the cellulose hydrophobicity (DS ≈ 0.87) and, thus, the compatibility between the modified fibres and the polyesters, was shown to be an adequate approach for obtaining homogeneous nanocomposites, especially in the case of Ac-Bc/PBF-*co*-PBDG-10/90 and -25/75, and Ac-BC/PBDG. A more extensive acetylation of the fibres could, in principle, increase the compatibility of the more hydrophobic furanoate polyesters (such as, PBF, PBF-*co*-PBDG-90/10),[29] but this would also have disrupted the characteristic BC nanostructure and thus would have extensively affected the properties of the ensuing materials. Another, possibility, worth considering in future work, will be the addition of an extra compatibility agent, or even a plasticiser acting also as a compatibility agent. Nevertheless, this would have brought an extra complexity to the data interpretation of the nanocomposite-systems, deviating from the present study as a more in-depth analysis of the basic principles governing cellulose/PBF-*co*-PBDG properties.

It is evident from the cross-section pictures (Figure 5.2 and Figure S5 of Supplementary data), the presence of Ac-BC nanofibres embedded within the polymeric matrix. Further, these results confirmed that the interfacial adhesion between the Ac-BC fibres and the polymeric matrices was particularly good for the high diglycolate content polyesters, namely PBF-*co*-PBDG-10/90, -25/75, and PBDG.

The nanocomposite hydrophobicity was evaluated through water contact angle (CA_{water}) measurements at several points in time for 40 s after the water droplet deposition. The main results are displayed in Figure 5.3 and summarised in Table S3 of Supplementary data.

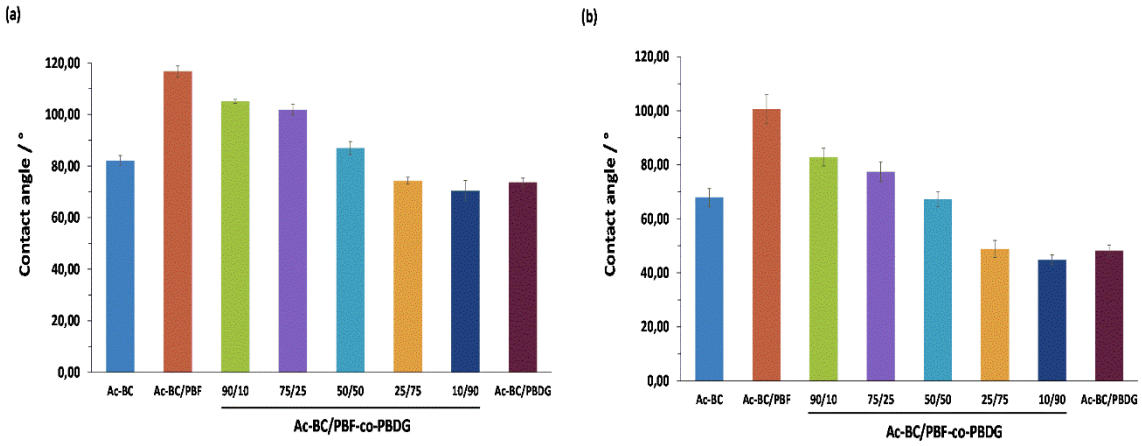

Figure 5.3. Water contact angles at (a) 0 and (b) 15 s.

The CA_{water} decreased drastically over the initial 5 s, and then roughly maintained constant. This behaviour was due to the initial re-orientation of the functional groups at surface of the films, allowing the water drops to spread more easily.[45] Among different nanocomposites, the CA_{water}, after 15 s, increased with the increasing furanoate content in the copolyester (from 45 to 100º), mostly due to the hydrophobic character of the furanoate-based polyesters.[41] The Ac-BC film showed an intermediate CA_{water} of approximately 67.9º after 15 s, in accordance with nanofibre affinity to the polyesters, and consequently good dispersion in the thermoplastic matrices, especially PBF-*co*-PBDG-50/50 to -10/90, and PBDG. The wide range of water contact angles covered by these nanomaterials, from highly hydrophobic (ca. 100.57º) to moderate hydrophilic (ca. 44.81º) was an interesting feature worth exploiting in different applications, such as, for example in packaging[29] or textiles.

3.3. Crystallinity and thermal behaviour

The nature of the crystalline domains of the nanocomposites prepared with a wide range of furanoate/diglycolate copolyesters and with Ac-BC fibers was evaluated by XRD (Figure 5.4 and Figure S6 of Supplementary Materials).

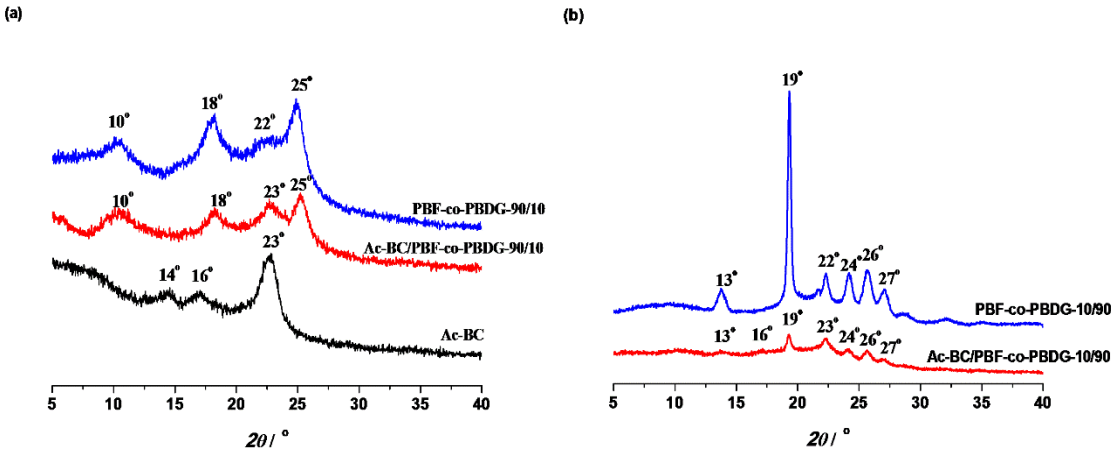

Figure 5.4. X-Ray diffractograms of: (a) Ac-BC/PBF-co-PBDG-90/10 nanocomposite film and corresponding Ac-BC film and PBF-co-PBDG-90/10 components, and (b) Ac-BC/PBF-co-PBDG-10/90 nanocomposite film and corresponding Ac-BC film and PBF-co-PBDG-10/90 components.

The nanocomposites prepared with the copolyesters containing a higher amount of furanoate moieties (*i.e.*, PBF-*co*-PBDG-90/10 to 50/50) roughly displayed the typical diffraction pattern of PBF, with strong reflections at 2θ ≈ 18 and 25º, and smaller peaks at 2θ ≈ 10 and 22º.[8] In the case of the diffractogram of the nanocomposite prepared with the copolyester containing the lowest amount of furanoate moieties (Ac-BC/PBF-*co*-PBDG-10/90), the main peaks observed were those typical of PBDG precursors, *viz:* 2θ ≈ 14, 19, 22, 24, 26, and 27º.[29] These results allowed one to associate the crystalline domain of Ac-BC/PBF-*co*-PBDG-90/10, 75/25, and 50/50 nanocomposites to PBF, whereas in the case of Ac-BC/PBF-*co*-PBDG-10/90, it was essentially related to PBDG. In addition, the XRD diffraction patterns of the nanocomposite films were all naturally related with the copolyesters counterparts (in the form of powder), despite some differences in the sharpness of the reflection peaks, as easily attested by comparing both (Figure S6 of Supplementary

data). These results could be associated with the incorporation of Ac-BC fibres into the polymeric matrix and/or due to solvent casting film formation conditions.

In the particular case of Ac-BC/PBF-*co*-PBDG-25/75, a more pronounced effect was noted; indeed this nanocomposite was amorphous, displaying accordingly on its diffractogram a pronounced amorphous halo cantered at 22º, despite its precursor displaying some crystallinity (see Figure S6 of Supplementary Materials).

Importantly, the thermal and mechanical behaviour of all nanocomposites were influenced by their degree of crystallinity and also by the nature of this domain, as discussed below.

All Ac-BC/PBF-*co*-PBDG nanocomposites and the corresponding individual components precursors were further characterised in terms of their thermal behaviour through DSC and TGA analyses (Table 5.1, Figure 5.5 and, Table S4 and Figures S7–S9 of Supplementary Materials).

Table 5.1. Important thermal values obtained from differential scanning calorimetry (DSC) and thermogravimetric analysis (TGA) analyses.

Sample	T_{cc} [1]/ ºC	T_g [1]/ ºC	T_m [1]/ ºC[1]	$T_{d,\ 5\%}$ [2]/ ºC	$T_{d,max}$ [2]/ ºC
Ac-BC/PBF	86.5	46.1	173.5	323.8	354.7; 384.2
Ac-BC/PBDG	-	−24.9	66.1 [3]	284.0	362.1; 384.0
Ac-BC/PBF-*co*-PBDG-					
90/10	76.3	25.8	162.9	305.8	354.9; 383.0
75/25	60.3	15.2	144.8	300.2	353.9; 376.6
50/50	-	−1.8	94.6	297.9	348.2; 380.7
25/75	-	−12.6	-	238.8	362.3; 378.6
10/90	-	−20.4	61.4 [3]	293.6	359.8; 384.8

[1] Determined by DSC from the second heating scan at 10 °C min^{-1}. [2] Determined by TGA at 20 °C min^{-1}. [3] Determined by DSC from the first heating scan at 10 °C min^{-1}.

The DSC traces of the nanocomposites (Table 5.1 and Figure 5.5) were in accordance with the semi-crystalline nature of the nanocomposites or instead with the amorphous character of one of these materials, as XRD results indicated. Therefore, the DSC traces of Ac-BC/PBF, Ac-BC/PBF-*co*-PBDG-90/10, -50/50 and -10/90, and Ac-Bc/PBDG displayed a glass transition (T_g), followed by a melting (T_m) event at -24.9 to 46.1 ºC, and 61.4 to 173.5 ºC, respectively. An additional cold crystallisation (T_{cc}) event was also observed after the T_g in the cases of Ac-BC/PBF, PBF-*co*-PBDG-90/10 and -75/25, which might be associated to an additional nucleation effect of Ac-BC fibres.[46] The corresponding traces of neat PBF and

PBF-*co*-PBDG-90/10 (co)polyesters (Figure S7 and Table S4 of Supplementary Material) did not showed a cold crystallisation event.

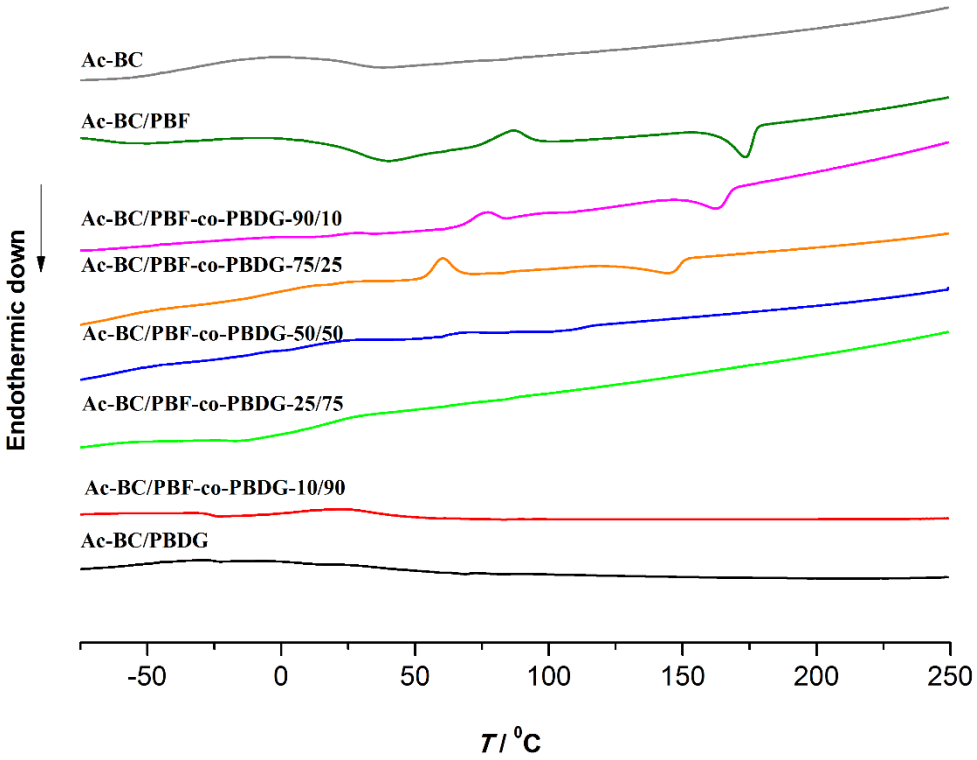

Figure 5.5. DSC traces of the nanocomposites and Ac-BC.

In regard to Ac-BC/PBF-*co*-PBDG-25/75, the corresponding thermogram displayed only a step in the baseline at *ca.* -12.6 ºC, attributed to the glass transition temperature, due to its essentially amorphous nature, in agreement with the XRD results.

For all nanocomposites, T_g decreased (around 13 ºC) with an increased amount of diglycolate units in the copolyester. In the same vein, the T_m of the nanocomposites also decreased from 173.5 to 61.4 ºC with an increasing amount of soft diglycolate segments. This trend was also observed in the case of neat (co)polyesters prepared in this work (Table S4 of Supplementary Material) and reported elsewhere.[29]

In addition, the T_g of the nanocomposite films tended to be higher than those obtained for the corresponding (co)polyester component, in agreement with the higher stiffness of the nanocomposites. For example, Ac-Bc/PBF-*co*-PBDG-75/25 had a T_g of 25.6 ºC, whereas the same parameter for PBF-*co*-PBDG-75/25 was 13.8 ºC. In regard to the T_m, the nanocomposites (Table 5.1) and the corresponding copolyesters synthesised in this work

(Table S4 of Supplementary Material) had very similar results, but they were higher than literature values.[29]

The typical TGA thermograms of the newly prepared furanoate nanocomposites (Table 5.1 and Figure S9 of Supplementary Material) displayed two major characteristic steps at maximum decomposition temperatures ($T_{d,max}$) of 348–362 ºC and 376–385 ºC. The first step was due to the Ac-BC decomposition and was quite close to that observed for the neat Ac-BC fibres (363.0 ºC) and comparable to previously reported results.[39] The other decomposition step was associated with the polyesters enriched fraction and was observed at higher temperatures than the related polyester precursor. For example, in the case of Ac-BC/PBF-*co*-PBDG-50/50 the second $T_{d,max}$ was equal to 380.7 ºC, whereas the same parameter was equal to 365.1 ºC for the PBF-*co*-PBDG-50/50 copolyester. These results were comparable to those reported for other nanocomposites of Ac-BC and poly(lactic acid).[39]

The nanocomposites were thermally stable up to 238–306 ºC (Table 5.1), indicating a decrease of the stability compared to the related polyesters (360–380 ºC) (Table S4 of Supplementary Materials). The same effect was previously reported with PEF/cellulose materials.[31] Additionally, one can notice, on both nanocomposites and the corresponding polyester component, an increase of the $T_{d,5\%}$ with the amount of furanoate incorporated into the polymeric matrix backbone. These thermal features enabled the establishment a maximum working temperature of up to 306 ºC for the novel nanocomposites.

3.4. Mechanical properties and permeability assays for oxygen

Tensile tests were performed to assess the mechanical performance of these novel furanoate-based nanocomposites and in particular to evaluate the effect of compounding cellulose nanofibres (Ac-BC) with PBF-co-PBDG copolyesters. The stress-strain behaviour of Ac-BC/PBF-co-PBDGs was revealed to be dependent on a complex interplay of factors, namely the chemical composition of the related (co)polyesters and the presence of nanofibres, as well as the crystallinity of the new materials. The main results are displayed in Figure 5.6 and summarised in Table S5.

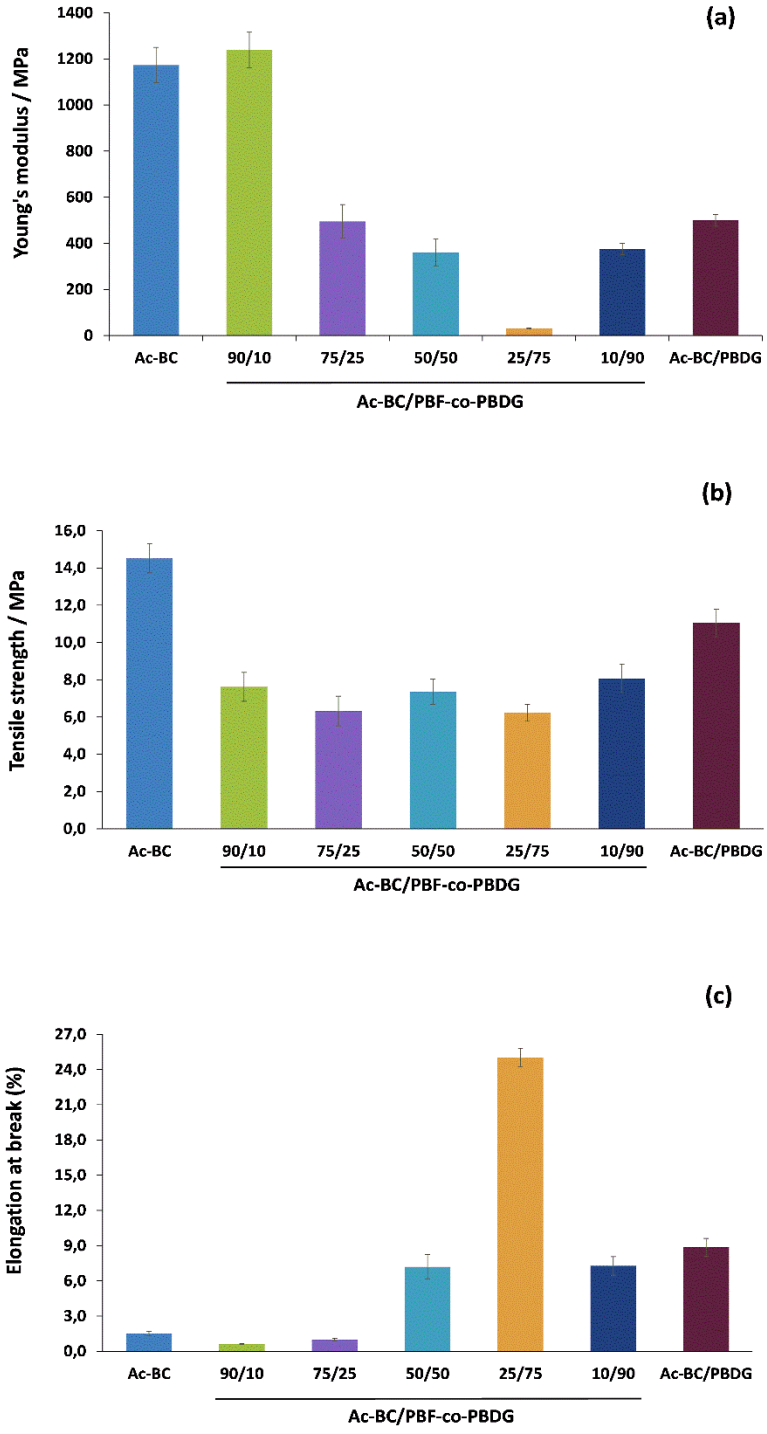

Figure 5.6. (a) Young's modulus, (b) tensile strength and (c) elongation at break of the nanocomposites and of the Ac-BC component.

Ac-BC/PBF-*co*-PBDG-90/10 exhibited the highest Young's modulus, approximately 1239.3 MPa, in accordance with this nanocomposite having the highest amount of rigid furanoate moieties. This result was significantly higher than that previous reported to the related film of the neat copolyester (ca. 373 MPa).[29] The cellulose fibres played here a reinforcing role in the nanocomposites, as well as due to the higher crystallinity of the copolyester prepared in this work, thus explaining the Young's modulus increase.

Importantly, the Young's modulus of Ac-BC/PBF-*co*-PBDG-90/10 (ca. 1239.3 MPa) was very close to that routinely reported for PBF,[11,24,29] and also very near to neat Ac-BC film (ca. 1172.8 MPa). This was a very interesting result because this nanocomposite had good mechanical properties, comparable to those of PBF; but had the advantage of being biodegradable oppositely to PBF.[29]

The other nanocomposites showed lower Young's modulus (ca. 499.9–30.3 MPa), decreasing with decreasing amounts of furanoate units from 75/25 to 25/75, but slightly increasing again to Ac-BC/PBF-*co*-PBDG-10/90 and PBDG. This inverted bell-shape trend behaviour for the first decreasing trend was in agreement with the decrease of stiff furanoate moieties; and for the second increasing trend it was most probably associated with an increase in crystallinity as prompted by the substantial amount of diglycolate segments, and thus a lower degree of randomness (as well as disclosed by XRD analysis). In addition, the nanocomposites Young's modulus results were typically much higher than those reported for the neat copolyesters films produced by Soccio et al.[29] due to the expectable reinforcing role of the cellulose fibres,[39] and due to a higher crystallinity of the herein prepared nanocomposites.

In terms of elongation at break, the nanocomposites prepared from copolyesters with higher amounts of diglycolate moieties displayed higher elongations due to the soft nature of these segments. The highest result was obtained with Ac-BC/PBF-*co*-PBDG-25/75 (ca. 25.02%). Despite this composite having a huge gain in elasticity, especially compared to cellulose fibres, the elongation at break was still lower than those of neat copolyesters.[29]

The nanocomposites barrier properties were evaluated in terms of permeability to oxygen, and preliminary results indicated that the nanocomposites and the corresponding (co)polyesters films prepared elsewhere[29] had similar permeabilities towards oxygen. Ac-BC/PBF-*co*-PBDG-90/10 showed to have a permeability to O_2 that was equal to 3.49×10^2 Barrer, whereas Ac-BC had 1.75×10^5, in accordance with the well-documented[44,47] superior

barrier properties of furanoate-based polymers. These were attractive properties worth exploiting for applications within packaging.

4. Conclusions

Furanoate-based (nano)composites using bacterial nano-cellulose was here reported for the first time, revealing great potential to broaden the properties of this material. In the present case study involving Ac-BC/PBF and Ac-BC/PBF-*co*-PBDGs nanocomposites, they were shown to have high stiffness (evaluated by the Young's modulus, from 30.3 to 1239 MPa) compared to the neat (co)polyesters counterparts. Concomitantly, these nanocomposites still displayed reasonable elasticity (elongation at break) compared e.g., to cellulose or PBF. These properties were only possible by judiciously tailoring the composition of the nanocomposites, especially the critical diglycolate/furanoate amount in the copolyester, as well as by compounding the (co)polyesters with acetylated cellulose (tailoring crystallinity, homogeneity, among other properties). Moreover, the permeabilities to oxygen results were quite attractive, being in the order of magnitude of PBF, justifying further exploitation of these nanocomposites for applications within packaging.

References

(1) Vilela, C.; Sousa, A. F.; Fonseca, A. C.; Serra, A. C.; Coelho, J. F. J.; Freire, C. S. R.; Silvestre, A. J. D. The Quest for Sustainable Polyesters–insights into the Future. *Polym. Chem.* **2014**, *5* (9), 3119–3141.

(2) Sousa, A. F.; Vilela, C.; Fonseca, A. C.; Matos, M.; Freire, C. S. R.; Gruter, G. J. M.; Coelho, J. F. J.; Silvestre, A. J. D. Biobased Polyesters and Other Polymers from 2,5-Furandicarboxylic Acid: A Tribute to Furan Excellency. *Polym. Chem.* **2015**, *6* (33), 5961–5983.

(3) Drewitt, J. G. N.; Lincoln, J. Improvements in Polymers. GB 621971 (A), 1946.

(4) Gandini, A.; Silvestre, A. J. D.; Neto, C. P.; Sousa, A. F.; Gomes, M. M. The Furan Counterpart of Poly (Ethylene Terephthalate): An Alternative Material Based on Renewable Resources. *J. Polym. Sci. Polym. Chem.* **2009**, *5* (c), 295–298.

(5) Papageorgiou, G. Z.; Tsanaktsis, V.; Papageorgiou, D. G.; Exarhopoulos, S.; Papageorgiou, M.; Bikiaris, D. N. Evaluation of Polyesters from Renewable Resources as Alternatives to the Current Fossil-Based Polymers. Phase Transitions of Poly(Butylene 2,5-Furan-Dicarboxylate). *Polymer* **2014**, *55* (16), 3846–3858.

(6) Jiang, M.; Liu, Q.; Zhang, Q.; Ye, C.; Zhou, G. A Series of Furan-Aromatic Polyesters Synthesized via Direct Esterification Method Based on Renewable Resources. *J. Polym. Sci. Polym. Chem.* **2012**, *50* (5), 1026–1036.

(7) Wu, B.; Xu, Y.; Bu, Z.; Wu, L.; Li, B. G.; Dubois, P. Biobased Poly(Butylene 2,5-Furandicarboxylate) and Poly(Butylene Adipate-Co-Butylene 2,5-Furandicarboxylate)s: From Synthesis Using Highly Purified 2,5-Furandicarboxylic Acid to Thermo-Mechanical Properties. *Polymer* **2014**, *55* (16), 3648–3655.

(8) Ma, J.; Yu, X.; Xu, J.; Pang, Y. Synthesis and Crystallinity of Poly(Butylene 2,5-Furandicarboxylate). *Polymer* **2012**, *53* (19), 4145–4151.

(9) Jiang, Y.; Woortman, A. J. J.; Alberda Van Ekenstein, G. O. R.; Loos, K. A Biocatalytic Approach towards Sustainable Furanic-Aliphatic Polyesters. *Polym. Chem.* **2015**, *6* (29), 5198–5211.

(10) Tsanaktsis, V.; Vouvoudi, E.; Papageorgiou, G. Z.; Papageorgiou, D. G.; Chrissafis,

K.; Bikiaris, D. N. Thermal Degradation Kinetics and Decomposition Mechanism of Polyesters Based on 2,5-Furandicarboxylic Acid and Low Molecular Weight Aliphatic Diols. *J. Anal. Appl. Pyrolysis* **2015**, *112*, 369–378.

(11) Zhu, J.; Cai, J.; Xie, W.; Chen, P.; Gazzano, M.; Scandola, M.; Gross, R. A. Poly(Butylene 2,5-Furandicarboxylate), a Biobased Alternative to PBT: Synthesis, Physical Properties, and Crystal Structure. *Macromolecules* **2013**, *46* (3), 796–804.

(12) Thiyagarajan, S.; Vogelzang, W.; J. I. Knoop, R.; Frissen, A. E.; Van Haveren, J.; Van Es, D. S. Biobased Furandicarboxylic Acids (FDCAs): Effects of Isomeric Substitution on Polyester Synthesis and Properties. *Green Chem.* **2014**, *16* (4), 1957–1966.

(13) Ma, J.; Pang, Y.; Wang, M.; Xu, J.; Ma, H.; Nie, X. The Copolymerization Reactivity of Diols with 2,5-Furandicarboxylic Acid for Furan-Based Copolyester Materials. *J. Mater. Chem.* **2012**, *22* (8), 3457–3461.

(14) Morales-Huerta, J. C.; Martínez De Ilarduya, A.; Muñoz-Guerra, S. Poly(Alkylene 2,5-Furandicarboxylate)s (PEF and PBF) by Ring Opening Polymerization. *Polymer* **2016**, *87*, 148–158.

(15) Matos, M.; Sousa, A. F.; Fonseca, A. C.; Freire, C. S. R.; Coelho, J. F. J.; Silvestre, A. J. D. A New Generation of Furanic Copolyesters with Enhanced Degradability: Poly(Ethylene 2,5-Furandicarboxylate)-Co-Poly(Lactic Acid) Copolyesters. *Macromol. Chem. Phys.* **2014**, *215* (22), 2175–2184.

(16) Sousa, A. F.; Guigo, N.; Pozycka, M.; Delgado, M.; Soares, J.; Mendonça, P. V.; Coelho, J. F. J.; Sbirrazzuoli, N.; Silvestre, A. J. D. Tailored Design of Renewable Copolymers Based on Poly(1,4-Butylene 2,5-Furandicarboxylate) and Poly(Ethylene Glycol) with Refined Thermal Properties. *Polym. Chem.* **2018**, *9* (6), 722–731.

(17) Morales-Huerta, J. C.; Ciulik, C. B.; De Ilarduya, A. M.; Muñoz-Guerra, S. Fully Bio-Based Aromatic-Aliphatic Copolyesters: Poly(Butylene Furandicarboxylate-Co-Succinate)s Obtained by Ring Opening Polymerization. *Polym. Chem.* **2017**, *8* (4), 748–760.

(18) Wu, L.; Mincheva, R.; Xu, Y.; Raquez, J. M.; Dubois, P. High Molecular Weight Poly(Butylene Succinate-Co-Butylene Furandicarboxylate) Copolyesters: From

Catalyzed Polycondensation Reaction to Thermomechanical Properties. *Biomacromolecules* **2012**, *13* (9), 2973–2981.

(19) Yu, Z.; Zhou, J.; Cao, F.; Wen, B.; Zhu, X.; Wei, P. Chemosynthesis and Characterization of Fully Biomass-Based Copolymers of Ethylene Glycol, 2,5-Furandicarboxylic Acid, and Succinic Acid. *J. Appl. Polym. Sci.* **2013**, *130* (2), 1415–1420.

(20) Zhou, W.; Wang, X.; Yang, B.; Xu, Y.; Zhang, W.; Zhang, Y.; Ji, J. Synthesis, Physical Properties and Enzymatic Degradation of Bio-Based Poly(Butylene Adipate-Co-Butylene Furandicarboxylate) Copolyesters. *Polym. Degrad. Stabil.* **2013**, *98* (11), 2177–2183.

(21) Zheng, M. Y.; Zang, X. L.; Wang, G. X.; Wang, P. L.; Lu, B.; Ji, J. H. Poly(Butylene 2,5-Furandicarboxylate-ε-Caprolactone): A New Bio-Based Elastomer with High Strength and Biodegradability. *Express Polym. Lett.* **2017**, *11* (8), 611–621.

(22) Papageorgiou, G. Z.; Papageorgiou, D. G. Solid-State Structure and Thermal Characteristics of a Sustainable Biobased Copolymer: Poly(Butylene Succinate-Co-Furanoate). *Thermochim. Acta* **2017**, *656* (September), 112–122.

(23) Kasmi, N.; Majdoub, M.; Papageorgiou, G. Z.; Bikiaris, D. N. Synthesis and Crystallization of New Fully Renewable Resources-Based Copolyesters: Poly(1,4-Cyclohexanedimethanol-Co-Isosorbide 2,5-Furandicarboxylate). *Polym. Degrad. Stabil.* **2018**, *152*, 177–190.

(24) Cai, X.; Yang, X.; Zhang, H.; Wang, G. Aliphatic-Aromatic Poly(Carbonate-Co-Ester)s Containing Biobased Furan Monomer: Synthesis and Thermo-Mechanical Properties. *Polymer* **2018**, *134*, 63–70.

(25) Wang, X.; Wang, Q.; Liu, S.; Wang, G. Biobased Copolyesters: Synthesis, Structure, Thermal and Mechanical Properties of Poly(Ethylene 2,5-Furandicarboxylate-Co-Ethylene 1,4-Cyclohexanedicarboxylate). *Polym. Degrad. Stabil.* **2018**, *154*, 96–102.

(26) Wang, J.; Liu, X.; Jia, Z.; Sun, L.; Zhang, Y.; Zhu, J. Modification of Poly(Ethylene 2,5-Furandicarboxylate) (PEF) with 1, 4-Cyclohexanedimethanol: Influence of Stereochemistry of 1,4-Cyclohexylene Units. *Polymer* **2018**, *137*, 173–185.

(27) Peng, S.; Bu, Z.; Wu, L.; Li, B. G.; Dubois, P. High Molecular Weight Poly(Butylene

Succinate-Co-Furandicarboxylate) with 10 Mol% of BF Unit: Synthesis, Crystallization-Melting Behavior and Mechanical Properties. *Eur. Polym. J.* **2017**, *96* (May), 248–255.

(28) Hu, H.; Zhang, R.; Wang, J.; Ying, W. Bin; Zhu, J. Synthesis and Structure-Property Relationship of Bio-Based Biodegradable Poly(Butylene Carbonate-Co-Furandicarboxylate). *ACS Sustain. Chem. Eng.* **2018**, *6* (6), 7488–7498.

(29) Soccio, M.; Costa, M.; Lotti, N.; Gazzano, M.; Siracusa, V.; Salatelli, E.; Manaresi, P.; Munari, A. Novel Fully Biobased Poly(Butylene 2,5-Furanoate/Diglycolate) Copolymers Containing Ether Linkages: Structure-Property Relationships. *Eur. Polym. J.* **2016**, *81*, 397–412.

(30) Hu, H.; Zhang, R.; Wang, J.; Ying, W. Bin; Zhu, J. Fully Bio-Based Poly(Propylene Succinate-Co-Propylene Furandicarboxylate) Copolyesters with Proper Mechanical, Degradation and Barrier Properties for Green Packaging Applications. *Eur. Polym. J.* **2018**, *102*, 101–110.

(31) Codou, A.; Guigo, N.; van Berkel, J. G.; de Jong, E.; Sbirrazzuoli, N. Preparation and Crystallization Behavior of Poly(Ethylene 2,5-Furandicarboxylate)/Cellulose Composites by Twin Screw Extrusion. *Carbohyd. Polym.* **2017**, *174* (July), 1026–1033.

(32) Achilias, D. S.; Chondroyiannis, A.; Nerantzaki, M.; Adam, K. V.; Terzopoulou, Z.; Papageorgiou, G. Z.; Bikiaris, D. N. Solid State Polymerization of Poly(Ethylene Furanoate) and Its Nanocomposites with SiO2 and TiO2. *Macromol. Mater. Eng.* **2017**, *302* (7), 1–15.

(33) Martino, L.; Guigo, N.; van Berkel, J. G.; Sbirrazzuoli, N. Influence of Organically Modified Montmorillonite and Sepiolite Clays on the Physical Properties of Bio-Based Poly(Ethylene 2,5-Furandicarboxylate). *Compos. Part B-Eng.* **2017**, *110*, 96–105.

(34) Martino, L.; Niknam, V.; Guigo, N.; Gabriël Van Berkel, J.; Sbirrazzuoli, N. Morphology and Thermal Properties of Novel Clay-Based Poly(Ethylene 2,5-Furandicarboxylate) (PEF) Nanocomposites. *RSC Adv.* **2016**, *6* (64), 59800–59807.

(35) Lotti, N.; Munari, A.; Gigli, M.; Gazzano, M.; Tsanaktsis, V.; Bikiaris, D. N.;

Papageorgiou, G. Z. Thermal and Structural Response of in Situ Prepared Biobased Poly(Ethylene 2,5-Furan Dicarboxylate) Nanocomposites. *Polymer* **2016**, *103*, 288–298.

(36) Codou, A.; Guigo, N.; Van Berkel, J. G.; De Jong, E.; Sbirrazzuoli, N. Preparation and Characterization of Poly(Ethylene 2,5-Furandicarboxylate)/Nanocrystalline Cellulose Composites via Solvent Casting. *J. Polym. Eng.* **2017**, *37* (9), 869–878.

(37) Tomé, L. C.; Gonçalves, C. M. B.; Boaventura, M.; Brandão, L.; Mendes, A. M.; Silvestre, A. J. D.; Neto, C. P.; Gandini, A.; Freire, C. S. R.; Marrucho, I. M. Preparation and Evaluation of the Barrier Properties of Cellophane Membranes Modified with Fatty Acids. *Carbohyd. Polym.* **2011**, *83* (2), 836–842.

(38) Sousa, A. F.; Vilela, C.; Matos, M.; Freire, C. S. R.; Silvestre, A. J. D.; Coelho, J. F. J. Polyethylene Terephthalate: Copolyesters, Composites, and Renewable Alternatives. In *Poly(ethylene terephthalate) based blends, composites and nanocomposites*; Visakh, P. M., Liang, M., Eds.; Elsevier, 2015; pp 113–141.

(39) Tomé, L. C.; Pinto, R. J. B.; Trovatti, E.; Freire, C. S. R.; Silvestre, A. J. D.; Gandini, A.; Neto, C. P. Transparent Bionanocomposites with Improved Properties Prepared from Acetylated Bacterial Cellulose and Poly(Lactic Acid) through a Simple Approach. *Green Chem.* **2011**, *13*, 419–427.

(40) Gomes, F. P.; Silva, N. H. C. S.; Trovatti, E.; Serafim, L. S.; Duarte, M. F.; Silvestre, A. J. D.; Neto, C. P.; Freire, C. S. R. Production of Bacterial Cellulose by Gluconacetobacter Sacchari Using Dry Olive Mill Residue. *Biomass and Bioenergy* **2013**, *55*, 205–211.

(41) Soares, M. J.; Dannecker, P. K.; Vilela, C.; Bastos, J.; Meier, M. A. R.; Sousa, A. F. Poly(1,20-Eicosanediyl 2,5-Furandicarboxylate), a Biodegradable Polyester from Renewable Resources. *Eur. Polym. J.* **2017**, *90*, 301–311.

(42) Vaca-Garcia, C.; Borredon, M. E.; A. Gaseta. Determination of the Degree of Substitution (DS) of Mixed Cellulose Esters by Elemental Analysis. *Cell Adhes. Migr.* **2001**, *8*, 225–231.

(43) Campo, M. C.; Magalhães, F. D.; Mendes, A. Carbon Molecular Sieve Membranes from Cellophane Paper. *J. Memb. Sci.* **2010**, *350* (1–2), 180–188.

(44) Araujo, C. F.; Nolasco, M. M.; Ribeiro-Claro, P. J. A.; Rudić, S.; Silvestre, A. J. D.; Vaz, P. D.; Sousa, A. F. Inside PEF: Chain Conformation and Dynamics in Crystalline and Amorphous Domains. *Macromolecules* **2018**, *51* (9), 3515–3526.

(45) Liukkonen, A. Contact Angle of Water on Paper Components: Sessile Drops versus Environmental Scanning Electron Microscope Measurements. *Scanning* **1997**, *19*, 411–415.

(46) Zhang, X.; Li, W.; Ye, B.; Lin, Z.; Rong, J. Studies on Confined Crystallization Behavior of Nanobiocomposites Consisting of Acetylated Bacterial Cellulose and Poly (Lactic Acid). *J. Thermoplast. Compos. Mater.* **2013**, *26* (3), 346–361.

(47) Burgess, S. K.; Leisen, J. E.; Kraftschik, B. E.; Mubarak, C. R.; Kriegel, R. M.; Koros, W. J. Chain Mobility, Thermal, and Mechanical Properties of Poly(Ethylene Furanoate) Compared to Poly(Ethylene Terephthalate). *Macromolecules* **2014**, *47* (4), 1383−1391.

Supplementary Materials

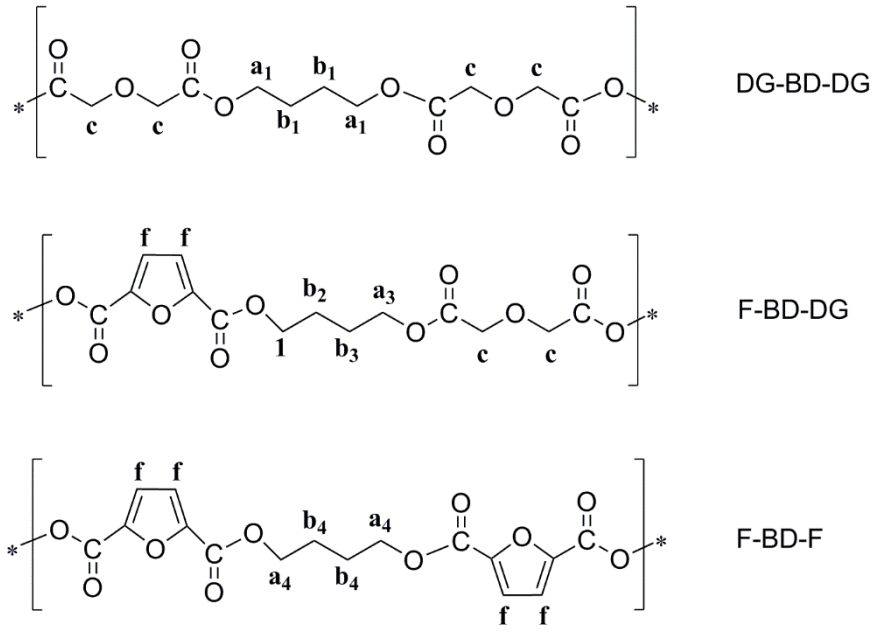

Scheme S1. Chemical structures of the triad units of the PBF-co-PBDG copolyesters.

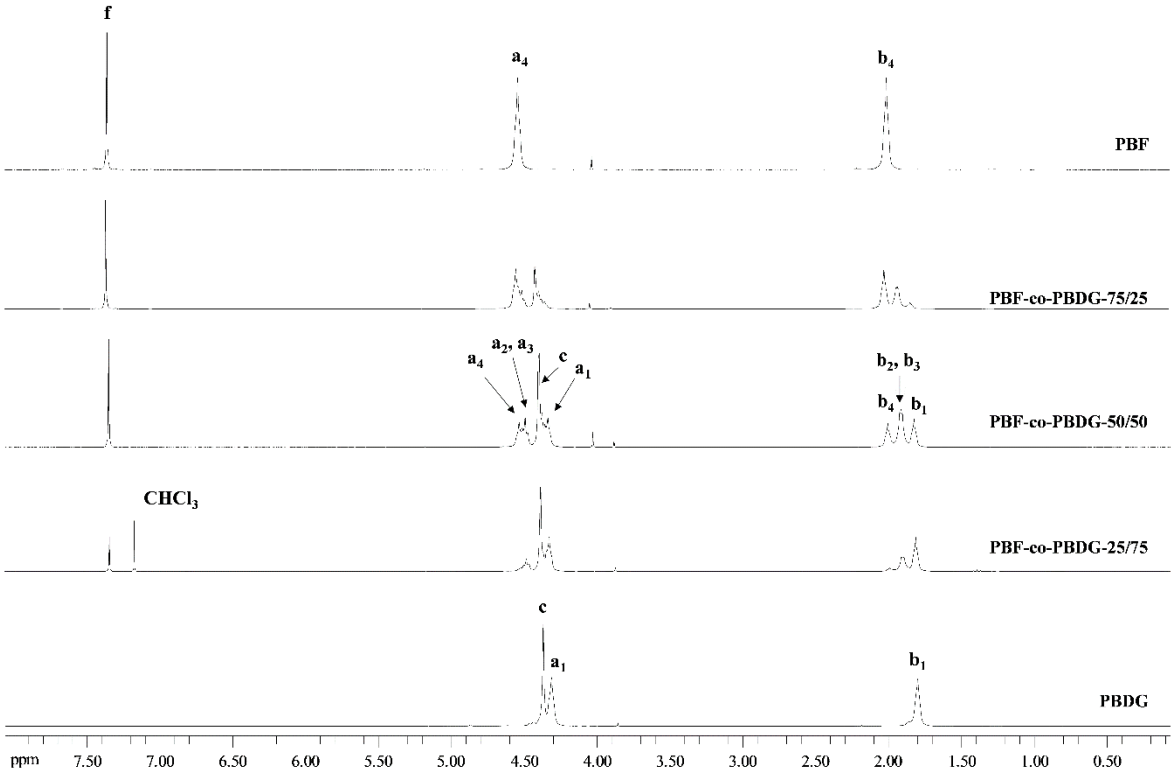

Figure S1. ^{1}H NMR spectra in TFA-*d* of PBF-co-PBDG copolyesters and related PBF and PBDG homopolyesters.

Table S1. Main ^{1}H NMR resonances of PBF-co-PBDG copolyesters and related PBF and PBDG homopolyesters**.**

δ / ppm	assignment	triads	integration area						
			PBF	PBF-co-PBDG-					PBDG
				90/10	75/25	50/50	25/75	10/90	
7.30	**f; C*H* (FDCA)**	**F-BD-F; F-BD-DG**	1.00	1.00	1.00	1.00	1.00	1.00	–
4.50	**a_4; OCH_2 (BD)**	**F-BD-F**	2.00	1.85	1.72	1.52	1.60	2.13	–
4.45	**a_2, a_3;OCH_2 (BD)**	**F-BD-DG**	–	0.31	0.85	1.16	3.89	13.80	–
4.36	**c; CH_2OCH_2 (DGA)**	**DG-BD-DG**	–	0.32	0.76	1.51	6.75	43.67	1.00
4.30	**a_1; OCH_2 (BD)**	**DG-BD-DG**	–	0.06	0.18	0.56	4.97	38.27	1.00
1.90	**b_4; OCH$_2$CH_2 (BD)**	**F-BD-F**	2.01	1.86	1.72	1.52	1.60	1.90	–
1.83	**b_2, b_3; OCH$_2$CH_2 (BD)**	**F-BD-DG**	–	0.33	0.85	1.29	3.93	11.89	–
1.80	**b_1; OCH$_2$CH_2 (BD)**	**DG-BD-DG**	–	0.05	0.13	0.59	4.94	38.76	1.01

Table S2. Comparison between the initial molar feed percentage and the real molar percentage of furanoate and diglycolate moieties.

(co)polymer	F/DG$_{feed}$ (mol%)	F/DG (mol%)
PBF	100/0	100.0/0
PBF-co-PBDG-		
90/10	90/10	86.2/13.8
75/25	75/25	72.5/27.5
50/50	50/50	57.0/43.0
25/75	25/75	22.9/77.1
10/90	10/90	4.4/95.6
PBDG	0/100	0/100.0

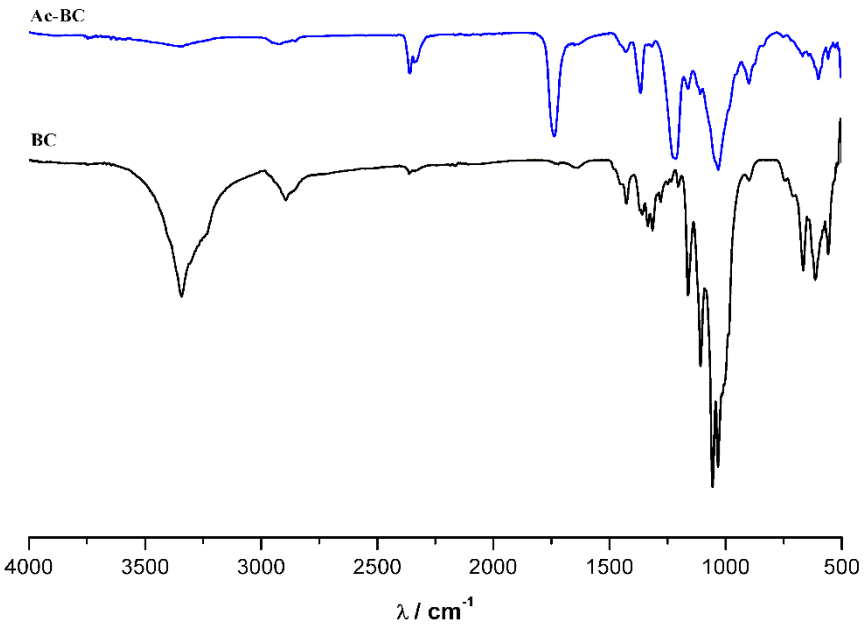

Figure S2. ATR FTIR spectra of the acetylated bacterial cellulose (Ac-BC) and of the unmodified bacterial cellulose (BC) fibres.

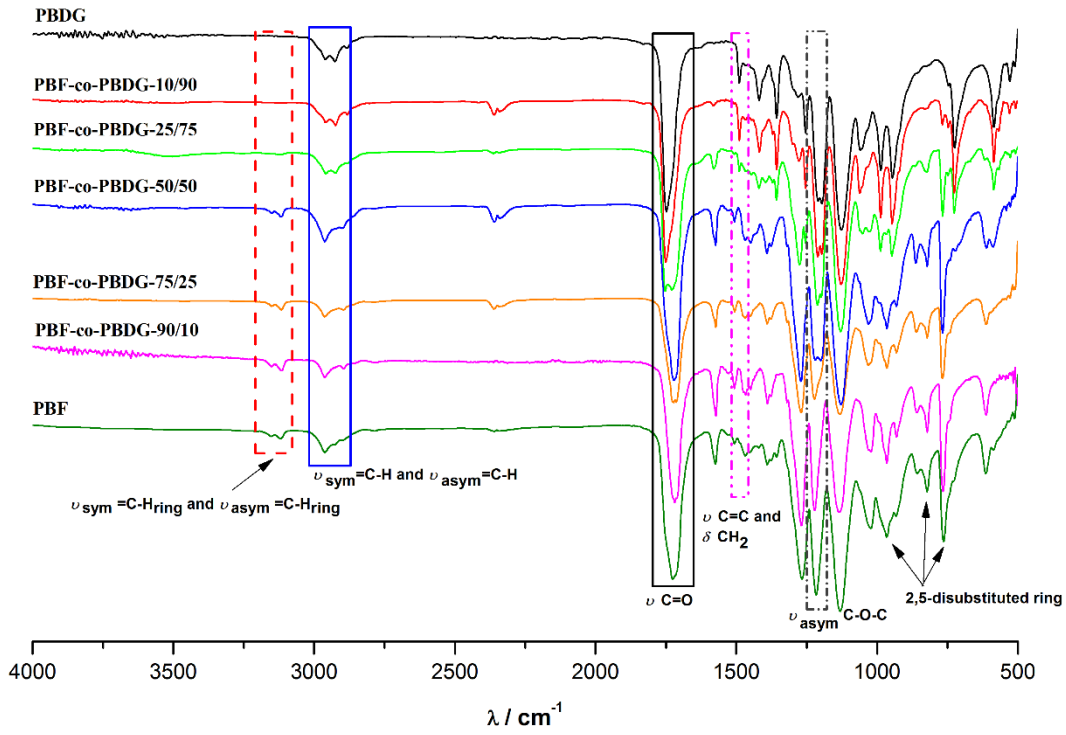

Figure S3. ATR FTIR spectra of PBF-co-PBDG copolyesters and of PBF and PBDG related homopolyesters.

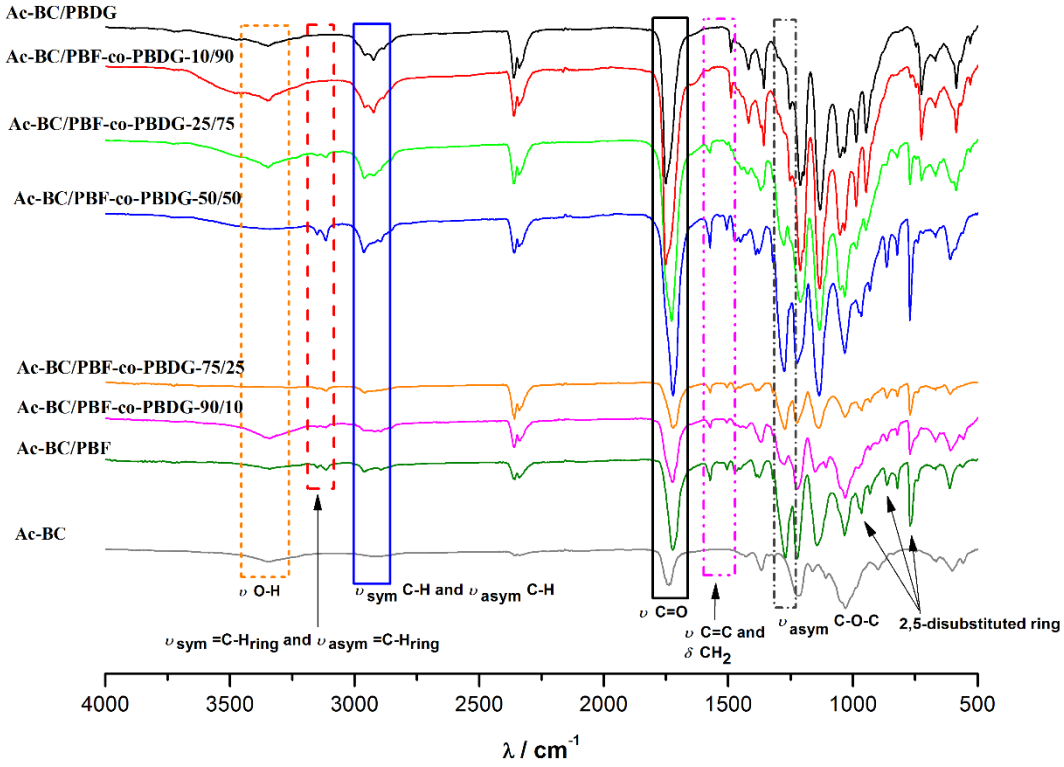

Figure S4. ATR FTIR spectra of all Ac-BC/PBF-64 co-PBDG nanocomposites.

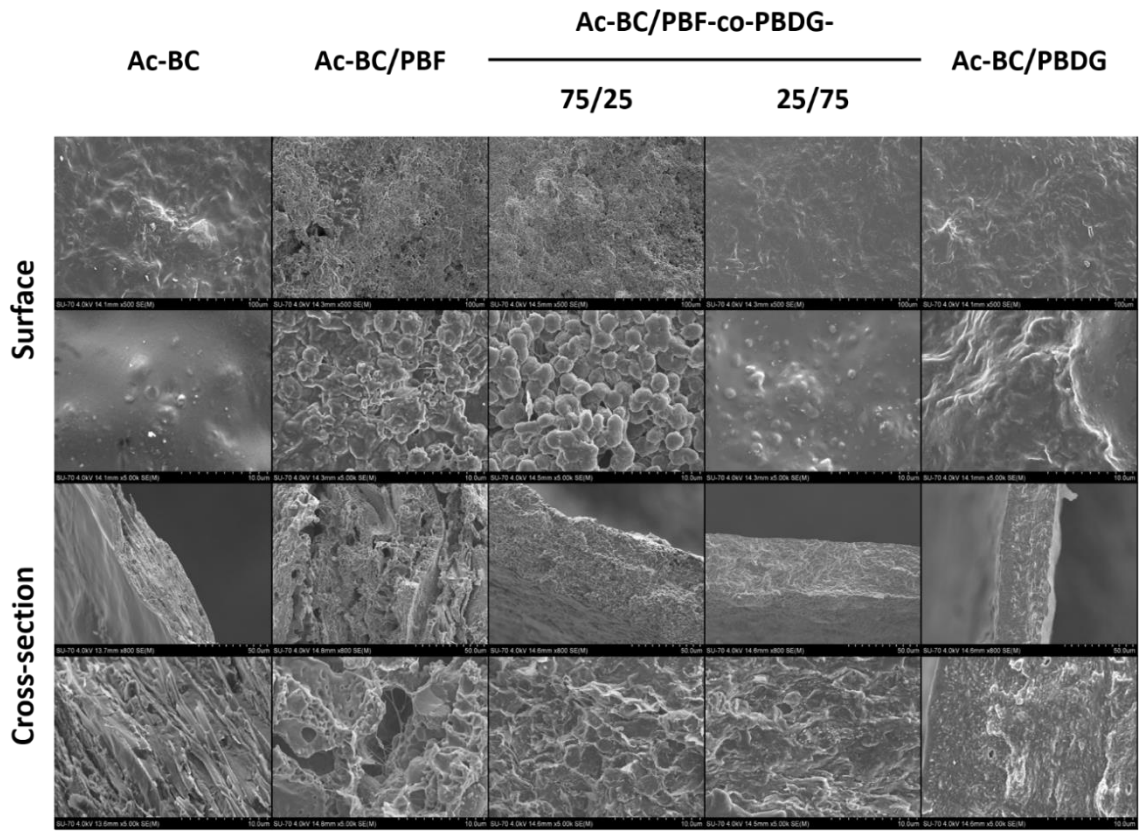

Figure S5. SEM micrographs of Ac-BC film and of the nanocomposites of the (**a**) surface (500 x and 5.0 kx) and 69 (**b**) cross-section (800 x and 5.0 kx).

Table S3. Water contact angles of the composites films measured at several points in time for 40 s.

Sample	CA_{water} / °							
	time / s							
	0	5	10	15	20	25	30	40
Ac-BC	82.10 ± 1.93	71.09 ± 2.34	69.22 ± 3.05	67.93 ± 3.33	67.45 ± 3.03	66.83 ± 3.32	66.48 ± 3.42	65.97 ± 3.60
Ac-BC/PBF	116.40 ± 2.11	102.43 ± 5.03	101.96 ± 4.52	100.57 ± 5.37	98.14 ± 4.36	97.37 ± 4.05	96.89 ± 3.84	96.45 ± 4.04
Ac-BC/PBF-co-PBDG-90/10	105.10 ± 0.77	87.36 ± 2.41	83.01 ± 3.30	82.84 ± 3.30	82.41 ± 3.25	82.44 ± 3.59	82.04 ± 3.62	81.67 ± 3.57
Ac-BC/PBF-co-PBDG-75/25	101.85 ± 2.08	85.47 ± 3.87	78.85 ± 3.51	77.40 ± 3.70	75.97 ± 3.82	73.96 ± 3.62	73.61 ± 3.26	72.28 ± 3.82
Ac-BC/PBF-co-PBDG-50/50	86.97 ± 2.49	72.32 ± 2.75	69.39 ± 3.11	67.24 ± 2.81	65.30 ± 2.51	64.04 ± 2.67	63.62 ± 2.74	62.15 ± 2.75
Ac-BC/PBF-co-PBDG-25/75	74.29 ± 1.37	53.56 ± 3.82	50.50 ± 3.45	48.82 ± 3.15	47.46 ± 2.34	46.85 ± 2.21	46.26 ± 2.05	45.10 ± 1.66
Ac-BC/PBF-co-PBDG-10/90	70.40 ± 3.96	46.56 ± 1.71	45.48 ± 1.78	44.81 ± 1.78	44.61 ± 1.48	44.37 ± 1.70	44.27 ± 1.73	43.36 ± 1.83
Ac-BC/ PBDG	73.65 ± 1.67	54.04 ± 4.32	49.84 ± 2.73	48.18 ± 2.06	47.57 ± 1.37	46.74 ± 1.79	46.69 ± 1.95	45.96 ± 1.92

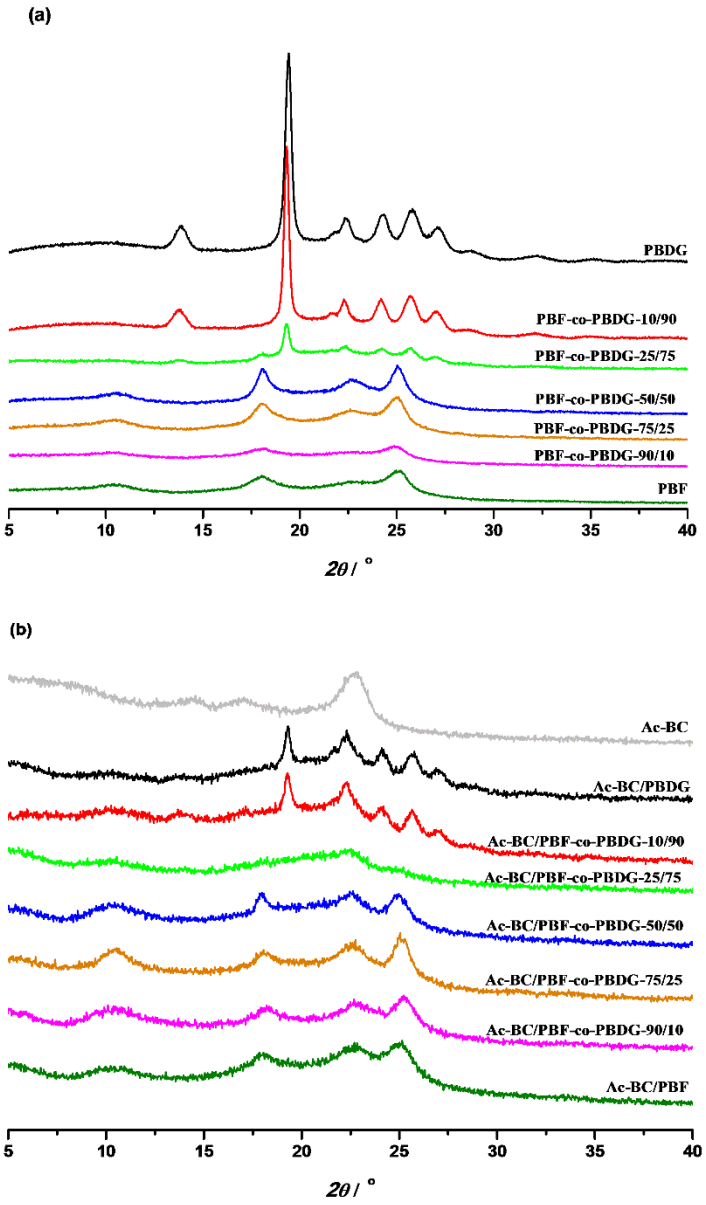

Figure S6. X-Ray diffractograms of the (a) neat (co)polyesters and (b) corresponding nanocomposites.

Table S4. Important thermal values of the (co)polyesters and Ac-BC obtained by DSC and TGA analyses.

sample	T_g / ºC	T_{cc} / ºC	T_m / ºC	$T_{d,\,5\%}$ / ºC	T_d / ºC
PBF	46.1	-	173.9	348.7	380.5
PBF-co-PBDG-		-			
90/10	25.1	-	161.7	328.6	368.4
75/25	13.8	81.5	136.2	303.1	360.3
50/50	-2.7	-	93.2	322.1	365.3
25/75	-17.6	-	48.0	305.4	378.1
10/90	-26.4	-	48.0	297.5	362.1
PBDG	-26.6	-	65.6	294.9	360.1
Ac-BC	-	-	-	278.2	363.0

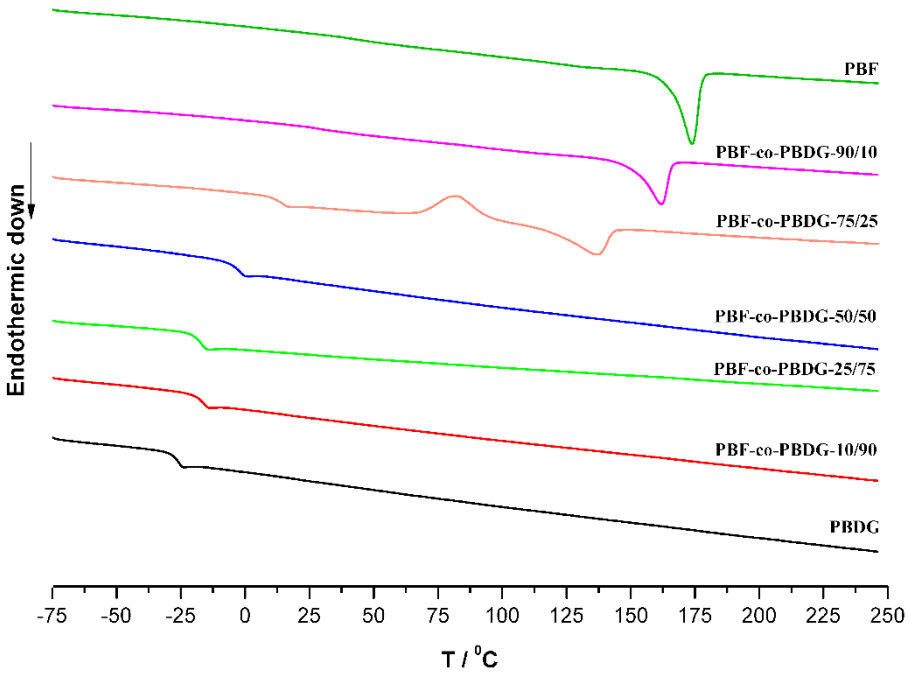

Figure S7. DSC traces of the PBF-co-PBDGs and related PBF and PBDG homopolyesters.

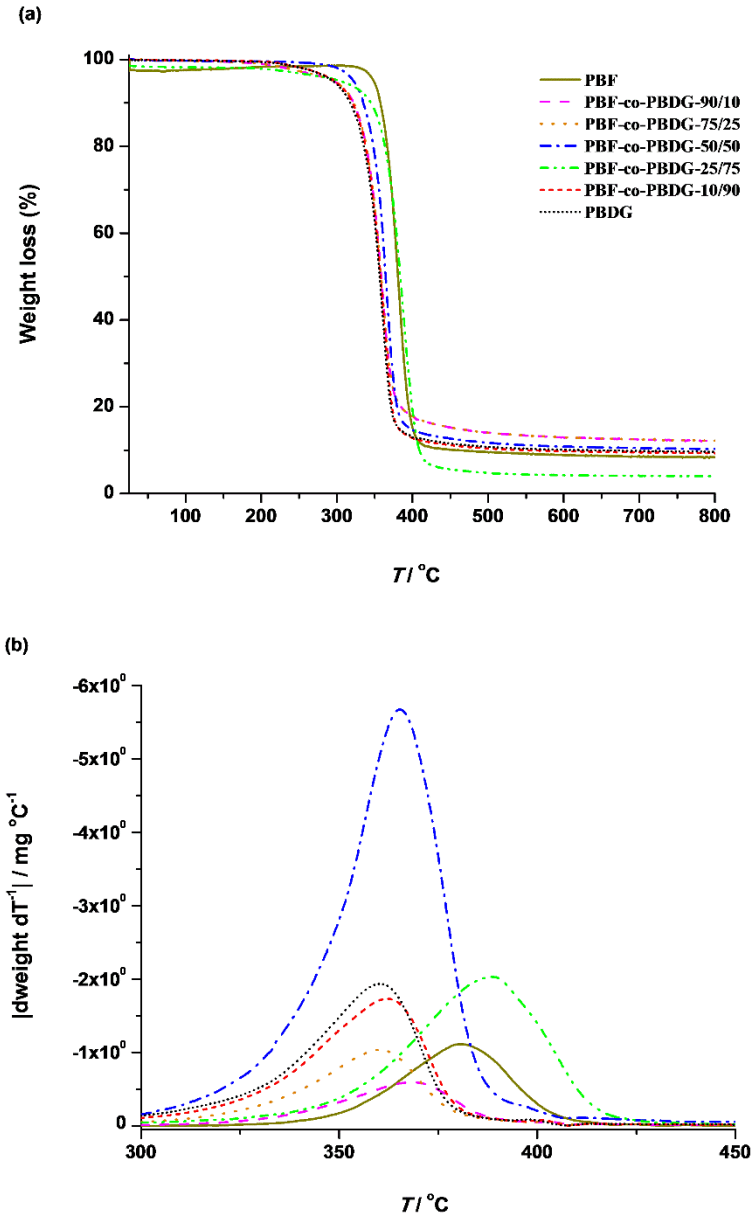

Figure S8. Thermogravimetric curves of the PBF-co-PBDGs and related PBF and PBDG homopolyesters: TGA (**a**) and (**b**) DTG.

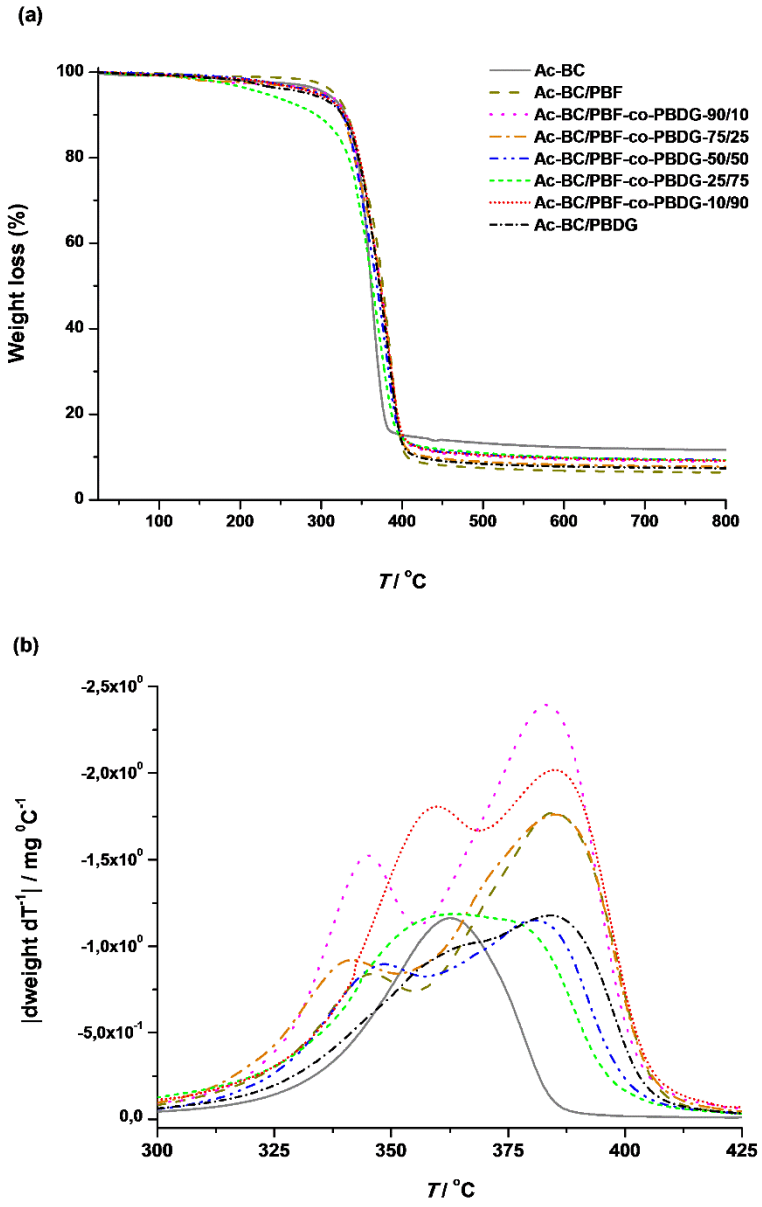

Figure S9. Thermogravimetric curves of the nanocomposites and Ac-BC: TGA (**a**) and (**b**) DTG.

Table S5. Young's modulus, elongation at breakage and tensile strength of the nanocomposites and of Ac-BC component.

sample [1]	**Young's modulus / MPa**	**Elongation at break (%)**	**Tensile strength / MPa**
Ac-BC	1172.8	1.57	14.51
Ac-BC/PBDG	499.8	8.85	11.05
Ac-BC/PBF-co-PBDG-90/10	1239.3	0.62	7.62
Ac-BC/PBF-co-PBDG-75/25	447.8	0.99	6.32
Ac-BC/PBF-co-PBDG-50/50	360.2	7.19	7.36
Ac-BC/PBF-co-PBDG-25/75	30.3	25.02	6.22
Ac-BC/PBF-co-PBDG-10/90	374.4	7.28	8.07

[1] Ac-BC/PBF nanocomposite was not evaluated by tensile testing due to its brittle character, which broken easily precluding its test.

PART C

FDCA-based ester as plasticiser for PVC formulations

Chapter VI – Replacing Fossil-based Di(2-ethylhexyl) Terephthalate by Sugar-based Di(2-ethylhexyl) 2,5-Furandicarboxylate for Benign PVC Plasticization: Synthesis, Materials, Preparation and Characterization

---

This chapter was submitted to ACS Sustainable Chemistry and Engineering journal as:

Marina Matos, Rosemeyre A. Cordeiro, Henrique Faneca, Jorge F. J. Coelho, Armando J. D. Silvestre, Andreia F. Sousa. Replacing fossil-based di(2-ethylhexyl) terephthalate by sugar-based di(2-ethylhexyl) 2,5-furandicarboxylate for benign PVC plasticization: synthesis, materials preparation and characterization.

Abstract

The worldwide regulatory demand for the elimination of non-phatalate compounds for poly(vinyl chloride) (PVC) plasticization has intensified the search for alternatives. Concomitantly, sustainability concerns have spotlighted the sugar-based 2,5-furandicarboxylic acid as one key renewable-chemical for the development of several products, namely di(2-ethylhexyl) 2,5-furandicarboxylate (DEHF) plasticizer. This study addresses the use of DEHF as a plasticizer for PVC under a realistic scenario of co-existence of both fossil- and renewable-based plasticizers: *i.e.*, PVC blends using mixtures of di(2-ethylhexyl) terephthalate ester (DEHT) and DEHF. The detailed structural, thermal and mechanical characterization of these materials showed that they have a set of interesting properties, compatible to those of commercial DEHT, namely a low glass transition (19.2-23.8 ºC) and enhanced elongation at break (up to 330%). Importantly, migration tests under different daily situations, such as for example exudation from food/beverages packages and medical blood bags, reveal very low weight loss percentages. For example, in both distilled water and PBS solution, weight loss does not exceed ca. 0.3% and 0.2%, respectively. Viability tests show, for the first time, that up to 500 μM of DEHF a fairly non-toxic profile is observed, as well as to DEHT. Overall, this study demonstrates that the combination of DEHF and DEHT plasticizers result in a noticeable plasticized PVC with an increase green content and with a benign profile.

KEYWORDS

Di(2-ethylhexyl) 2,5-furandicarboxylate; di(2-ethylhexyl) terephthalate; PVC sustainable plasticizers; renewable resources; benign plasticizers.

1. Introduction

Poly(vinyl chloride) (PVC) is one of the most widely used thermoplastic polymers in respect to the worldwide plastics' consumption. In fact, according to a recent market study,[1] in 2016, over 42 million tons of PVC were consumed, corresponding to over 16% of total plastics demand, and it is continuously growing. PVC is routinely plasticized in order to increase its flexibility, workability or distensability,[2,3] and thus, to decrease the melting (T_m)

and glass transition (T_g) temperatures, as well as, the elastic modulus, in order to meet the requirements of several applications in food/beverage packaging, dialysis bags, blood bags, tubing systems, children toys, among many others.[4] Free plasticizers are relatively low molecular weight molecules that interact with PVC electrophilic C-Cl groups, mainly in the amorphous regions, reducing polymer-polymer chains interactions. The most used plasticizers were for decades esters of phthalic acid derivatives,[5] mainly di(2-ethyl-1-hexyl) orthophthalate ester (DEHP or DOP). However, its use has raised several concerns associated to migration issues overtime and especially due to the severe adverse health effects (especially when it enters the blood stream).[6] In fact DEHP has successively been banned in the EU, and consequently non-phthalate plasticizers have become more widely used (reference [7] and references therein). This is the case of di(2-ethylhexyl) terephthalate ester (DEHT), DEHP structural isomer but which is not associated to toxic effects.[6] However, both DEHP and DEHT plasticizers are derived from fossil resources.

In recent years, motivated by sustainability awareness an increasing attention and concern on the massive use of petroleum-based products[8] (including plasticizers) has called for a paradigm shift towards the development of renewable-based ones. In this vein, several alternatives to DEHT and toxic DEHP have been disclosed,[9,10] namely tung oil-,[11,12] cardanol-,[13,14] poly(caprolactone)-[9] and poly(hexane succinate)-based[10] plasticizers. 2,5-Furandicarboxylic acid (FDCA) is a well-recognized sugar-based monomer, structurally related with terephthalic acid (TPA) and the precursor of several polyesters with thermal and mechanical properties very similar to those prepared from fossil-TPA.[8,15] Moreover, unlike phthalates, furan compounds are easily metabolized and FDCA itself is a common human urinary metabolite.[16] Therefore, its use in broader applications, including as a benign plasticizer, besides in polymer synthesis, is of upmost interest. However, there are only a few reports on this subject,[17,18] specifically on the synthesis of di(2-ethylhexyl) 2,5-furandicarboxylate (DEHF) and its use in PVC blends.[17,18] The PVC-DEHF studied blends (between 10-50 phr of plasticizer) showed to have an elongation at break within 57-249% (slightly lower than DEHP), a T_g between 1-59 ºC; to be thermally stable up to 189-225ºC; and the migration in hexane was at most around 9%. Despite these relatively promising mechanical and thermal performance some important properties, like DEHF cytotoxicity, migration studies using broader spectra of model solvents (including water), and the volatile resistance behavior remained unknown. Moreover, in a more realistic scenario, at the

industrial scale, the replacement of petroleum-based DEHT with renewable counterparts (*e.g*. DEHF) will be hampered due to relevant economic issues related to cost-competitiveness. In this vein, the partial replacement of DEHT by DEHF is a logical approach worth exploring in order to increase the designated 'green-content'.[19]

Therefore, in this study different ratios of DEHF/DEHT were used to assess the progressive replacement of fossil-based DEHT by more sustainable DEHF in PVC formulations, and increase the compatibility/affinity of the mixture of plasticizers with the PVC matrix. These new PVC blends were characterized in detail using several structural, thermal and mechanical techniques, namely ATR FTIR, DRX, TGA, DMTA and tensile tests. Migration stability of the plasticizers was assessed, through chemical and volatile resistance tests. Further, the cytotoxicity of DEHF was evaluated, for the first time, in terms of cell viability tests in order to foresee its wide application as a benign PVC plasticizer.

2. Experimental

2.1. Materials

2,5-Furandicarboxylic acid (>98%) was purchased from TCI Europe N.V. 2-Ethyl-1-hexanol (≥99.6%), stearic acid (95%), anhydrous sodium sulfate (≥99.0%), zinc stearate purum and Dulbecco's modified Eagle's medium - high glucose (DMEM-HG) were supplied by Sigma Aldrich-chemicals Corp. Sulfuric acid (96%), sodium chloride (≥99.0%) and deuterated chloroform (99.8 % D) were acquired from Acros Organics. Chloroform and cyclohexane (HPLC grade) were purchased from Fisher Scientific and Panreac Applichem, respectively. Activated carbon (granules with density of 2 g/cm^3) was obtained by VWR Chemicals. Di(2-ethyl-1-hexyl) 1,4-terephthalate (DEHP) (DOTP- 168 Eastman) was supplied by Eastman Chemical Company and PVC resin (VICIR S1200; K-Fikentscher value of 70 corresponding to number-average molecular weight equal to 59 000 and a polydispersity of 1.97)[20] was provided from CIRES, *Lda*. (Portugal). All chemicals were used as received, without further purification.

2.2. Synthesis of di(2-ethyl-1-hexyl) 2,5-furandicarboxylate (DEHF)

In this study DEHF was synthesized via Fisher esterification following an adapted procedure described elsewhere.[21,22] Briefly, 5.0 g of FDCA (32.0 mmol) and 25.0 g of 2-ethyl-1-hexanol (192.2 mmol) (diacid:diol, 1:6 mol/mol) were reacted in the presence of concentrated sulfuric acid (1 wt%, total diacid weight) and kept at 160 ºC for 6 h. The resulting reaction product was washed with an aqueous NaCl solution (30% m/v) until it reached pH 7, and then extracted with chloroform. The extracted DEHF was dried and weighted. DEHF was isolated as a light-yellow liquid at room temperature in 94 % yield. The purity and molecular structure of the isolated compound was also confirmed by ATR FTIR (Figure S1), NMR (Figure S2 and S3) and GC-MS analyses (Figure S4) and was in accordance with previously reported data.[18] ATR FTIR (ν/cm^{-1}): 3126 (=C–H); 2957, 2927 and 2859 (υ C–H, methylene and methyl groups); 1719 (C=O); 1581 (C=C); 1461, 1380, 1271 and 1220 (C–O); 1017 (furan ring breathing); 968, 822 and 764 (2,5-dibustituted furan ring) (Figure S1). ^{1}H NMR (300 MHz, $CDCl_3$, δ, ppm): 7.20 (s, 2H, H3,H4), 4.25-4.28 (2d, 4H, H6), 1.69-1.77 (m, 2H, H7), 1.30-1.50 (m, 16H, H10, H11, H12), 0.92-0.98 (2t,12H, H9, H13) (Figure S2). ^{13}C NMR (75 MHz, $CDCl_3$, δ, ppm): 158.3 (2,5- C=O); 147.0 (C2/C5); 118.1 (C3/C4); 67.9 (C6); 38.8 (C7); 30.3 (C10); 28.9 (C11); 23.8 (C8); 22.9 (C12); 14.0 (C13); 11.0 (C9) (Figure S3). MS (EI) *m/z* (relative intensity %): 380 $[M]^{+\cdot}$ (1), 269 (17), 251 (14), 223 (5), 157 (100), 112 (31), 70 (35), 57 (9) (Figure S4).

2.3. Preparation of the PVC-DEHF/DEHT films

Plasticized PVC films (Table 6.1) were prepared by pre-mixing PVC-K70 resin (40.0 g), stearic acid (0.3 per hundred resin (phr)), zinc stearate (1 phr) and a mixture of DEHP/DEHF plasticizers in different relative amounts (Table 6.1) for *ca*. 5 min and vigorously hand-stirring. Subsequently, the ensuing mixtures were allowed to rest for 30 min, and after that period they were mixed using a two-roll mild (Collin machine type W-150P), at 140 ºC and 1600 rpm for 5 min. The mixtures were compression-molded (Carver press Model 3851) using a steel mold (110 mm × 110 mm × 2 mm) and heated until reaching 140 ºC and after standing for 2 min pressed at 28 tons until a thickness of 2 mm was reached, and finally depressed, and fast cooled to room temperature.

Table 6.1. Compositions of the different PVC-DEHF/DEHT formulations prepared.

Components	Formulations					
	Pure PVC	**PVC1**	**PVC2**	**PVC3**	**PVC4**	**PVC5**
	Amount / g					
PVC resin -K70	40.0 (100 phr[a])	40.0 (100 phr)	40.0 (100 phr)	40.0 (100 phr)	40.0 (100 phr)	40.0 (100 phr)
DEHT	-	22.0 (55 phr)	20.0 (50 phr)	18.0 (45 phr)	16.0 (40 phr)	14.0 (35 phr)
DEHF	-	0.0 (0 phr)	2.0 (5 phr)	4.0 (10 phr)	6.0 (15 phr)	8.0 (20 phr)
Stearic acid	-	0.12 (0.3 phr)	0.12 (0.3 phr)	0.12 (0.3 phr)	0.12 (0.3 phr)	0.12 (0.3 phr)
Zinc stearate	-	0.40 (1.0 phr)	0.40 (1.0 phr)	0.40 (1.0 phr)	0.40 (1.0 phr)	0.40 (1.0 phr)

[a]phr- per hundred resin

2.4. Characterization techniques

Viscosity and density of DEHF plasticizer were measured using an automated SVM 3000 Anton Paar rotational Stabinger viscometer-densimeter, at atmospheric pressure, within the temperatures range of 293.15 to 323.15 K ± 0.02 K.

Attenuated total reflectance Fourier transform infrared (ATR FTIR) spectra were obtained using a PARAGON 1000 Perkin-Elmer FTIR spectrometer equipped with a single-horizontal Golden Gate ATR cell. The spectra were recorded after 128 scans, at a resolution of 4 cm^{-1}, within the range of 500 to 4000 cm^{-1}. The ATR FTIR spectra of all samples were normalized relatively to the vibrational peak at 2953 cm^{-1}.

^{1}H and ^{13}C NMR spectra were recorded using a Bruker AMX 300 spectrometer, operating at 300 or 75 MHz, respectively. All chemical shifts (δ) were expressed as parts per million, downfield from tetramethylsilane (used as the internal standard).

Gas chromatography-mass spectrometry (GC-MS) analyses were performed using a Trace gas chromatograph (2000 series) equipped with a Thermo Scientific DSQ II mass spectrometer (Waltham, MA). Separation of compounds was carried out in a DB-1 J&W capillary column (30 m × 0.32 mm inner diameter, 0.25 μm film thickness) using helium as the carrier gas (35 cm s^{-1}). The chromatographic conditions were as follows: initial temperature equal to 80 °C for 5 min; then temperature raised up to 260 °C at a temperature rate of 4 °C min^{-1}; and finally up to 285 °C, at 2 °C min^{-1} and maintained for 8 min. the injector temperature was 250 °C; transfer-line temperature equal to 290 °C; and split ratio of 1:33. The mass spectrometer was operated in the electron impact (EI) mode with an energy

of 70 eV, and data were collected at a rate of 1 scan s^{-1} over a range of *m/z* 33–700. The ion source was kept at 250 °C. The sample was prepared dissolving DEHF in chloroform (1 mg/mL).

X-ray diffraction (XRD) analyses were performed using a Philips X'pert MPD diffractometer operating with CuKα radiation (λ = 1.5405980 Å) at 40 kV and 50 mA. Samples were scanned in the 2θ range of 5 to 50°, with a step size of 0.04°, and time per step of 50 s.

Thermogravimetric analysis (TGA) were carried out with a Setaram SETSYS analyzer equipped with an alumina plate. Thermograms were recorded under a nitrogen flow of 20 mL min^{-1} and heated at a constant rate of 10 °C min^{-1} from room temperature up to 800 °C. Thermal decomposition temperatures were taken at the onset of significant weight loss (≥5%) and at maximum decomposition temperatures from the heated samples ($T_{d,5\%}$ and T_d, respectively).

Dynamic mechanical thermal analyses (DMTA) were performed with a Tritec 2000 DMA Triton, operating in tension mode, except for pure PVC, for which a material pocket accessory was used, operating in the single cantilever mode. Tests were performed at 1 and 10 Hz and the temperature was varied from -100 to 150 ºC, at 2 ºC min^{-1}. The glass transition temperature (T_g) was determined as the maximum peak value of tan δ.

Tensile tests were obtained with an Instron 5564 tensile testing machine at a cross-head speed of 10 mm min^{-1} using a 500 N static load cell. The tensile test specimens were rectangular strips (50 mm × 10 mm × 2 mm) pre-conditioned for 72 h at 25 °C. Each measurement was repeated at least five times.

The chemical resistance tests were performed in agreement with the Standard Test Method ASTM D 1239-98.[23] PVC-DEHF/DEHT specimens (10 mm × 10 mm × 2 mm) were pre-conditioned at 23 ± 2ºC with a humidity of 50 ± 5 %, for 24 h. After this period, the specimens were immerged in 10 ml of the chosen solvent (distilled water, sodium phosphate buffer at pH~ 7, or cyclohexane), at 23 ± 2ºC for 48 h. The films were then removed from the liquid, washed thoroughly with distilled water and dried. Each measurement was repeated at least three times. The weight loss percentage was calculated using the expression: $Weight\ loss\ (\%) = \frac{W_i - W_f}{W_i} \times 100$ where, W_i and W_f stand for the specimen weights prior and after chemical resistance tests, respectively.

Volatile resistance tests were performed according to the international standard ISO 176-2005,[24] to determine the loss of plasticizers through the activated carbon method. PVC-DEHF/DEHT specimens (10 mm ×10 mm × 2 mm) were placed on the center of activated carbon at 40 ºC for 48 h. After this period, samples were washed with distillate water and dried. Each measurement was repeated at least three times. The weight loss was determined using the same equation represented above.

2.5. Citotoxicity assays

The cytotoxicity of the plasticizers was evaluated in the 3T3-L1 cell line acquired from ATCC. For this purpose, 35×10^3 3T3-L1 cells were seeded onto 48-well culture plate, 24 h prior to incubation with the compounds (cells were used at 70% confluence). Then, cells were incubated with different concentrations of the plasticizers for 48 and 72 h, and the cell viability was assessed by a modified Alamar Blue assay.[25] This assay measures the redox capacity of the cells due to the production of metabolites as a result of cell growth. Briefly, the cell culture medium of each well was replaced with 0.3 mL of DMEM-HG containing 10% (v/v) of *Alamar Blue* (0.1 mg/mL in PBS) and, after 1 h of incubation at 37 °C, 170 μL of the supernatant were collected from each well and transferred to 96-well plates. The absorbance was measured at 570 and 600 nm in a SPECTRAmax PLUS 384 spectrophotometer (Molecular Devices, Union City, CA). Cell viability was calculated as a percentage of the control cells (cells not treated with the plasticizers) according to the ratio: $(A_{570} - A_{600})_{treated\ cells} / (A_{570} - A_{600})_{control\ cells} \times 100$. The data are expressed as mean ± standard deviation obtained from n = 9 (from three independent experiments).

3. Results and Discussion

The partial replacement of fossil-based DEHT plasticizer in PVC formulations was accomplished by preparing several mixtures incorporating increasing amounts of renewable-based DEHF (Table 6.1). In the first step, DEHF was synthesized by a Fisher esterification of FDCA and 2-ethyl-1-hexanol, under acidic conditions (Scheme 1), and its structure probed by FTIR, NMR and MS spectroscopies (Figures S1-S4) with a molecular weight equal to 380.30 (Table S1); followed, in the second step, by DEHF mixture with DEHT; and

then, finally, compounding the plasticizers mixture with PVC resin, and also with stearic acid and zinc stearate, selected as lubricant and heat stabilizer, respectively.[26,27]

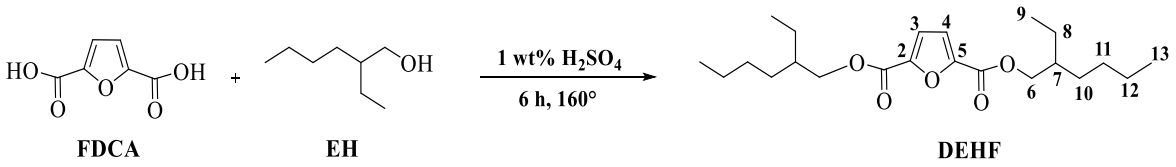

Scheme 1. Synthesis of DEHF.

Interestingly, it was noted that DEHF has the same density (0.98) but slightly lower viscosity (55 cP) than DEHT (63 cP) (Table S1), which could facilitate its dispersion within the PVC matrix, and in this way also facilitate dispersion in the case of the DEHF/DEHT mixtures.

3.1. Structural characterization of PVC-DEHF/DEHP films

The PVC-DEHF/DEHT films and their main components, *i.e.*, DEHF and DEHT plasticizers, as well as the pure PVC were studied by ATR FTIR spectroscopy (Figure 6.1). The spectrum of DEHF is in accordance with its expected structure, and with a previous report,[18] displaying: symmetrical and asymmetrical C–H stretching vibrations of the furanic ring (ν_{sym} =C–H$_{ring}$ and ν_{asym} =C–H$_{ring}$) near 3141 and 3162 cm^{-1} (Figure S1); asymmetrical and symmetrical C-H stretching of the methyl and methylene groups of the EH moieties (ν_{asym} –C-H and ν_{sym} –C-H) at 2958, 2928, 2873 and 2860 cm^{-1}, respectively;[18,28,29] one intense band at 1719 with a shoulder at around 1740 cm^{-1} arising from the carbonyl stretching vibration, typical of ester groups (ν C=O). The presence of the higher wavenumber band at 1740 cm^{-1} is most likely associated with plasticizer-plasticizer associations involving the carbonyl groups.[30] Also detected were CH_3 in plane deformation (δ CH_3) at 1380 cm^{-1}; aromatic C-H in plane angular deformation vibration at 1270 cm^{-1}; near 941 cm^{-1} the out of plane *trans* deformation vibration (ω C-H);[18] and the typical vibrational modes of 2,5-disubstituted furanic ring near 980, 823, and 764 cm^{-1}.

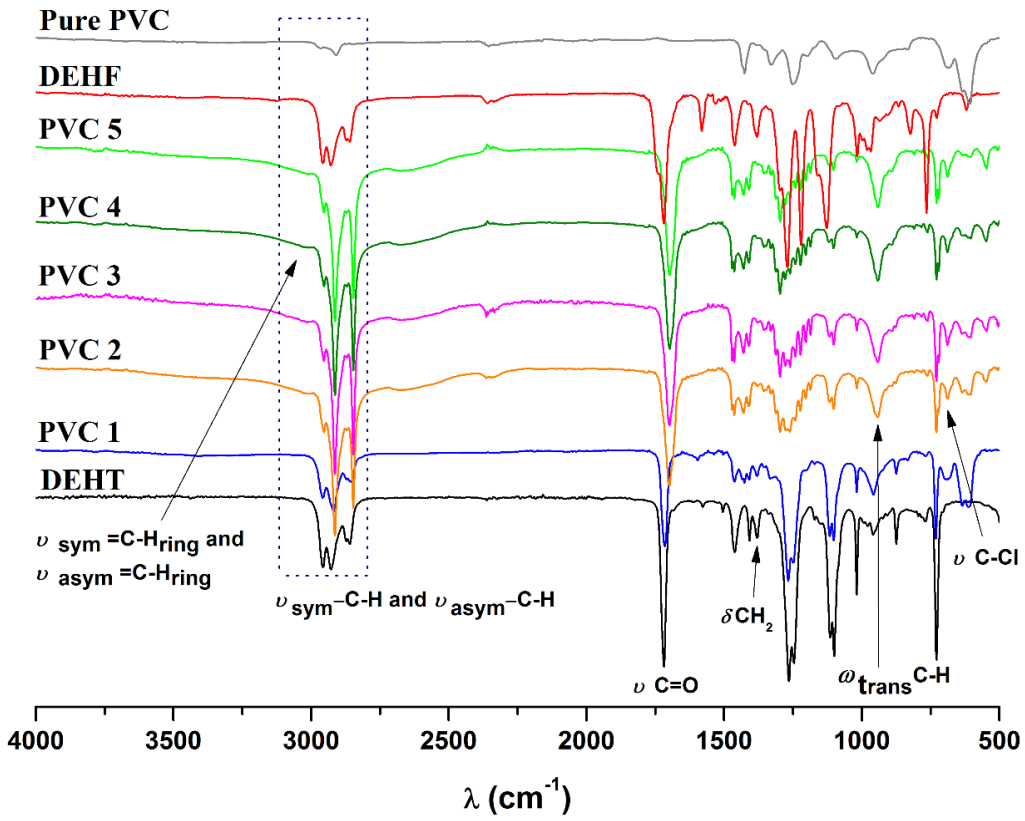

Figure 6.1. Normalized ATR FTIR spectrum of all PVC films, and DEHF and DEHT plasticizers.

The spectrum of the fossil-based DEHT is quite similar to that of DEHF counterpart, except for the bands at 3100 cm^{-1}, arising from the C-H stretching mode of the benzenic ring and those of 1,4-disubstituted benzenic ring at 728 cm^{-1}. The spectrum of the pure PVC showed the main characteristic vibrational bands of this polymer (Figure 6.1), *viz.*: C-H stretching on neighboring C-Cl group at 2966 cm^{-1}; asymmetrical and symmetrical C-H stretching ($\nu_{asym,sym}$ –C-H) at 2908 cm^{-1}; CH_2 deformation at 1425 cm^{-1}; CH_2 deformation at 1328 cm^{-1}, Cl-CH out of plane angular deformation at 1252 cm^{-1}; out of plane *trans* deformation at 958 cm^{-1} and the C-Cl bond stretching vibrations in the region between 660-580 cm^{-1}.[31–33]

As expected, the ATR FTIR spectra of the PVC-DEHF/DEHT blends (Figure 6.1) displayed the characteristic bands of the two main components, *i.e.*, the plasticizers and the pure PVC. The characteristic vibrational peaks of the other additives were not distinguishable in the spectra of the films.

Probing PVC-plasticizer compatibility. It is well known that an enhanced compatibility/miscibility of a polymer-plasticizer blend is essentially the result of physical interactions between the components of the mixture which could be followed by infrared spectroscopy.[2,3] As previously suggested, in the particular case of PVC-aromatic ester plasticized blends, for example, PVC-DEHT or PVC-DEHP, the main interactions are essentially of dipole-dipole nature involving the polarized carbon−chlorine (C−Cl) and the carbonyl (C=O) groups of PVC and plasticizer, respectively.[28,30,33] The vibrational modes stemming from these groups denounced the blends compatibility and will be studied in more detail.

From the neat plasticizers to the ensuing blends, a red-shift of the C=O stretching band from 1718 cm^{-1} to lower wavenumbers, *e.g.* to 1715 cm^{-1} for PVC1, and to near 1700 cm^{-1} for all the other blends was observed (Figure 6.1), in accordance with Tabb *et al.* findings.[33] This result is indicative of interactions between the plasticizers and the PVC polymer chains and in accordance with an effective plasticization process.[28,29,34] However, in a previous study by Yu *et al.*[18] about PVC-DEHF films, no shift of this band was observed, which was attributed to probable weak interaction between the plasticizer and the PVC matrix. Oppositely, the herein presented results support the enhanced compatibility of the present PVC plasticization system involving both DEHF and DEHT. Both the nature of plasticizers mixture and the methodology used to prepare the PVC formulations, by a pre-mixture procedure between all the components for a period of 30 minutes, contribute to the enhanced compatibility.

Other important spectral changes, in the region between 660-580 cm^{-1} (Figure 6.2), attributed to the C–Cl stretching vibration modes (ν C-Cl) were clearly observed. There was both a broadening and splitting of the band associated with the atactic PVC fraction (amorphous domains), centered at 608 cm^{-1}, especially in the case of the blends prepared with higher amounts of DEHF compared with neat PVC. Furthermore, the band at 638 cm^{-1} related to crystalline domains of PVC remained essentially unchanged, except for DEHF amounts higher than 27% (PVC4). Similar observations were denoted in several other previous studies, and were pointed out as evidence of a strong interaction between PVC and the plasticizer.[13,35] Moreover, this is consistent with the classical plasticization process essentially affecting the amorphous domains of PVC, through a solvation process.[33] Hence, for the present PVC-DEHF/DEHT system similar conclusions can be inferred. In particular,

revealing that DEHF/DEHT mixture of plasticizers could improve the plasticization process, increasing the compatibility between the different compounds in the PVC formulations.

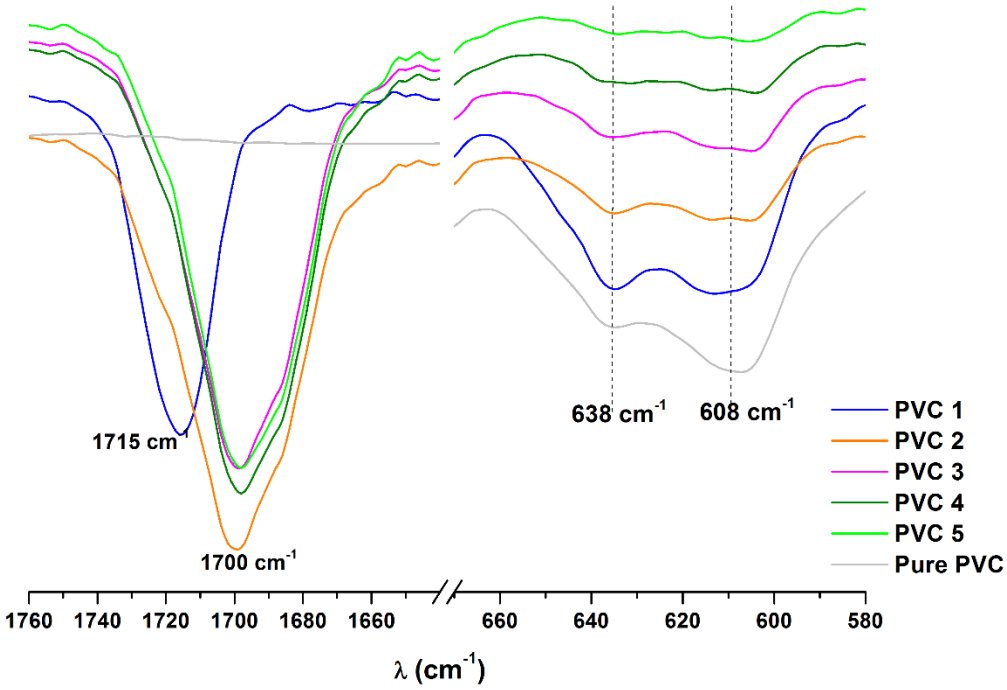

Figure 6.2. ATR FTIR spectra of all PVC-DEHF/DEHT blends in the C=O and C-Cl stretching regions.

The XRD patterns of all plasticized films (Figure 6.3) evidenced their essentially amorphous nature, with nonetheless, some broad crystallinity peaks at $2\theta \approx 16.5$, 18.4 and 24.4 º, in agreement with literature and ATR FTIR results.[36,37] The pure PVC pattern, was consistent with the PVC-DEHF/DEHT patterns, although evidencing higher degree of crystallinity.

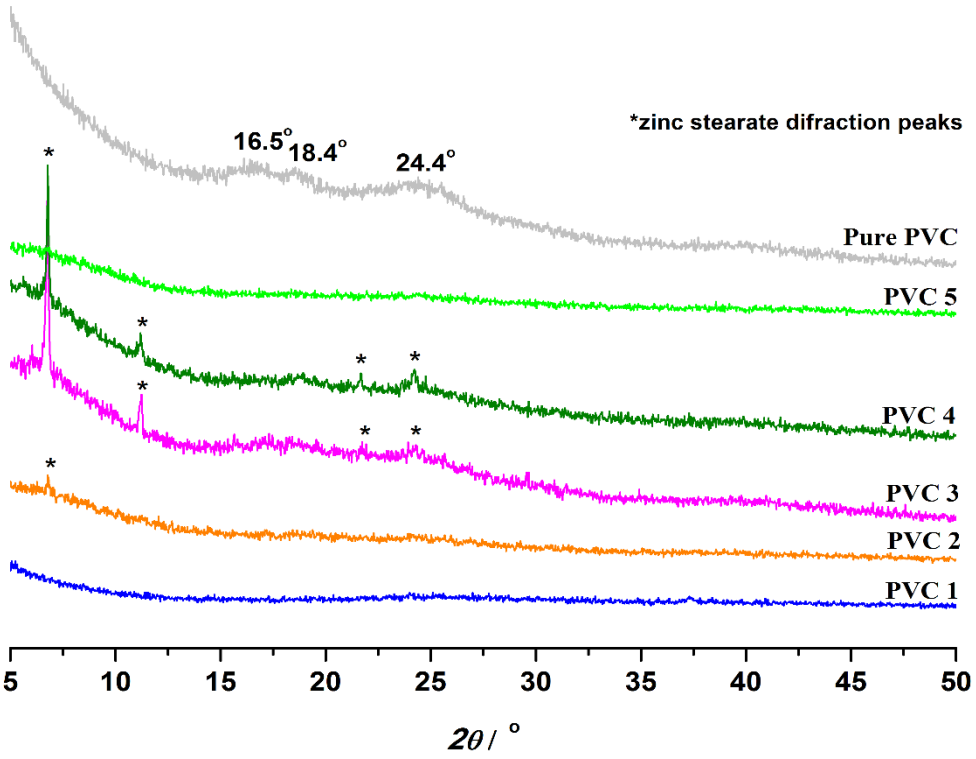

Figure 6.3. X-Ray diffractograms of all DEHF/DEHT-based PVC films and pure PVC.

3.2. Mechanical behaviour

3.2.1. Dynamic mechanic thermal analyses

All blends were analyzed by DMTA to evaluate the influence of using DEHF/DEHT plasticizers on their dynamical-mechanical properties. Figure 6.4 shows the tan δ and storage modulus (E') traces of DEHF/DEHT-based PVC films, recorded in tension mode, at constant frequency (1 Hz). Figure S5 displays the loss modulus (E'') traces. The main results are summarized in Table S2.

The tan δ curves (Figure 6.4(a)) of all plasticized PVC films displayed a single maximum corresponding to a α transition, ascribed to the glass transition (T_g), with values ranging from 19.2 to 23.8 ºC, typically decreasing with the increasing content of DEHF in the blend (PVC1-3). However, going into further detail, a small shift to higher T_g values occurred in the case of those blends incorporating the highest relative amounts of DEHF (PVC4 and 5). This could be related to the existence of more rigid DEHF molecules in the blends, leading to a slightly increase on T_g values, in similarity to FDCA-based polyesters.[38,39]

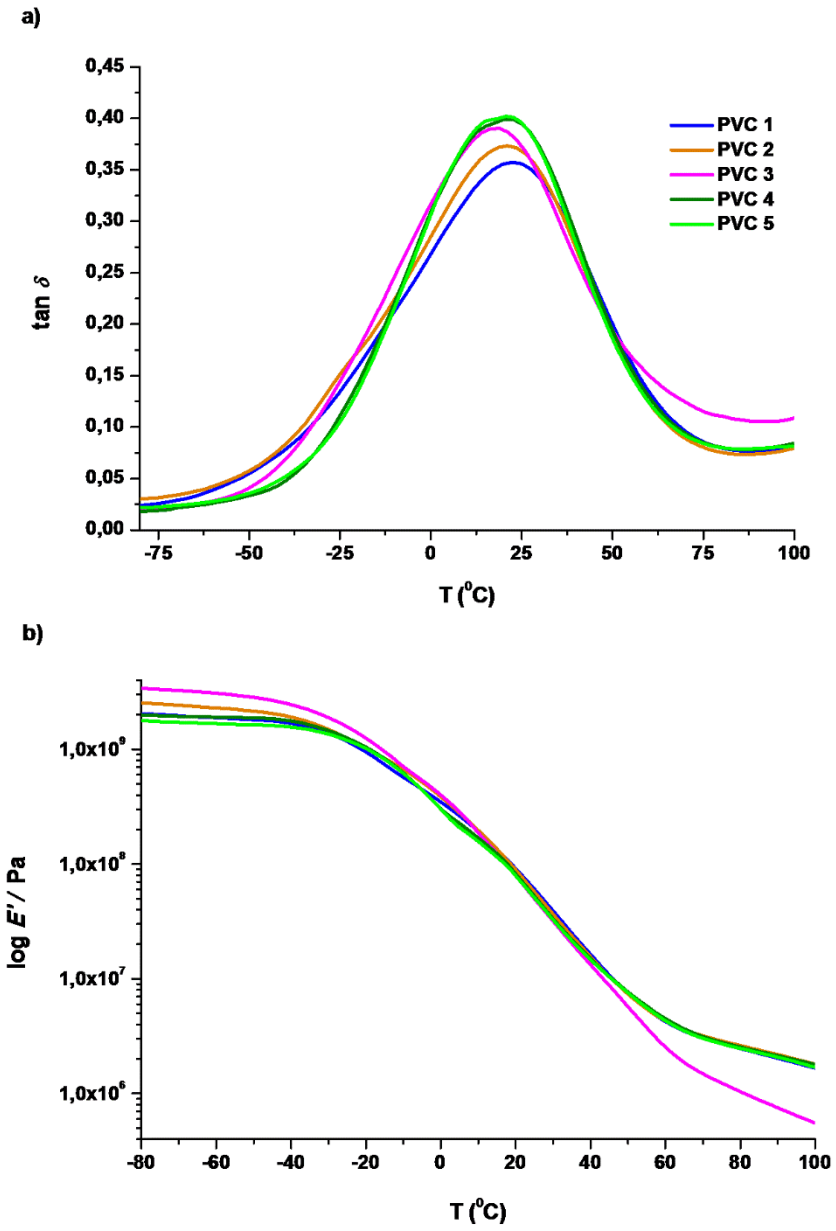

Figure 6.4. Main results of DMTA analyses a) tan δ and b) E' traces of all plasticized PVC films.

In comparison with the tan δ curve of pure PVC, the maximum was at much higher temperatures than in the case of the blends, approximately 97.4 °C. These results are in accordance with literature results on pure PVC and on other plasticized systems incorporating DEHF or other 2,5-FDCA-based esters,[17,18] DEHT,[12,40] and binary mixtures of DEHT with other plasticizers.[29,41,42] Importantly, the appearance of a single T_g on the tan δ traces of plasticized PVC films, and shifted to lower values, reaching a difference of *e.g.*

77 ºC relatively to PVC3 formulation, suggested the compatibility between the plasticizers and PVC as already ATR FTIR results suggested.[42,43]

The blends' storage modulus traces (Figure 6.4 (b)) clearly show three main regions, *viz.*: one region below the glass transition corresponding to an almost constant high modulus, ranging from 551-695 MPa at -10 ºC; followed by an abrupt decrease of the modulus due to T_g transition; finally, at higher temperatures, the modulus reached its minimum and maintained roughly constant between 38 to 43 MPa at 25 ºC. In general, the storage modulus of the blends were far below from that of pure PVC (e.g. 12-13 MPa at 40 ºC *vs.* 377 MPa at 40 ºC, respectively),[44] indicating an improvement of the flexibility of the PVC-DEHF/DEHT films. In addition, comparing the use DEHF/DEHT mixtures of plasticizers (PVC2-5) with the single use of DEHT (PVC1), *E´ and E´´* were higher in the former case, most probably due to the incorporation of stiff furan plasticizer (Table S2 and Figure S5). Nevertheless, incorporating relatively higher amounts of DEHF the modulus tend to decrease.

Furthermore, comparing PVC-DEHF/DEHT blends with those previously reported based only on the single use of renewable DEHF as plasticizer, this study clearly highlighted the enhanced flexibility of the former, since they had lower *E'*.[18] For example, PVC-DEHF (50 phr) presented an *E´* equal to 91 MPa at 23 ºC.[18] In this respect, the DEHF/DEHT binary system seems to be not only a valuable approach in view of progressively replacing fossil-based plasticizers, but also due to their compatible properties.

3.2.2. Tensile tests

Table 6.2 summarizes the Young's modulus, tensile strength and elongation at break of all plasticized PVC blends. The most interesting result observed was the fact that the elongation at break of DEHF/DEHT based formulations increased from 247 % in PVC-DEHT (PVC1) to 330% in PVC-DEHF/DEHT (PVC3), and tensile strength increased from 13.19 MPa (PVC1) to 17.46 MPa (PVC3), respectively, indicating an enhancement on the flexibility of PVC blends. However, such trend was not detected in the case of the highest amounts of DEHF used, *i.e.*, in the case of PVC4 and PVC5. This latter evidence was perfectly aligned with the DMTA results, showing that DEHF content higher than 10 phr can change the final mechanical properties.

Table 6.2. Main results of Young's modulus, elongation at breakage and tensile strength determined at 25 ºC.

Formulations	Young's modulus (MPa)	Elongation at break (%)	Tensile strength (MPa)
Pure PVC	153.87 ± 6.3[a]	180.37 ± 5.16[a]	30.33 ± 0.28[a]
PVC1	8.96 ± 0.26	246.64 ± 9.38	13.19 ± 0.55
PVC2	8.20 ± 0.14	316.26 ± 9.65	16.37 ± 0.51
PVC3	7.58 ± 0.29	330.34 ± 11.66	17.46 ± 0.54
PVC4	7.72 ± 0.45	238.63 ± 4.26	13.35 ± 0.24
PVC5	8.69 ± 0.31	225.76 ± 7.49	14.57 ± 0.37

[a] Determined by Jia *et al.*[45].

As expected, comparing DEHF/DEHT plasticized PVC (PVC2-5) with the non-plasticized one,[14] as well as, with DEHT-based PVC film (PVC1 formulation), an improvement on the flexibility was achieved, but at the expense of the Young's modulus decrease (see Figure S6). In addition, enhanced flexibility was also achieved for all range of DEHF/DEHT ratios compared with PVC-DEHF, displaying a maximum increase on the elongation at break of around 82 %.[18]

3.3. Thermogravimetric analysis

DEHF and DEHT plasticizers, as well as, all the related PVC formulations were characterized in terms of their thermogravimetric behavior through TGA analysis, and the main results are summarized in Table 6.3 and Figure S7.

TGA thermograms of DEHF/DEHT-based PVC films (PVC1 to PVC5) exhibited two major decomposition steps, (Figure S7), in agreement with other plasticized PVC systems.[11,45,46] The first step was comprehended between 200-380 °C, showing the higher weight loss of the PVC films (around 72 %), and was related to dechlorination of PVC and formation of polyenes, as well as to the thermal decomposition of the plasticizers. The second degradation step was found between 420 and 530 ºC, with an observed lower weight loss (around 13 %), and it occurred mainly due to the evolution of toluene and methylated aromatics coming from the decomposition of the polyenes.[47]

Table 6.3. Decomposition at 5, 10 and 50% weight loss ($T_{d,5\%}$, $T_{d,10\%}$ and $T_{d,50\%}$) and maximum decomposition ($T_{d,max}$) temperatures of plasticized PVC films, and their pure components counterparts.

Formulations	$T_{d,5\%}$ (ºC)	$T_{d,10\%}$ (ºC)	$T_{d,50\%}$ (ºC)	$T_{d,max1}$ (ºC)	$T_{d,max2}$ (ºC)	Weight loss (%)		Residue (%)
						1st step	2nd step	
						200 - 380 ºC	420 - 530 ºC	
DEHF	175.9	237.8	318.8	349.8	-	-	-	0.01
DEHT	279.0	297.3	343.1	360.5	-	-	-	0.07
Pure PVC	268.7	274.6	303.2	286.4	461.7	58.2	23.7	3.46
PVC1	241.9	262.0	308.2	305.0	455.7	71.8	13.5	8.85
PVC2	243.0	263.3	308.5	298.7	460.3	72.1	12.8	9.93
PVC3	250.0	262.7	306.1	297.5	459.4	71.7	12.6	13.22
PVC4	245.1	264.0	308.0	295.1	459.2	72.6	12.6	10.44
PVC5	247.3	263.2	304.6	292.3	458.3	72.2	12.1	12.75

For all range of DEHF/DEHT ratios used in the blends an expected increase of the $T_{d,max1}$ compared with pure PVC (286 ºC) was observed.[45,47] This was directly related to the incorporation of high-thermal behavior plasticizers in the blends. Indeed, the maximum degradation temperatures of DEHF and DEHT plasticizers were *ca*. 349 and 361 ºC, respectively. In terms of $T_{d,max2}$, no relevant variation was observed, except for a general decrease of this parameter in the case of the blends compared with the pure PVC counterpart.

Moreover, a decrease on both $T_{d,5\%}$ and $T_{d,10\%}$ of the plasticized PVC films compared with the non-plasticized PVC was noted, mostly due to the lower evaporation/degradation temperature of the DEHF plasticizer. Despite these results, the ensuing DEHF/DEHT-based PVC films presented a higher thermal stability than those prepared from a single plasticizer, either DEHF[18] or DEHT (PVC1), in agreement with the occurrence of strong interactions between the mixture of plasticizers and PVC matrix, favoring the blend stability.

3.4. Chemical and volatile resistance tests

The new PVC blends of binary mixtures of DEHF/DEHT were evaluated in terms of plasticizers migration stability, simulating potential DEHF/DEHT migration under daily situations, such as for example exudation from food/beverages packages and medical blood bags. In practice, the weight loss percentages by leaching of plasticizers from PVC specimens to distilled water, sodium phosphate buffer (pH~ 7) and to cyclohexane were

determined (chemical resistance).[48] Additionally, the PVC blends were buried in active carbon and the PVC weight loss assessed (volatile resistance), simulating for example the case of plasticizers migration from baby nipples to solid medium. The main results of weight loss are summarized in Figure 6.5 and Table S3.

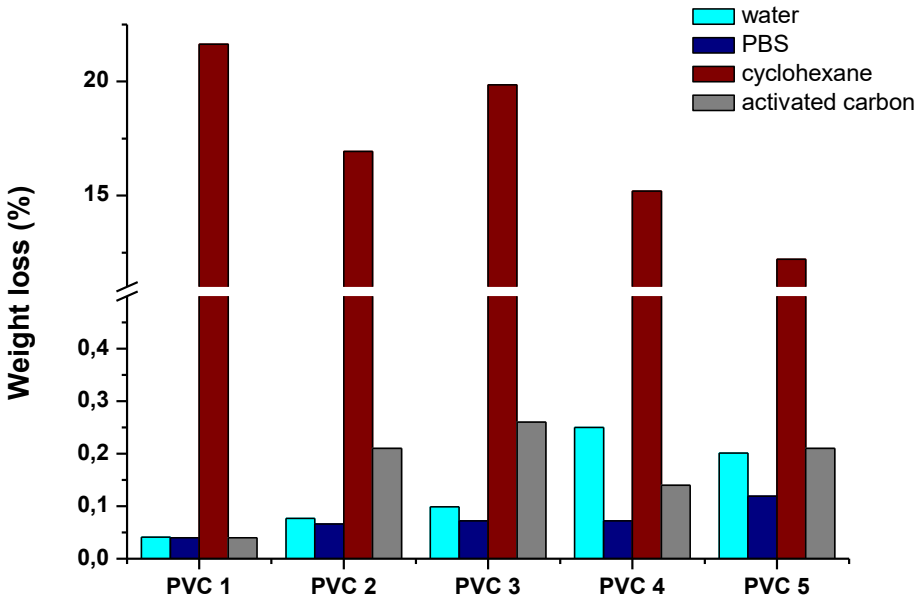

Figure 6.5. PVC blends weight loss percentage results determined from the chemical and volatile resistance tests.

The weight loss percentages of all DEHF/DEHT plasticized PVC blends in both distilled water and PBS solution, were very low, not exceeding *ca.* 0.3% and 0.2%, respectively, due to the hydrophobic nature of the plasticizers. These findings indicated that the DEHF/DEHT mixture of plasticizers were quite compatible with the PVC matrix, in accordance with the FTIR results. Importantly, these low leaching values clearly showed that they were not easily extracted.

PVC-DEHT film (PVC1) had the lowest weight loss values in distilled water, followed very closely by all the other plasticized systems studied: PVC2<PVC5<PVC3<PVC4. In general, all weight losses observed for PVC-DEHF/DEHT and PCV-DEHT samples were of the same magnitude as to previously published results, or even lower.[10–12,40,41] For example, migration tests in distilled water conducted in the same conditions as those carried

out in the present study reported a weight loss of around 0.22% to PVC/DEHP, and of *ca*. 0.20% to a PVC/cardanol-based plasticizer blend.[40]

An overall trend of the cyclohexane migration tests was that the weight loss results were much higher than those obtained in aqueous media (water or PBS), which is easily understood considering the essentially hydrophobic nature of both plasticizers and cyclohexane. The PVC-DEHT (PVC1) weight loss was higher than those obtained for the DEHF/DEHT-based films (PVC2-5), most probably to a higher solubility of DEHT in cyclohexane. This is a very interesting fact enabling the consideration of a new wide range of applications, especially for materials to be used in contact with foods with high fat content, such as, blood, foods, among others.

Volatile resistance results (Figure 6.5 and Table S3) were quite similar to chemical resistance ones, displaying a maximum weight loss percentage of *ca*. 0.3% for PVC3. A general trend of both chemical and volatile tests was that up to a DEHF/DEHT ratio equal to 10/45 phr/phr (PVC3) the weight loss percentages increased but decreased thereafter for higher values of DEHF/DEHT ratios. This behavior was also in agreement with the thermal and mechanical results reported before. Moreover, in the case of DEHF-based PVC films,[18] similar results were obtained for formulations incorporating a DEHF content higher than 30 phr. This trend could indicate, on the one hand, that for DEHF/DEHT ratios lower than 10/45 (PVC2 and 3), DEHT plasticizer dominated the interactions with the PVC matrix, whereas DEHF molecules acted as a secondary plasticizer. On the other hand, for the higher DEHF/DEHT ratios (higher than 10/45), DEHF plasticizer played a major role instead, and one could conjecture that it was also involved in relevant PVC-plasticizer interactions, hindering the migration process.

Importantly, chemical resistance and volatile resistance tests of the new DEHF/DEHT binary mixtures showed weight loss percentage values far below the specified limits for food and medical applications (weight loss < 50 % of the plasticizer content, according the Standard test D 1239-98).[23] Another important result that is worth to highlight here is that the very small migration of the plasticizers observed from the PVC blend will not be enough to negatively influence stiffness/flexibility of the PVC materials along their life-cycle.

3.5. Citotoxicity assays

Toxicity is one of the majors health concerns associated to plasticizers routinely used in common 'plastics'.[49] Actually, in this context legislators have banned DEHP from some EU countries. The present study did not neglect this important issue and despite all the other evidenced adequate plasticizing properties (both in terms of thermal and mechanical behaviour together with low migration profile) also the cytotoxicity profile of DEHF, using the Alamar blue assay in 3T3-L1 cell line, was evaluated for the first time. For comparison reasons, cell viability in the presence of commercially used DEHT was also evaluated under the same conditions. The main results are displayed in Figure 6.6.

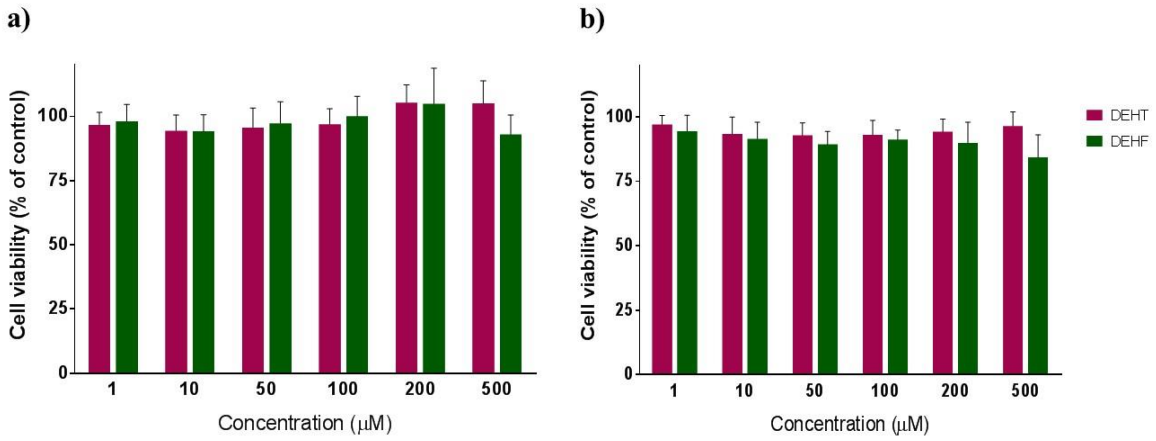

Figure 6.6. Cell viability in 3T3-L1 cell line after (a) 48 hours and (b) 72 hours of incubation in the presence of DEHF or DEHT plasticizers. Values represent the mean ± standard deviation (n = 9).

3T3-L1 mouse cells were incubated for 48 and 72 h in the presence of different amounts of DEHF and DEHT (ranging from 1 to 500 μM). According to the Alamar blue assay results, plasticizers didn't exhibit significant toxicity in 3T3-L1 cells, up to a concentration of 500 μM and for a period of 48 and 72 h. Approximately 100% cell viability was obtained with both DEHF and, as expected, also with DEHT, after 72 h of incubation (Figure 6.6). Generally, materials that promote a cell viability higher than 80% are considered as biocompatible.[25]

4. Conclusions

In summary an effective strategy to prepare plasticized PVC blends with higher 'green content' based on the combination of the renewable-based DEHF and the fossil based DEHT compounds is reported. The ensuing PVC/DEHF-DEHT materials showed to have enhanced compatibility between PVC matrix - mixture of plasticizers, compared to single use of DEHF,[18] confirmed by FTIR spectroscopy. In this regard, all PVC blends spectra display a red-shift of the C=O stretching band from 1718 cm^{-1} to lower wavenumbers, in accordance with the occurrence of dipole-dipole interactions,[33] and an effective plasticization process. Accordingly, these new PVC blends showed to have a reduced T_g, from around 97 to 20 °C, together with an enhanced elongation at break (up to 330 %) but at the expense of some reduction of its stiffness with Young's modulus of approximately 8 MPa. Importantly, both migration tests and cell viability assays using 3T3-L1 cell line showed promising results in terms of applications prospects. For example, migration tests of PVC/DEHF-DEHT blends in water showed that the weight loss will at the most be equal to 0.3%, despite some increase compared to PVC/DEHT (≈ 0.1%), but still quite low values were obtained. In terms of cytotoxicity of DEHF samples up to 500 μM, for a maximum period of 72 h, an almost 100% cell viability was observed.

References

(1) Ceresana. Polyvinyl chloride (PVC) market report https://www.ceresana.com/en/market-studies/plastics/polyvinyl-chloride/ (accessed Oct 5, 2018).

(2) Immergut, E. H.; Mark, H. F. Principles of Plasticization. In *Plasticization and Plasticizer Processes*; Platzer, N. A. J., Ed.; American Chemical Society: Washington, DC, 1965; pp 1–26.

(3) Daniels, P. H. A Brief Overview of Theories of PVC Plasticization and Methods Used to Evaluate PVC-Plasticizer Interaction. *J. Vinyl Addit. Technol.* **2009**, *15* (4), 219–223.

(4) Carroll, W. F.; Johnson, R. W.; Moore, S. S.; Paradis, R. A. 5-Poly(Vinyl Chloride). In *Applied Plastics Engineering Handbook*; Kutz, M., Ed.; Elsevier, 2011; pp 61–76.

(5) Rahman, M.; Brazel, C. S. The Plasticizer Market: An Assessment of Traditional Plasticizers and Research Trends to Meet New Challenges. *Prog. Polym. Sci.* **2004**, *29* (12), 1223–1248.

(6) Wirnitzer, U.; Rickenbacher, U.; Katerkamp, A.; Schachtrupp, A. Systemic Toxicity of Di-2-Ethylhexyl Terephthalate (DEHT) in Rodents Following Four Weeks of Intravenous Exposure. *Toxicol. Lett.* **2011**, *205* (1), 8–14.

(7) Larsson, K.; Lindh, C. H.; Jönsson, B. A.; Giovanoulis, G.; Bibi, M.; Bottai, M.; Bergström, A.; Berglund, M. Phthalates, Non-Phthalate Plasticizers and Bisphenols in Swedish Preschool Dust in Relation to Children's Exposure. *Environ. Int.* **2017**, *102*, 114–124.

(8) Sousa, A. F.; Vilela, C.; Fonseca, A. C.; Matos, M.; Freire, C. S. R.; Gruter, G. J. M.; Coelho, J. F. J.; Silvestre, A. J. D. Biobased Polyesters and Other Polymers from 2,5-Furandicarboxylic Acid: A Tribute to Furan Excellency. *Polym. Chem.* **2015**, *6* (33), 5961–5983.

(9) Choi, W.; Chung, J. W.; Kwak, S. Y. Unentangled Star-Shape Poly(ε-Caprolactone)s as Phthalate-Free PVC Plasticizers Designed for Non-Toxicity and Improved Migration Resistance. *ACS Appl. Mater. Interfaces* **2014**, *6* (14), 11118–11128.

(10) Gao, C.; Zhang, X.; Sun, J.; Yuan, Z.; Han, S.; Liu, Y.; Ji, S. Poly(Hexane Succinate) Plasticizer Designed for Poly(Vinyl Chloride) with a High Efficiency, Nontoxicity, and Improved Migration Resistance. *J. Appl. Polym. Sci.* **2018**, *135* (25).

(11) Chen, J.; Wang, Y.; Huang, J.; Li, K.; Nie, X. Synthesis of Tung-Oil-Based Triglycidyl Ester Plasticizer and Its Effects on Poly(Vinyl Chloride) Soft Films. *ACS Sustain. Chem. Eng.* **2018**, *6* (1), 642–651.

(12) Li, M.; Li, S.; Xia, J.; Ding, C.; Wang, M.; Xu, L.; Yang, X.; Huang, K. Tung Oil Based Plasticizer and Auxiliary Stabilizer for Poly(Vinyl Chloride). *Mater. Des.* **2017**, *122* (16), 366–375.

(13) Lee, S.; Park, M. S.; Shin, J.; Kim, Y. W. Effect of the Individual and Combined Use of Cardanol-Based Plasticizers and Epoxidized Soybean Oil on the Properties of PVC. *Polym. Degrad. Stabil.* **2018**, *147*, 1–11.

(14) Jia, P.; Hu, L.; Shang, Q.; Wang, R.; Zhang, M.; Zhou, Y. Self-Plasticization of PVC Materials via Chemical Modification of Mannich Base of Cardanol Butyl Ether. *ACS Sustain. Chem. Eng.* **2017**, *5* (8), 6665–6673.

(15) Gandini, A.; Silvestre, A. J. D. A.; Neto, C. P.; Sousa, A. F.; Gomes, M. The Furan Counterpart of Poly(Ethylene Terephthalate): An Alternative Material Based on Renewable Resources. *J. Polym. Sci. Polym. Chem.* **2009**, *47* (1), 295–298.

(16) Koenig, K.; Andreesen, J. R. Xanthine Dehydrogenase and 2-Furoyl-Coenzyme. A Dehydrogenase from Pseudomonas Putida Fu1: Two Molybdenum-Containing Dehydrogenases of Novel Structural Composition. *J. Bacteriol.* **1990**, *172* (10), 5999–6009.

(17) Sanderson, R. D.; Schneider, D. F.; Schreuder, I. Synthesis and Evaluation of Dialkyl Furan-2,5-Dicarboxylates as Plasticizers for PVC. *J. Appl. Polym. Sci.* **1994**, *53* (13), 1785–1793.

(18) Yu, Z.; Zhou, J.; Zhang, J.; Huang, K.; Cao, F.; Wei, P. Evaluating Effects of Biobased 2,5-Furandicarboxylate Esters as Plasticizers on the Thermal and Mechanical Properties of Poly (Vinyl Chloride). *J. Appl. Polym. Sci.* **2014**, *131* (20), 1–10.

(19) VanDyke, M. S.; Tedesco, J. C. Understanding Green Content Strategies: An Analysis of Environmental Advertising Frames from 1990 to 2010. *Int. J. Strateg. Commun.* **2016**, *10* (1), 36–50.

(20) Coelho, J. F. J.; Gonçalves, P. M. F. O.; Miranda, D.; Gil, M. H. Characterization of Suspension Poly(Vinyl Chloride) Resins and Narrow Polystyrene Standards by Size Exclusion Chromatography with Multiple Detectors: Online Right Angle Laser-Light

Scattering and Differential Viscometric Detectors. *Eur. Polym. J.* **2006**, *42* (4), 751–763.

(21) Waskitoaji, W.; Triwulandari, E.; Haryono, A. Synthesis of Plasticizers Derived from Palm Oil and Their Application in Polyvinyl Chloride. *Procedia Chem.* **2012**, *4*, 313–321.

(22) Matos, M.; F. Sousa, A.; H. C. S. Silva, N.; S. R. Freire, C.; Andrade, M.; Mendes, A.; J. D. Silvestre, A. Furanoate-Based Nanocomposites: A Case Study Using Poly(Butylene 2,5-Furanoate) and Poly(Butylene 2,5-Furanoate)-Co-(Butylene Diglycolate) and Bacterial Cellulose. *Polymers* **2018**, *10* (8), 810.

(23) ASTM D 1239. *Standard Test Method for Resistance of Plastic Films to Extraction by Chemicals*; US, 1998; Vol. 08.

(24) ISO 176-2005. *Plastics-Determination of Loss of Plasticizers-Activated Carbon Method*; 2005; Vol. 3.

(25) Korsmeyer, R. W.; Gurny, R.; Doelker, E.; Buri, P.; Peppas, N. A. Mechanisms of Solute Release from Porous Hydrophilic Polymers. *Int. J. Pharm.* **1983**, *15* (1), 25–35.

(26) Wang, M.; Song, X.; Jiang, J.; Xia, J.; Li, M. Binary Amide-Containing Tung-Oil-Based Ca/Zn Stabilizers: Effects on Thermal Stability and Plasticization Performance of Poly(Vinyl Chloride) and Mechanism of Thermal Stabilization. *Polym. Degrad. Stabil.* **2017**, *143*, 106–117.

(27) Naqvi, M. K.; Unnikrishnan, P. A.; Sharma, Y. N.; Bhardwaj, I. S. Effect of Calcium and Zinc Carboxylates on the Thermal Stabilisation of PVC. *Eur. Polym. J.* **1984**, *20* (1), 95–98.

(28) Gonzalez, N.; Fernandez-Berridi, M. J. Fourier Transform Infrared Spectroscopy in the Study of the Interaction Between PVC and Plasticizers: PVC/Plasticizer Compatibility. *Appl. Polym. Sci.* **2008**, *107*, 1294–1300.

(29) Coltro, L.; Pitta, J. B.; Madaleno, E. Performance Evaluation of New Plasticizers for Stretch PVC Films. *Polym. Test.* **2013**, *32* (2), 272–278.

(30) Lai, H.; Wang, Z.; Wu, P.; Chaudhary, B. I.; Sengupta, S. S.; Cogen, J. M.; Li, B. Structure and Diffusion Behavior of Trioctyl Trimellitate (TOTM) in PVC Film Studied by ATR-IR Spectroscopy. *Ind. Eng. Chem. Res.* **2012**, *51* (27), 9365–9375.

(31) Ramesh, S.; Leen, K. H.; Kumutha, K.; Arof, A. K. FTIR Studies of PVC/PMMA

Blend Based Polymer Electrolytes. *Spectrochim. Acta - Part A Mol. Biomol. Spectrosc.* **2007**, *66* (4–5), 1237–1242.

(32) Rajendran, S.; Uma, T. Lithium Ion Conduction in PVC-LiBF4 Electrolytes Gelled with PMMA. *J. Power Sources* **2000**, *88* (2), 282–285.

(33) Tabb, D. L.; Koenig, J. L. Fourier Transform Infrared Study of Plasticized and Unplasticized Poly(Vinyl Chloride). *Macromolecules* **1975**, *8* (6), 929–934.

(34) Demertzis, P. G.; Riganakos, K. A.; Akrida-Demertzi, K. Study of Compatibility of PVC and Polyester-Type Plasticizer Blends by Inverse Gas Chromatography. *Eur. Polym. J.* **1990**, *26* (2), 137–140.

(35) Beltrán, M.; García, J. C.; Marcilla, A. Infrared Spectral Changes in PVC and Plasticized PVC during Gelation and Fusion. *Eur. Polym. J.* **1997**, *33* (4), 453–462.

(36) Silva, M. A. da; Adeodato Vieira, M. G.; Gomes Maumoto, A. C.; Beppu, M. M. Polyvinylchloride (PVC) and Natural Rubber Films Plasticized with a Natural Polymeric Plasticizer Obtained through Polyesterification of Rice Fatty Acid. *Polym. Test.* **2011**, *30* (5), 478–484.

(37) Brunner, A. J. X-Ray Diffraction Pattern of Poly (Vinylchloride). *Polym. Lett.* **1972**, *10*, 379–383.

(38) Burgess, S. K.; Leisen, J. E.; Kraftschik, B. E.; Mubarak, C. R.; Kriegel, R. M.; Koros, W. J. Chain Mobility, Thermal, and Mechanical Properties of Poly(Ethylene Furanoate) Compared to Poly(Ethylene Terephthalate). *Macromolecules* **2014**, *47* (4), 1383−1391.

(39) Araujo, C. F.; Nolasco, M. M.; Ribeiro-Claro, P. J. A.; Rudić, S.; Silvestre, A. J. D.; Vaz, P. D.; Sousa, A. F. Inside PEF: Chain Conformation and Dynamics in Crystalline and Amorphous Domains. *Macromolecules* **2018**, *51* (9), 3515–3526.

(40) Chen, J.; Liu, Z.; Nie, X.; Zhou, Y.; Jiang, J.; Murray, R. E. Plasticizers Derived from Cardanol : Synthesis and Plasticization Properties for Polyvinyl Chloride (PVC). *J. Polym. Res.* **2018**, *25* (128).

(41) Wang, M.; Song, X.; Jiang, J.; Xia, J.; Ding, H.; Li, M. Plasticization and Thermal Behavior of Hydroxyl and Nitrogen Rich Group-Containing Tung-Oil-Based Ester Plasticizers for PVC. *New J. Chem.* **2018**, *42* (4), 2422–2431.

(42) Li, Y.; Wang, C.; Wang, G.; Qu, Z. Application of the Long-Chain Linear Polyester in Plastification of PVC. *J. Wuhan Univ. Technol. Mater. Sci. Ed.* **2008**, *23* (1), 100–

104.

(43) Haryono, A.; Triwulandari, E.; Jiang, P. Interaction between Vegetable Oil Based Plasticizer Molecules and Polyvinyl Chloride, and Their Plasticization Effect. *AIP Conf. Proc.* **2017**, *1803*.

(44) Zakaria, N. a.; Yahya, S. Y. S.; Isa, M. I. N.; Mohamed, N. S.; Subban, R. H. Y. Conductivity and Dynamic Mechanical Studies of PVC/PEMA Blend Polymer Electrolytes. *Adv. Mater. Res.* **2010**, *93–94* (January), 429–432.

(45) Jia, P.; Zhang, M.; Liu, C.; Hu, L.; Feng, G.; Bo, C.; Zhou, Y. Effect of Chlorinated Phosphate Ester Based on Castor Oil on Thermal Degradation of Poly (Vinyl Chloride) Blends and Its Flame Retardant Mechanism as Secondary Plasticizer. *RSC Adv.* **2015**, *5* (51), 41169–41178.

(46) Wang, Q.; Wu, W.; Tang, Y.; Bian, J.; Zhu, S. Thermal Degradation Kinetics of Plasticized Poly(Vinyl Chloride) with Six Different Plasticizers. *J. Macromol. Sci. Part B* **2017**, *56* (6), 420–434.

(47) Yu, J.; Sun, L.; Ma, C.; Qiao, Y.; Yao, H. Thermal Degradation of PVC: A Review. *Waste Manag.* **2016**, *48* (December), 300–314.

(48) Kovačić, T.; Mrklić, Ž. The Kinetic Parameters for the Evaporation of Plasticizers from Plasticized Poly(Vinyl Chloride). *Thermochim. Acta* **2002**, *381* (1), 49–60.

(49) Fernandez-Canal, C.; Pinta, P.-G.; Eljezi, T.; Larbre, V.; Kauffmann, S.; Camilleri, L.; Cosserant, B.; Bernard, L.; Pereira, B.; Constantin, J.-M.; et al. Patients' Exposure to PVC Plasticizers from ECMO Circuits. *Expert Rev. Med. Devices* **2018**, *15* (5), 377–383.

Supporting Information

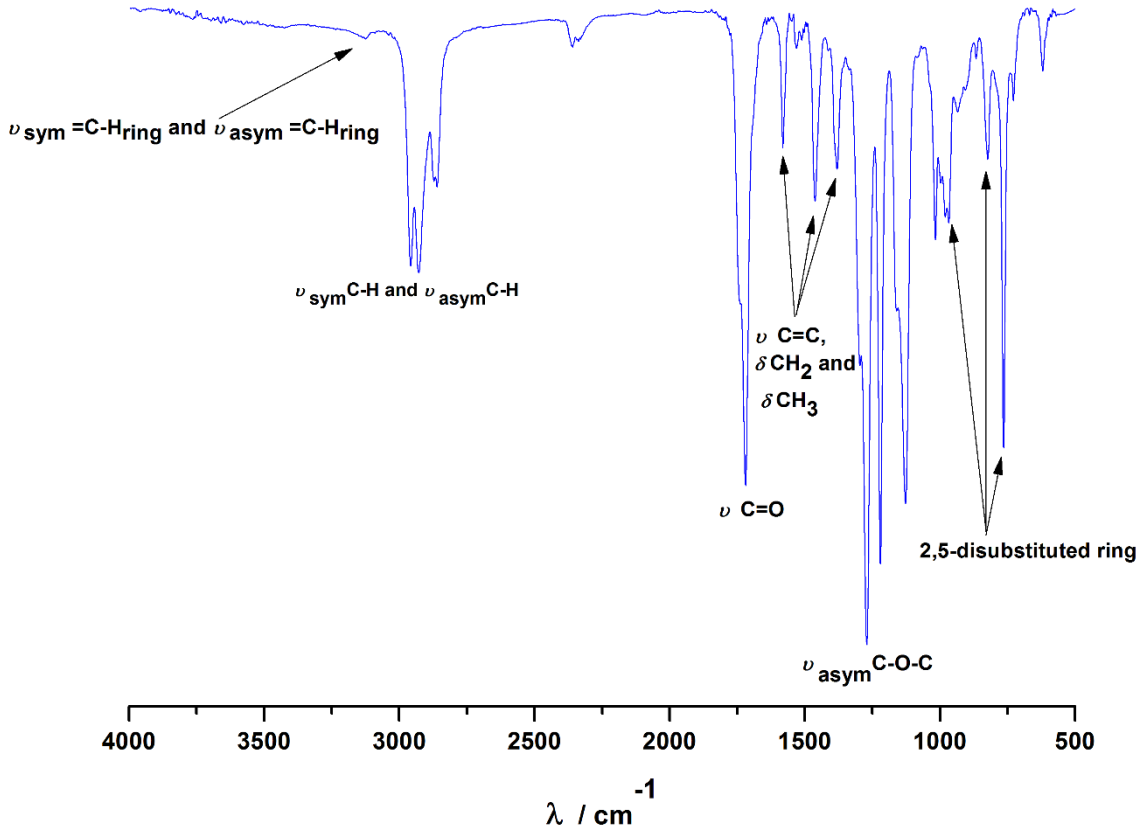

Figure S1. ATR FTIR spectrum of DEHF plasticizer.

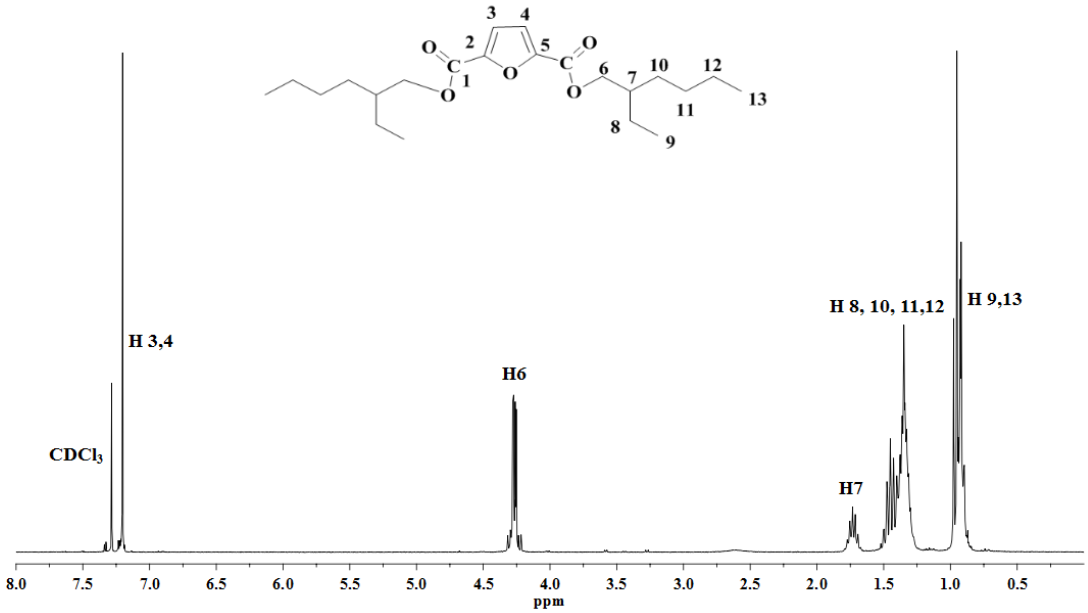

Figure S2. ^{1}H NMR spectrum of DEHF ($CDCl_3$).

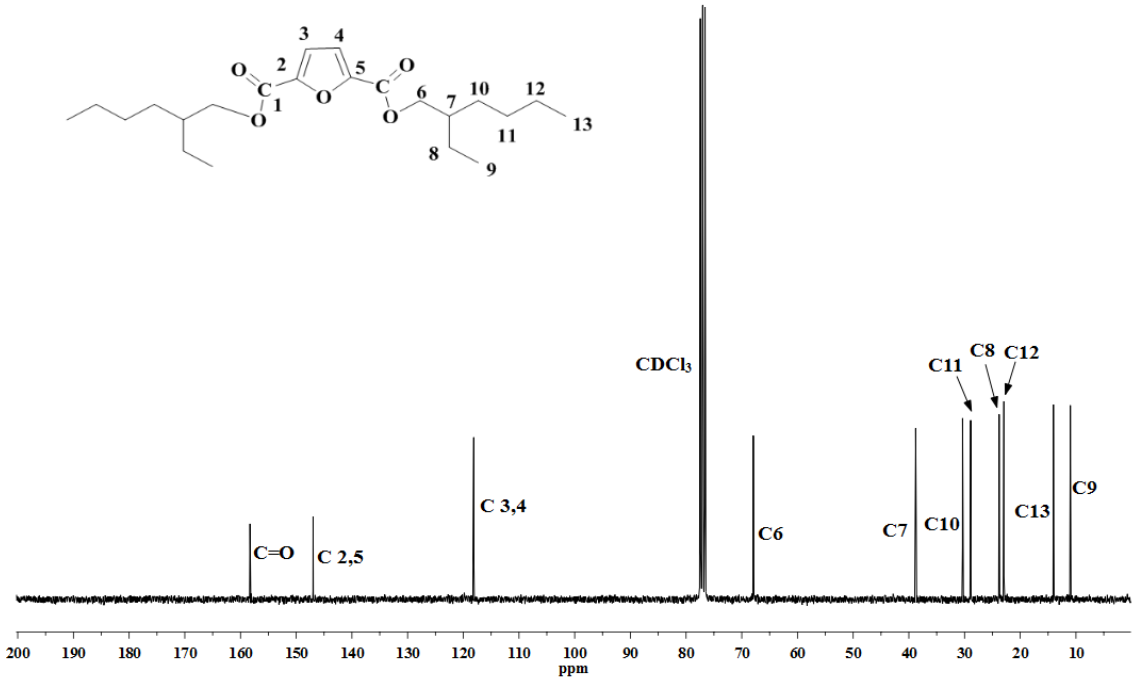

Figure S3. ^{13}C NMR spectrum of DEHF ($CDCl_3$).

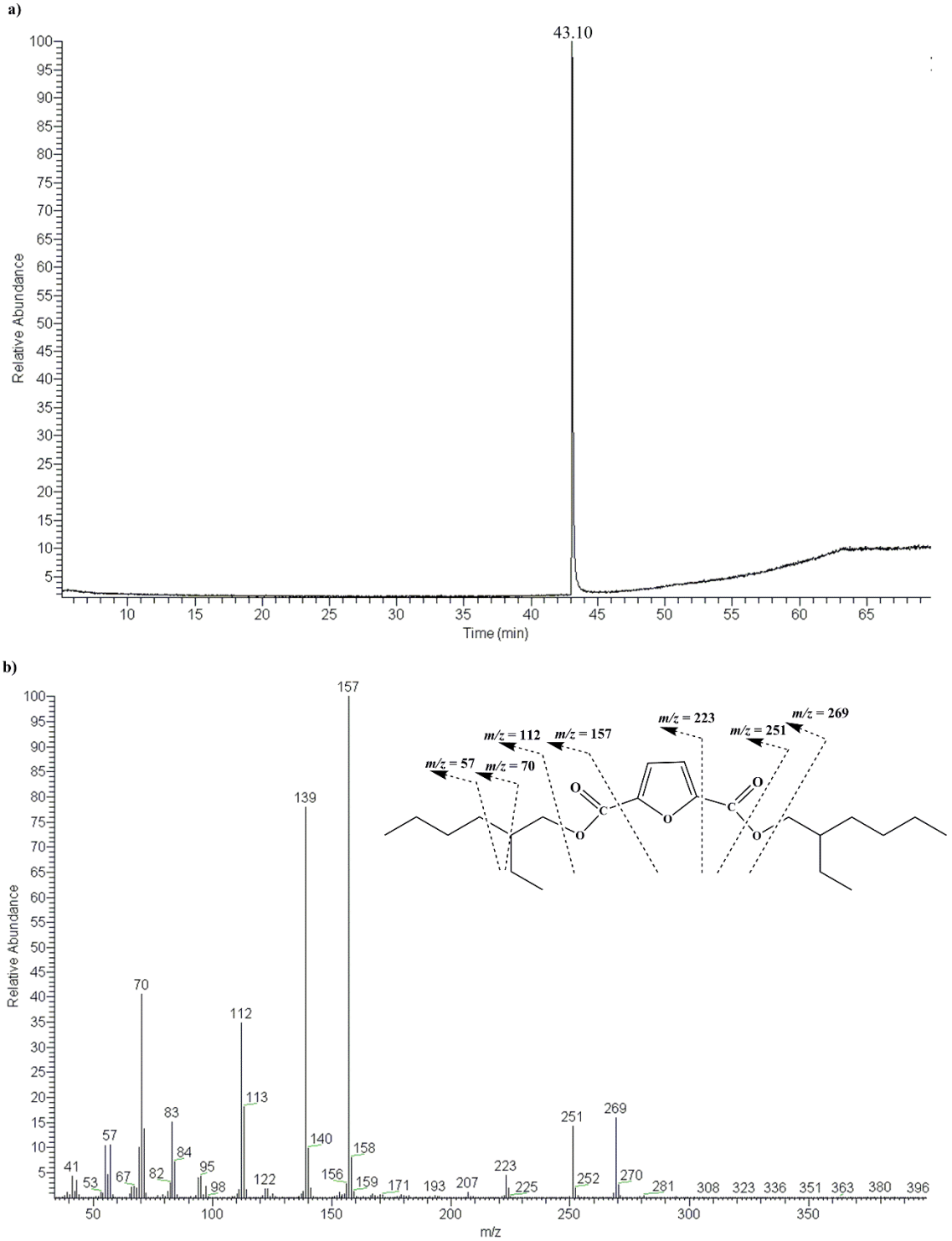

Figure S4. Main results from GC-MS analysis a) GC chromatogram and b) MS spectra of DEHF.

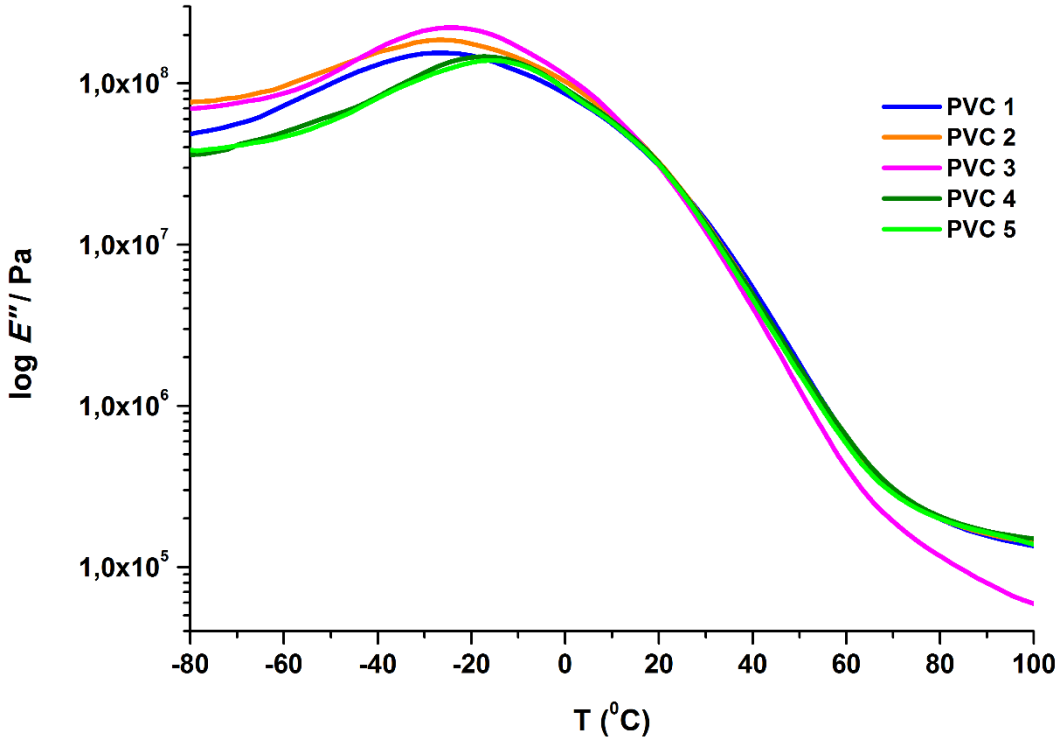

Figure S5. *E´´* traces of all PVC films.

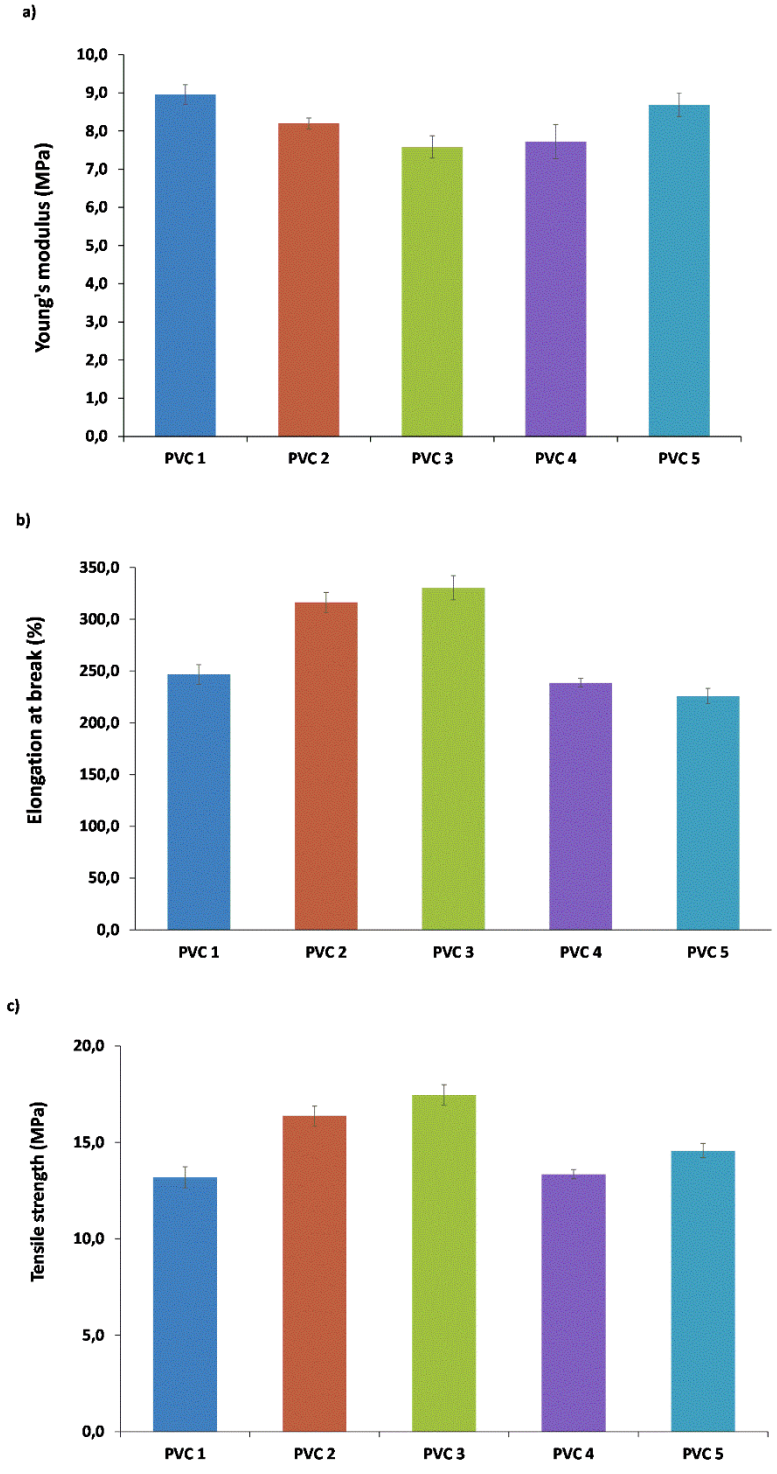

Figure S6. Mechanical properties of all PVC-DEHF/DEHT blends: a) Young's modulus, b) elongation at break and c) tensile strength.

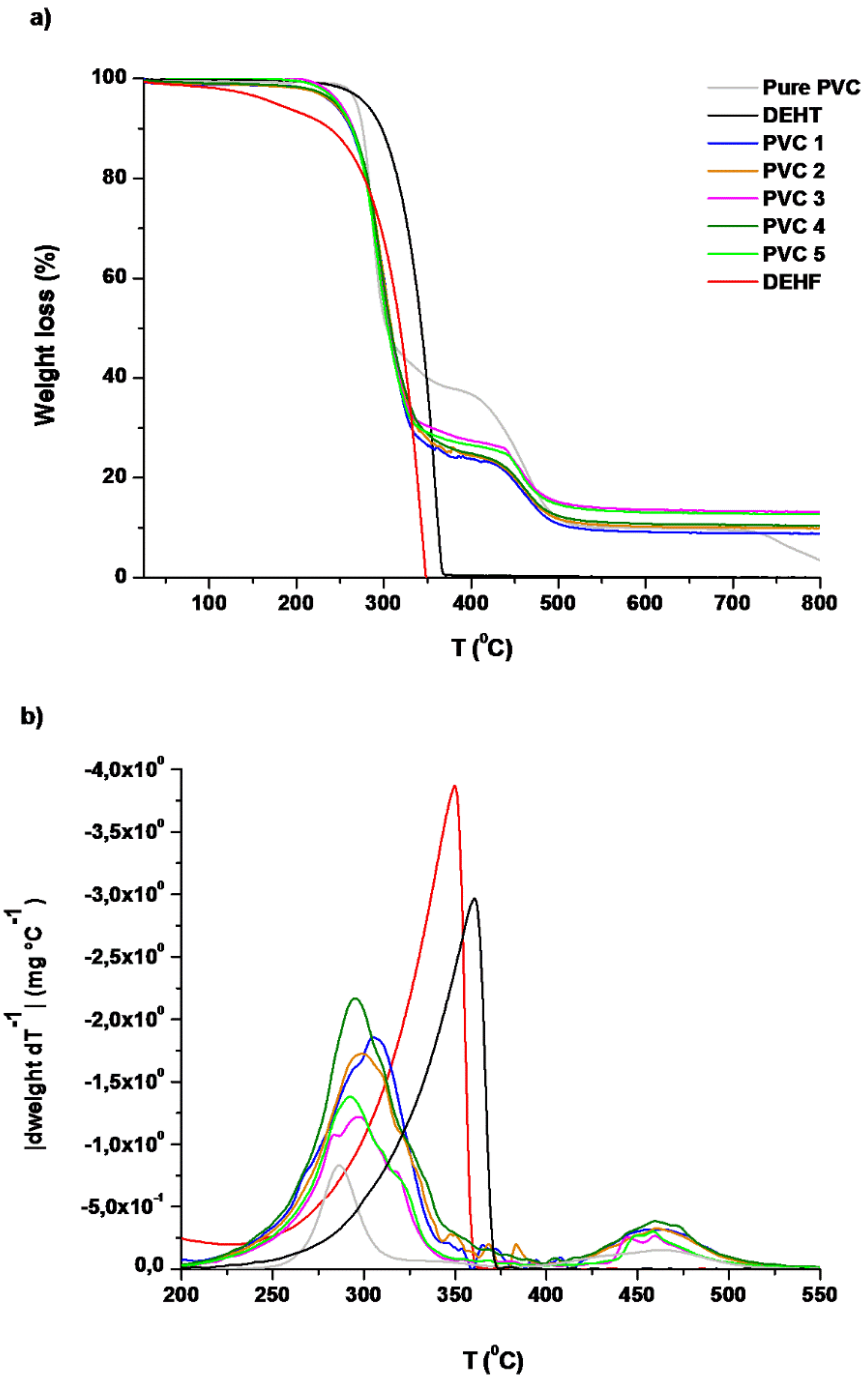

Figure S7. TGA (a) and DTG (b) thermograms of all PVC-DEHF/DEHT blends, related DEHF and DEHT plasticizers and pure PVC.

Tables:

Table S1. Chemical characteristics of the different plasticizers.

Plasticizers	Molecular formula	Molecular weight	Viscosity (cP at 25 ºC)	Density (g/cm^3)
DEHF	$C_{22}H_{36}O_5$	380.53	55	0.98
DEHT	$C_{24}H_{38}O_4$	390.56	63	0.98

The relative uncertainty of the dynamic viscosity is ±0.35%.

Table S2. Glass transition (T_g) and storage modulus (E') at -10 ºC and 25 ºC of all PVC-DEHF/DEHT blends.

Formulations	T_g (ºC)	E' (MPa)		
		at $T_{-10ºC}$	at T_g	at $T_{25ºC}$
Pure PVC	97.4[a]	-	-	-
PVC 1	23.5	551.8	50.6	42.9
PVC 2	22.1	658.2	56.9	42.2
PVC 3	20.4	694.7	58.5	38.2
PVC 4	21.1	617.3	55.2	39.4
PVC 5	21.5	649.7	56.1	40.2

[a] Determined by DMTA using material pocket technology.

Table S3. PVC blends weight loss percentage results determined from the chemical and volatile resistance tests.

chemicals	Formulations				
	PVC1	PVC2	PVC3	PVC4	PVC5
	Weight loss (%)[a]				
water	0.04	0.08	0.26	0.27	0.09
PBS	0.04	0.07	0.17	0.13	0.13
cyclohexane	21.40	16.93	19.86	15.19	12.20
activated carbon	0.04	0.21	0.26	0.14	0.21

[a]Error deviations were less than or equal to 0.01%.

PART D

Chapter VII – Concluding Remarks and Perspectives

1. Concluding Remarks

The demand for new renewable-based polymers and materials has increased in the last decades, mostly due to environmental concerns. In this context, it has been demonstrated that FDCA-based materials prepared in this thesis could be promising renewable alternatives to fossil-based counterparts. In fact, in general terms, all prepared materials, besides being prepared from renewable resources (at least partially) have shown attractive thermal and/or mechanical properties, very similar to those based on non-renewable counterparts, namely from TPA.

This work was essentially focused on the synthesis of FDCA-based polyesters and nanocomposites thereof. This study also explored the FDCA-based ester as a plasticiser for PVC (PART B and C, respectively).

The first study was related to the synthesis of a new furanic-cycloaliphatic homopolyester with enhanced thermal features, namely PCdF. Moreover, a comparative study between PCdF and PCF, since they are structurally related, and also a comparison with their non-renewable counterpart was done. Their synthesis through two-step bulk polytransesterification reaction using titanium (IV) butoxide as catalyst lead to homopolyesters with the highest molecular weights PCdF and PCF were characterised in detail by several techniques, showing to be semi-crystalline materials with high glass transition temperatures (T_g values of 175 e 105 ºC for PCdF and PCF, respectively), and thermally stable up to 377 ºC. These results are in agreement with the literature, showing that incorporation of the more rigid structure cyclohexanediol into the polymeric chain backbone lead to an increase on the thermal properties. Moreover, it was found that, the absence of the CH_2 group on PCdF homopolyester, also lead to higher T_g than PCF, as well as higher thermal stability when compared with their related petroleum-based counterpart. These homopolyesters could find several interesting industrial applications, worth exploring in the future, namely in optical films or in injection moulding materials, in similarity to PCT.

The second study was devoted to the synthesis of poly(ester-ether)s (PEEs) copolymers. These materials are known to incorporate both stiff and soft units in their polymer chain, displaying good thermal stability and also a large working temperature interval between their T_g and T_m values, turning possible their processability at lower temperatures than for example PBF. A series of poly(ester-ether)s (PEEs) copolymers were prepared using different

PBF/PPO ratios to tune the final thermal properties of these materials. In fact, when small amounts of PPO were incorporated into polymer chain, the ensuing copolyesters presented a semi-crystalline character similar to that of PBF, however when similar amounts of PBF and PPO were used the resulting material was unable to crystallise. Despite some decrease of their thermal properties when compared with the PBF homopolyester, their maximum degradation temperatures were still reasonable (T_d between 340-365 ºC). Moreover, a sharp decreased on their T_g was noted, specially when compared with PBF (values ranging from -42.3 to -32.6 ºC and 75.6 ºC for PEEs and PBF, respectively). Due to their tuneable thermal properties, they can be easily processed as thermoplastic materials.

In the third study nanocomposite films were prepared by solvent-casting based on poly(butylene 2,5-furandicarboxylate)-co-(butylene diglycolate) (PBF-co-PBDG) copolyesters and acetylated bacterial cellulose (Ac-BC). A balance between flexibility, prompted by the PBF-co-PBDG polymeric matrix; and the high strength prompted by the bacterial cellulose fibres, enabled the preparation of a wide range of new nanocomposite materials. In fact, by incorporating 30 weight % of Ac-BC and higher amounts of PBDG, these reinforced materials showed an increased stiffness (Young's modulus up to 1239 MPa) and enhanced elasticity (elongation at break values up to 25.0 %) compared to their neat (co)polyester counterparts. In terms of oxygen gas barrier properties, similar results were obtained for nanocomposites and their related (co)polyesters, expanding the exploitation of these materials for packaging applications.

Besides the need to find new renewable-based polymers, it is also important to try to replace also other petroleum-based products used in the most variate number of industrial applications. In this vein, this study also explored the partial replacement of DEHT by a FDCA-based monomer, namely the di(2-ethylhexyl) 2,5-furandicarboxylate (DEHF) for PVC formulations. DEHF was mixed with DEHT until 20 per hundred resin (phr) (55 phr on total PVC formulation), and the resulting PVC blends have shown similar glass transitions temperatures (19.2 to 23.8 ºC) to those obtained with commercial DEHT, enhanced flexibility (elongation at break up to 330%) and even higher compatibility with PVC matrix. Furthermore, very low weight loss percentages were observed through migration tests, increasing their potential for applications in food/beverages packages and medical blood bags. For example, in cyclohexane, weight loss was higher in the case of PVC blends prepared with DEHT as single plasticizer, when compared with PVC-DEHF/DEHT

blends. Interestingly, viability tests showed, that up to 500 μM, both plasticizers displayed a non-toxic profile, showing that the combination of DEHF and DEHT plasticizers into PVC formulations increased not just the green content, but also the wide range of applications.

In conclusion, this thesis dealt with the synthesis of several FDCA-based materials with quite interesting properties, which pump up a panoply of renewable possible substitutes to those prepared from petroleum resources mainly based on fossil based TPA. Moreover, the materials prepared in this study revealed to be an important contribution for a more sustainable society.

2. Perspectives

As refereed above the main goal of this thesis was the development of new FDCA-based polymers and nanocomposites, opening new perspectives for new work to be explored. In fact, in the future, further work could be performed in order to complement these materials characterisations. It will be very interesting to obtain some answers to the following topics:

1. characterisation of the mechanical properties of some materials, namely PCdF homopolyesters and PBF-co-PPOF copolyesters;

2. study of the biodegradability (under compostable conditions) of all copolyesters and nanocomposites prepared in this study;

3. deep evaluation of plasticisers citotoxicity, *i.e.*, the use of human line cells in *in vitro* tests, and forward also, in *in vivo* tests;

4. synthesis and characterisation of new chemicals and materials based on FDCA;

5. the synthesis of new nanomaterials.